UNIVERSITY OF CALIFORNIA
RIVERSIDE

I. Synthesis and Bioactivity of Novel Proteasome Inhibiting Syrbactins and II. Peptide Assembly by Ligation of Hydroxyl Amino Acids and Mildly Activated Esters

A Dissertation submitted in partial satisfaction
of the requirements for the degree of

Doctor of Philosophy

in

Chemistry

by

Nicole Amber Bakas

September 2017

Dissertation Committee:
Dr. Michael Pirrung, Chairperson
Dr. Christopher Switzer
Dr. Richard Hooley

The Dissertation of Nicole Amber Bakas is approved:

_____

_____

_____

Committee Chairperson

University of California, Riverside

Acknowledgement

First and most importantly, I would like to thank my husband, Kendall Bakas. Kendall, thank you for all the unconditional patience, love and support you have provided during all the failures, successes and meltdowns of my graduate career. Thank you for not only believing in me, but also helping me learn to believe in myself. I would also like to thank all of my family for their continued love and support through all the craziness of these past five years.

I would also like to acknowledge the Minority Access to Research Careers-Undergraduate Student Training in Academic Research (MARC U*) Program at UC Riverside, which funded my initial exploration and research as an undergraduate. Thanks to this program, I gained an interest in synthetic organic chemistry that led to my decision to pursue a PhD.

As for my wonderful lab mates, thank you all for your support and your ability to make the long workdays more manageable. You all have certainly made the last five years more interesting and fun. A special thanks to Dr. Ambadi Sudhakar for being such an excellent mentor and bestowing his vast organic chemistry knowledge upon an eager mind and to Dr. Luca Gambini for always being helpful and providing his peptide chemistry expertise.

I would also like to acknowledge Dr. Andre Bachmann, Chad Schultz and Lisette Yco for conducting the biological testing on the NAM syrbactin compounds. I would also like to thank Dr. Dan Borchardt for all his technical assistance with instrumentation over

the past five years. A special thanks to Prisciliano Saavedra for the countless times you have helped me with all my purchasing, shipping, stock room, and many other laboratory needs.

I would like to acknowledge UC Riverside, the Department of Education and the National Science Foundation (CHE 1362737) for their financial support, which made all this work possible. Additionally, thank you to the UC Riverside Dean's distinguished fellowship and the Department of Education Graduate Assistance in Areas of National Need fellowship (award #P200A120170) was greatly appreciated and allowed me to focus more effort on research.

Lastly, I would like to thank my advisor Dr. Pirrung for his mentorship and support, both financially and intellectually. Dr. Pirrung, your guidance has helped me achieve goals I once believed were out of reach.

ABSTRACT OF THE DISSERTATION

I. Synthesis and Bioactivity of Novel Proteasome Inhibiting Syrbactins and
II. Peptide Assembly by Ligation of Hydroxyl Amino Acids and Mildly Activated Esters

by

Nicole Amber Bakas

Doctor of Philosophy, Graduate Program in Chemistry
University of California, Riverside, September 2017
Dr. Michael C. Pirrung, Chairperson

Part one describes the synthesis and bioactivity of syrbactin derivatives. The syrbactins are a class of structurally similar natural products that were discovered to effectively induce apoptosis in various cancer cell lines through irreversible binding and inhibition of the constitutive proteasome. The success of proteasome inhibitors bortezomib and carfilzomib as cancer therapeutics has promoted further interest in the syrbactins. Previous work conducted by the Pirrung laboratory exploring the structure-activity relationship of syrbactin analogs has inspired the investigation into the synthesis of a unique set of syrbactin derivatives in efforts to create next-generation proteasome inhibitors with improved potency and enhanced overall efficacy. In this work, a novel set of syrbactin based derivatives have been proposed, synthesized, and the biological activities have been evaluated. Additionally, thiasyrbactin derivatives have been discovered to have unique properties resulting in rare and selective inhibition of the immunoproteasome. The immunoproteasome has been linked to a variety of diseases

including various cancers, autoimmune, and neurodegenerative diseases, and is therefore, a novel therapeutic target.

Part two describes the development of peptide assembly by ligation of hydroxyl amino acids threonine and homoserine with mildly activated esters. Many advances in the field of peptide chemistry have occurred allowing for the synthesis and bioevaluation of complex peptides and proteins. The development of native chemical ligation (NCL), a chemoselective cysteine-based peptide-coupling technique, provided a breakthrough in the chemical synthesis of peptides. Cysteine is one of the least abundant amino acids in natural peptides; thus, additional ligation methods based on other amino acids are essential. Recently, the Pirrung laboratory has developed a method of peptide assembly reacting β-hydroxylamines including serine, with activated esters to form amide bonds. This strategy mimics the mechanism of NCL via transesterification and subsequent acyl transfer to form a native peptide bond at the ligation site. In this work, peptide assembly with mildly activated esters has been successfully extended to the hydroxyl amino acids threonine and homoserine, expanding the scope of this ligation method. The utility of this method was further demonstrated by the synthesis of the opossum peptide, antivenom lethal toxin neutralizing factor-10 (LTNF-10).

Table of Contents

List of Figures

List of Schemes

List of Tables

List of Abbreviations

AA	Amino acid
Ac	Acetyl
AcOH	Acetic acid
Ala	Alanine
Asp	Aspartic acid
aq	Aqueous
9-BBN	9-Borabicyclo[3.3.1]nonane
Bn	Benzyl
Boc	*tert*-Butyloxycarbonyl
C-L	Caspase-like
Cbz	Carbobenzyloxy
CM	Cyanomethyl
COSY	Correlation spectroscopy
2-CTC	2-Chlorotrityl chloride
CT-L	Chymotrypsin-like
Cys	Cysteine
DBU	1,8-Diazabicyclo[5.4.0]undec-7-ene
DCC	*N,N′*-Dicyclohexylcarbodiimide
DCM	Dichloromethane
DIPEA	*N,N*-Diisopropylethylamine
DKP	Diketopiperazine

DMF	Dimethylformamide
EDCI	*N*-(3-Dimethylaminopropyl)-*N*-ethylcarbodiimide hydrochloride
EtOAc	Ethyl acetate
equiv	Equivalent
FDA	Food and Drug Administration
Fmoc	Fluorenylmethyloxycarbonyl
FT-IR	Fourier transform infrared spectroscopy
GlbA	Glidobactin A
HIP	1,1,1,3,3,3-Hexafluoroisopropyl
HOBt	Hydroxybenzotriazole
HPLC	High-performance liquid chromatography
Hse	Homoserine
HSQC	Heteronuclear single quantum coherence
HWE	Horner–Wadsworth–Emmons reaction
IC_{50}	Half-maximal inhibitory concentration
Ile	Isoleucine
IR	Infrared
K_i	Inhibition constant
Leu	Leucine
LTNF	Lethal toxin-neutralizing factor
M	Molarity
MeOH	Methanol

MM	Multiple myeloma
MS	Mass spectroscopy
NB	Neuroblastoma
NCI	National Cancer Institute
NCL	Native chemical ligation
NHS	*N*-Hydroxysuccinimide
NMP	*N*-Methylpyrrolidone
NMR	Nuclear magnetic resonance
NOESY	Nuclear Overhauser Spectroscopy
PFP	2,2,3,3,3-Pentafluoro-1-propyl
Phe	Phenylalanine
PMA	Phosphomolybdic acid
Pro	Proline
RCM	Ring closing metathesis
SAL	Salicylaldehyde
SAR	Structure-activity relationship
sat	Saturated
Ser	Serine
SPPS	Solid phase peptide synthesis
SylA	Syringolin A
SylB	Syringolin B
TBD	Triazabicyclodecene

TCICA	Trichloroisocyanuric acid
TEA	Triethylamine
TEMPO	2,2,6,6-Tetramethyl-1-piperidinyloxy
Tf	Triflate
TFA	Trifluoroacetic acid
TFE	2,2,2-Trifluoroethyl
THF	Tetrahydrofuran
Thr	Threonine
T-L	Trypsin-like
TLC	Thin layer chromatography
TMEDA	Tetramethylethylenediamine
Val	Valine

Part 1: Synthesis and Bioactivity of Novel Proteasome Inhibiting Syrbactins

Chapter 1: Syrbactin Introduction

1.1 Isolation and Structure

The syrbactins are a class of structurally similar peptide-based natural products including the glidobactins, syringolins, cepafungins, and luminmycins. Each of these natural products has a 12-membered macrolactam core containing an α,β–unsaturated amide and exhibit diverse biological activities by a common mechanism of irreversible inhibition of the proteasome.[1]

The glidobactins were first isolated in 1988, by Oka and coworkers from the fermentation of the bacterial strain *Polyangium brachysporum* sp. nov. found in a soil sample obtained in Greece, as a collection of seven structurally similar natural products designated glidobactins A-G (Figure 1.1).[2-4] However, it was discovered several years later by the Dudler group that the originally assigned bacteria strain was incorrect, resulting in the reassignment to the class of proteobacteria, *Burkholderiales*.[5] Glidobactin A (GlbA) was isolated as the major product, while glidobactins B-H were isolated as minor products.

The chemical structures of these natural products were determined by spectral analysis of compounds isolated from the hydrolysis of the natural products.[6] The 12-membered macrolactam core of these compounds contains two unnatural amino acid residues: *erythro*-4-hydroxy-L-lysine and the trans α,β-unsaturated-γ amino acid 4-(S)-amino-2(*E*)-pentenoic acid.[5] The side chains of the glidobactins are composed of a

threonine residue attached to varying unsaturated fatty acids. In comparison to GlbA, the structures of glidobactins B-F have varying fatty acid side chain residues, while glidobactin G has a hydroxymethyl group instead of a methyl substituent on the macrolactam core (Figure 1.1).

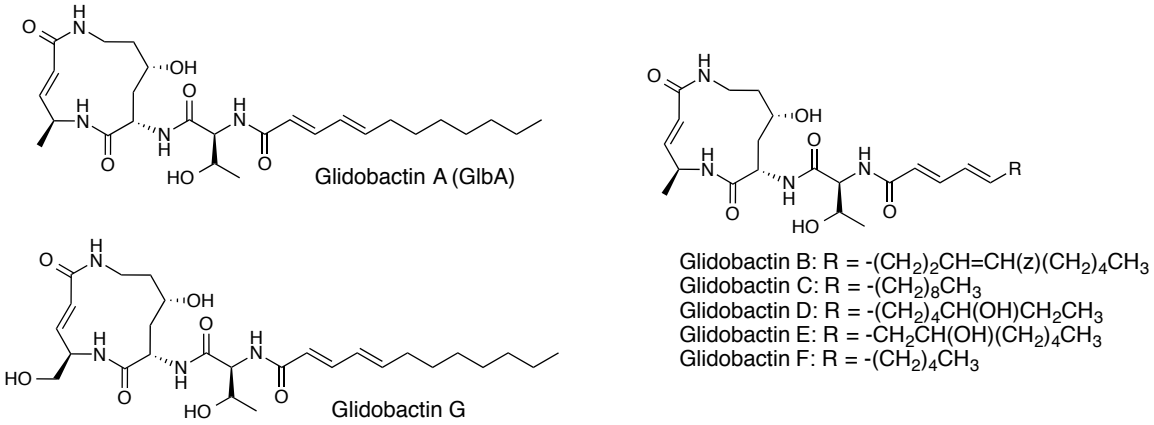

Figure 1.1: Structures of Glidobactins A-G.

In 1990, Terui and coworkers isolated the cepafungins from the bacteria strain *Pseudomonas* sp. found in a soil sample collected in Japan.[7-8] Three natural products were isolated and the chemical structures were determined by extensive spectroscopic analysis of compounds isolated from the hydrolysis of the natural products.[7-8] Cepafungin I was the major product while cepafungin II and III were the minor products (Figure 1.2). The cepafungins have the same 12-membered macrolactam core of GlbA, but have different alkyl side chain residues. Structure elucidation studies demonstrated that the compound isolated as cepafungin II had an identical structure to GlbA.

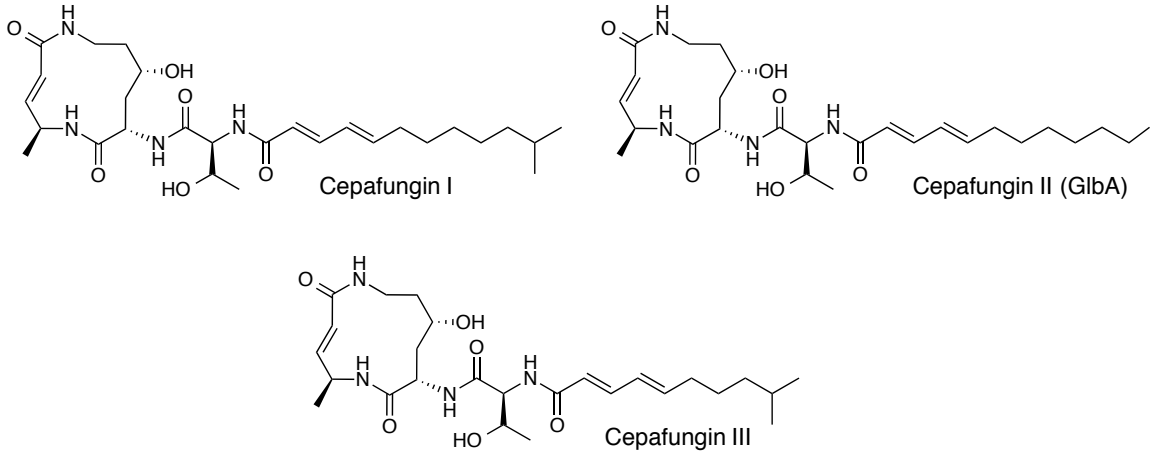

Figure 1.2: Structures of Cepafungins I, II, and III.

In 1998, Dudler and coworkers isolated syringolin A from the secretion of the bacterial plant pathogen *Pseudomonas syringae* pv. *Syringae,* and it was discovered to have antifungal activity in rice.[9] Further investigation led to the discovery of five additional structurally similar products denoted syringolin B-F.[10] The structure of each of the products was determined by extensive spectroscopic analysis (Figure 1.3). These compounds vary in the unsaturation of the macrolactam and in the two amino acid residues connected by a urea residue that make up the side chain. Syringolin A (SylA) has a 12-membered macrolactam core consisting of two trans olefins and two unnatural amino acid residues: 3,4-dehydrolysine and the trans α,β-unsaturated-γ amino acid 5-methyl-4-amino-2-hexenoic acid.[5] Syringolins C, D, and F have the same macrolactam structure as SylA. Syringolin B (SylB) and syringolin E have a macrolactam containing a single trans olefin in the macrolactam and are constructed from the natural amino acid lysine instead of 3,4-dehydrolysine. Additionally, these natural products also vary in the

nature of the amino acids linked by the urea residue in the side chain, consisting of a combination of valine and isoleucine (Figure 1.3).

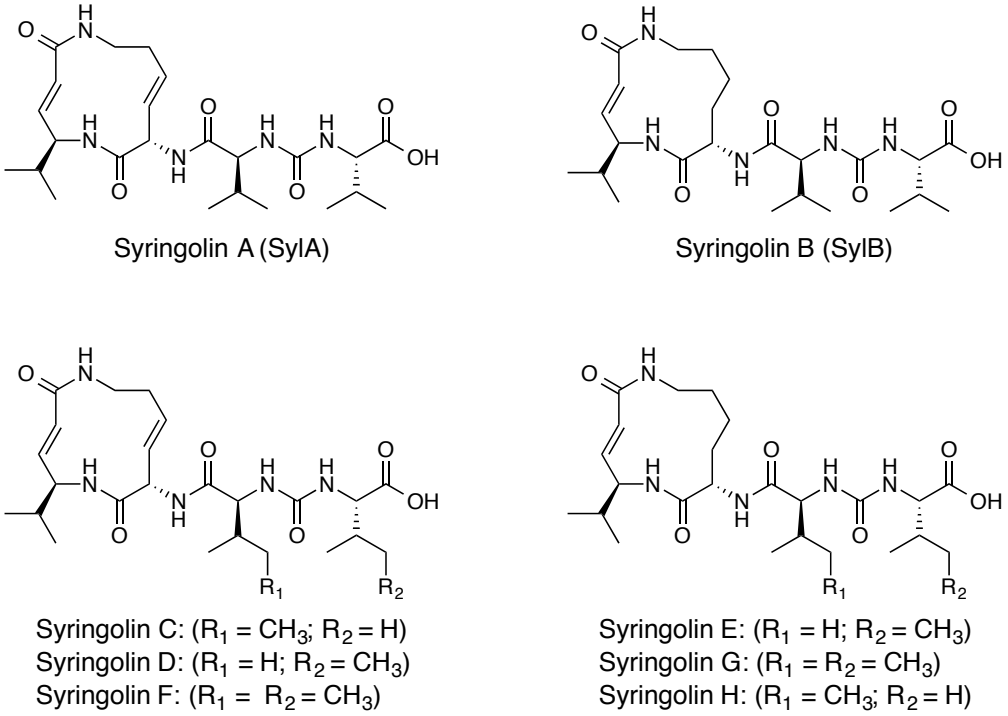

Figure 1.3: Structures of Syringolins A-H.

In 2012, Müller and coworkers discovered two more syringolin natural products, syringolin G and H, by cloning the partial syringolin gene cluster (*sylCDE*) and expressing the gene in *E. coli* (Figure 1.3).[11] Additionally, Müller and coworkers discovered the structurally similar natural product luminmycin A from *Photorhabadus luminescens* by heterologous expression in *E. coli*.[12] The structure was deduced from extensive spectroscopic analysis to be the deoxy-derivative of GlbA (Figure 1.4).

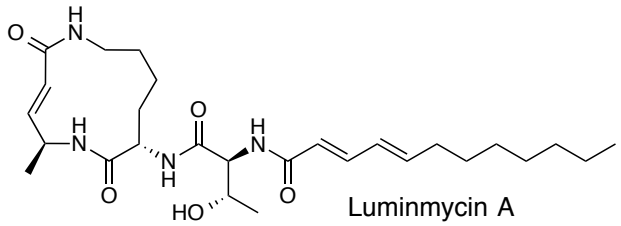

Figure 1.4: Structure of Luminmycin A.

The syrbactins are all structurally similar natural products consisting of a 12-membered macrolactam ring core containing an α,β-unsaturated amide. These molecules vary in the degree of unsaturation of the macrolactam core, amino acid substitutions, and modifications to the side chain. The glidobactins and the cepafungins have identical macrolactam cores connected to a threonine residue, but differ by the unsaturated fatty acid residues attached to the threonine residue of the side chain. Luminmycin A has essentially the same structure as GlbA, but lacks the hydroxyl substituent of the macrolactam core. The syringolins have more distinct features containing amino acid substitutions in the macrolactam core with varying degrees of unsaturation, including one or two trans olefins in the ring. Additionally, the alkyl side chain consists of two amino acids, a combination of valine and isoleucine residues connected by a urea linkage. Although these natural products have several structural variations, each of the syrbactins has similar biological activity. These compounds exhibit a broad range of antifungal activity and antitumor activity against various cancer cell lines.[1 2, 5-6, 12-13]

1.2 Syrbactin Biological Activity: Proteasome Inhibition

The syrbactins including GlbA, SylA, and SylB have been discovered to irreversibly inhibit the eukaryotic proteasome.[1] The proteasome is a large multi-protein complex within cells that is responsible for protein degradation. Proteasomal protein degradation has a crucial role in many biological processes including cell division, proliferation, immune response, gene expression, and apoptosis.[14-15] The eukaryotic 20S proteasome is a large symmetrical cylindrical protease that contains four heptameric rings: two outer α-rings and two inner β-rings consisting of seven structurally similar α- and β-subunits (Figure 1.5).[15] The α-rings act as a gateway into the complex, while the β-rings form a proteolytic inner chamber.[15] The α-rings facilitate the transport of ubiquitin tagged or damaged proteins into the proteolytic center for degradation.[16] Of the seven distinct β- subunits, only three catalytic subunits have proteolytic activity, including the β1, β2, and β5 subunits, representing caspase-like (C-L), trypsin-like (T-L), and chymotrypsin-like (CT-L) activities, respectively.[1, 15, 17] The caspase-like activity cleaves peptides after acidic amino acid residues, the trypsin-like activity cleaves after basic amino acid residues, and the chymotrypsin-like activity cleaves after hydrophobic amino acid residues.[15, 17]

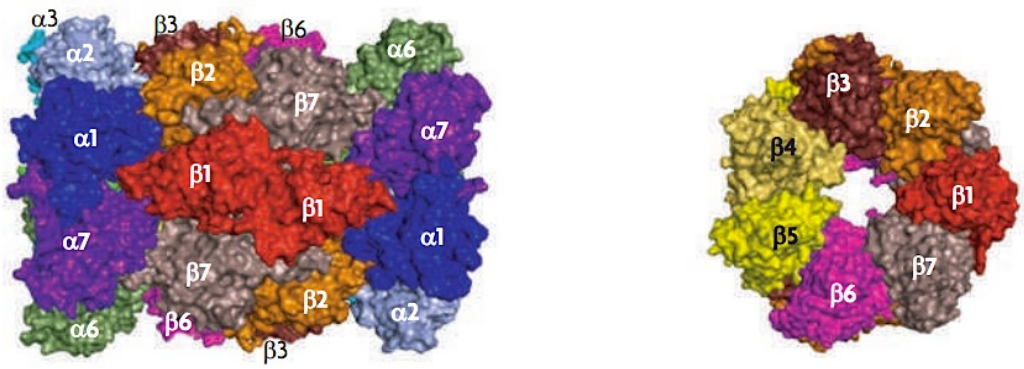

Figure 1.5: Structure of the eukaryotic 20S proteasome: side view of the proteasome (left), top view of the β-ring (right). (Images copied from Murata, S; Yashiroda, H; Tanaka, K. *Nat. Rev. Mol. Cell. Biol.* **2009**, 10, 104-115.)[15]

The eukaryotic proteasome is classified into two types— the constitutive proteasome and immunoproteasome. The constitutive proteasome is found in most mammalian cells, while the immunoproteasome is found predominately in immune cells.[18-19] The immunoproteasome has similar catalytic activity to the constitutive proteasome, but has subtle differences in the subunit composition.[18-19] Compared to the constitutive proteasome, the immunoproteasome also has enhanced CT-L and T-L activities and reduced C-L activity.[18] It can also degrade a broader range of protein substrates including: ubiquitinated proteins, pathogens, oxidized proteins, and protein aggregates.[18]

Inhibition of the proteasome causes an accumulation of proteins within the cell, preventing cell division and ultimately causing apoptosis.[20-21] The relative contribution of each of the different catalytic sites in the degradation of proteins depends on the composition of the protein substrates. Simultaneous inhibition of the three catalytic sites is key to have the greatest cytotoxic effect and induce apoptosis.[20] Disregulation of the

proteasome activity has been linked to a variety of diseases including various cancers, autoimmune diseases, and inflammatory diseases.[18, 21-22] Thus, proteasome inhibition is a novel mechanism to exploit for a broad range of therapeutic applications.

The syrbactins were originally discovered to have anticancer properties by causing apoptosis in various cancer cell lines, but the mechanism of action was unknown. GlbA demonstrated activity against leukemia and melanoma[2], and SylA demonstrated activity against neuroblastoma and ovarian cancer cell lines with IC_{50} (50% inhibition) values ranging between 20-25 μM.[13] In 2008, Groll and coworkers discovered that the syrbactins bioactivity was the result of proteasome inhibition, and they obtained a crystal structure of SylA bound to the yeast 20S proteasome to evaluate the mechanism of action.[1] Analysis of the crystal structure revealed that the syrbactins covalently bind to the catalytic sites of the proteasome with varying affinities resulting in irreversible proteasome inhibition.[1] The syrbactins covalently bind to the proteasome by way of an oxa-Michael 1,4-addition reaction between the α,β-unsaturated amide in the syrbactin macrolactam and the hydroxyl group of the terminal threonine residue of the proteasome catalytic subunit (Figure 1.6).[1, 17] The reaction is promoted by a nearby glycine residue, which stabilizes the enolate formed in the transition state by hydrogen bonding. The produced ether bond results in the irreversible inhibition of the proteasome catalytic site.

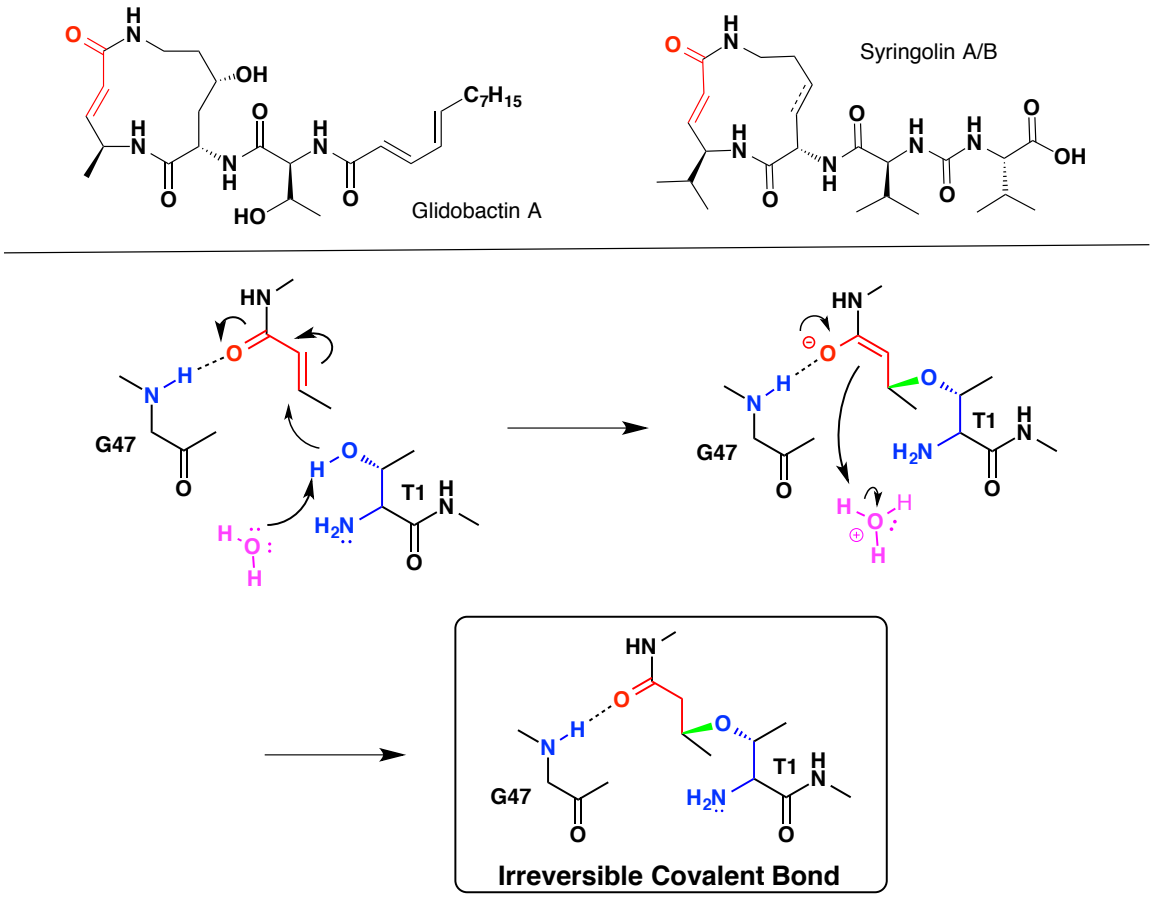

Figure 1.6: Syrbactin irreversible proteasome binding mechanism.[1]

Although the mode of inhibition is the same for each of the catalytic sites, the syrbactins have varying subunit activities (Table 1.1). *In vitro* studies reveal that SylA inhibits each of the catalytic sites, having the highest affinity for the β5 site with an inhibition constant (K_i) of 843 ± 8.4 nM.[1, 17] GlbA is a more potent inhibitor of the β5 site with a K_i of 49 ± 5.4 nM, but has less activity against the β2 site and does not inhibit the β1 site even at high concentrations.[17] SylB was determined to be the least potent inhibitor with a K_i of 7.78 ± 2.26 μM for the β5 site, and like GlbA it does not inhibit the β1

subunit even at high concentrations. Structural analysis of the crystal structures were used to provide insight into the structural features that result in the observed relative activities of the syrbactins (Figure 1.7). The only structural difference between SylA and SylB is the additional alkene in the macrolactam core, which results in the increased activity and potency of proteasome inhibition. The macrolactam also influences the catalytic subunit selectivity, as seen for the selective inhibition of the β1 site by SylA, and not by GlbA or SylB. The increased ring strain in the SylA macrolactam could result in a more reactive α,β-unsaturated amide system.[23] Additionally, the strained conformation of the SylA macrolactam core is speculated to react more favorably with the proteasome due to entropic factors to alleviate ring strain, in addition to forming an antiparallel β-sheet conformation that has more favorable interactions with the proteasome active site.[1] The crystal structure of GlbA bound to the yeast proteasome revealed a hydrophobic binding pocket near the catalytic site that is occupied by the lipophilic side chain of the molecule, providing additional stabilization that could result in the observed enhanced inhibition activity.[17] Additionally, GlbA has a smaller methyl substituent near the reactive site on the macrolactam, whereas SylA has an isopropyl group. The smaller alkyl group of GlbA can reduce possible steric interactions within the catalytic site and facilitate a more favorable reaction with the proteasome.

Syrbactin	Catalytic Site	Inhibition Constant (K_i)
GlbA	C-L (β1)	no inhibition
	T-L (β2)	2.0 ± 0.6 μM
	CT-L (β5)	49 ± 5.4 nM
SylA	C-L (β1)	minimal activity
	T-L (β2)	6.7 ± 0.7 μM
	CT-L (β5)	843 ± 8.4 nM
SylB	C-L (β1)	no inhibition
	T-L (β2)	107.8 ± 39.2 μM
	CT-L (β5)	7.78 ± 2.26 μM

Table 1.1: Syrbactin inhibition constants (K_i) for the caspase-like, trypsin-like, and chymotrypsin-like activities of the human 20S proteasome.[17]

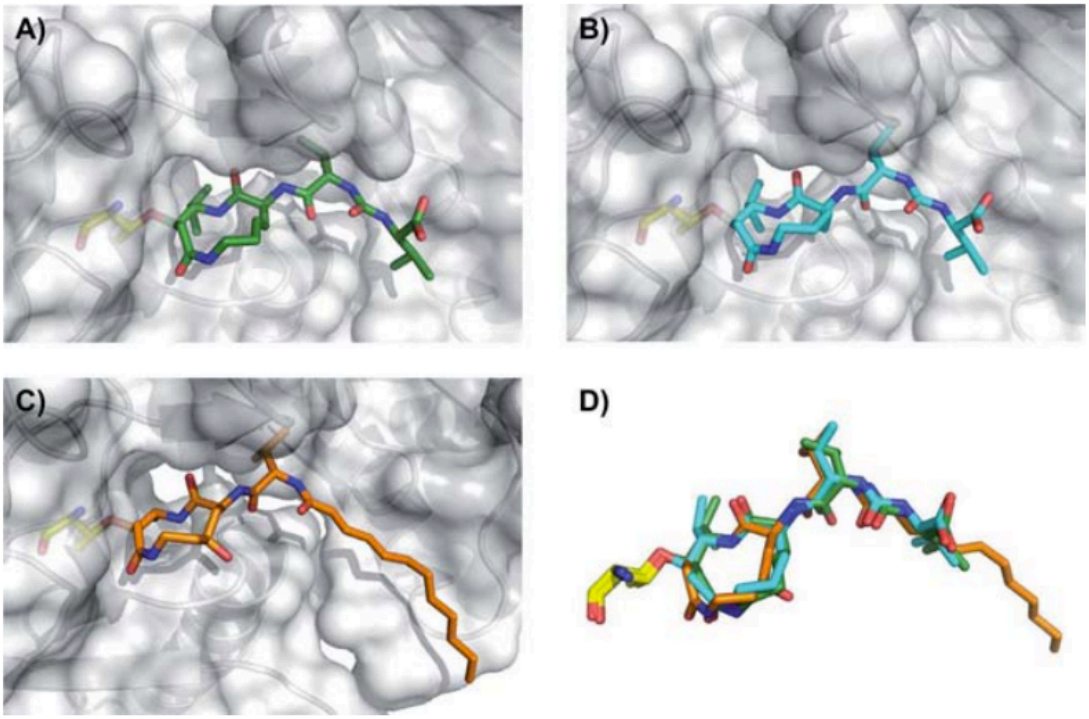

Figure 1.7: Structural analysis of the syrbactins bound to the β5 subunit of the yeast 20S proteasome complex: A) syringolin A, B) syringolin B, C) glidobactin A, and D) structural superimposition of syringolin A, syringolin B, and glidobactin A. (Image copied from Krahn, D; Ottamann, C; Kaiser, M. *Nat. Prod. Rep.,* **2011**, 28, 1854-1867.)[17]

As a result of their unique ability to irreversibly inhibit the proteasome by a novel mechanism, the biological activities and the structure-activity relationships of the syrbactins have been extensively studied. Total syntheses of the natural products have been developed, and the synthesis and evaluation of syrbactin derivatives have been achieved in the aim of creating syrbactin-based proteasome inhibitor therapeutics.

1.3 Proteasome Inhibitor Therapeutics

Bortezomib (Velcade®) is a small dipeptide boronic acid that was introduced in 2003 as the first U.S. Food and Drug Administration (FDA) approved proteasome inhibitor therapeutic for the treatment of relapsed and refractory multiple myeloma (MM) and mantle cell lymphoma (Figure 1.8).[24] This drug potently and reversibly inhibits the proteasome with the greatest effect against the β5 CT-L catalytic activity.[21] Despite the success of the drug as an anticancer agent, there have been several limitations to its use. Not all patients with MM respond to treatment with bortezomib, and many who do often develop resistance to the drug or ultimately relapse.[25] In addition, there are a broad range of adverse effects resulting from its use, including asthenic conditions, gastrointestinal distress, hypotension, neutropenia, peripheral neuropathy, and thrombocytopenia, which often lead to the discontinuation of treatment.[25-26]

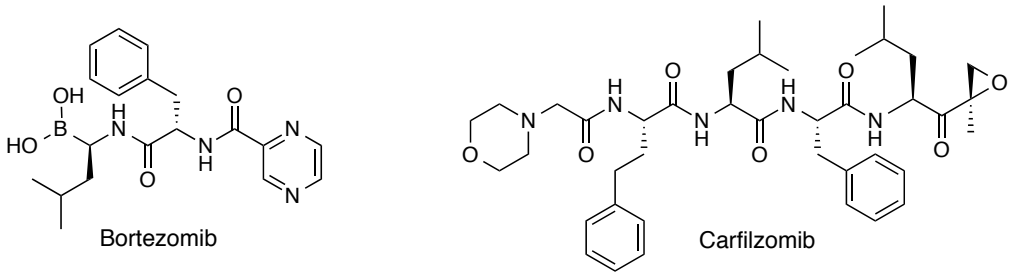

Figure 1.8: Structure of FDA approved proteasome inhibitor drugs bortezomib and carfilzomib.

Second generation proteasome inhibitors have been developed in the effort to improve efficacy and decrease toxicity. Carfilzomib (Kyprolis®) is an epoxyketone-based drug approved by the FDA in 2012, as the second proteasome inhibitor for the treatment of relapsed and refractory MM (Figure 1.8).[27] Carfilzomib potently and irreversibly inhibits the CT-L active site of the proteasome with more selectivity and with less off target reactivity than bortezomib, resulting in lower overall toxicity.[28] Additionally, this anticancer drug has been able to overcome bortezomib issues of drug resistance in MM cell lines.[27] Due to the success of the current proteasome inhibitor drugs bortezomib and carfilzomib, a variety of new proteasome inhibitor drugs are currently under clinical evaluation, including delanzomib, oprozomib, ixazomib, and marizomib (Figure 1.9).[29]

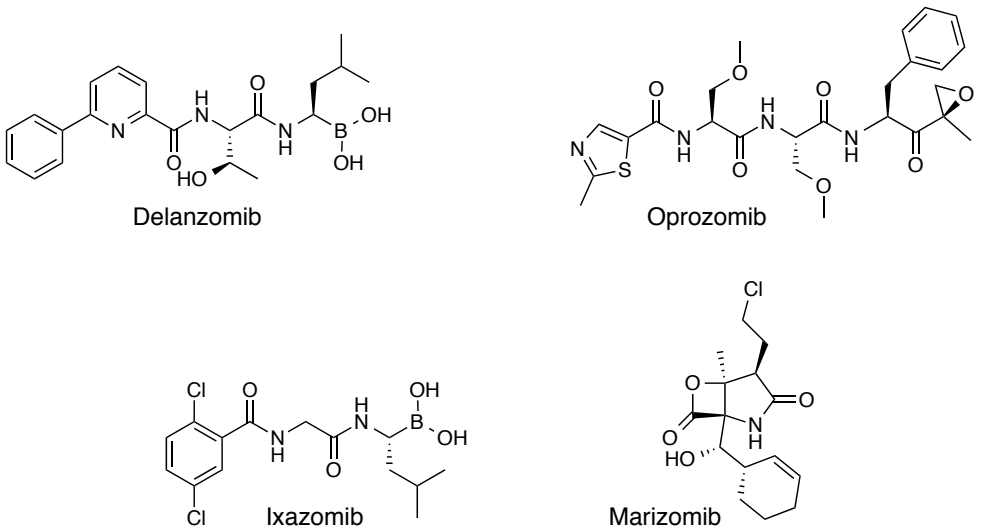

Figure 1.9: Structures of proteasome inhibitor drugs currently under clinical evaluation.

The development of proteasome inhibitors with improved potency and enhanced overall efficacy has been the focus of immense research. The syrbactins have a unique natural structure and are potent inhibitors of the proteasome. Since their isolation and discovery of their unique mode of proteasome inhibition, there has been a lot of research focused on the synthesis of the syrbactins to further evaluate their biological activities and therapeutic potential.

1.4 Total Syntheses of the Syrbactins

The success of the proteasome inhibitor cancer therapeutics bortezomib and carfilzomib and the unique ability of the syrbactins to potently inhibit the proteasome by a novel mechanism has sparked the interest into the syrbactins. In the past few decades

there have been various total syntheses of the syrbactins, GlbA, SylA, and SylB, to further evaluate their biological activities and explore their potential use as cancer therapeutics. The main challenge in the syntheses of the syrbactins has been the formation of the strained twelve membered macrolactam. A variety of approaches have been utilized in attempt to overcome the challenges of macrocyclization.

In 1988, Oka and coworkers completed the first successful chemical synthesis of glidobactin A. It was synthesized using fragments obtained from structure elucidation studies by the hydrolysis of the isolated natural product.[6] The linear cyclization precursor **1.1** was synthesized by conventional solution phase peptide coupling, followed by macrolactamization using N,N'-dicyclohexylcarbodiimide (DCC) and hydroxybenzotriazole (HOBt) in dimethylformamide to afford GlbA in 2.3% yield (Scheme 1.1).

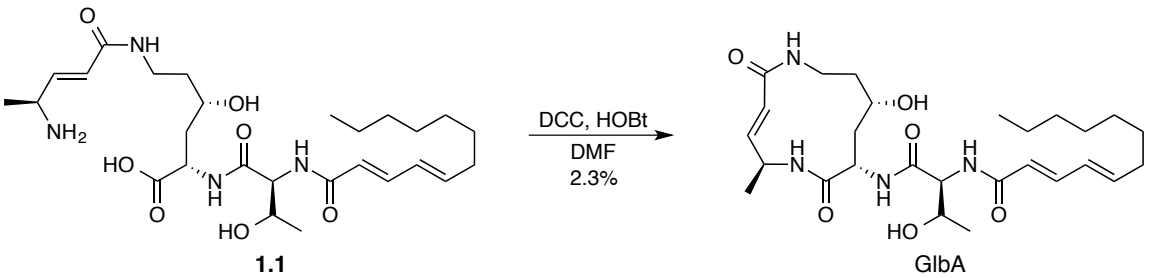

Scheme 1.1: Key step in the first synthesis of GlbA by Oka.

In 1991, Meng and Hesse attempted to synthesize the deoxy-glidobactin A core, glidobamine **1.3**.[30] This macrolactamization approach differed from Oka's synthesis by forming the macrolactam by peptide coupling at the least hindered position of the

molecule. However, formation of the macrolactam was unsuccessful using conventional coupling reagents including DCC, DEPC, and DPPA, even under high dilution conditions (Scheme 1.2).[30] Their lack of successful ring closure was attributed to the lack of the bulky substituents in the macrolactam precursor or intramolecular hydrogen bonding, which could assist in bringing the reactive ends closer together and facilitate the cyclization reaction.[30]

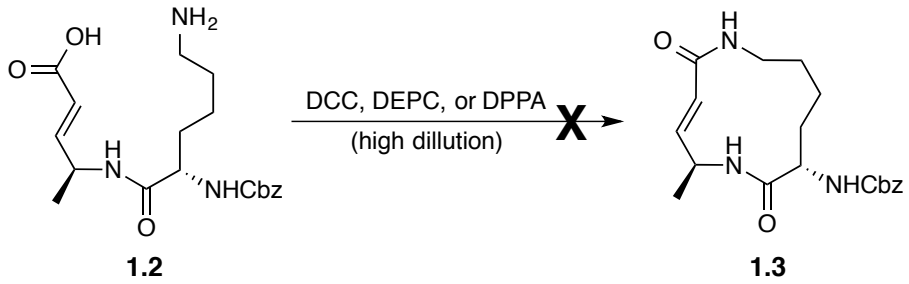

1.2 **1.3**

Scheme 1.2: Failed attempt of the synthesis of the deoxy-GlbA macrolactam by Meng and Hesse.

Meng and Hesse explored a different approach for the formation of the glidobamine macrolactam **1.3** by ring expansion utilizing a method of N-N bond cleavage.[30] The unfunctionalized GlbA core **1.5** was successfully synthesized by the reductive cleavage of the N-N bond of the bicyclic hydrazide **1.4** in 83% yield, demonstrating the utility of this method (Scheme 1.3). The glidobamine macrolactam **1.3** could be synthesized in a similar approach from the reaction of hydrazine **1.6** and lactone **1.7** to provide the bicyclic hydrazide **1.8**, followed by ring expansion by the reductive

cleavage of the N-N bond (Scheme 1.3). However, formation of the hydrazine **1.6** was not successful, and thus, the synthesis of glidobamine **1.3** was not accomplished.

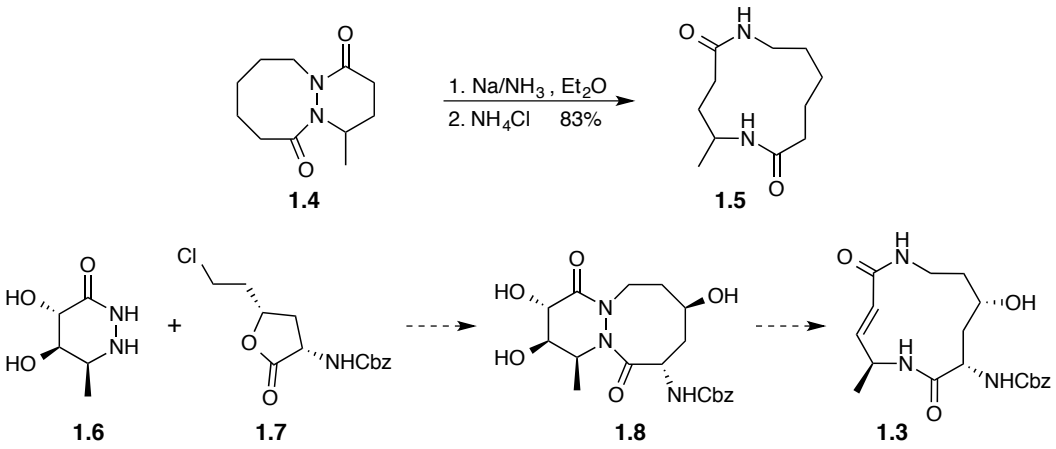

Scheme 1.3: Meng and Hesse's approach to synthesize glidobamine by reductive ring opening via N-N bond cleavage.

In 1992, Schmidt and coworkers designed a successful synthesis of GlbA following a similar macrolactamization approach to Oka's synthesis, by cyclization at the same position containing the α,β-unsaturated-γ-alanine residue.[31] This synthesis varied by the formation of the macrolactam prior to the attachment of the lipophilic side chain (Scheme 1.4). The cyclization strategy was performed over two steps, utilizing the corresponding pentafluorophenol activated ester of **1.9** under high dilution to provide macrolactam **1.10** in 20% yield. The side chain was attached by subsequent deprotection and coupling reactions to provide GlbA. This was the first total synthesis of GlbA.

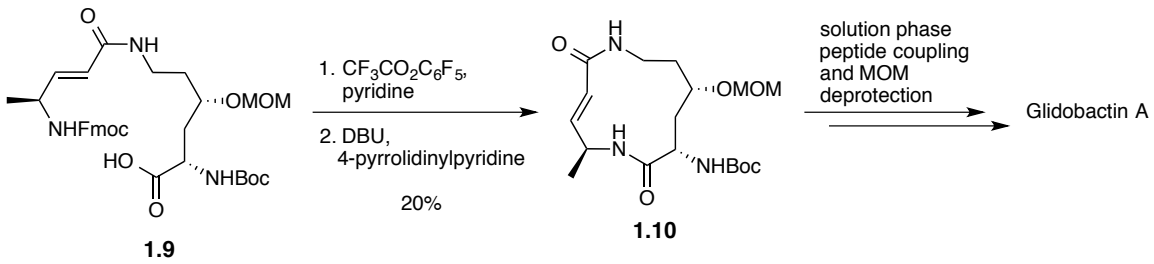

Scheme 1.4: Key steps of Schmidt's synthesis of GlbA.

In 2009, Kaiser and coworkers accomplished the total synthesis of SylA and SylB.[23] In their approach, the macrocyclization was performed with prior attachment of the lipophilic side chain. The overall strategy for the synthesis of SylB followed Oka's approach in the synthesis of GlbA by ring closure utilizing conventional peptide coupling on a preassembled linear precursor to afford the target product (Scheme 1.5). Macrolactamization of **1.12** was performed utilizing PyBOP and HOAt coupling reagents under high dilution to provide the cyclized product **1.13** in 30% yield. Subsequent deprotection of the side chain of **1.13** with piperidine provided SylB in 73% yield. SylB was successfully synthesized in 9 steps starting from N-Boc valine methyl ester **1.11** in 7.8% overall yield.

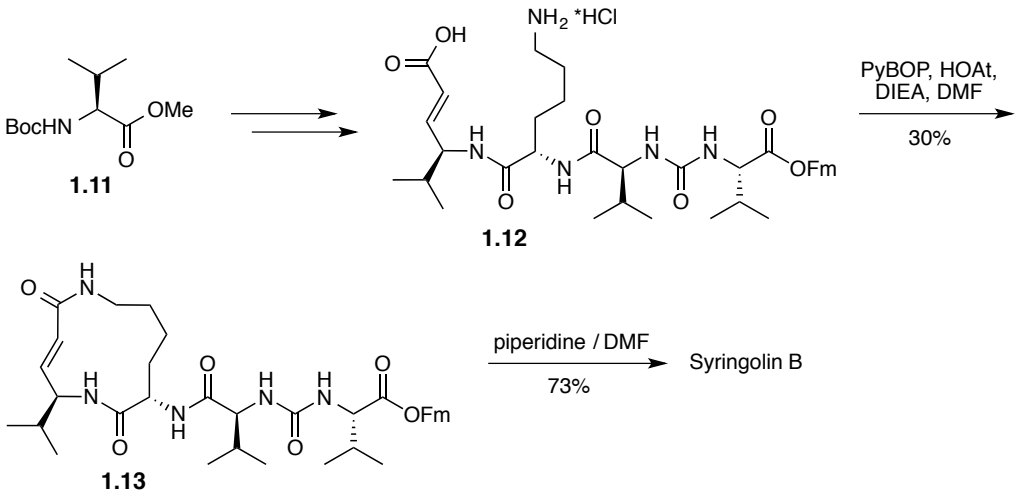

Scheme 1.5: Key steps in Kaiser's synthesis of SylB.

Kaiser and coworkers tried to implement a similar approach in their synthesis of SylA; however, the macrolactamization strategy did not result in the desired product formation. The synthesis of SylA was accomplished utilizing a ring-closing metathesis (RCM) based strategy (Scheme 1.6).[23] The RCM of **1.14** using Grubbs II catalyst provided the macrolactam precursor **1.15** in 49% yield. The side chain residue was then attached to **1.15** by peptide coupling of the preassembled side chain. The α,β-unsaturated amide was then generated by deprotection of the diol, formation of the corresponding thiocarbonate, and subsequent Corey-Winter elimination.[23] SylA was successfully synthesized in 16 steps starting from N-Boc valine methyl ester **1.11** in 9.1% overall yield. Additionally, Kaiser and coworkers provided an alternative synthesis for SylA applying the same RCM based strategy, by forming the α,β-unsaturated amide prior to the attachment of the side chain (Scheme 1.7).[32] This modified approach was used in the synthesis of a variety of SylA derivatives for the evaluation of their structure-activity relationship.

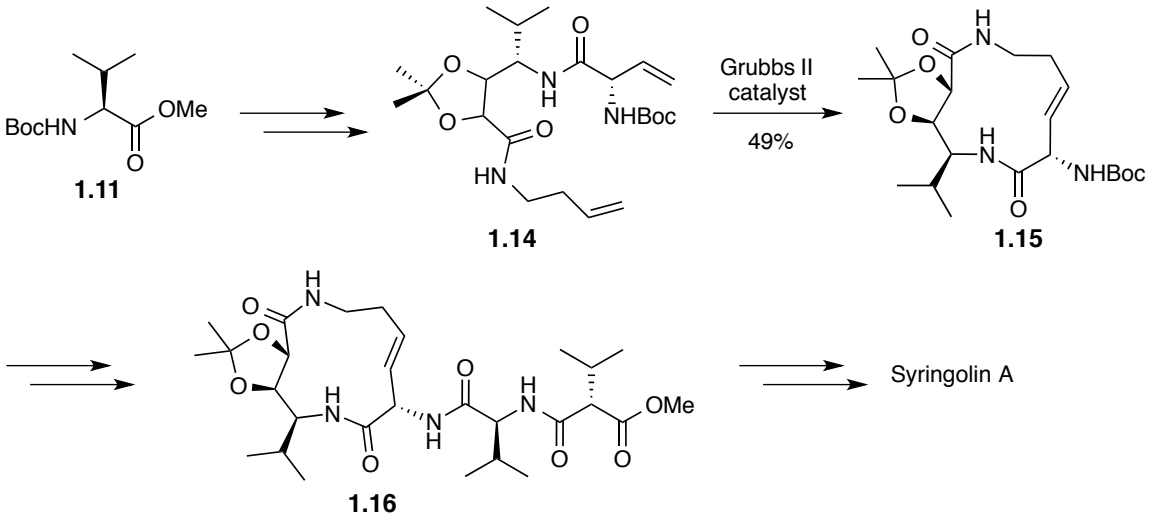

Scheme 1.6: Key steps in Kaiser's synthesis of SylA.

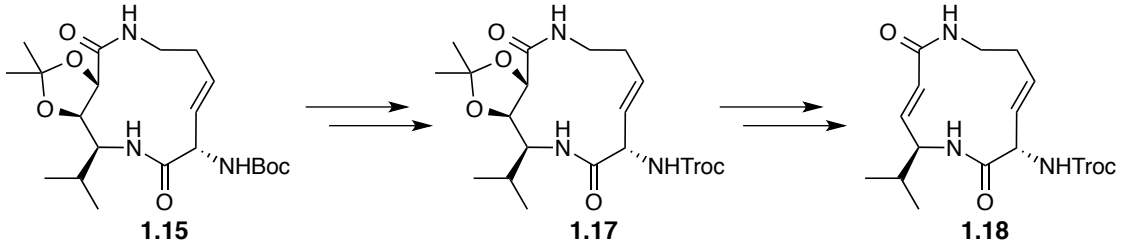

Scheme 1.7: Alternative route by Kaiser to synthesize SylA macrolactam.

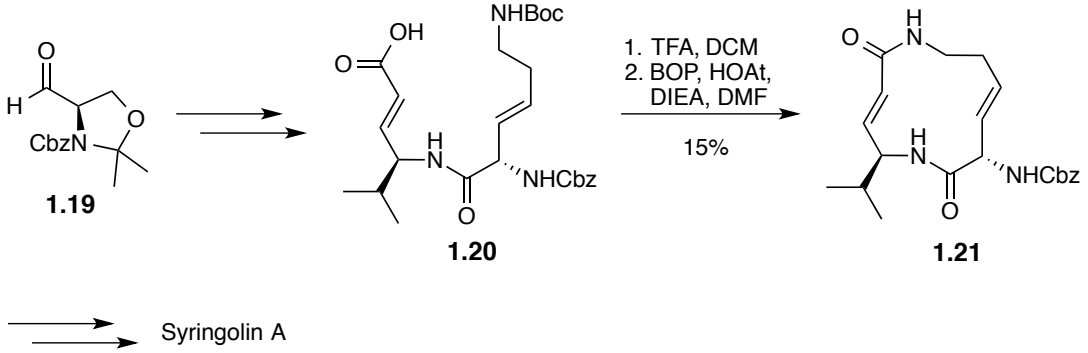

Scheme 1.8: Key steps in Dai and Stephenson's SylA synthesis.

In 2010, Dai and Stephenson[33] accomplished a total synthesis of SylA utilizing macrolactamization to form the macrolactam core, similar to the approach used by Kaiser[23] for the synthesis of SylB (Scheme 1.8). The ring closure reaction was performed by an intramolecular coupling reaction of **1.20** with BOP, HOAt and DIPEA to provide the SylA macrolactam **1.21** in 20% yield. Subsequent coupling of the preassembled side chain completed the synthesis. SylA was successfully synthesized in 13 steps starting from L-valine and Garner's aldehyde **1.19** in 3.5% overall yield.

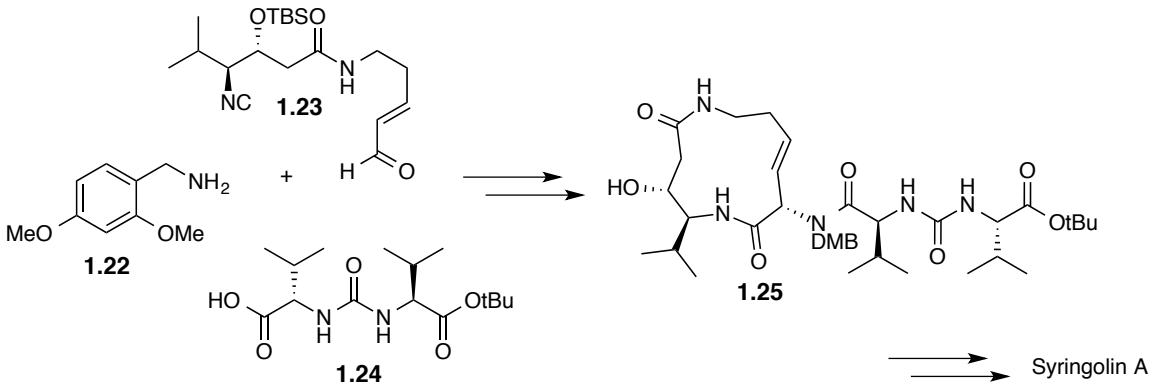

Scheme 1.9: Key steps in Ichikawa's SylA synthesis utilizing an Ugi reaction.

In 2012, Ichikawa and coworkers developed the total synthesis of SylA utilizing an intramolecular three-component Ugi reaction (Scheme 1.9).[34] The fragments **1.23** and **1.24** were preassembled and reacted together with 2,4-dimethyoxybenzylamine **1.22** to provide compound **1.25** in 32% yield. Subsequent formation of the α,β-unsaturated amide and deprotection provided SylA. A variety of derivatives have been synthesized utilizing this strategy to study the structure-activity relationship of SylA.

1.5 Pirrung Syringolin Synthesis

The Pirrung laboratory has reported the total syntheses of SylA and SylB by macrocyclization utilizing an intramolecular Horner-Wadsworth-Emmons (HWE) reaction.[35-36] The goal of the work was to provide an efficient and diversity oriented synthetic route based on lysine, which could be readily applied to the synthesis of syrbactin derivatives by the substitution of structurally variant reagents.

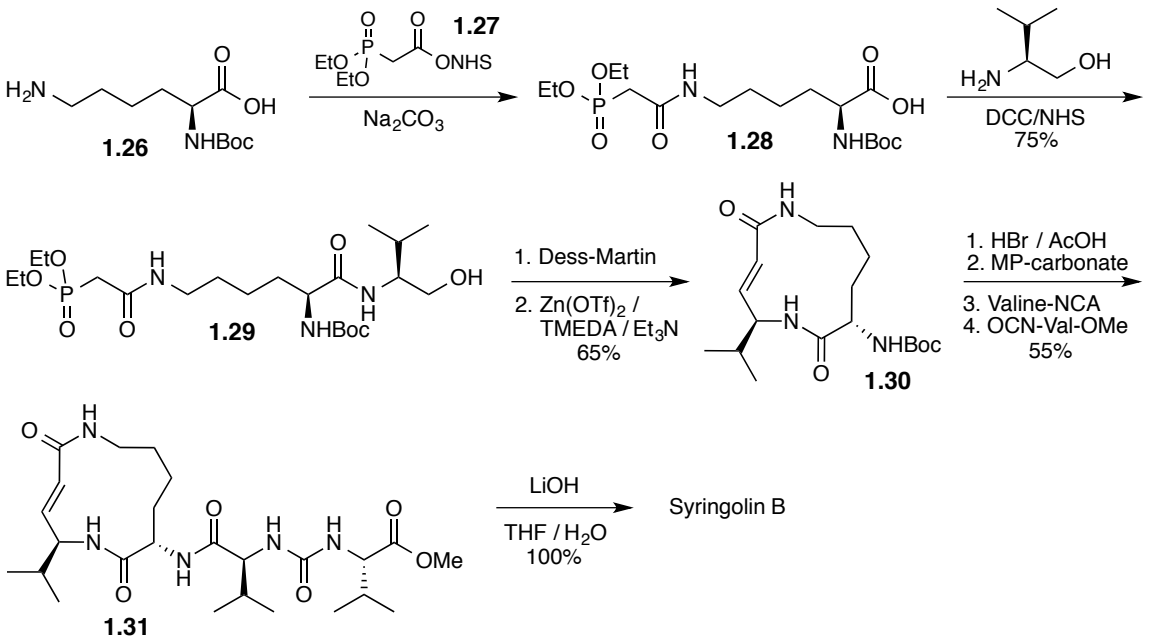

Scheme 1.10: Pirrung total synthesis of syringolin B.

The synthesis of SylB was initially examined (Scheme 1.10). The macrolactam precursor was synthesized in two steps starting from the commercially available α–amino protected lysine. *N*-Boc lysine **1.26** was reacted with the phosphono N-hydroxysuccinimide (NHS) activated ester **1.27** to provide the ε-

phosphonocarboxylate/α-Boc derivative **1.28**, which was then coupled with L-valinol using the conventional peptide coupling reagents DCC and NHS to provide **1.29** in 75% yield, over the two steps.

A variety of reaction conditions were examined for the transformation of **1.29** to the corresponding aldehyde and the subsequent HWE reaction to provide the macrolactam **1.30**. Oxidation using Dess-Martin periodinane (DMP) gave the best results providing the corresponding crude aldehyde in good yield and purity, which could be used directly in the next step.[36] In addition, a variety of conditions were examined to optimize the HWE macrocyclization reaction. The reaction of the aldehyde with sodium bis(trimethylsilyl)amide (NaHMDS) in THF resulted in decomposition and the Roush-Masamune LiCl/DBU conditions provided no reaction. The use of potassium carbonate and 18-crown-6 provided the desired macrolactam **1.30**, but excess crown ether made the purification of the product difficult.[36] The HWE reaction protocol implemented was a method developed by Schauer and Helquist for the synthesis of α,β-unsaturated amides with high selectivity for the *E* alkene configuration.[37] DMP oxidation of **1.29** followed by the application of the HWE reaction following the protocol by Schauer and Helquist utilizing zinc triflate, tetramethylethylenediamine (TMEDA), and triethylamine in high dilution in THF, provided the macrolactam **1.30** in 65% yield. The *N*-Boc group was removed using hydrobromic acid in acetic acid to give the amine salt in quantitative yield. Treatment with the ion-exchange base resin MP-carbonate provided the free amine, which was then acylated by reaction with valine *N*-carboxyanhydride (NCA), followed by reaction with valine methyl ester-isocyanate **1.32** to provide **1.31** in 55% yield over

the four steps. Saponification of **1.31** gave SylB in quantitative yield. In an alternative approach, coupling of the macrolactam **1.30** free amine with the preassembled side chain **1.33**, similar to the route applied by Kaiser in the synthesis of SylA[32], provided **1.31** in a less impressive 50% yield. The preassembled side chain was synthesized by the reaction of valine methyl ester-isocyanate **1.32** with valine *tert*-butyl ester, followed by subsequent NHS activation (Scheme 1.11). The initial route offers a more efficient method for the side chain preparation. Additionally, this route allows for the introduction of side chain modifications by direct substitutions of various amino acid NCA and isocyanate derivatives into the synthesis.

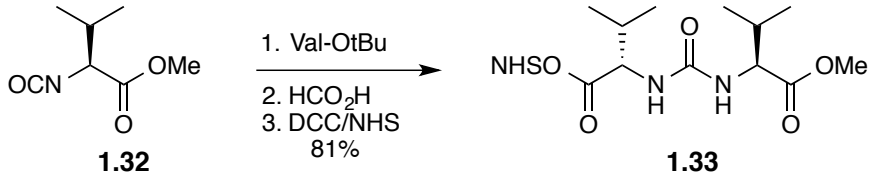

Scheme 1.11: Synthesis of syringolin side chain.

With the success of the macrocyclization with the HWE reaction and synthesis of SylB, the synthesis of SylA was then examined (Scheme 1.12).[35] The phosphono-alcohol macrolactam precursor **1.38** was synthesized over four steps starting from N-Cbz vinylgycine **1.34**. Peptide coupling of *N*-Cbz vinylglycine with valinol was performed using 1-isobutoxycarbonyl-2-isobutoxy-1,2-dihydroquinoline (IIDQ) to provide **1.35** in 83% yield. The cross-metathesis using Grubbs second-generation catalyst with **1.35** and 1-bromo-3-butene gave the product **1.36** exclusively as the *E* stereoisomer in 69% yield. Intermediate **1.36** was then reacted with sodium azide to introduce the nitrogen, which

was then converted to the corresponding amine utilizing the Staudinger reaction with triphenylphosphine.[35] Coupling of the phosphono NHS ester **1.27** provided the macrolactam precursor **1.38** in 72% yield. The oxidation of **1.38** with DMP followed by the HWE reaction conditions provided the macrolactam **1.39** in 81% yield. Although SylA has increased ring strain compared to SylB due to the second alkene in the macrolactam, the HWE cyclization reaction worked exceptionally well. The macrolactam **1.39** was then deprotected with hydrobromic acid, neutralized with MP-carbonate resin, and acylated to the side chain activated NHS ester **1.33** to afford the SylA methyl ester **1.40** in 73% yield. Deprotection of the methyl ester provided SylA in 92% yield.

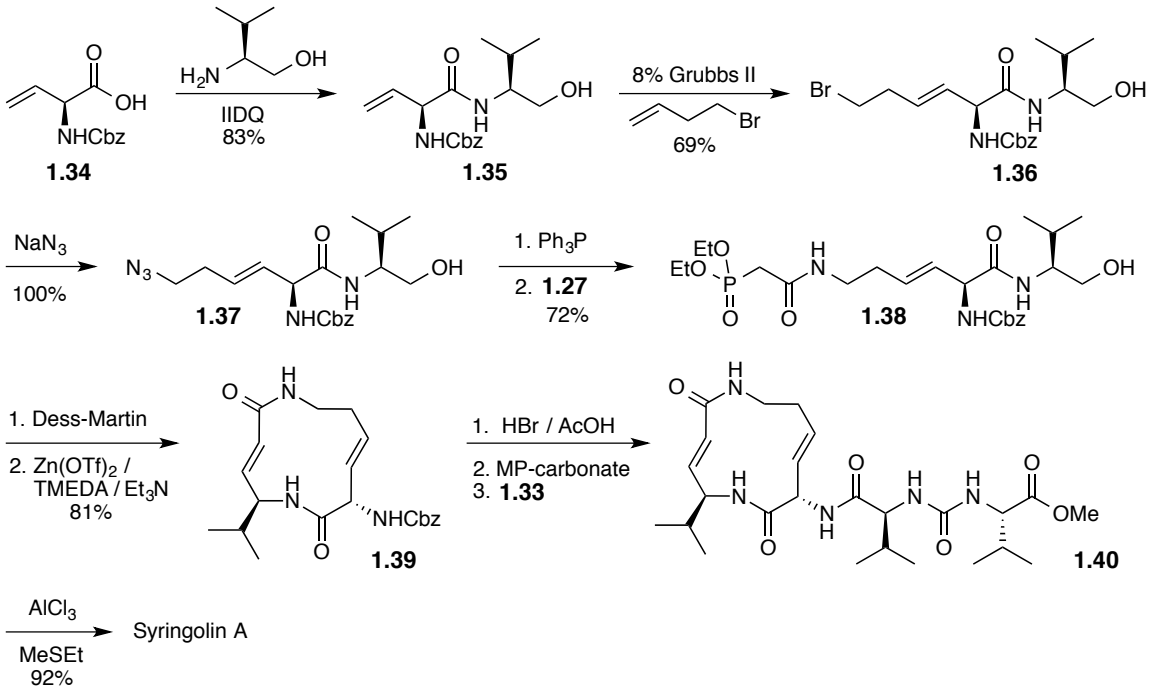

Scheme 1.12: Pirrung total synthesis of syringolin A.

The total syntheses of the syringolins were successful, providing SylA and SylB in significantly improved yields than previously reported syntheses of the natural products. SylB was synthesized in seven steps with 27% overall yield and SylA was synthesized in ten steps with 22% overall yield. These efficient and versatile syntheses have been used to create a variety of syrbactin derivatives for the evaluation of their proteasome inhibitory biological activities and structure-activity relationship.

1.6 Second-Generation Syrbactin Derivatives

With the successful syntheses of SylA and SylB and the desire to improve the syrbactin proteasome inhibition, a variety of syrbactin analogs have been created and their biological activities have been evaluated (Figure 1.10). In addition, the structure-activity relationship (SAR) of the syrbactins has been extensively studied.

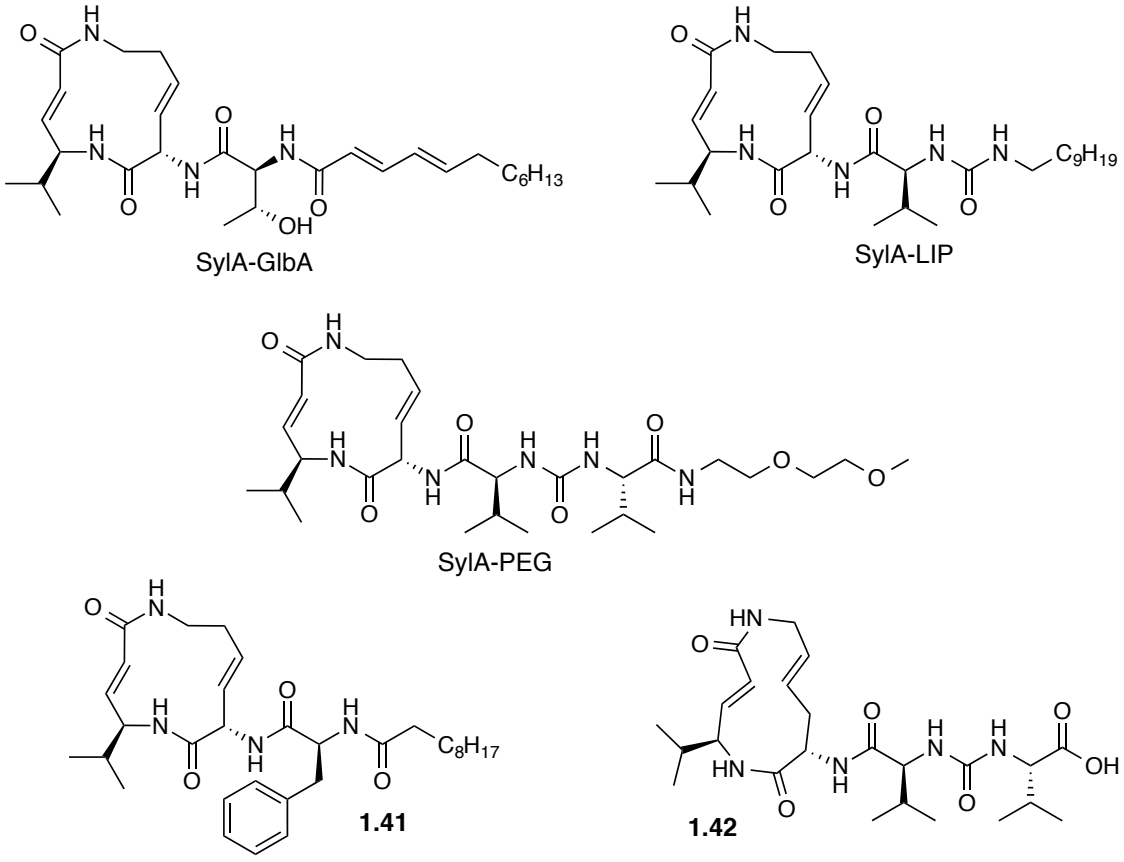

Figure 1.10: Structures of syrbactin derivatives by other groups: SylA-GlbA, SylA-LIP, SylA-PEG, SylA derivative **1.41** and iso-SylA derivative **1.42**.

To determine the effect of the side chain on proteasome inhibition, the Kaiser group synthesized the SylA-LIP syrbactin derivative containing the SylA macrolactam core and a lipophilic saturated alkyl chain similar to GlbA.[23] SylA-LIP was discovered to

be one of the most potent syrbactin derivatives with a K_i of 8.65 ± 1.33 nM for the CT-L activity, which is more than 100 times more potent than SylA, and more than 6 times more potent than GlbA (Table 1.2).[23] Similar to SylA, SylA-LIP inhibited each of the catalytic sites with the greatest affinity for the CT-L site, but had significantly improved activity.[23] The use of a lipophilic alkyl side chain significantly improved proteasome inhibition activity. The Kaiser group also demonstrated the beneficial effect of the lipophilic side chain by the synthesis and evaluation of the syrbactin hybrid SylA-GlbA, which contained the SylA macrolactam core and the GlbA side chain.[14, 24] SylA-GlbA also demonstrated a drastic improvement in activity for each of the catalytic sites, similar to SylA-LIP, having a K_i of 12.5 ± 1.5 nM for the CT-L activity (Table 1.2).[24] The effect of SylA-GlbA proteasome inhibition on cancer cell viability of various multiple myeloma, neuroblastoma, and ovarian cancer cells was evaluated. It was determined that SylA-GlbA was significantly more potent (100-2000 fold depending on the cancer line) than SylA, and was most potent against multiple myeloma cancer cell lines.[24]

Syrbactin Derivative	**Catalytic Site**	**Inhibition Constant (K_i)**
SylA-LIP[a]	C-L (β1)	943 ± 100 nM
	T-L (β2)	79.6 ± 29.3 nM
	CT-L (β5)	8.65 ± 1.33 nM
SylA-GlbA[b]	C-L (β1)	3.7± 1.2 μM
	T-L (β2)	136.9 ± 12.4 nM
	CT-L (β5)	12.5 ± 1.5 nM

[a] Values from reference 23. [b] Values from reference 24.

Table 1.2: Syrbactin derivative SylA-LIP and SylA-GlbA inhibition constants (K_i) for the caspase-like, trypsin-like, and chymotrypsin-like activities of the human 20S proteasome.

Additional *in vivo* studies were conducted to compare the proteasomal inhibition activity of the syrbactins SylA and GlbA with the derivatives SylA-LIP and SylA-PEG against neuroblastoma, multiple myeloma and ovarian cancer cell lines.[32, 38] Interestingly, GlbA was most effective at inhibiting the proliferation of cancer cells.[38] SylA-LIP was effective in all the cancer cell lines, with the greatest activity against MM cell lines, while SylA and SylA-PEG had minimal effect on cancer cell viability.[38] These results suggest that the hydrophobic side chains of GlbA and SylA-LIP allow these molecules to enter the cell allowing them to induce cytotoxicity by proteasome inhibition.[38] SylA and SylA-PEG cannot pass through the cell membrane as readily resulting in diminished effect on cancer cell viability.[38] Therefore, in the design of syrbactin based cancer therapeutics it is necessary to incorporate a lipophilic side chain to facilitate cell permeability in order to achieve proteasome inhibition and effectively induce cancer cell cytotoxicity.

Ichikawa and coworkers have focused their efforts in studying the structure-reactivity relationship of SylA developing the potent syrbactin inhibitor **1.41** (Figure 1.10).[34, 39-40] The incorporation of the phenylalanine-decanoyl side chain to the SylA macrolactam core enhanced the β5 proteasome activity compared to SylA providing a K_i of 0.14 nM.[39] A variety of alkyl and aryl residues were evaluated in the effort to introduce a larger substituent than the valine residue of the SylA side chain to better occupy a hydrophobic pocket identified in the crystal structure of SylA bound to the proteasome.[34] The introduction of the phenylalanine residue provided a large increase in inhibitory activity.[34] Additionally, a saturated alkyl chain was applied to the side chain in order to occupy the hydrophobic pocket of the proteasome active site and allow for ample

cell permeability.[34] The optimal length of the lipophilic alkyl side chain was evaluated, and it was determined that an alkyl chain between eight and eleven carbons best fit into the hydrophobic pocket of the proteasome active site, with the decanoyl alkyl chain giving the greatest increase in proteasome activity.[39]

Additionally, Ichikawa and coworkers synthesized the iso-SylA analog **1.42**, which potently inhibits the CT-L site with a K_i of 1.53 nM (Figure 1.10).[40] Initial SAR studies comparing iso-SylA and SylA demonstrated that the transposition of the double bond did not improve proteasome activity.[40] However, incorporation of the phenylalanine-decanoyl side chain residue in combination with the transposed olefin resulted in greater proteasome activity of the iso-SylA analog **1.42** compared to SylA.[40]

1.7 Syrbactin Derivatives Synthesized by the Pirrung Laboratory

The Pirrung laboratory has also focused on synthesizing syrbactin derivatives with improved biological activity (Figure 1.11). The syrbactin derivatives SylB-LIP,[36, 41] dGlbA-LIP,[36, 41] oxa-SylA-LIP,[36, 42] T-03,[41] and TIR-199[22] were each synthesized utilizing the versatile syntheses that were developed by the Pirrung laboratory for SylA and SylB,[35-36] by introducing simple reagent substitutions into the synthetic route. The side chain design incorporating a valine-dodecyl urea residue was influenced by the greater proteasome inhibition potency of GlbA among the natural syrbactins and the lipophilic side chain of the potent syrbactin proteasome inhibitor SylA-LIP[32] by Kaiser.

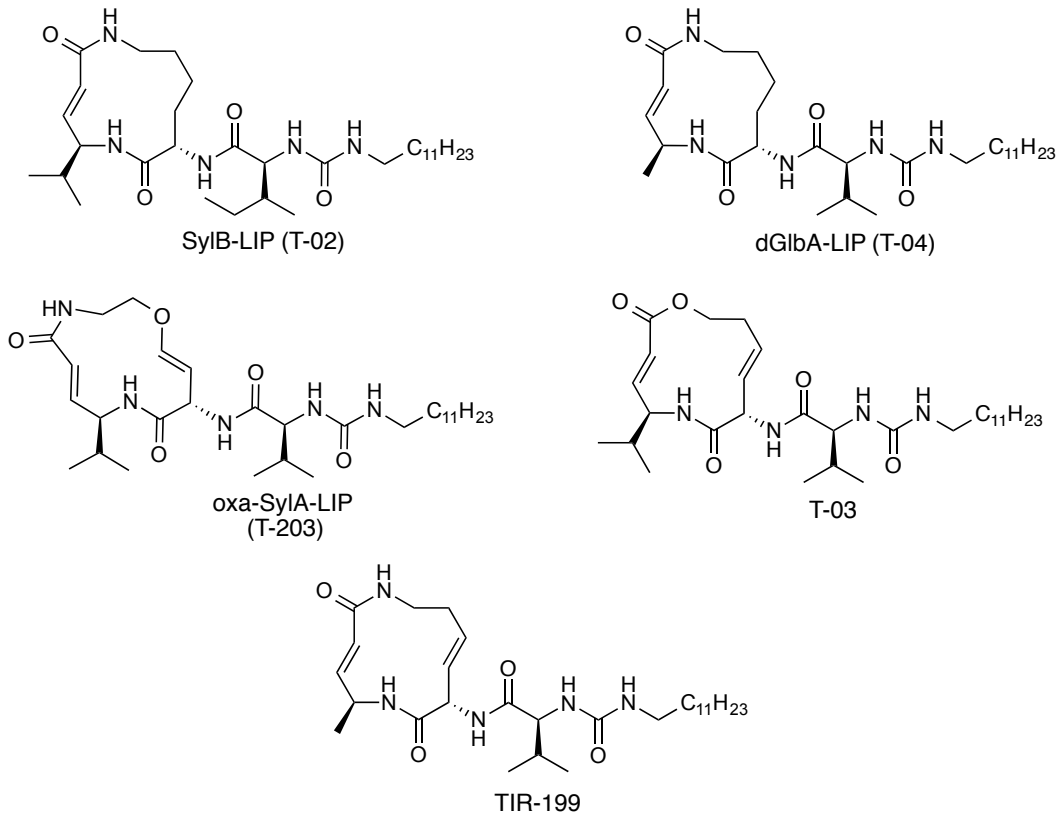

Figure 1.11: Structures of the syrbactin analogs synthesized by the Pirrung group: SylB-LIP, dGlbA-LIP, oxa-Syl-LIP, T-03, and TIR-199.

SylB-LIP was inspired by SylA-LIP, incorporating the SylB macrolactam core with a modified isoleucine-dodecyl alkyl urea side chain to evaluate the hydrophobic interactions of the proteasome-binding pocket. dGlbA-LIP has a deoxy-glidobactin A macrolactam core with a lipophilic side chain to evaluate the effect of reduced steric interactions at the site of the reaction with the proteasome. The oxa-SylA-LIP incorporates a vinyl ether into a 13-member macrolactam core with the valine-dodecyl alkyl urea side chain. Compound T-03 has an α,β-unsaturated macrolactone replacing the macrolactam of SylA in an attempt to improve nucleophilic addition reaction with the proteasome. Finally, TIR-199 incorporates a combination of features from SylA and

GlbA, having the more active SylA macrolactam core with the methyl substituent found in GlbA, and the incorporation of the valine-dodecyl urea side chain. Maintaining a degree of structural similarity in these derivatives allowed the SAR to be readily discerned.

The results of the biological activity evaluation of these syrbactin derivatives offer a better understanding of the structural features that affect the syrbactin biological activity. These analogs were each evaluated for their proteasome inhibition activity against the proteasome catalytic subunits and the effect on the proliferation of multiple myeloma (MM) and neuroblastoma (NB) cell lines.[22, 36, 41-42] Each of these analogs had a significant improvement in proteasome inhibition activity compared to SylA (IC_{50} greater than 20 μM) and comparable to the potency of SylA-LIP (IC_{50} of 3.2 μM, NB: SK-N-SH).[22, 36] SylB-LIP and dGlbA-LIP had IC_{50} values of about 1 μM and oxa-SylA-LIP had an IC_{50} value of 0.4 μM in NB cell lines SK-N-AS and MYCN-2,[36] while T-03 was intrinsically less potent.[41] However, TIR-199 was discovered to be one of the most potent SylA derived syrbactin derivatives to date, having an IC_{50} value of less than 0.05 μM for MM1.RL multiple myeloma cell line and about 0.1 μM for MYCN-2 NB cell line.[22] These IC50 values reveal a greater than 250-fold increase in potency compared to SylA (39 μM in MM1.RL cells).[22]

The evaluation of the SAR comparing these analogs reveal that the combination of the more reactive SylA macrolactam with the less hindered methyl substituent, and the lipophilic side chain residue drastically improve syrbactin biological activity as demonstrated with the improvement of the IC_{50} values of TIR-199 in comparison to the

other syrbactin derivatives. Switching from a SylA macrolactam to the macrolactone in T-03 did not improve the biological activity. However, introduction of the larger SylA-like macrolactam with the vinyl ether in oxa-SylA-LIP drastically improved the activity, however TIR-199 maintaining the natural macrolactam core was more potent. These analogs each inhibit the proteasome in a dose dependent manner with the greatest activity for the chymotrypsin-like (β5) catalytic subunits, reduced activity for the trypsin-like (β2) subunit, and minimal activity toward the caspase-like (β1) subunit.[22, 41] Computational modeling of TIR-199 with the chymotrypsin-like catalytic site revealed that the valine-dodecyl urea side chain was crucial for the stability of TIR-199 in the binding site by interaction with a nearby hydrophobic pocket in the proteasome catalytic site, resulting in the improved activity.[22]

As a result of the enhanced potency, TIR-199 has been extensively studied in numerous *in vivo* and *in vitro* proteasome activity and cytotoxicity assays, and was also evaluated by the National Cancer Institute (NCI) to determine the effects on tumor cell growth by conducting a NCI-60 human tumor line screen.[22] The NCI-60 screen revealed that TIR-199 induces dose-dependent cell death in a wide range of tumor cell types including leukemia, breast, CNS, colon, kidney, lung, ovarian, skin and prostate cancers.[22] Due to the success of TIR-199 in these assays demonstrating potent proteasome inhibition, TIR-199 was evaluated in preclinical screenings and was the first syrbactin proteasome inhibitor to be evaluated in animal studies.[22] Thus, TIR-199 is a promising anticancer agent with broad application potential against various tumor cell types.[22]

1.8 Conclusion

Much progress in the development and synthesis of syrbactin based proteasome inhibitors for the use as next-generation cancer therapeutics has occurred. The syrbactin derivative TIR-199, developed in the Pirrung laboratory, has demonstrated the most potential for the use as an anticancer therapeutic due to potent proteasome inhibition causing cytotoxicity in various tumor lines. However, poor aqueous solubility of TIR-199 limits it's therapeutic potential. Further research into the development of novel syrbactin based proteasome inhibitors for therapeutic value is driven by the desire to develop more potent syrbactin derivatives with improved aqueous solubility and drug uptake by a practical and modular synthesis.

Chapter 2: Syrbactin Results and Discussion

2.1 Introduction

The clinical success of proteasome inhibitors bortezomib and carfilzomib as cancer therapeutics has sparked the interest into the syrbactin natural products. In recent years, there has been a substantial amount of progress in the study of the biological activity and structure activity relationship (SAR) of the syrbactin proteasome inhibition. The creation of syrbactin analogs to explore reactivity and improve the potency of these compounds for use as potential proteasome based therapeutics has been the focus of many researchers. Several syntheses of the natural products have been reported over the years, and many analogs have been prepared and evaluated (Chapter 1). However, adequate aqueous solubility is a persistent issue and further research is needed to improve the drug uptake, as well as overall efficacy of syrbactin based proteasome inhibition. Previous work conducted by the Pirrung laboratory exploring the SAR of syrbactin analogs[22, 35-36, 41] has inspired the investigation into the synthesis of a unique set of syrbactin derivatives in efforts to create next-generation proteasome inhibitors with increased solubility, improved potency and inhibitory properties.

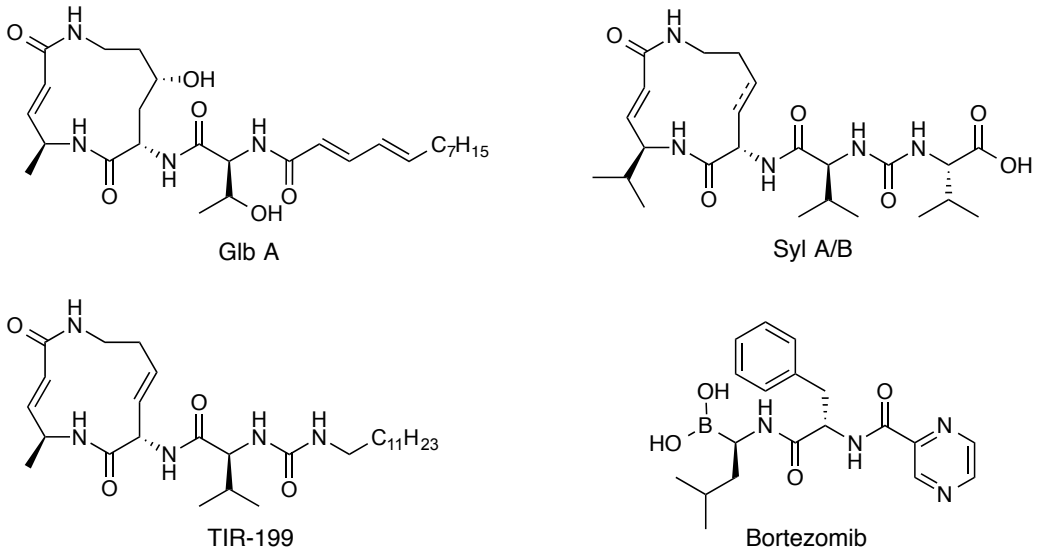

Figure 2.1: Structures of glidobactin A, syringolins A and B, TIR-199, and bortezomib (Velcade®).

As previously described, the Pirrung laboratory has developed versatile total syntheses of SylA and SylB.[35-36] A variety of syrbactin analogs have been synthesized utilizing the outlined method, including the potent inhibitor TIR-199, which was the first syrbactin to demonstrate activity against tumor cell lines in animal studies.[22] TIR-199 has been evaluated in preclinical assays, however low aqueous solubility has impeded further studies of bioactivity and cellular transport. The goal of this project is to provide potent TIR-199 inspired analogs by a synthetically simplified route with the incorporation of modifications to enhance solubility and improve bioavailability. The incorporation of hydrophilic functionalities to the syrbactin structure will decrease the overall lipophilicity of the molecules, which is a method used to improve drug solubility.[43] The challenge will be to increase the solubility while maintaining a degree of hydrophobicity in the side

chain necessary to fill the hydrophobic binding pocket of the proteasome without compromising bioactivity.

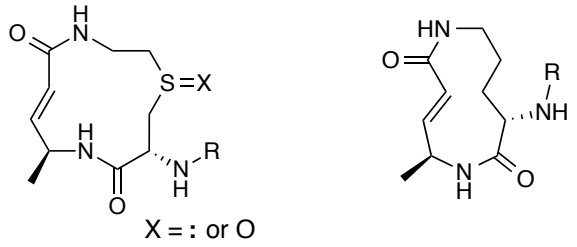

Figure 2.2: Macrolactam structures of the proposed analogs.

The design of the syrbactins synthesized in this work were based on the concise and versatile synthesis of syringolin B developed by the Pirrung laboratory,[36] and were inspired by the potent syrbactin analog TIR-199. The key structural features of TIR-199 include the methyl group substituent of the macrolactam and the long saturated side chain. These analogs will incorporate two sets of unique macrolactam cores (Figure 2.2). Introduction of the sulfur into the macrolactam will provide a synthetic handle that can be used to enhance solubility by oxidation to the corresponding sulfoxide. Additionally, the sulfoxide at this position of the macrolactam resembles the hydroxyl substituent of GlbA. The other set of analogs will contain a smaller, eleven-membered macrolactam core to mimic the ring strain induced by the secondary alkene of TIR-199, while providing a simplified synthetic route.

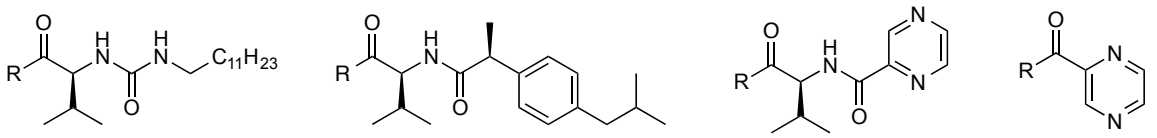

Figure 2.3: Structures of the proposed syrbactin side chain residues.

A diverse array of side chains will be examined in the synthesis of the syrbactin analogs in this work (Figure 2.3). Most of the side chains will maintain the valine residue attachment to enable the SAR of the varying side chain residues to be evaluated. The side chain residues include a long saturated alkyl chain, ibuprofen, and the pyrazine residue found in bortezomib. The saturated alkyl urea side chain is similar to that of GlbA and is similar to the side chain that was originally applied to syrbactin analogs by Kaiser[32] to provide a simplified and more easily accessible hydrophobic side chain. The valine-dodecyl urea alkyl side chain has been incorporated in a variety of syrbactin analogs, like TIR-199, to enable the SAR of syrbactin analog macrolactam cores to be easily distinguished. Maintaining this functionality will allow for a similar evaluation of the SAR of the macrolactam core of the syrbactin analogs in this work. The valine-ibuprofen and valine-pyrazinamide residues will be used to reduce the lipophilicity of the compounds and improve solubility. The ibuprofen will provide a hydrophobic residue with branching, unsaturation, and chirality, and the pyrazine will provide a more polar/hydrophilic character. Alkyl branching and chirality can reduce the size/volume of the compound making solvation easier and can also reduce planarity of the compound eliminating negative intermolecular interactions to improve solubility.[44-46] Introduction of a polar side chain residue should increase the overall hydrophilicity of the compound and

improve solubility.[44] Directly attaching the pyrazinamide residue to the macrolactam core will result in analogs inspired by the structure of bortezomib. This connection provides the same spatial relationship between the electrophilic carbon of the unsaturated amide that binds to the proteasome and the pyrazine residue, similar to that seen in bortezomib (Figure 2.4).

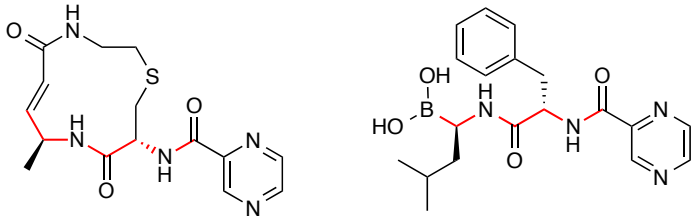

Figure 2.4: Structure of bortezomib-inspired thiasyrbactin analog.

In this work, a novel set of syrbactin derivatives will be synthesized and evaluated. Computational analysis of the syrbactin derivatives synthesized will be conducted to compare the physiochemical properties that affect drug-likeness including hydrophobicity and solubility. The biological activity will be evaluated by *in vitro* proteasome activity assays and cell viability assays. Variation of the macrolactam core and side chain functionalities in these analogs, while maintaining the general structural features of TIR-199, will enable the SAR to be readily evaluated.

2.2 Synthesis of Thiasyrbactin Analogs

The design of the thiol ether-based syrbactin analogs allows for the concise synthesis based on the previously reported synthesis of syringolin B by the Pirrung laboratory,[35-36] which can be applied to any lysine analog. The commercially available lysine analog L-4-thialysine hydrochloride **2.1** was utilized in this synthesis (Scheme 2.1). Initially, **2.1** was coupled with the NHS activated phosphono ester **2.2** followed by *N*-Boc protection to afford the crude ε-phosphonocarboxylate/α-Boc derivative **2.3** as a mixture. Due to the high polarity of the compound, it was used crude in the next step. We anticipated that the primary amine would be more reactive than the secondary amine, resulting in the desired functionalized product. However, the coupling of **2.3** with L-alaninol using DCC and NHS resulted in a mixture of products including the doubly *N*-Boc protected dipeptide **2.5** and the α-phosphonoacetatamide/ε-Boc product **2.6** along with the desired macrolactam precursor **2.4** in low yield. Therefore an alternative approach was explored to optimize the yield of the desired product.

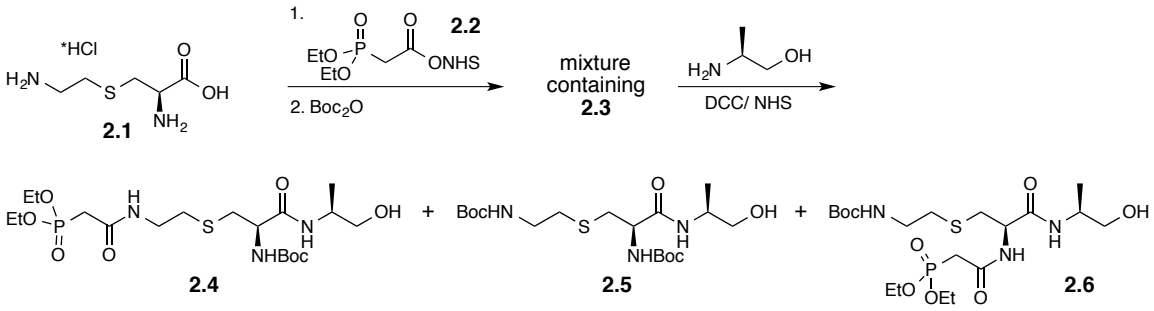

Scheme 2.1: Initial attempt at the synthesis of the macrolactam precursor **2.4**.

To improve the yield of the functionalized thialysine product **2.3**, 9-borabicyclo[3.3.1]nonane (9-BBN) was explored as a transient protecting group for the α-amine, to allow the selective acylation of **2.2** with the primary amine side chain of thialysine. Sánchez and coworkers previously developed a method using 9-BBN as a transient protecting group for the chemoselective functionalization of amino acid side chains of several amino acids including tyrosine, aspartic acid, glutamic acid, ornithine, and lysine.[47] The method involves the complexation of 9-BBN-H with the corresponding amino acid, followed by side chain manipulation, and subsequent 9-BBN cleavage (Figure 2.5).

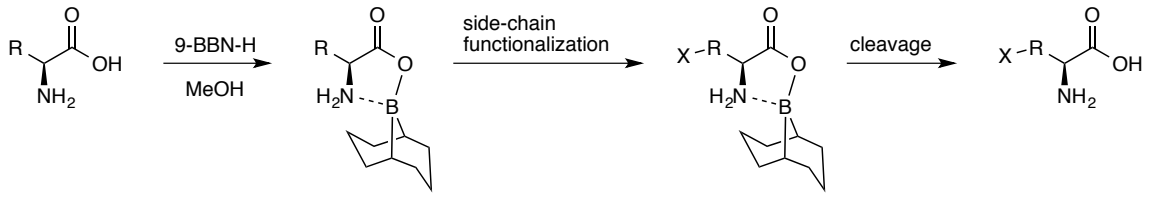

Figure 2.5: Use of transient 9-BBN protection for chemoselective amino acid side chain functionalization.

With the success of previously reported examples of selective lysine functionalization,[47] this method was applied to thialysine **2.1** (Scheme 2.2). Thialysine **2.1** was protected by treatment with 9-BBN to afford the complexed product **2.7**. Subsequent reaction with **2.2** followed by aqueous work up to cleave the 9-BBN protecting group resulted in **2.8** in 55% yield over the two steps. *N*-Boc protection by treatment with Boc anhydride and triethylamine afforded compound **2.3** in 52% yield.

The protocol utilizing the transient 9-BBN protection added additional steps to the synthesis and resulted in a diminished overall yield.

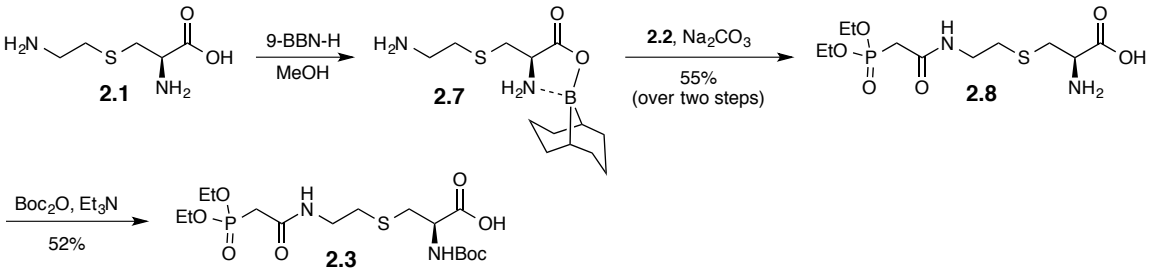

Scheme 2.2: Synthesis of ε-phosphonoacetatamide/α-Boc compound **2.3** utilizing 9-BBN transient α-amino protection.

Since the method using the 9-BBN transient protection to selectively functionalize **2.1** was not very effective, the initial synthetic pathway was reexamined and optimized to improve the product yield (Scheme 2.3). The reaction of **2.1** with the phosphonate NHS ester **2.2** was discovered to be very sluggish. Allowing this step to proceed longer before the addition of the Boc anhydride resulted in drastically improved yields of the desired compound **2.3** to 83%. Coupling of L-alaninol with DCC and NHS afforded the precursor **2.4** in 68% yield. Small quantities of the doubly Boc-protected **2.5** and α-phosphonoacetatamide/ε-Boc **2.6** compounds were also formed, but in reduced amounts.

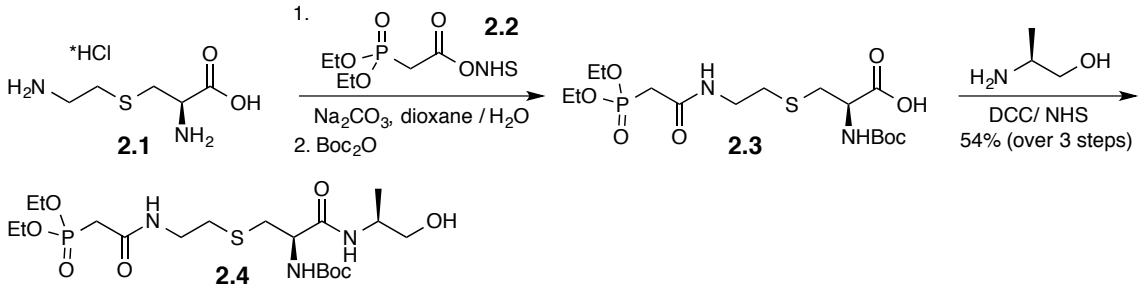

Scheme 2.3: Optimized synthesis of the macrolactam precursor **2.4**.

The synthesis of the macrolactam precursor **2.4** was also explored by peptide ligation with mildly activated esters and β-hydroxylamines developed previously in the Pirrung laboratory (Scheme 2.4).[48] First, **2.3** was converted to the mildly activated cyanomethyl ester **2.9** by the alkylation reaction with chloro- or bromoacetonitrile and base, followed by subsequent ligation with L-alaninol to afford **2.4** in 40% yield. Although this method provides a racemization free route to the desired product, diminished overall yields deemed this route unfavorable.

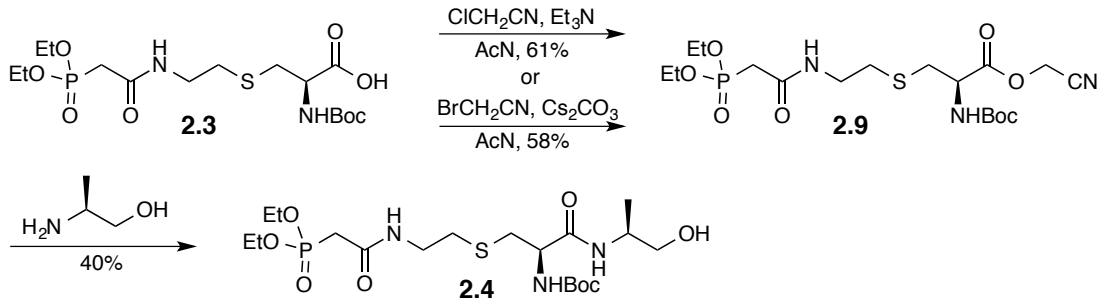

Scheme 2.4: Alternative synthetic route of the macrolactam precursor **2.4** by alaninol ligation.

With the precursor **2.4** in hand, the next step was the synthesis of the thia-macrolactam core (Scheme 2.5). Dess-Martin periodinane oxidation of **2.4** gave the aldehyde intermediate that was used crude in the next step to minimize the possibility of enolization. Next, the Horner-Wadsworth-Emmons (HWE) reaction was performed following the protocol developed by Schauer and Helquist[37] by reaction promoted by triethylamine, zinc triflate, and tetramethylethylenediamine (TMEDA) in high dilution in THF, to form the thia-macrolactam **2.10** in 58% yield. This method of cyclization utilizing the HWE reaction has been successfully implemented in previous syrbactin syntheses by the Pirrung laboratory.[22, 35-36]

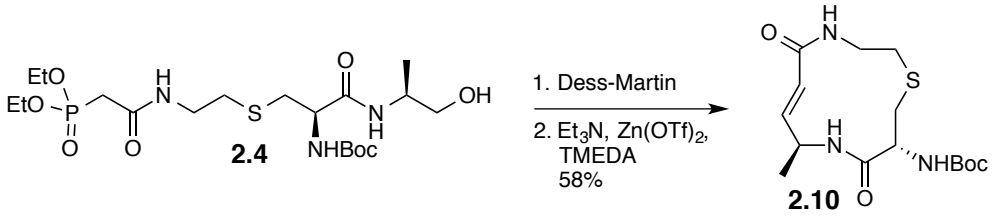

Scheme 2.5: Synthesis of the thia-macrolactam core **2.10**.

Side chain functionalization of the thia-macrolactam **2.10** was then pursued. The *N*-Boc group was removed from **2.10** by treatment with a solution of hydrochloric acid in ethyl acetate, and the resulting hydrochloride salt was neutralized with MP-carbonate base resin. The free amine was then coupled with the NHS activated ester of Fmoc-valine to afford compound **2.11** in 58% yield. Removal of the *N*-Fmoc group followed by reaction with dodecyl isocyanate to install the urea side chain provided the first analog

2.12 in 75% yield. Oxidation of **2.12** with sodium periodate provided the sulfoxide **2.13** as a single stereoisomer in 60% yield.

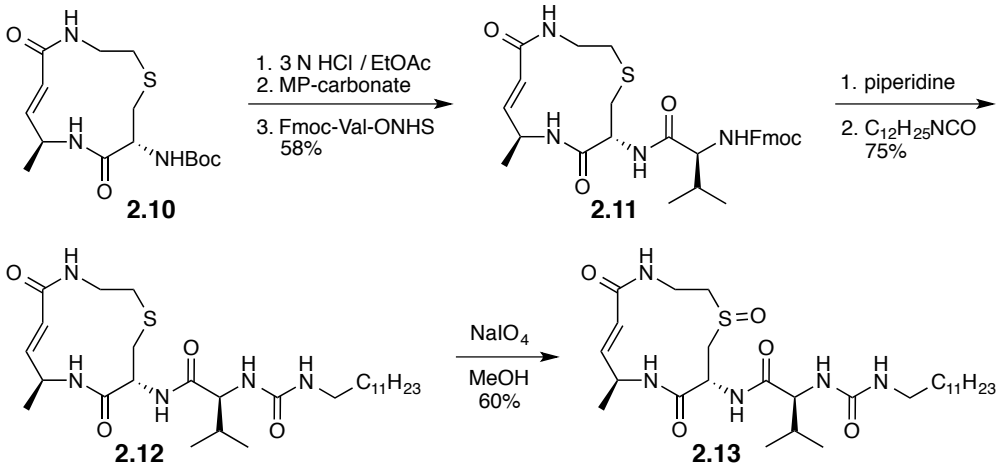

Scheme 2.6: Synthesis of the TIR-199/GlbA analogs **2.12** and **2.13**.

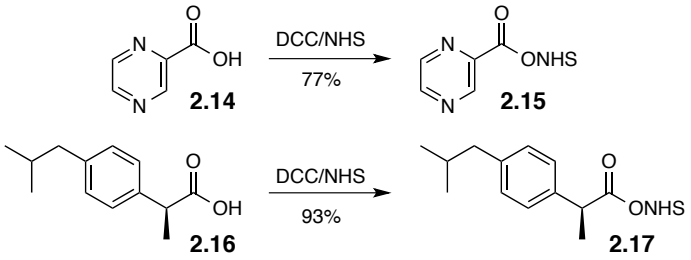

Scheme 2.7: Synthesis of the side chain NHS active esters **2.15** and **2.17**.

The side chains of the other target analogs were installed using NHS activated esters of pyrazine carboxylic acid **2.15** and (S)-(+)-ibuprofen **2.17**, which were prepared by conventional DCC and NHS coupling, in 77% and 93% yields respectively (Scheme 2.7). The valine substituted macrolactam **2.11** was deprotected with piperidine and coupled with each of the activated esters (Scheme 2.8). Coupling with the pyrazine NHS

ester **2.15** provided **2.18** in 42% yield. Similarly, reaction with ibuprofen NHS ester **2.17** gave **2.19** in 73% yield.

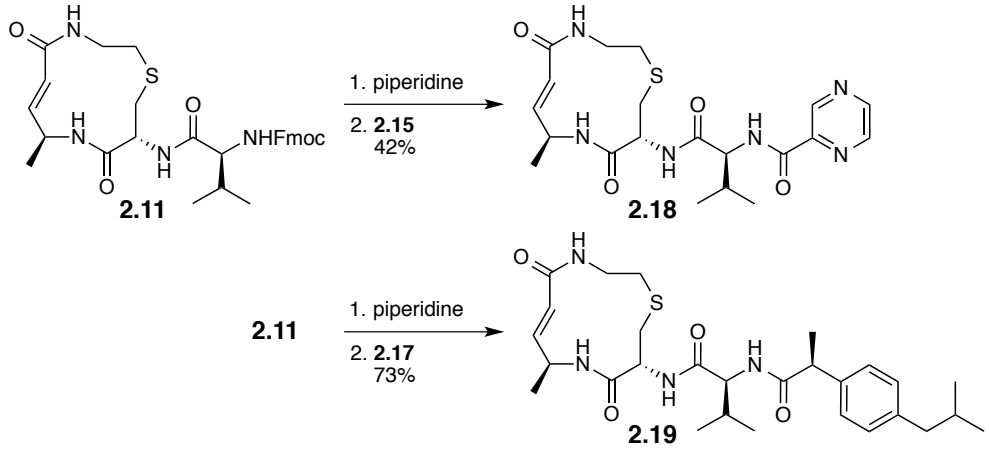

Scheme 2.8: Synthesis of TIR-199/GlbA analogs **2.18** and **2.19**.

The bortezomib inspired analogs were synthesized in a similar manner (Scheme 2.9). The thia-macrolactam **2.10** was deprotected with acid and converted to the free amine with base resin, as previously described. It was then coupled with pyrazine NHS ester **2.15** to provide analog **2.20** in 48% yield. Oxidation of **2.20** with sodium periodate gave the corresponding sulfoxide **2.21** as a single stereoisomer in 98% yield.

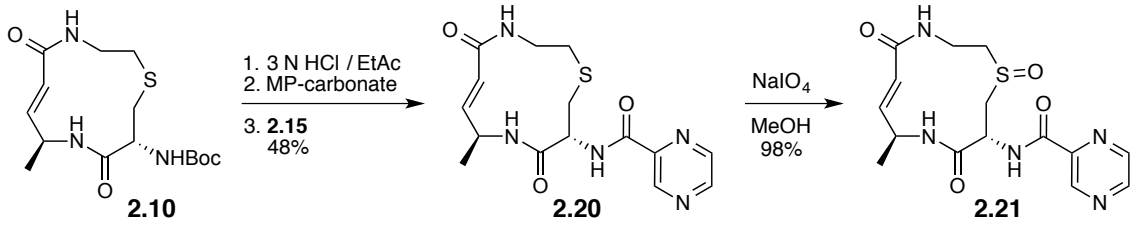

Scheme 2.9: Synthesis of bortezomib and GlbA inspired analogs **2.20** and **2.21**.

Additionally, analogs **2.20** and **2.21** containing the pyrazine carboxamide side chain were also synthesized by reaction with 2,3-pyrazinedicarboxylic anhydride (PCA). Klumpp and coworkers demonstrated that various pyrazine carboxamides could be prepared by reaction of amines with PCA in good yields.[49] Reaction of PCA with valine ethyl ester gave the corresponding coupled product in near quantitative yield,[49] supporting the application of this method for the synthesis of the syrbactin analogs. The mechanism proposed for this reaction by Klumpp and coworkers is shown in Figure 2.6, via ring opening of the anhydride by reaction with an amine, decarboxylation to afford the corresponding *N*-heterocyclic carbene, and subsequent proton transfer to provide the pyrazine carboxamide product.[49] The syrbactin analogs were alternatively synthesized utilizing this methodology, as shown in Scheme 2.10. The thia-macrolactam intermediate **2.10** was deprotected with acid, neutralized to the free amine with MP-carbonate base resin, and reacted with PCA to provide **2.20** in 18% yield. Analogously, the valine substituted macrolactam **2.11** was deprotected with piperidine and reacted with PCA to afford **2.18** in 30% yield. Unfortunately, the resulting product yields of the two reactions were much lower than anticipated.

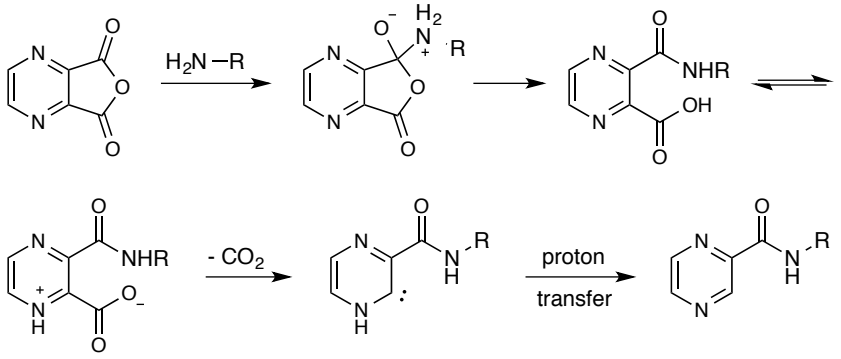

Figure 2.6: Proposed mechanism of the reaction of 2,3-pyrazinedicarboxylic anhydride with amines.[49]

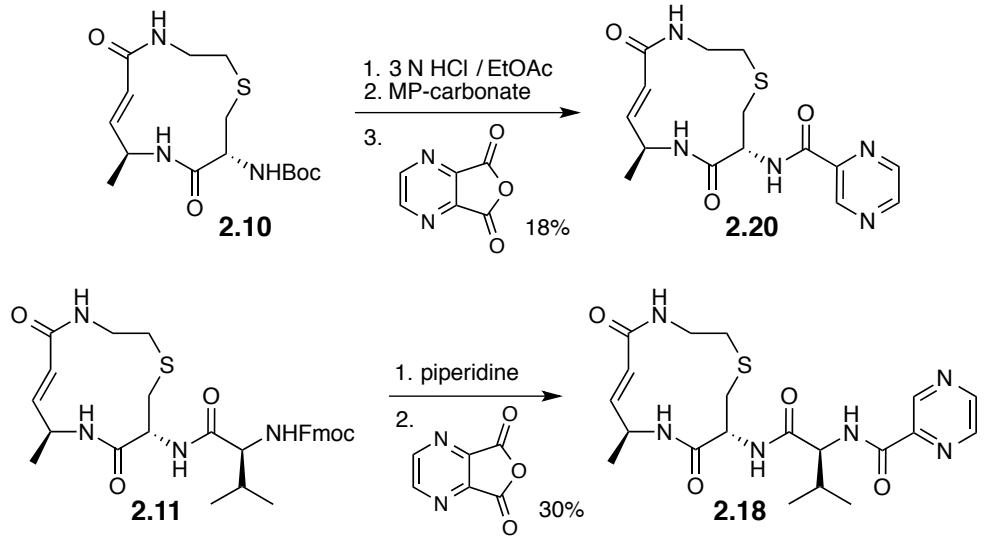

Scheme 2.10: Alternative synthesis of the analogs **2.16** and **2.17** using 2,3-pyrazinedicarboxylic anhydride.

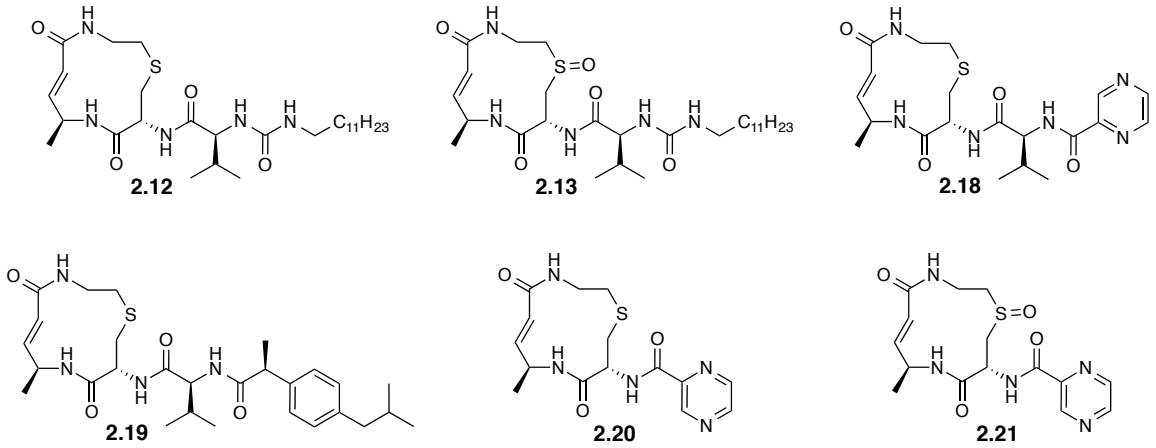

Figure 2.7: Synthesized thiasyrbactin analogs.

Thus far, the synthesis of six unique thiasyrbactin analogs has been accomplished (Figure 2.7). In subsequent sections of this chapter, the physiochemical properties, biological activities, and SAR of these syrbactin analogs will be evaluated.

2.3 Stereochemical/Conformational Analysis of the Thiasyrbactin Macrolactam

Introduction of a sulfoxide in the thiasyrbactin macrolactam of analogs **2.13** and **2.21** created a new stereocenter that needed to be evaluated and assigned stereochemistry. The assignment of the stereochemistry was accomplished by spectral comparison of these derivatives to a simplified sulfoxide model **2.22**, which was extensively studied by various NMR techniques. The oxidation of macrolactam **2.10** with sodium periodate provided the sulfoxide macrolactam **2.22** model used in this study as a single stereoisomer in 89% yield (Scheme 2.11).

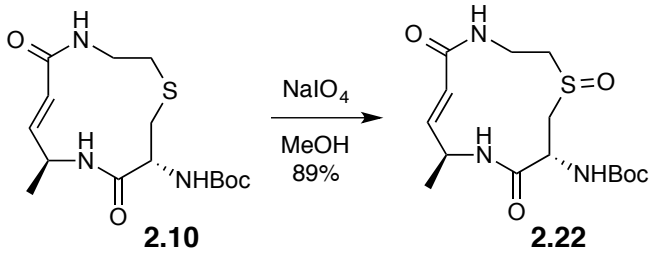

2.10 **2.22**

Scheme 2.11: Synthesis of the sulfoxide model **2.22**.

The conformational analysis of the thiasyrbactin macrolactam was accomplished by extensive evaluation of various NMR spectra of macrolactam **2.10** and the corresponding sulfoxide **2.22**. The NMR data collected on these compounds include high field proton, carbon, COSY, NOESY, and HSQC spectra. The data collected from these spectra are reported in Table 2.1. Conformational models of the thia-macrolactams **2.10** and **2.22** were constructed to aid in the understanding of the chemical and biological properties of the thiasyrbactins and to assign the sulfoxide configuration in the oxidized analogs (Figure 2.8). The COSY data were used to identify and assign the protons of the model compounds. The NOESY data were used to identify proximal transannular hydrogens, which significantly limited the possible conformations of the macrolactam. There are two main low-energy conformations of the macrolactam determined by molecular modeling, with the sulfide pointing above or below the nominal plane of the ring. Using the information provided by the spectral data and NOE correlations, the conformation of the thia-macrolactam **2.10** was modeled, having the sulfide pointed below the plane (Figure 2.8). The NOE correlations between H-6 and both H-2a and H-12a, and the coupling constant between H-11 and H-12a support this conformation. If the

sulfide was pointing above the plane, the protons on carbon 12 would be pointed downward, which would cause the dihedral angles between H-11 and H-12a/12b to be closer to 135°. This would result in a larger coupling constant than is observed.

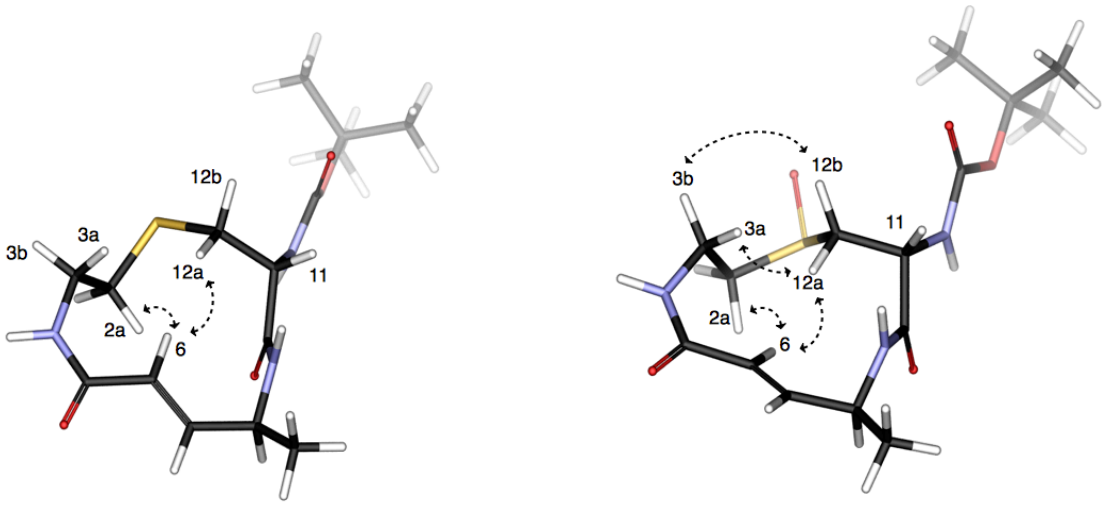

Figure 2.8: The conformations of thia-macrolactam **2.10** (left) and the sulfoxide macrolactam **2.22** (right) consistent with the spectral data.

	Compound **2.10**				Compound **2.22**			
Position	δ_C[a]	δ_H[b], mult. (*J*, Hz)	COSY	NOESY	δ_C[a]	δ_H[b], mult. (*J*, Hz)	COSY	NOESY
1-S								
2	32.4	a: 2.47, m	2b, 3a, 3b	6	54.5[c]	a: 3.29, m	2b, 3a, 3b	6
		b: 2.70, ddd (5.1, 8.6, 14.0)	2a, 3a, 3b[d]			b: 2.96, ddd (7.2, 8.9, 13.9)	2a, 3a, 3b	
3	42.0	a: 3.50, m	2a, 2b, 3b	12a	37.4	a: 3.70, m	2a, 2b, 3b	12a
		b: 3.22[d], m				b: 3.48, ddd (4.5, 6.9, 16.1)	2a, 2b, 3a	12b
5	170.8				169.7			
6	121.3	6.45, d (15.7)	7	2a, 12a	120.0	6.15, d (15.4)	7, 8	2a, 12a
7	146.0	6.72, dd (4.9, 15.6)	6, 8		149.5	6.92, dd (4.8, 15.4)	6, 8	
8	48.0	4.52, m	7, 8-Me		47.9	4.57, m	6, 7, 8-Me	
8-Me	18.8	1.33, d (7.1)			18.7	1.33, d (7.1)	8	
10	172.7				171.0			
11	53.8	4.43, m	12a, 12b		52.9	4.77, t (3.5)	12a, 12b	
12	34.1	a: 3.00, dd (6.1, 14.4)	11, 12b	3a, 6	54.5[c]	a: 3.14, dd (3.8, 14.4)	11, 12b	3a, 6
		b: 3.22[d], m				b: 3.77, dd (3.2, 14.4)	11, 12a	3b
2’	157.2				157.1			
4’	81.1				81.4			
5’	28.8	1.45, s	8		28.8	1.45, s	8	

[a]Recorded at 126 MHz. [b]Recorded at 700 MHz. [c]The carbon signals 2 and 12 of compound **2.22** overlap. [d]The proton signals of 3b and 12b in compound **2.10** overlap.

Table 2.1: NMR data for thia-macrolactams **2.10** and **2.22**.

Proton	δ (ppm)	*J* (Hz)	Θ (deg)[a]	Θ (deg)[b]
C2α	3.29[c]	C2β	gem	gem
		C3α	68	-
		C3β	156	-
C2β	2.96	C2α - 13.9	gem	gem
		C3α - 8.9	168	170
		C3β - 7.2	32	20
C3α	3.70[c]	C3β	gem	gem
		C2α	68	-
		C2β	168	-
C3β	3.48	C3α - 16.1	gem	gem
		C2α - 6.9	156	150
		C2β - 4.5	32	41
C11	4.77	C12α - 3.5	48	47
		C12β - 3.5	52	47
C12α	3.14	C12β - 14.4	gem	gem
		C11 – 3.8	48	45
C12β	3.77	C12α - 14.4	gem	gem
		C11 – 3.2	52	49

[a]from modeled structure **2.12**; [b]calculated from the Karplus equation; [c]multiplet

Table 2.2: The J-coupling values for sulfoxide macrolactam **2.22** with modeled and implied dihedral angles.

The conformation of the sulfoxide **2.22** was then explored. Oxidation of **2.10** by sodium periodate from the less hindered position would result in the reaction from the equatorial direction producing the beta sulfinyl group shown in the model of **2.22** in Figure 2.8. Analysis of the NMR spectra enabled the conformation and sulfoxide configuration of compound **2.22** to be confirmed. The proton NMR of **2.22** show that the

protons adjacent to the sulfoxide are deshielded, but the relationships among the hydrogens, both in terms of dipolar and scalar couplings, are very similar to **2.10**, supporting a similar conformation with the sulfur atom positioned below the ring plane. The sulfoxide compound **2.22** has additional NOE correlations between H-3b and H-12b, and H-3a and H-12a, strengthening the case for the conformation with the sulfur atom pointing downward with a slight inward rotation of carbon 3. Additionally, this structure would lack NOE correlations between the protons on carbons 3 and 12 if the ring was oriented with the sulfur atom above the plane. The greatest deshielding is experienced by H-2a, which has a dihedral angle with the sulfoxide of about 162°, supporting the beta sulfinyl configuration (Figure 2.9). This dihedral angle relationship between the sulfoxide and the adjacent proton H-2a provides the greatest downfield shift when a sulfide is converted to the sulfoxide.[50] The dihedral angles of **2.22** were calculated using the Karplus equation from the observed proton NMR coupling constants and compared to the dihedral angles of the conformational model, and are reported in Table 2.2. The calculated and the observed dihedral angles of the model were very similar and only vary by 6° or less. The dihedral angles between H-11 and H-12a, and H-11 and H-12b were calculated from the coupling constants of H-12a and H-12b to be 45° and 49°. The dihedral angles of the conformational model were determined to be 48° and 52° respectively, and reasonably agreed with the calculated values. The dihedral angles further support the conformation of **2.22** with the sulfur atom pointing below the plane of the ring.

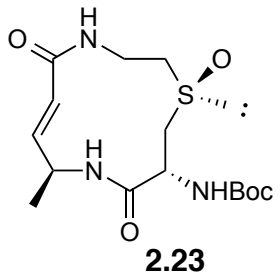

2.23

Figure 2.9: Thiasyrbactin sulfoxide configuration assigned to compound **2.22**.

Using the information provided by the spectral data, the conformation of the sulfoxide macrolactam **2.22** was modeled, having a similar conformation to **2.10** with the assigned sulfoxide stereochemistry of a beta sulfinyl group (Figure 2.9). Based on this analysis, the sulfoxides of the oxidized thiasyrbactin derivatives **2.13** and **2.21** were assigned the beta configuration due to the spectral similarities to the model **2.22**.

2.4 Synthesis of Ornithine Based Syrbactin Analogs

The proposed strained syrbactin derivatives were synthesized in a similar manner as the thiasyrbactin. The design of these analogs allows for the implementation of the syringolin B synthesis developed by the Pirrung group,[35-36] utilizing the commercially available lysine analog *N*-Boc ornithine **2.24** (Scheme 2.12). Initially, *N*-Boc ornithine **2.24** was reacted with the phosphono ester **2.2** to afford the corresponding phosphonocarboxylate **2.25**. Intermediate **2.25** was then coupled with L-alaninol using the conventional coupling protocol with DCC and NHS to afford the phosphonoacetatamide macrolactam precursor **2.26** in 88% yield over the two steps.

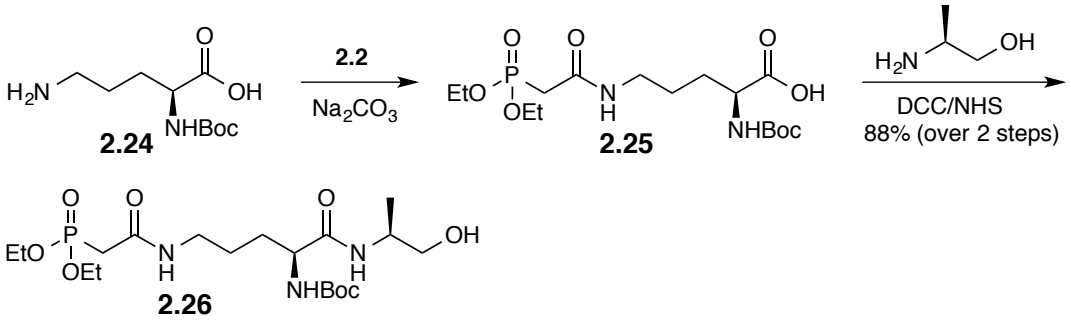

Scheme 2.12: Synthesis of the macrolactam precursor **2.26**.

The synthesis of the macrolactam precursor **2.26** was also explored by peptide ligation with the mildly activated cyanomethyl ester and β-hydroxylamine L-alaninol (Scheme 2.13). Compound **2.25** was converted to the corresponding cyanomethyl ester **2.27** by the alkylation reaction with chloro- or bromoacetonitrile and base, with the method using the chloroacetonitrile giving the best results providing **2.27** in 92% yield. Subsequent ligation with L-alaninol provided **2.26** in 40% yield, which is similar to the ligation yield obtained in the thiasyrbactin synthesis. Although the activated ester **2.27** was obtained in high yield, the poor ligation reaction limited the utility of this route. The initial synthetic route was superior.

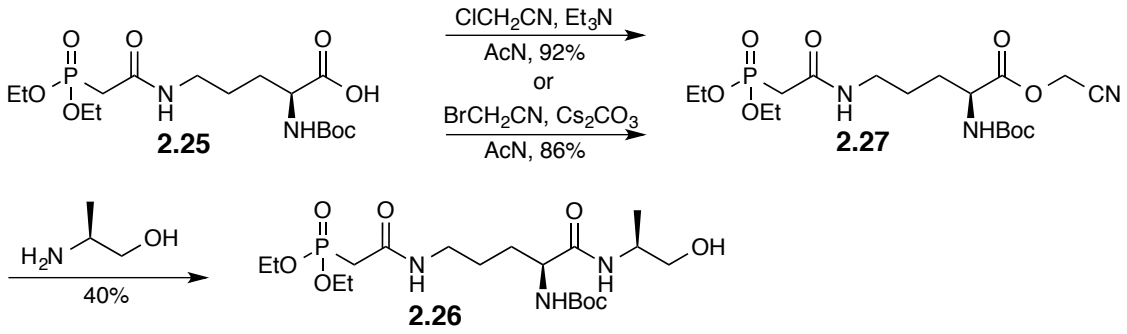

Scheme 2.13: Alternative synthetic route of the macrolactam precursor **2.26** by alaninol ligation.

Next, the synthesis of the eleven-membered macrolactam was examined (Scheme 2.14). Formation of the more strained macrolactam was more difficult than the traditional twelve membered ring core of the syrbactins. Cyclization was performed using the same method as the thiasyrbactins by the HWE reaction. Oxidation of **2.26** with Dess-Martin periodinane gave the corresponding aldehyde, which was used crude in the next step. The HWE cyclization reaction was performed by treatment of the aldehyde with triethylamine, zinc triflate, and TMEDA at low concentration in THF, but only a small amount of macrolactam **2.28** was formed, as observed by proton NMR. Attempts to isolate this compound by column chromatography were unsuccessful. Efforts to optimize the product yield by modifying the reaction conditions were also unsuccessful. Due to the additional strain induced by the reduction of the ring size, the synthesis of macrolactam **2.28** was unattainable with these reaction conditions.

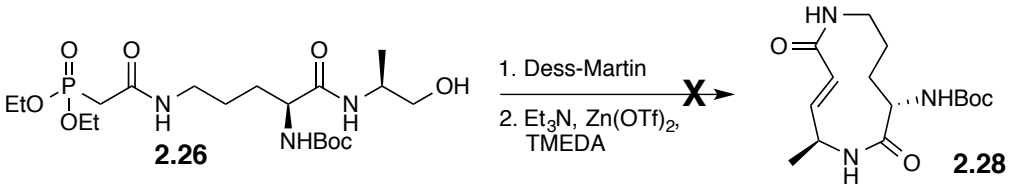

Scheme 2.14: Attempted synthesis of the strained macrolactam core **2.28** by the HWE reaction.

2.5 Alternative Syrbactin Derivatives

It was envisioned that a unique variant of the strained macrolactam core could be achieved by applying the Ramberg-Backlund reaction to the thiasyrbactin macrolactam to

generate an eleven-membered core similar to TIR-199 and SylA with the second olefin in the macrolactam ring (Scheme 2.15). Upon oxidation of the thiasyrbactin macrolactam to the sulfone, the Ramberg-Backlund reaction could be applied to generate the α-halo sulfone and convert it into an alkene by treatment with base and elimination of sulfur dioxide (Figure 2.10).

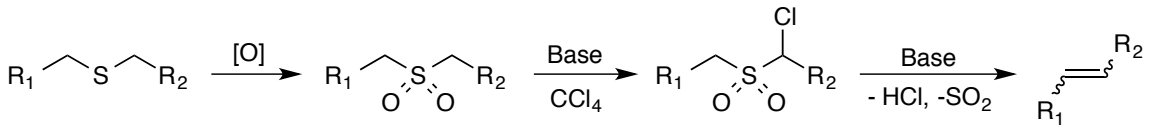

Figure 2.10: General scheme of the Ramberg-Backlund reaction.

The synthesis of **2.30** was attempted by applying the method utilized by Gonnade and coworkers in their synthesis of the neuraminidase inhibitor drug, Tamiflu (Scheme 2.15).[51] The thiasyrbactin macrolactam **2.10** was treated with oxone to afford the corresponding sulfone **2.29** in quantitative yield. Treatment of **2.29** with potassium hydroxide and carbon tetrachloride in *tert*-butanol provided **2.30** in 31% yield. As a result of a low yield accompanied by the ample loss in mass from the starting sulfoxide to the product, only a small quantity of pure compound was obtained. In depth spectral analysis of the product is needed to determine the *E* or *Z* configuration of the generated alkene. The reaction parameters can be modified to promote *E* alkene formation, by employing a stronger base like potassium *tert*-butoxide. The modified Ramburg-Backlund reaction utilizing a sulfoxide in place of the sulfone has recently been reported to provide improved yields in the formation of strained ring systems[52] and may be superior in this

instance. Further scale up and optimization of this synthetic route is needed to complete the synthesis of these syrbactin analogs. Additionally, the optimization of this method can provide an alternative and simplified synthetic route toward SylA/TIR-199 inspired syrbactin derivatives with two alkenes in the macrolactam core.

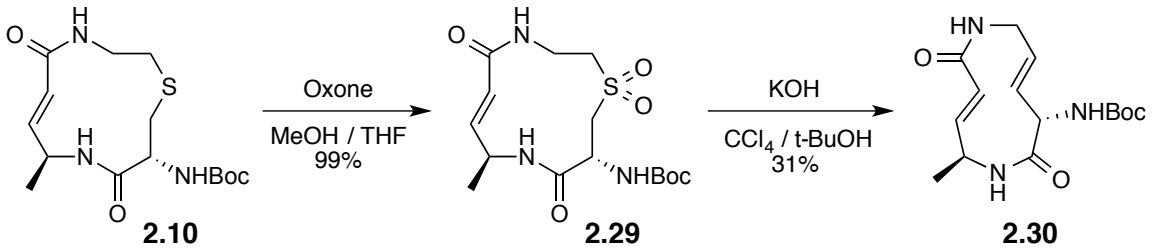

Scheme 2.15: Synthetic route toward TIR-199 like macrolactam core **2.30**.

2.6 Analysis of Syrbactin Analog Drug-likeness

The physicochemical properties of all the synthesized syrbactin analogs in this study (Figure 2.7) were evaluated computationally and compared to the parent syrbactin GlbA and the potent syrbactin derivative TIR-199 to determine the relative drug-likeness of these compounds. Properties including hydrophilicity and solubility were calculated using the web-based properties calculator, AquaSol,[53] used for drug development to predict aqueous solubility of prospective drug compounds, and the FAF-Drugs3[54] web server used to evaluate various physiochemical properties for drug discovery and design. The results of these computational calculations on hydrophilicity and solubility are summarized in Table 2.3. Introduction of the sulfur to the macrolactam and modifications

to the side chain of these syrbactin derivatives were applied to increase the overall solubility of the compounds. Generally, high compound solubility and moderate lipophilicity are required for enhancing *in vitro* drug activity.[43] Greater lipophilicity results in a decrease in aqueous solubility,[43] so the right balance is needed to improve solubility while preserving the lipophilicity in the side chain needed to occupy the hydrophobic pocket of the proteasome to maintain inhibitory activity. The log P value is a measure of lipophilicty, the log S value is a measure of solubility and log Sw is a measure of aqueous solubility. A high log P value greater than 5 is generally associated with poor drug solubility.[43] TIR-199 and structurally similar thiasyrbactin **2.12** have very similar physiochemical properties. Incorporation of the sulfoxide increases the overall hydrophilicity of the molecule, as demonstrated by the log P calculations for **2.13** and **2.21**. The overall lipophilicity of **2.18**, **2.20**, and **2.21** decreases considerably with the incorporation of the more polar pyrazinamide side chain, and is accompanied by an increase in overall solubility. The most drastic increase in solubility is seen in the bortezomib inspired thiasyrbactin analogs **2.20** and **2.21**, which do not contain the valine residue in the side chain. Thiasyrbactin **2.21** highlights the utility of the sulfoxide to increase hydrophilicity and improve solubility. Introduction of the ibuprofen residue to the side chain in **2.19** increases the relative hydrophilicity compared to TIR-199 and thiasyrbactin analog **2.12** with the dodecyl side chains, but only improves the solubility slightly. The thiasyrbactin analogs are computationally predicted to have an overall increase in solubility and hydrophilicity compared to TIR-199.

Compound	NAM #	M_r (Da)	log P[a]	Log S[b]	Log S_w[a]
TIR-199	-	533	5.95	-4.51	-5.91
GlbA	-	520	3.12	-3.89	-4.24
2.12	105	553	5.51	-4.65	-5.75
2.13	135	569	3.89	-4.36	-4.83
2.18	95	448	-0.05	-3.56	-2.33
2.19	93	531	3.86	-4.52	-5.09
2.20	41	349	-0.76	-3.03	-1.50
2.21	111	365	-2.38	-2.91	-0.58

Table 2.3: Calculated properties affecting thiasyrbactin drug-likeness including molecular weight, hydrophobicity, and solubility. [a]Calculated using the method in Lagorce *et al.*, *Nucleic Acids Res.* 43:W200-W207 (2015).[54] [b]Calculated using the method in Lusci *et al*., J. *Chem. Inf. Model* 53:1563-1575.[53]

2.7 Biological Evaluation

The thiasyrbactin derivatives (Figure 2.7) were evaluated for their ability to inhibit each of the catalytic subunits of the constitutive proteasome and immunoproteasome, as well as for cytotoxic activity against neuroblastoma cancer cells. The biological studies discussed in this section were preformed in collaboration with the Bachmann laboratory at MSU. In vitro proteasome activity assays were conducted to determine the extent of proteasome inhibition of each of the catalytic sites (Figure 2.11). Luminogenic substrates consisting of short peptides specific for each of the catalytic sites tagged with aminoluciferin are added to a mixture of the proteasome along with the syrbactin inhibitor. When the proteasome is not inhibited, the luminogenic substrates are cleaved by the proteasome, releasing the aminoluciferin. Upon addition of luciferase to the mixture and reaction with ATP, the aminoluciferin will produce light. The extent of

proteasome inhibition is related to the amount of light produced. The amount of light produced indirectly correlates to the extent of proteasome inhibition- when the proteasome is inhibited, less light is produced relative to a control. The cell viability assays were conducted in a similar manner, using a colorimetric method to determine the amount of viable cells remaining after treatment with the proteasome inhibitors (Figure 2.11). After the cells have been treated with the proteasome inhibitor, a tetrazolium reagent is added to the cells, and upon reaction with NADPH or NADH produced in viable cells, the reagent is converted to the corresponding formazan chromogenic product, which can be measured by absorbance. The quantity of formazan product produced is directly proportional to the amount of viable cells- if the cells are dead, a decrease in absorbance intensity is measured relative to a control.

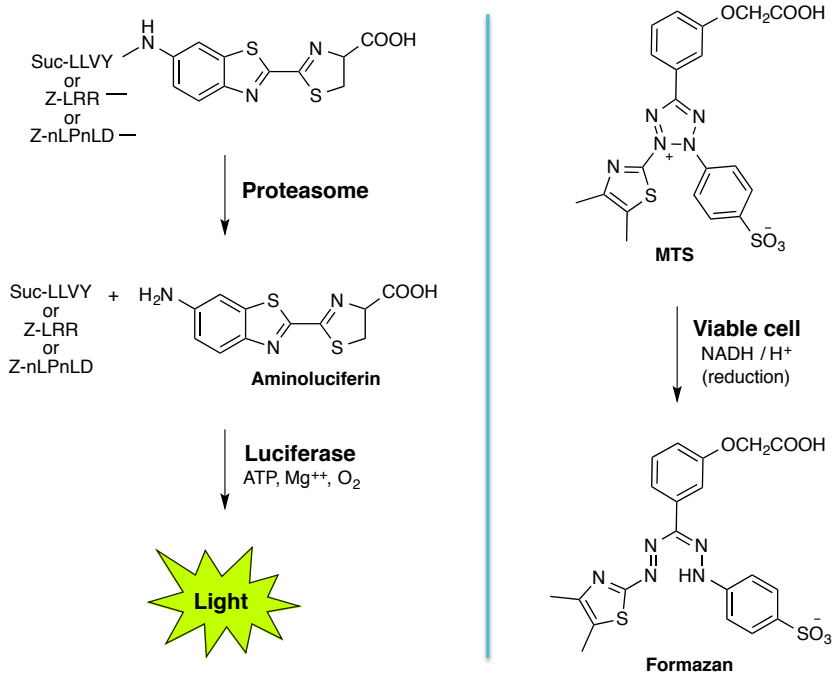

Figure 2.11: General scheme of the biological assays: mechanism of proteasome activity (left) and cell viability (right).

The biological activities and proteasome inhibitory properties of each of the thiasyrbactins were evaluated. To evaluate the inhibitory activity of the thiasyrbactins, *in vitro* assays were performed and the proteasome inhibition activities were measured at the three catalytic sites β1 (C-L), β2 (T-L), and β5 (CT-L) of the constitutive proteasome and immunoproteasome (Figure 2.12). For control comparison, the FDA-approved peptide boronic acid proteasome inhibitor bortezomib (BTZ) and the peptide epoxyketone immunoproteasome inhibitor ONX-0914 were included in these assays. The K_i-50 inhibition constants are recorded in Table 2.4. The bortezomib like thiasyrbactin derivatives **2.20** and **2.21** (NAM-41 and NAM-111, respectively) had minimal activity in these assays, with negligible inhibition of each of the proteasome catalytic sites. In comparison to compound **2.18** (NAM-95), the valine residue is necessary for proteasome inhibition. The thiasyrbactins **2.12** (NAM-105), **2.13** (NAM-135), **2.18** (NAM-95), **2.19** (NAM-93) predominantly inhibited the CT-L and T-L activities of the constitutive proteasome, but more potently and more selectively inhibited the T-L activity of the immunoproteasome with negligible effect on the CT-L and C-L sites. In contrast, BTZ inhibited the CT-L and C-L catalytic sites indiscriminately, and did not inhibit the T-L activity at all. The immunoproteasome inhibitor ONX-0914 exhibited higher potency against the immunoproteasome CT-L activity compared to the CT-L activity of the constitutive proteasome, but also inhibited the C-L and T-L activities of both proteasome types at higher concentrations. Thus, **2.12**, **2.18**, and **2.19** more selectively target the T-L site of the immunoproteasome with Ki-50 values at 1.39, 0.75, and 0.74 μM, respectively, and have no effect at concentration less than 10 μM on the CT-L and T-L

activities (Table 2.4). Although **2.13** follows the same trend of inhibition, the activity against the T-L site is significantly lower (Figure 2.12).

The thiasyrbactins **2.12** and **2.13**, which maintain the same general features of TIR-199, demonstrate different activities against the proteasome. TIR-199 strongly inhibits the CT-L and T-L sites but has minimal activity against the C-L site of both the constitutive proteasome and immunoproteasome.[22] However, thiasyrbactins **2.12** and **2.13** inhibit the CT-L activity of the constitutive proteasome and the T-L activity of the immunoproteasome (Figure 2.12). Thus, modification to the macrolactam core impacted the inhibitory properties of the thiasyrbactins dramatically. The attempt to improve solubility by oxidation of the thia-macrolactam core resulted in the reduction of inhibition as shown by the decrease in activity of **2.13** compared to **2.12** (Figure 2.12). The selective inhibition of the T-L activity of the immunoproteasome is much greater with **2.18** and **2.19** with the incorporation of the pyrazine and ibuprofen side chain residues, with **2.19** being the most potent inhibitor.

To study the biological effects of these thiasyrbactins, the inhibition activities on the viability of human neuroblastoma cells were examined at varying concentration for 24 hours (Figure 2.13). Thiasyrbactins **2.13**, **2.18**, and **2.19** exhibited minimal effect on the three neuroblastoma cell lines MYCN2, SK-N-Be2c, and SK-N-SH, even at the highest concentration tested (1 μM). In contrast, **2.12** significantly inhibited the viability of MYCN2 and SK-N-SH cells by about 30% to 50% relative to the DMSO control. TIR-199 strongly inhibited the viability of MYCN2 and SK-N-SH cells as previously reported[22] with little effect on SK-N-Be2c, a cell line originally derived from a highly

metastatic MYCN-amplified neuroblastoma tumor that exhibits chemoresistance. BTZ exhibited strong cytotoxic effects against each of the neuroblastoma cell lines, but most notably in MYCN2 and SK-N-SH cell lines at 0.1-1 μM resulting in no detection of cell viability.

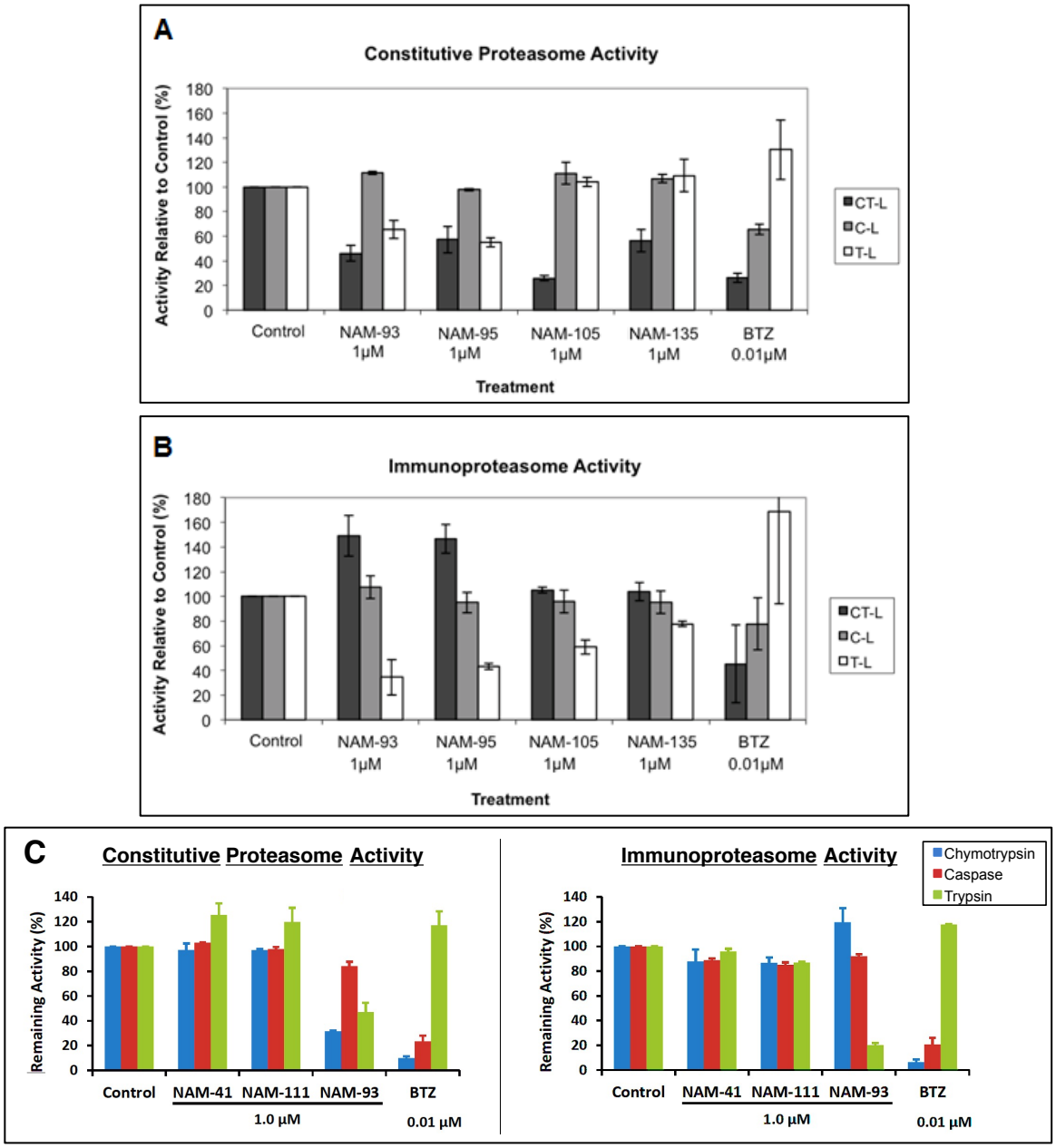

Figure 2.12: Effect of the thiasyrbactins on *in vitro* proteasome activity. (A) Constitutive proteasome and (B) immunoproteasome treated with 1μM **2.12** (NAM-105), **2.13** (NAM-135), **2.18** (NAM-95), **2.19** (NAM-93) for two hours. (C) Constitutive proteasome (left) and immunoproteasome (right) treated with 1μM **2.20** (NAM-41), **2.21** (NAM-111), and **2.19** (NAM-93) for two hours. BTZ was included as a control comparison. The data shown are from three independent experiment (n=3).

Compound	Constitutive Proteasome		Immunoproteasome		Catalytic Site
	Ki-50 (μM)	SD	Ki-50 (μM)	SD	
2.12	0.28	0.07	>10	-	CT-L (β5)
	>10	-	>10	-	C-L (β1)
	1.76	0.78	1.39	0.11	T-L (β2)
2.18	1.22	0.18	>10	-	CT-L (β5)
	>10	-	>10	-	C-L (β1)
	0.92	0.12	0.75	0.03	T-L (β2)
2.19	0.91	0.18	>10	-	CT-L (β5)
	>10	-	>10	-	C-L (β1)
	1.07	0.19	0.74	0.06	T-L (β2)
ONX-0914	0.56	0.19	0.11	0.02	CT-L (β5)
	2.07	0.30	1.32	0.21	C-L (β1)
	1.11	0.06	1.34	0.22	T-L (β2)
BTZ	0.01	0.00	0.01	0.00	CT-L (β5)
	0.02	0.00	0.03	0.01	C-L (β1)
	1.37	0.11	0.78	0.03	T-L (β2)

Table 2.4: Calculated Ki-50 values of *in vitro* inhibition of the thiasyrbactins on sub-catalytic activities of the constitutive proteasome and immunoproteasome.

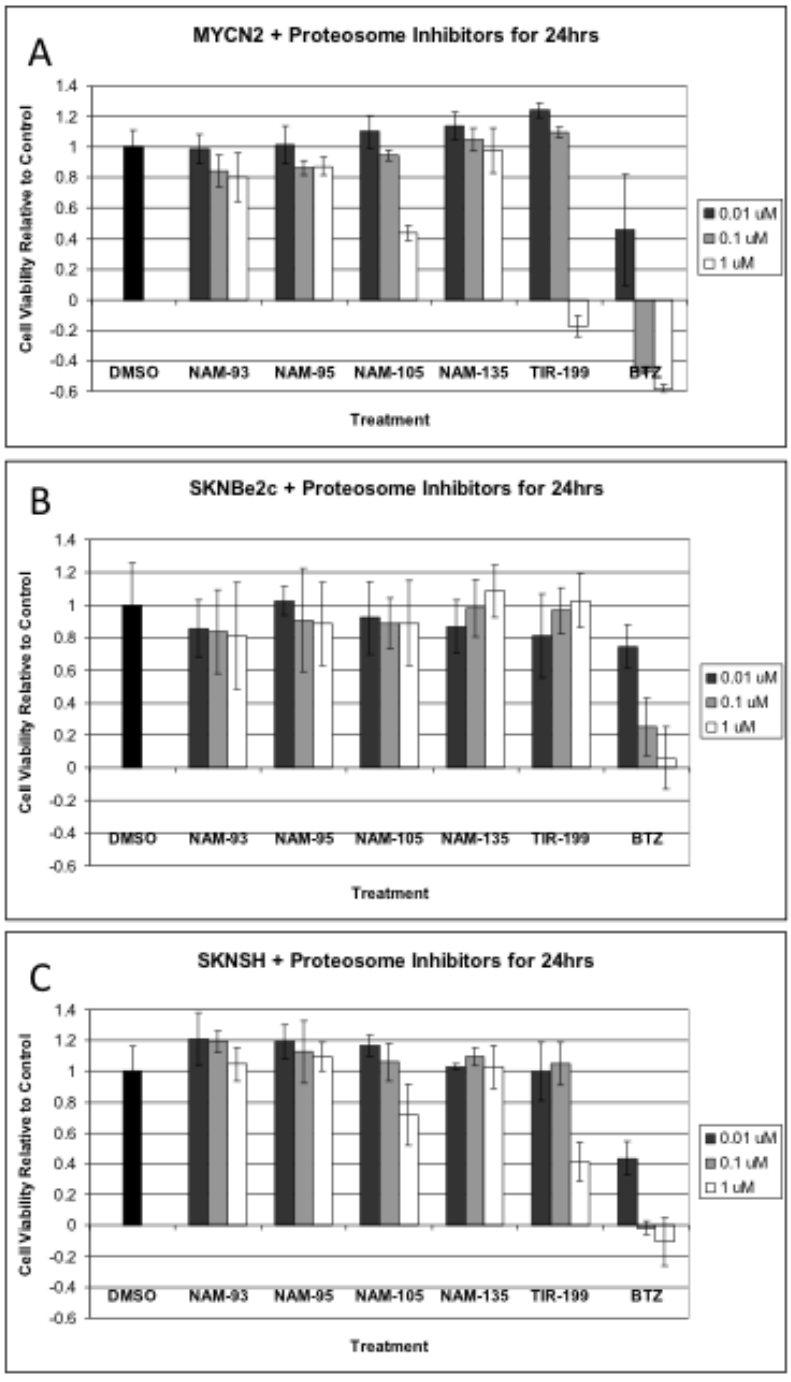

Figure 2.13: Effect of thiasyrbactins on the viability of human neuroblastoma cancer cells. (A) MYCN2, (B) SK-N-Be2c, and (C) SK-N-SH neuroblastoma cells were treated with the inhibitors **2.12** (NAM-105), **2.13** (NAM-135), **2.18** (NAM-95), and **2.19** (NAM-93) for 24 hours at three different concentrations (0.01, 0.1, and 1 μM). Bortezomib (BTZ) was included as a control and TIR-199 as a reference. Data shown are from two independent experiments, each performed in triplicate wells (n=6).

2.8 Conclusion

The desired goal to provide methods to enhance the solubility of syrbactin analogues by an efficient synthetic route has been accomplished in this work. However, the synthesis of the strained ornithine based analogs was not successful. Although the solubilities of the syrbactin analogs were enhanced, they did not have more activity toward proteasome inhibition. This study resulted in the discovery of syrbactin analogs with selective inhibition of the trypsin-like catalytic site of the constitutive proteasome and immunoproteasome. The thiasyrbactins **2.18** and **2.19** inhibit the chymotrypsin-like (β5) and trypsin-like (β2) sites of the constitutive proteasome and selectively inhibit the trypsin-like site of the immunoproteasome, whereas TIR-199 is an indiscriminate and potent inhibitor of the chymotrypsin-like and trypsin-like subunits of the constitutive and immunoproteasome,[22] and bortezomib indiscriminately inhibits the chymotrypsin-like (β5) and caspase-like (β1) subunits. The stimulation of the β5 subunit of the immunoproteasome was observed when the β2 subunit was inhibited. Similar instances of increased sub-site activity with simultaneous inhibition of other active sites have been observed with other proteasome inhibitors, including bortezomib (Figure 2.12). The selective inhibition of the T-L site is likely the result of unique interactions of the thiasyrbactins **2.18** and **2.19** within the proteasome binding pocket resulting in greater subunit affinity. Evaluation of the crystal structure of the thiasyrbactins bound to the immunoproteasome and molecular modeling simulations are necessary to determine the key proteasome-substrate interactions that result in the unique activity. Data from these

studies can be exploited for the synthesis of syrbactins with increased proteasome selectivity and inhibition potency.

Given the preference for the inhibition of the immunoproteasome catalytic activity which is only found in select cells, the weak biological activity of the thiasyrbactins against the neuroblastoma cell lines was not surprising. Compound **2.12** demonstrated the most activity of the thiasyrbactins, demonstrating activity in the MYCN2 and SK-N-SH cell lines, but the extent of inhibition was quite unimpressive. Thiasyrbactins **2.18** and **2.19** are more drug-like and soluble than TIR-199, though their potency as proteasome inhibitors were poorer resulting in less favorable biological activity.

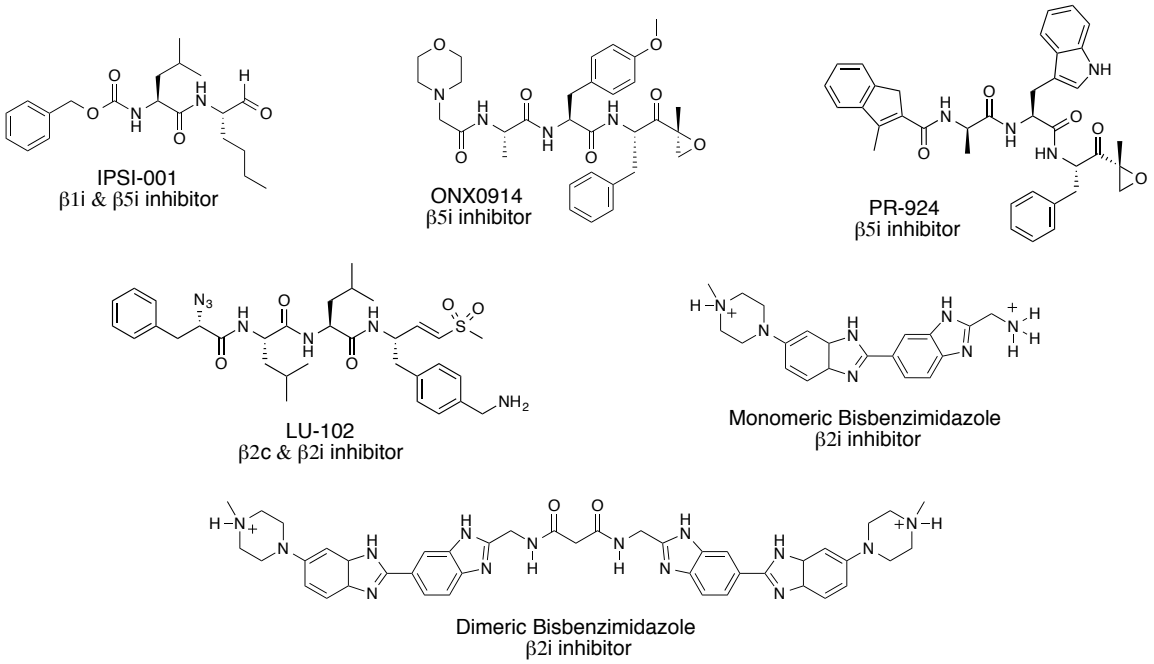

Figure 2.14: Structures of previously reported immunoproteasome inhibitors.

The overexpression of the immunoproteasome has been linked to a variety of autoimmune and neurodegenerative diseases including Huntington disease, Alzheimer disease, inflammatory bowel disease, and cancer.[18, 55] The immunoproteasome is thus a novel therapeutic target for proteasome inhibition. There are several reports of selective inhibitors of the immunoproteasome, but there are only a few that are selective for the $\beta2_i$ trypsin-like subunit.[55-59] Examples of selective immunoproteasome inhibitors include: IPSI-001,[55] ONX0914,[59] PR-924,[59] LU-102,[56-57] and monomeric and dimeric bisbenzimidazoles,[58] shown in Figure 2.14. The compound IPSI-001 inhibits the $\beta1_i$ and $\beta5_i$ subunits, whereas ONX0914 and PR-924 selectively inhibit the $\beta5_i$ subunit of the immunoproteasome.[58] The molecule LU-102 is an indiscriminate inhibitor selective for the β2 subunit and has been used in combination with multiple myeloma drugs bortezomib and carfilzomib to improve the efficacy of the therapy and overcome the challenge of drug resistance.[56-57] The bisbenzimidazoles were demonstrated to selectively inhibit the trypsin-like ($\beta2_i$) site, however their biological activity is not limited to proteasome inhibition and their structures are not particularly appropriate to be used as drugs.[58] Although the thiasyrbactin inhibitors **2.18** and **2.19** are not very potent, they have the potential to be useful in further studies of the immunoproteasome to evaluate the therapeutic value of selective $\beta2_i$ inhibition. Unlike other immunoproteasome inhibitors, the syrbactin structure has better drug-like potential. Further development of the thiasyrbactins is needed to provide analogs with improved inhibition properties that would be better suited for *in vivo* studies of the immunoproteasome activity.

Part 2: Peptide Assembly by Ligation of Hydroxyl Amino Acids and Mildly Activated Esters

Chapter 3: Peptide Chemistry Introduction

3.1 Significance of Peptide Chemistry

Proteins and peptides are biological molecules of varying complexity and diversity that perform many highly specific and important biological cellular functions.[60] These biologically active molecules have been subjected to immense research in order to determine their structure and understand their specific biological function.[61] The isolation of proteins and peptides from their natural source is often impractical and difficult to obtain pure samples in sufficient quantities.[60, 62] The use of recombinant DNA technologies can provide access to large amounts of peptide and allows for site-specific amino acid modifications for the analysis of the structure function relationship, but it is limited to the incorporation of natural amino acid residues.[60, 62] Additionally, post-translational modification of phosphorylation, glycosylation, and ubiquitination are not readily applicable with these techniques.[63]

The development of protein chemical synthesis has been used to overcome some of these limitations of molecular biology by allowing the synthesis of large quantities of peptide for analysis, and the incorporation of controlled site-specific modifications to a protein, not limited to natural amino acid residues.[60] A variety of modification can be applied, including the incorporation of non-coded amino acid residues, isotopic labels, fluorophores, and post-translational modifications by phosphorylation, glycosylation and ubiquitination.[63-64] The introduction of these modifications has allowed the extensive

evaluation of peptide and protein structures by various biophysical techniques, including NMR spectroscopy, infrared spectroscopy, fluorescence spectroscopy, electrophysiology, and crystallography,[63-64] as described in Figure 3.1.

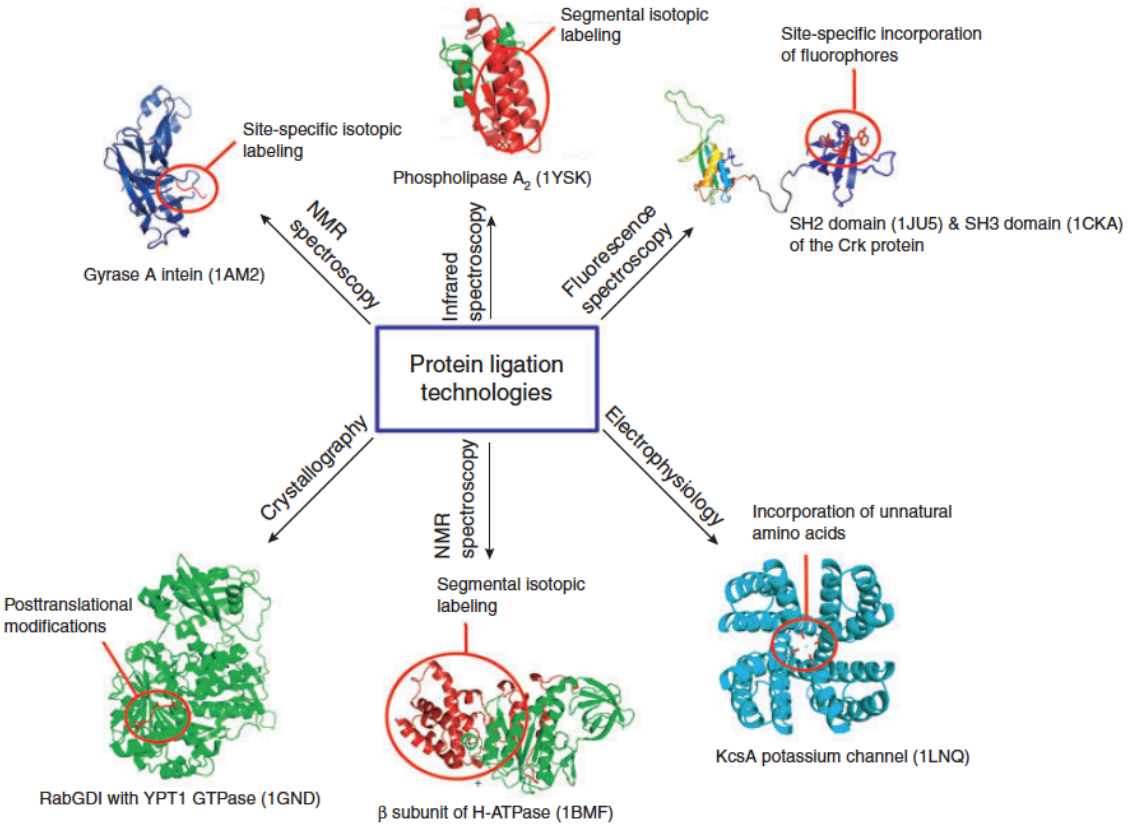

Figure 3.1: The introduction of site-specific modifications into proteins by chemical synthesis enables the study of peptide structure and function by a variety of biophysical techniques. (Image copied from Muralidharan, V; Muir, T. W. *Nat. Methods* **2006**, 3, 429-438.)[64]

3.2 Introduction to Peptide Ligation Chemistry

The field of peptide chemistry has developed drastically over the past hundred years[65-66] since the first dipeptide synthesis by Emil Fischer in 1901[67], with many notable achievements including the development of solid phase peptide (SPPS) chemistry[68] and native chemical ligation[69] (NCL). The development of various amino-protecting groups and coupling reagents has allowed for the synthesis of larger peptides.[66] Protein chemical synthesis has provided a great advance in the field of peptide chemistry, enabling the evaluation of the physical properties and biological activities of various peptides and proteins.[62] As a result, an increasing number of peptides are being use as therapeutics.[66, 70] The limitations of peptide chemistry methods prevent the synthesis and evaluation of more complex and unique peptides, providing inspiration for further advancements to the field.

3.3 Solid Phase Peptide Synthesis

Introduced by Robert Merrifield in 1963, solid phase peptide synthesis (SPPS) has provided a great advancement to the field of peptide chemistry.[68] SPPS permits the preparation of peptides on an insoluble polymer based support by step-wise coupling of protected amino acids (Figure 3.2). The C-terminal protected amino acid residue is attached to a resin linker, and the peptide is assembled by subsequent deprotection, coupling and washing steps. Excess quantities of coupling reagents and amino acids are utilized to promote rapid coupling reaction rates. After the reaction is compete, the excess

reagents and byproducts are easily removed by filtration and washing of the peptide bound solid support, eliminating tedious purification steps. Once the target peptide is synthesized, it is cleaved from the resin support to afford the free peptide. In 1984, Merrifield was awarded the Nobel Prize in Chemistry for his contributions to peptide chemical synthesis revolutionizing the field of peptide chemistry with the development of SPPS.

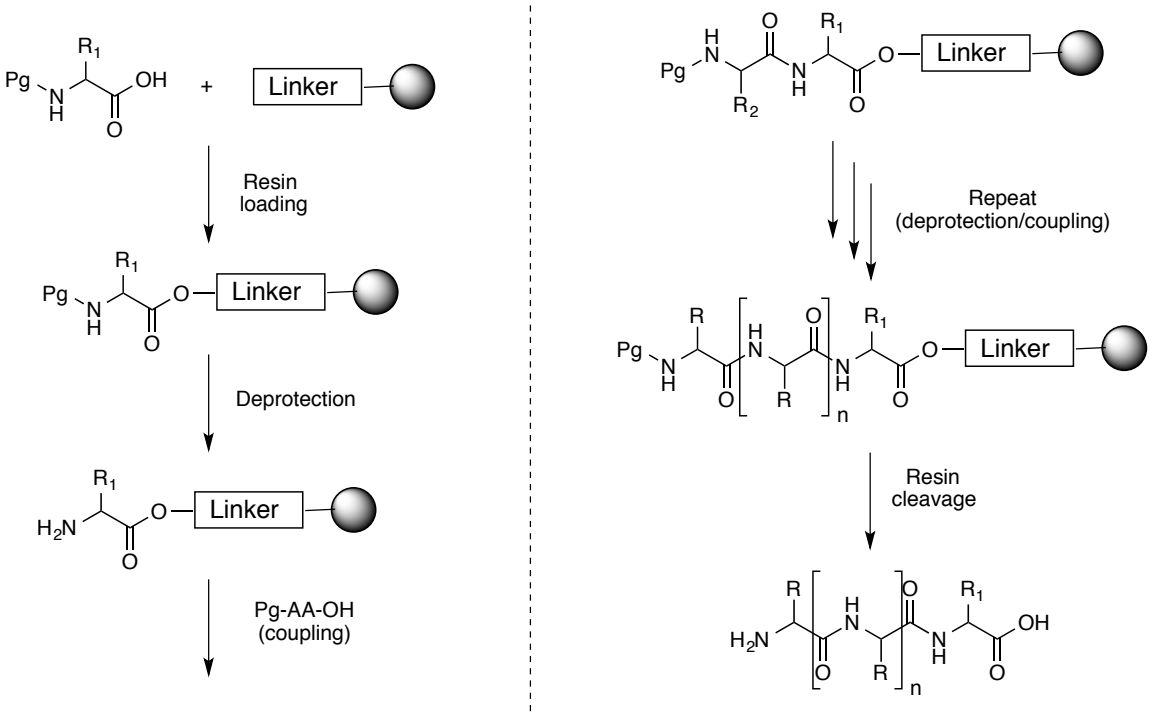

Figure 3.2: General scheme of solid phase peptide synthesis.

The method of SPPS has been further developed and advanced to expand the scope of the method for the synthesis of more diverse and challenging peptides. All aspects of the method have been refined including resin scaffolds and linkers, N^{α}-

protecting groups, side chain protecting groups, coupling reagents, and cleavage cocktails.[71] There are two general protocols for SPPS, differentiated by the N-terminal amino acid protecting groups utilized: *tert*-butyloxycarbonyl (Boc), initially introduced by Merrifield and fluorenylmethyloxycarbonyl (Fmoc). These SPPS protocols differ in the methods of *N*-terminal protecting group removal and cleavage of the peptide from the resin support. In Boc-SPPS, N^{α}-deprotection is conducted with trifluoroacetic acid (TFA) and resin cleavage is done with hydrofluoric acid (HF) whereas Fmoc-SPPS utilizes secondary amine bases like piperidine for N^{α}-amino acid deprotection and TFA to cleave the peptide from the resin. Kent and coworkers developed an *in situ* neutralization Boc SPPS method, utilizing ten minute coupling reactions allowing for the synthesis of seventy-five residues a day.[72] However, this method is not as desirable as Fmoc SPPS due to the use of hazardous HF, requiring cautious handling due to its highly toxic and corrosive nature, whereas the Fmoc SPPS method utilizes much milder conditions. Generally, N^{α}-Fmoc deprotection is performed using a diluted solution of piperidine (20% volume in DMF), and peptide cleavage from the resin support and global side chain deprotection is achieved by treatment with TFA. Additionally, Fmoc SPPS can be performed with automated peptide synthesizing instruments utilizing microwave irradiation for efficient peptide synthesis.[71] Various structural modifications can be incorporated into SPPS allowing for the synthesis of phosphopeptides, O- and N-glycopeptides, N^{α}-methylated peptides, peptoids, pseudopeptides, and other modified peptides.[71]

SPPS is the most common method used to synthesize peptides and small proteins.[71] Although SPPS has many advantages including efficiency of peptide synthesis, elimination of tedious purification steps, and increased rate of synthesis, there are crucial limitations to the method. Most of the shortcomings arise in the synthesis of larger peptides. Some peptides are often difficult to synthesize and result in low purity, diminished overall yield, or the method fails to produce the desired peptide sequence.[71] These problems typically arise due to steric hindrance at the coupling site and both intermolecular and intermolecular aggregation of the peptide resulting from hydrogen bonding and hydrophobic properties of the peptide.[71] Additionally, incomplete coupling or deprotection reactions can lead to amino acid deletions in the sequence resulting in an accumulation of byproducts, making the peptide more difficult to purify. These effects are more pronounced in the syntheses of large peptides, thus SPPS is most routinely used to synthesize peptides of about fifty amino acid residues or smaller.[73] Various chemical ligation strategies have been developed to use in combination with SPPS to overcome the limitations of the synthesis of large peptides and proteins. In a convergent approach, smaller peptide fragments are synthesized efficiently by SPPS and are chemoselectively coupled together to afford the complete peptide. A variety of ligation techniques have been developed in this effort.

3.4 Native Chemical Ligation

Native chemical ligation (NCL), introduced by Kent in 1994, was a major advancement in the chemical synthesis of peptides and proteins.[69] This method consists of an unprotected C-terminal peptide thioester and an unprotected N-terminal cysteine peptide chemoselectively reacting to generate a native peptide bond (Scheme 3.1). NCL is based on the concept of peptide synthesis by thiol-capture and intramolecular acyl transfer developed by Kemp in 1989.[74] The high chemoselectivity of the reaction is achieved due to the unique 1,2-mercaptoamine functionality of the N-terminal cysteine, differentiating it from other cysteine residues that may be present in the peptide fragments to be ligated. The reaction occurs in aqueous media at neutral pH and proceeds through an initial transthioesterification reaction between the terminal cysteine and thioester residues, followed by an intramolecular 1,4 S→N acyl transfer to afford the native peptide bond at the ligation site. The use of excess thiol of the same composition of the thioester is added to inhibit disulfide formation.[69, 75] The thioesters are generally synthesized from alkylation of alkyl halides, like benzyl bromide, with peptide thiocarboxylates generated by SPPS on a thioester resin.[69, 75] The rate of ligation is dependent on the reactivity of the leaving group of the thioester. Exploiting the ability of thioesters to readily undergo thiol exchange reactions, thiol additives including thiophenol have been employed in NCL to generate a more reactive thioester to enhance the rate of ligation.[75] Various catalysts have been evaluated in the search for the optimal thiol additive to enhance the efficiency of NCL, with thiophenol and (4-carboxylmethyl)thiophenol (MPAA) having the best reactivity.[76] The thiol additives

serve the dual function of acting as reducing agents to prevent disulfide bond formation and promote the ligation reaction.

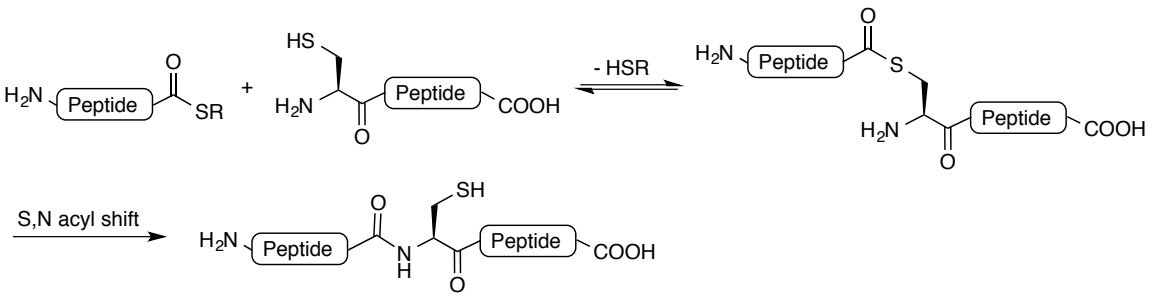

Scheme 3.1: Native chemical ligation.

It has been demonstrated that all twenty amino acids can be used at the C-terminus in NCL, however, the use of bulky β-branched residues including valine, isoleucine, and proline are not favorable due to very slow ligation rates.[77] Although many peptides have been synthesized using NCL, cysteine is one of the least abundant amino acids, consisting of only 1.7% of the residues in natural peptides,[78] thus limiting the applications of this method. Many strategies have been developed over the years to broaden the applications of NCL.

3.5 Methionine Ligation

In 1998, Tam and Yu introduced a methionine ligation technique, applying the strategy of NCL with homocysteine, followed by selective S-methylation to convert the homocysteine residue to methionine (Scheme 3.2).[79] Ligation of homocysteine proceeds through a 1,5 S→N acyl shift resulting in a six-membered ring transition state, which forms slower and is considered less favorable than the five-membered ring transition state attained by the 1,4 S→N acyl shift in NCL.[80] Regardless, the acyl transfer in the ligation of homocysteine occurs rapidly enough to afford the peptide bond. Due to the lack of selectivity of the methylation step, peptides containing unprotected cysteine residues other than at the ligation site are not compatible with this method, limiting the utility of this approach.[81]

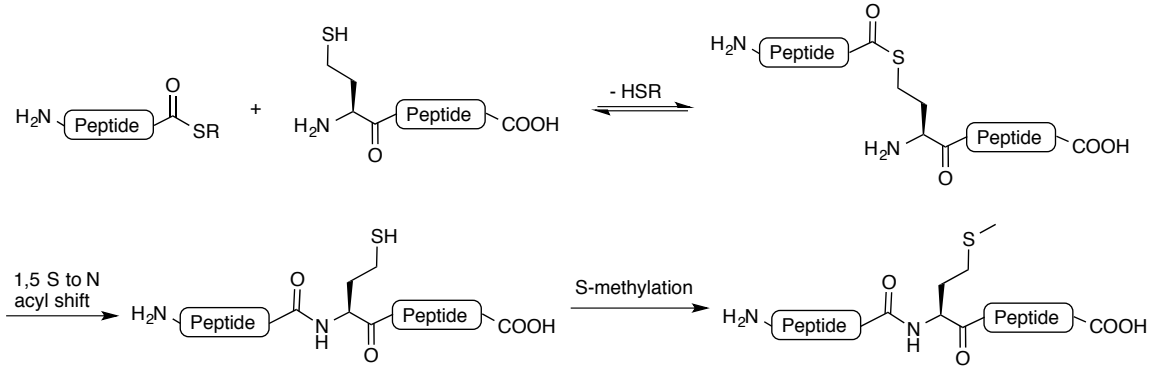

Scheme 3.2: Methionine ligation.

3.6 Thiol Auxiliaries in NCL

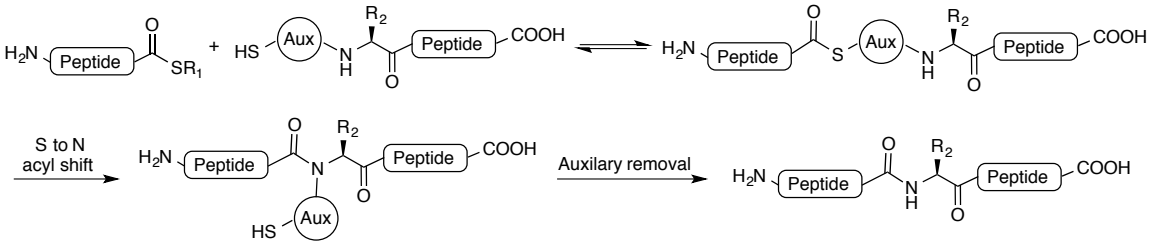

Scheme 3.3: Native chemical ligation utilizing thiol-auxiliary.

To overcome the limitation resulting from the requirement of a cysteine residue in NCL, various removable thiol-containing auxiliaries have been developed to use as cysteine surrogates in NCL (Scheme 3.3).[82-88] The thiol auxiliaries are attached to the end of the N-terminal peptide and react with C-terminal peptide thioesters, in the same manner as cysteine in NCL. After ligation, the auxiliary is then removed to provide the native peptide. A variety of auxiliaries have been developed and implemented in NCL (Figure 3.3). For this method to be practical, the auxiliary must efficiently undergo transthioesterification, promote acyl transfer, and be readily removed after the ligation. High ligation rates were only observed with the use of thiol auxiliaries when at least one of the amino acids at the ligation junction was a glycine residue.[73] The use of thiol-auxiliaries in NCL is not very successful due to slow ligation reaction rates associated with bulky amino acid residues, resulting in poor ligation yields.[80]

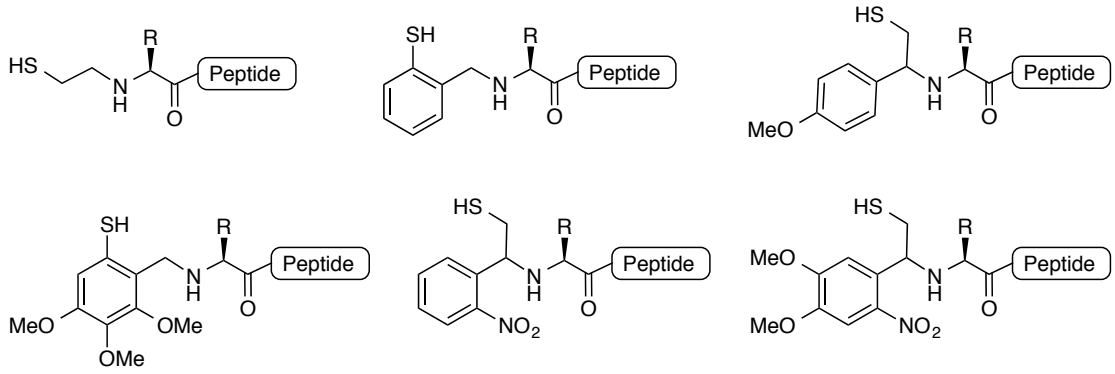

Figure 3.3: Examples of thiol-auxiliaries for use in NCL.

3.7 Ligation-Desulfurization Application in NCL

In an effort to expand the scope of NCL to amino acid residues other than cysteine, the strategy of ligation-desulfurization was developed using unnatural thiol or selenol containing amino acids. The thiol/selenol amino acid derivatives have been used in place of cysteine to perform NCL, and subsequent post-ligation desulfurization/deselenization techniques are applied to restore the natural amino acid at the ligation site.

Yan and Dawson initially developed the method of desulfurization in 2001, applying NCL to a non-cysteine residue by converting cysteine to an alanine residue (Figure 3.4).[81] Desulfurization of cysteine was achieved by metal mediated reduction with hydrogen gas and either palladium or Raney nickel catalyst, with Raney nickel being the most efficient catalyst.[81] Methionine, tryptophan, and unprotected cysteine residues are not compatible with this method due to the lack of selectivity of the reduction conditions, limiting the utility of this approach.[80] In addition, Raney nickel has been

observed to cause epimerization of secondary alcohols and the reduction of thiols, thioethers, and thioesters, prompting the need for a non-metal based desulfurization technique.[89]

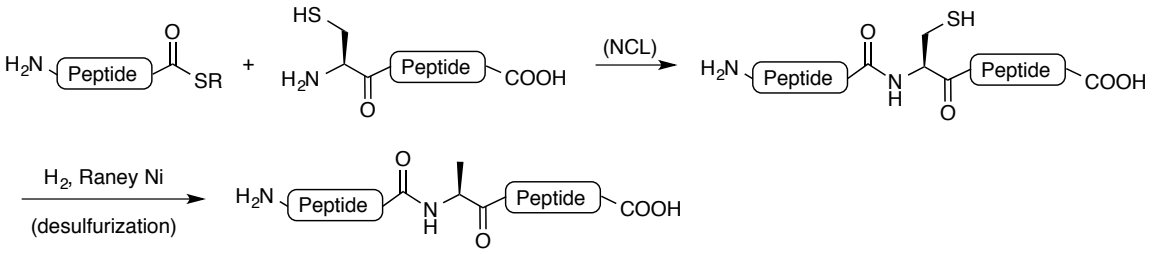

Scheme 3.4: Alanine ligation by the application of ligation-desulfurization to NCL.

In 2007, Wan and Danishefsky developed a selective free-radical based desulfurization technique that can tolerate a variety of functionalities including methionine and N-acetamidomethyl (Acm) protected cysteine residues.[89] This approach utilizes tris(2-carboxyethyl)phosphine (TCEP) and the water soluble radical initiator 2,2'-azobis[2-(2-imidazolin-2-yl)propane]dihydrochloride (VA-044) to selectively reduce free cysteine residues to alanine under aqueous conditions.[89] Additionally, this protocol has been successfully applied to the deselenolization of the unnatural amino acid selenocysteine to the corresponding reduced alanine residue.[89] With the success of this desulfurization technique, this method has been extended to the ligation of a variety of other synthetic thiol and selenol amino acids. Additionally, Guo and coworkers have recently developed another method of cysteine reduction, by way of a visible-light

induced radical desulfurization protocol with selectivity for cysteine reduction in the presence of other sulfur containing functionalities.[90]

The development of these selective and mild metal-free reduction protocols has inspired the efforts to develop methods of ligation at other amino acid residues utilizing the NCL-desulfurization technique. A variety of unnatural thiol containing amino acid residues have been applied to NCL, with the use of β-thiol residues in a cysteine-like ligation and γ-thiol residues to mimic a homocysteine-like ligation. The ligation of thiolated amino acids exhibit increased reaction rates and improved reaction scope in comparison to the method of ligation of thiol auxiliaries.[83] Of these unnatural amino acids, only β-thiol valine (penicillamine) and γ-thiol proline are commercially available. The syntheses of a variety of unnatural thiol containing amino acid residues have been developed.[80] The method of ligation-desulfurization has been applied in the ligation of a variety of other amino acid residues including: valine[91-92], phenylalanine[93-94], leucine[95-96], lysine[97-99], proline[100-101], threonine[102], glutamine[103], tryptophan[104], arginine[105], and aspartic acid[106]. A variety of complex peptide targets have been successfully synthesized utilizing this methodology, including the HIV-1 Tat protein[96], a mucin 1 glycopeptide oligomer[105], modified chemokine receptor CXCR4 (1-38) fragment[106], and human parathyroid hormone (hPTH)[107].

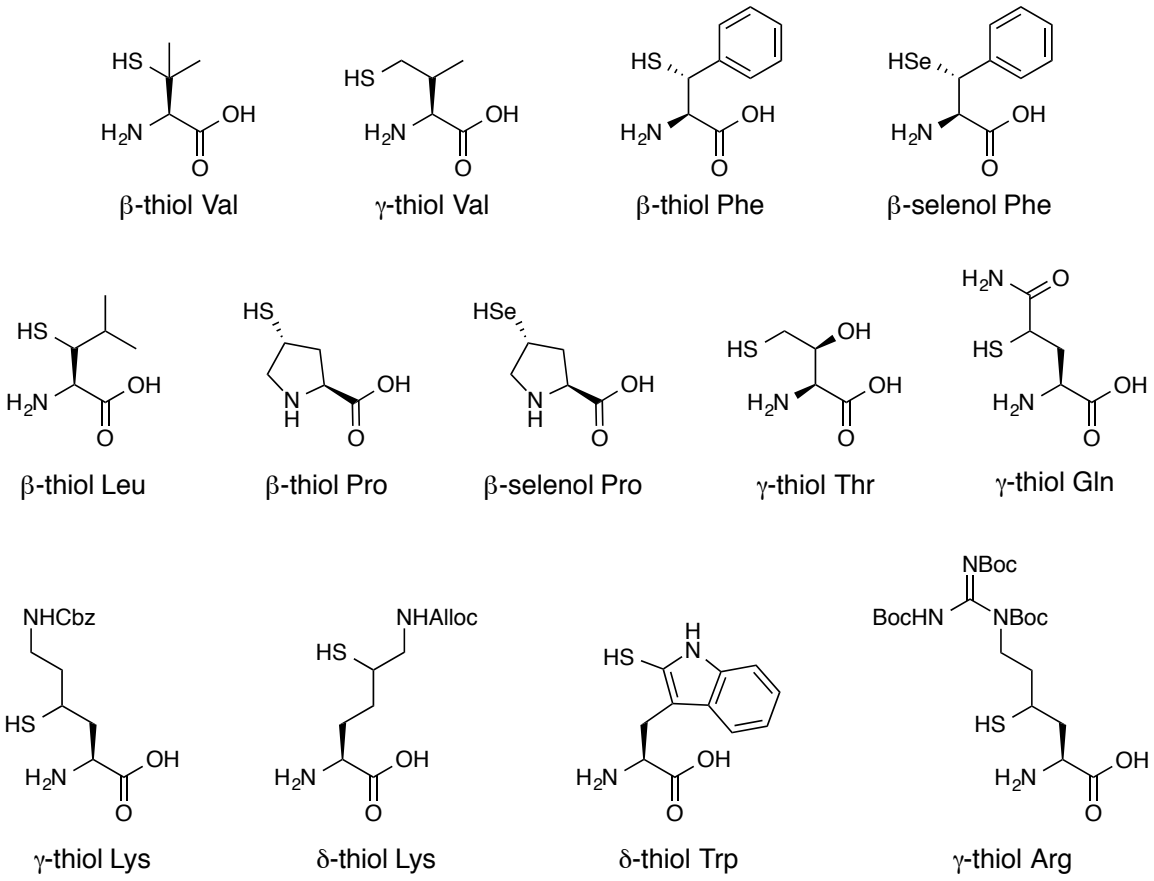

Figure 3.4: Synthetic thiol amino acid cysteine surrogates for NCL.

The common strategy to synthesize thiol or seleno containing amino acids is by functional group substitution, exchanging a hydroxyl group for a thiol group.[80] However, the introduction of a β–, γ–, or δ– hydroxyl group to natural amino acids is challenging, resulting in risks of racemization, lengthy syntheses, and low overall yields. A variety of cysteine surrogates have been synthesized and applied to NCL by the ligation-desulfurization technique (Figure 3.4). However, these unnatural amino acids are not commercially available and take between seven and sixteen steps to synthesize with relatively low overall yield.[80] Additionally, the desulfurization step reduces all cysteine

residues in a peptide in addition to the cysteine at the ligation site[80, 108], thus requiring the protection of all other cysteine residues in the ligated peptide. The added steric bulk and decreased electrophilicity of synthetic secondary and tertiary thiols reduce the overall rate of the ligation.[83, 108] The lack of accessibility of these thiol-amino acids and issues with selectivity of the desulfurization process limits the application of this method. In the effort to broaden the utility of chemical protein synthesis, a variety of unique ligation methods have been developed that do not depend on cysteine.

3.8 Staudinger Ligation

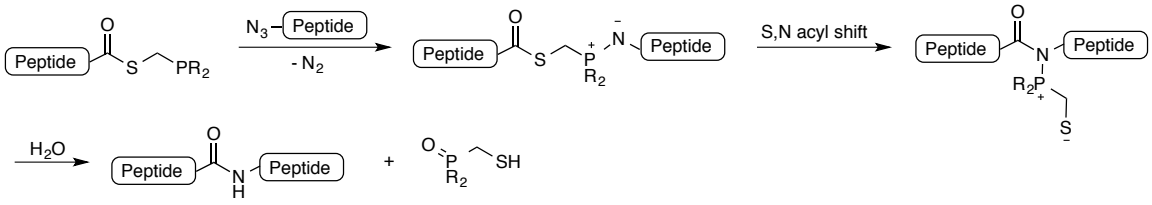

Scheme 3.5: Staudinger ligation.

The Staudinger ligation was introduced independently by Bertozzi[109] and Raines[110] in 2000, as a method of chemoselective ligation based on the Staudinger reaction between an azide and phosphine (Scheme 3.5). In the Staudinger ligation, a phosphine reacts with an azide to form an aza-ylide, followed by an intramolecular acyl shift to from an amidophosphonium salt. Hydrolysis of the salt results in the formation of the native amide bond and phosphine oxide. While this method has yet to be developed

for the synthesis of peptides, it has demonstrated utility in the applications of cell surface engineering[111] and site-specific protein immobilization[112-113].

3.9 KAHA ligation

In 2006, Bode introduced the α-ketoacid-hydroxylamine (KAHA) ligation in which a C-terminal peptide α-ketoacid and N-terminal peptide hydroxylamine react by way of chemoselective, decarboxylative condensation to form a native peptide bond (Scheme 3.6).[114-117] The reaction can be conducted with unprotected peptide fragments in various polar solvents, it is not limited to peptides containing an N-terminal cysteine or thiol derivative, and produces carbon dioxide and water as byproducts.

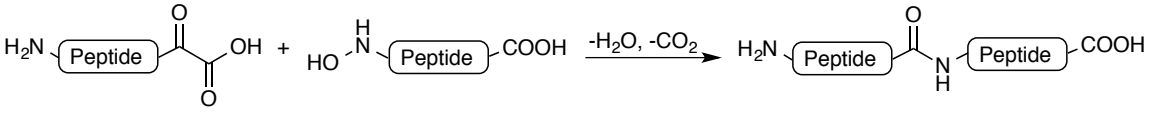

Scheme 3.6: KAHA ligation.

The α-ketoacids are prepared by standard coupling of a stable cyclic cyanosulfur ylide to the C-terminal peptide fragment followed by oxone oxidation to afford the ketoacid (Scheme 3.7).[115] Many unprotected and protected amino acid residues are compatible under the oxidative conditions; however minimal epimerization was observed upon oxidation.[115] The synthesis was extended to create a cyanosulfur ylide linker that can be introduced to a solid support to allow the preparation of α-ketoacids using

standard Fmoc- based SPPS.[116] The hydroxylamine fragments were prepared on single amino acid monomers protected as the N-benzylidene nitrone, which are chemically stable, and can be readily incorporated into SPPS (Scheme 3.7).[117] Amino acid esters are alkylated with bromoacetonitrile, oxidized with mCPBA to a cyano-nitrone, which is then hydrolyzed to the hydroxylamine and isolated as the oxalate salt. The free hydroxylamines are prone to oxidation resulting in oxime formation as the major side product of the ligation.[117] The oxalate salt was reacted with benzaldehyde and base resulting in stable nitrone protected hydroxylamino acids without epimerization.

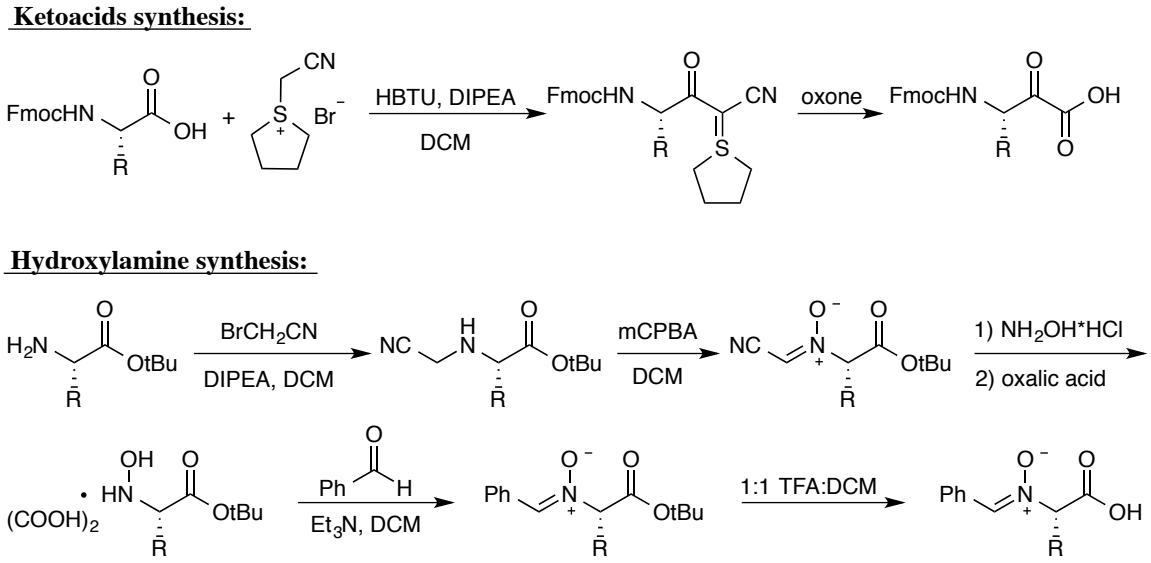

Scheme 3.7: Synthesis of key intermediates of the KAHA ligation.

Figure 3.5: Structures of a) 5-oxaproline, and b) oxazetidine amino acids used in KAHA ligation.

More stable, cyclic hydroxylamino acids were later developed and incorporated with the KAHA ligation, including 5-oxaproline[118-119] and oxazetidine amino acid[120], resulting in homoserine and serine forming ligations (Figure 3.5). These cyclic hydroxylamino acids are not sensitive to ligation or purification conditions, do not result in oxime formation, and can be ligated under aqueous conditions, unlike O-unsubstituted hydroxylamines.[118] This ligation method has been used to synthesize a variety of peptide targets including: a fragment of human glucagon-like peptide (GLP-1)[121], cyclic antibiotic peptide Gramicidin S[122], Pup[118], a derivative of the ubiquitin-fold modifier 1 (UFM1)[123], the 12kDa calcium-binding protein S100A4[120], betatrophin[124], and various other proteins.

3.10 Imine Ligation with Salicylaldehyde Esters

This approach of imine ligation was first introduced by Kemp[125] and developed by Tam[126-127] in 1994. Tam and coworkers utilized the approach of imine induced proximity acyl transfer to ligate unprotected peptide segments containing a C terminal glycolaldehyde with N-terminal cysteine, threonine, and serine containing peptides to form pseudoproline residue at the ligation site (Scheme 3.8). The glycolaldehyde reacts

with the amine to form an imine which cyclizes with the S- or O- nucleophile of the cysteine, serine, or threonine residue to form a thiazolidine or oxazolidine intermediate.[126-127] The cyclic intermediate then undergoes a 1,4 acyl transfer to afford the pseudoproline ligated product. The pseudoproline product is quite stable and the formation of the native peptide linkage was not achieved.[127] This method has been used to synthesize various peptides including an epidermal growth factor-like peptide consisting of fifty amino acid residues[128] and analogs of the antimicrobial peptide bactenecin 7 consisting of fifty-nine amino acid residues in length[129].

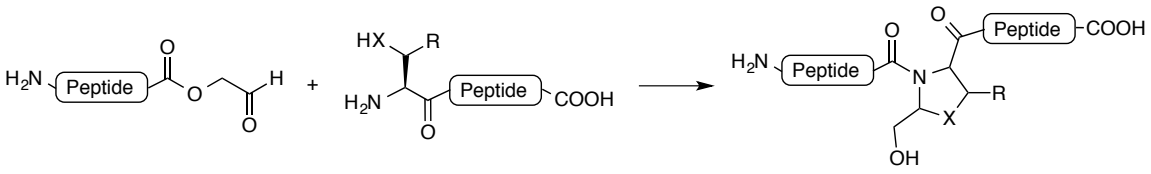

Scheme 3.8: Tam imine ligation- formation of pseudoproline at the ligation site.

In 2010, Li and coworkers expanded the method of imine ligation and developed a method of chemical ligations between serine and threonine with peptide salicylaldehyde esters to form a natural peptide linkage (Scheme 3.9).[130] The challenge was to determine a method that would transform the stable pseudoproline intermediate into the native peptide bond. Introduction of the salicylaldehyde (SAL) ester was envisioned to increase the rate of the β-hydroxyl group reaction with the imine or the O→N acyl shift, however the acyl shift would proceed through a less favorable 1,5 shift.[130] Utilizing a SAL ester at the C-terminus has the advantage of forming an intermediate with an N,O-benzylidene

acetal group which can be removed under acidic conditions by treatment with TFA to release the ligated peptide containing the native peptide bond at the ligation site.[130]

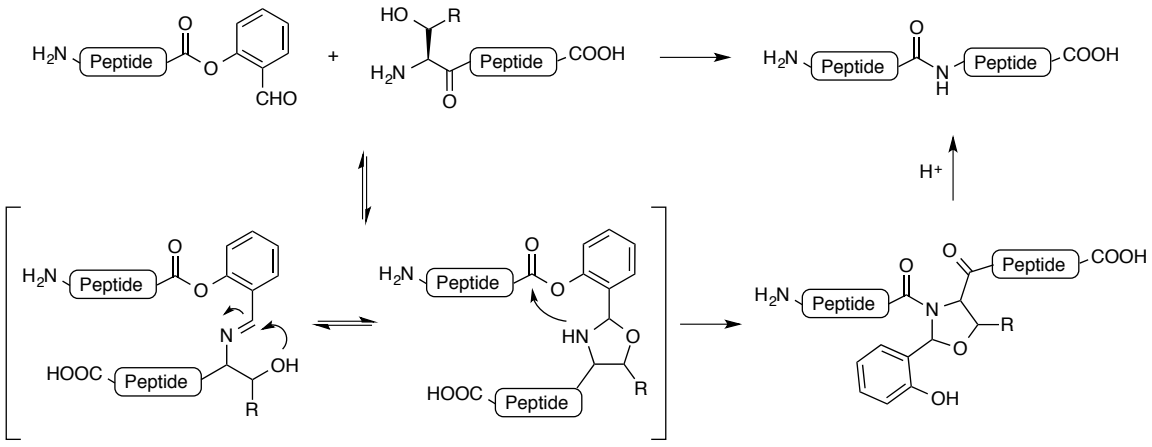

Scheme 3.9: Li imine ligation with salicylaldehyde esters.

The scope of the serine/threonine ligation with SAL amino acid esters was evaluated using an unprotected peptide model with serine at the N-terminus.[131] It was determined that ligation of β-branched amino acids and proline resulted in slow ligation rates, with proline and arginine having the slowest ligation rates.[131] Amino acids with nucleophilic side chains, including aspartic acid, glutamic acid, and lysine are not compatible with the ligation technique due to the instability of the SAL ester.[131] Thus, the method tolerates seventeen of the twenty natural amino acids and has been used to synthesize a variety of target peptides by ligation of peptide fragments synthesized by SPPS. Due to the instability of the SAL ester under Fmoc deprotection conditions of treatment with piperidine, the SAL ester was synthesized by a post-Fmoc-SPPS derivatization approach where the ester is formed by on-resin phenolysis of the C-

terminal peptide N-acyl-benzimidazolinone (Nbz) (Scheme 3.10).[132-133] Subsequent treatment with TFA to remove the side chain protecting groups results in the desired unprotected SAL ester. Alternatively, the SAL ester can be synthesized by Boc-SPPS techniques by ozonolysis of a peptide attached to a 2'-hydroxyl cinnamate linked to AM resin, however cysteine, methionine and tryptophan are not compatible with this method (Scheme 3.10).[133]

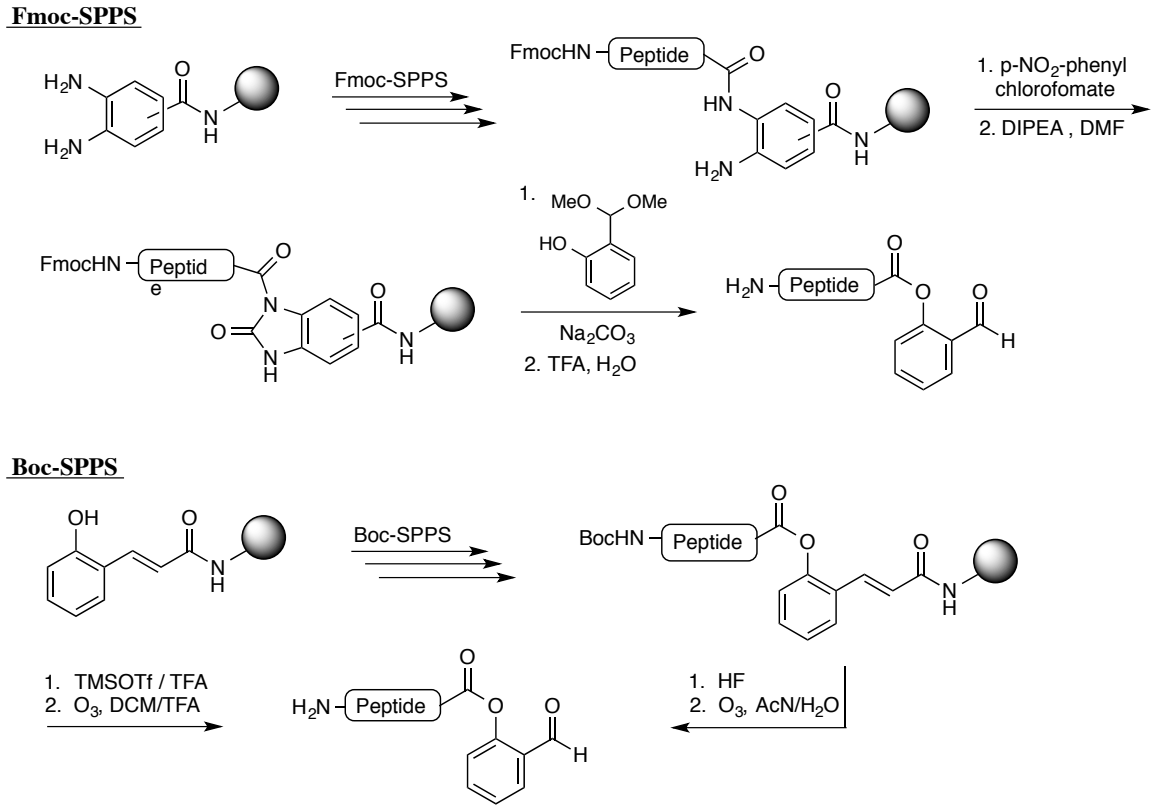

Scheme 3.10: Synthesis of salicylaldehyde esters by Fmoc and Boc SPPS.

This ligation method has successfully been used to synthesize a variety of complex peptide targets including the novel antibacterial teixobactin[134], therapeutic

peptides ovine-corticoliberin and Forteo[132, 135], the human erythrocyte acylphosphatase protein[132], and human growth hormone-releasing hormone (hGH-RH)[136].

3.11 Serine Peptide Assembly

The Pirrung laboratory has developed a method of peptide assembly by ligation of β-hydroxyamines and mildly activated esters.[48, 137] Various lactones and amino acid cyanomethyl (CM) activated esters were demonstrated to react with 1,2-amino alcohols by initial intermolecular transesterification, followed by rearrangement of the ester to the amide by an intramolecular O→N transacylation.[48, 137] This ligation method of transesterification/transacylation follows a similar mechanism to NCL (Scheme 3.11).

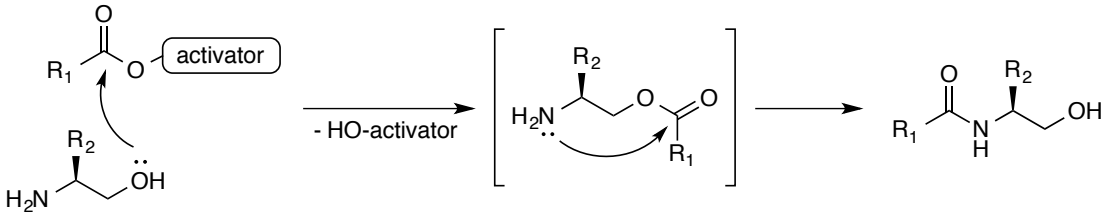

Scheme 3.11: Mechanism of the reaction of activated esters and 1,2-amino alcohols.

The mechanism of this transformation was supported by reactions of acetyl (Ac) valine CM ester with structural variants of the amino alcohol alaninol (Scheme 3.12).[137] When Ac-valine CM ester reacts with alaninol under ambient conditions, the ligation reaction is complete after 72 hours. However, when alaninol TBS ether is used for the ligation, no reaction is observed, demonstrating the essential nature of the alcohol in

these reactions. When N,N-dimethylalaninol is used, only the transesterification product is formed after 72 hours. Additionally, when alaninol N-formamide is used there is no reaction demonstrating the necessity of the basic nitrogen to facilitate transesterification. Hydroxylamines have unique reactivity due to the internal hydrogen bonding between the basic amine and hydroxyl group, which can enhance the reactivity of the hydroxylamine and facilitate transesterification.[48] These results demonstrate that the pathway of these reactions proceeds through a transesterification-transacylation mechanism and not by direct acylation.

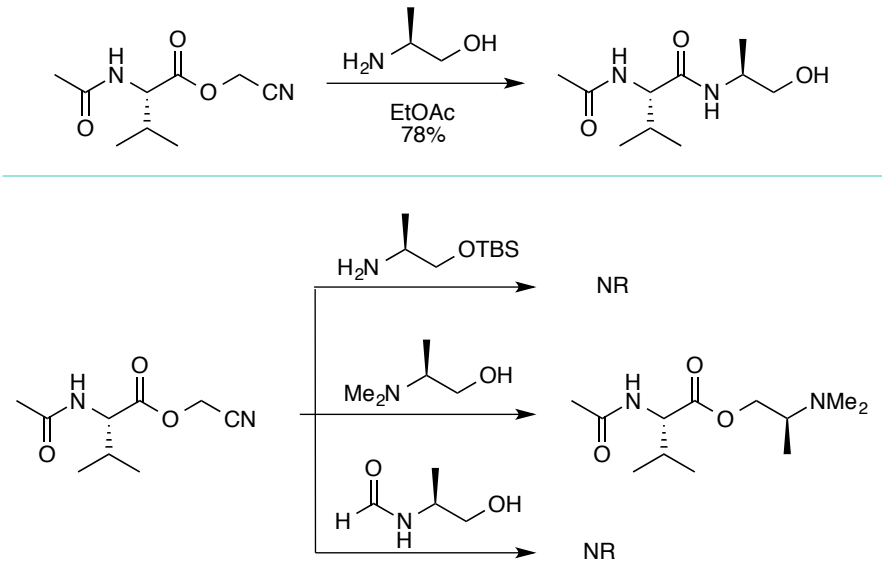

Scheme 3.12: Reactions supporting the transesterification/transacylation mechanism in the ligation of β-hydroxylamines and mildly activated esters.[137]

Various reaction parameters including solvent, additives, reaction time, and temperature were investigated to optimize the hydroxylamine peptide assembly. The use of nonpolar solvents enhances the rate of ligation.[48] Hydrocarbon-based solvents

including hexane and cyclohexane gave the best results, but poor reactant solubility limited their use. It is hypothesized that nonpolar solvents do not interfere with the internal hydrogen bonding that results in the intrinsic reactivity of the hydroxylamines in peptide assembly.[48] Various transesterification catalysts were also investigated and acetic acid and triazabicylodecene (TBD) proved effective at enhancing the rate of reaction.[48] Additionally, the amide ligations proceeded more quickly with microwave heating than at ambient temperatures. The optimized ligation conditions required a combination of nonpolar solvents and transesterification catalysts.

Hydroxylamine peptide assembly was initially studied by the ligation with alaninol as a serine surrogate, and *N*-acetyl amino acid CM esters to represent the C-terminus of a peptide segment. The relative reactivity of different C-terminal amino acids was then examined (Table 3.1).[137] The peptide assembly reactions were performed with a 50% excess of alaninol at 1 M concentrations in ethyl acetate. Ethyl acetate was used as the solvent to provide a relatively nonpolar reaction environment that can adequately dissolve the ligation reactants.[137] A variety of different C-terminal amino acids were ligated, as shown in Table 3.1. Notably, many bulky amino acids including valine and proline were well tolerated in the peptide assembly, while bulky β-branched C-terminal residues are a significant problem in NCL.[77]

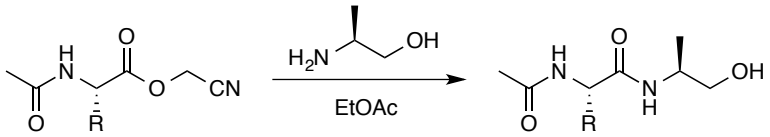

Entry	Ac-AA	Time[a] (h)	Yield (%)	Time[b] (min)	Yield (%)
a	Val	72	78	90	78
b	Leu	72	38	90	53
c	Phe	48	76	90	76
d	Met	48	90	90	91
e	Pro	72	64	90	54
f	Gly	72	72	90	73
g	(Trt)Asn	24	79	ND	ND
h	(Bn)Cys	48	78	ND	ND

[a]Ambient temperature. [b]Microwave heating, 100 °C.

Table 3.1: Peptide amide bond formation with alaninol and N-acetylamino cyanomethyl esters (Table copied from Pirrung, M. C. et al. *Eur. J. Org. Chem.* **2016**, 5633-5636).[137]

When the peptide assembly was extended to the ligation with serine ethyl ester, the reactions were sluggish and yields were less impressive, inspiring the search for better C-terminal activating esters to improve serine peptide assembly.[137] *N*-Boc valine was used to investigate the reactivity of various esters in the ligation with alaninol as a serine surrogate. The reaction times of the ligation reactions with varying mildly activating esters were examined utilizing the standard ligation conditions (Table 3.2). Although CM esters (Table 3.2, entry d) have been used previously in the peptide assembly reactions, it was one of the slower reacting esters examined. There was a substantial increase in reaction rate using fluorinated and vinyl esters, with the fastest being the (methyl trifluorocrototonate)yl (Table 3.2, entry m). Of the fluorinated esters, hexafluoroisoproyl (HIP) and trifluoroethyl (TFE) esters had drastically improved reactivity over CM. Subsequent ligation reactions with the most reactive *N*-Boc valine esters, the fluorinated

and vinyl esters (Table 3.2, entries h-m), and serine ethyl ester were examined. Reaction with HIP and TFE esters resulted in yields greater than 90% in 20-32 hours, whereas the vinyl esters resulted in diminished yields due to the formation of various side products. Thus the HIP and TFE esters were discovered to have the best reactivity. These activated amino acid esters can be prepared by Sn2 reactions with commercially available reagents, eliminating the concern of racemization from activation of a peptide C-terminus and oxazolone formation. The activated esters have also been shown by various control reactions to be racemization resistant under the ligation conditions including microwave heating.[137]

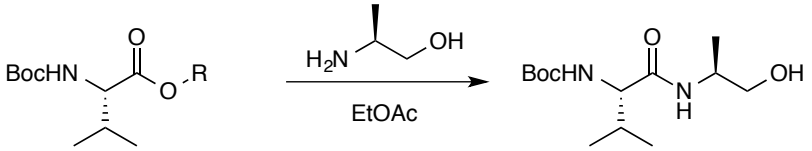

Entry	R	Time (h)
a	CH_2SCH_3	84
b	CH_2CCl_3	80
c	CH_2CH_2Cl	76
d	CH_2CN	70
e	CH_2CHCl_2	54
f	CH_2SOCH_3	50
g	$CH_2SO_2CH_3$	48
h	CH_2CF_3	32
i	$CH_2CF_2CF_3$	28
j	$CH(CF_3)_2$	18
k	$C{=}CH_2[C(CF_3)_2CF_2CF_3]$	18
l	$(MeO_2C)C{=}CH(CO_2Me)$	15
m	$(CF_3)C{=}CH(CO_2Me)$	8

Table 3.2: Reactivity of various mildly activated Boc valine esters with alaninol (Table copied from Pirrung, M. C. et al. *Eur. J. Org. Chem.* **2016**, 5633-5636).[137]

Peptide assembly by ligation of mildly activated amino acids with serine provides a unique approach to amide formation for the synthesis of peptides. These reactions are performed in organic media at high concentrations resulting in favorable process mass intensity making the method greener than most conventional means of peptide coupling.[137] The activated esters can be used in excess and are recoverable after the reaction and can be reused in subsequent ligation reactions. Amino acids with bulky/branched substituents are well tolerated at the ligation site and there is no risk of racemization. The relative abundance of serine in natural peptides is 6.9% (4th abundant), provides greater utility of peptide assembly over NCL that relies on ligation of cysteine, which has a relative abundance of 1.7%.[78] Additionally, peptide assembly can be extended to the ligation of other hydroxyl amino acids.

3.12 Conclusion

Many powerful ligation methods have been developed to expand the scope of peptide chemical synthesis, providing ligation methods that can be applied to a variety of amino acid residues. Many of these methods are very distinct and can be applied independently or orthogonally in peptide syntheses. Recent advances have allowed the synthesis of a wide variety of complex peptides and proteins demonstrating the vast utility of current peptide ligation methodologies.[83] As a result, a variety of peptides have been extensively evaluated and have found applications in medicinal and biotechnology research.[66, 70] It is important to continue to extend the repertoire of ligation methodologies

to enable the synthesis and evaluation of unique bioactive peptides to assess their biological properties and therapeutic potential.

Chapter 4: Peptide Assembly Results and Discussion

4.1 Introduction

The Pirrung laboratory has recently introduced a method of ligation utilizing β-hydroxylamines with mildly activated esters and has applied this technique to serine ligation.[48, 137] This technique mimics the concept of NCL via an intermolecular transesterification, followed by an intramolecular 1,4 O→N acyl transfer. The present work focused on the extension of peptide assembly to other hydroxyl amino acids, threonine and homoserine, broadening the scope of this ligation technique. Oxidation of homoserine post ligation will yield an aspartic acid residue at the ligation site, similar to the concept of using homocysteine in NCL, and post ligation modification to provide a route for methionine ligation.[79] The goal of this project is to study the structure-reactivity relationship in amide ligation of threonine and homoserine with mildly activated esters including 1,1,1,3,3,3-hexafluoroisopropyl (HIP), 2,2,2-trifluorethyl (TFE), and cyanomethyl (CM) esters, which were previously determined by our group to be optimal activators for this type of ligation.[137] The utility of peptide assembly will be demonstrated by the synthesis of the opossum antivenom, lethal toxin neutralizing factor-10 (LTNF-10). The results of this work will enable greater access to ligation junctions that can be used to ligate peptide fragments with this method for preparative peptide synthesis.

4.2 Threonine Ligation

With the success of the ligation with serine and mildly activated esters, the use of threonine with this method will be investigated. Previous work by the Pirrung laboratory on the ligation of β-hydroxylamines with activated esters demonstrated that secondary alcohols could perform the transesterification and transacylation necessary for the ligation to form an amide peptide bond, as demonstrated by the ligation of 1-amino-2-propanol (Figure 4.1) .[48] Threonine contains the required 1,2-hydroxylamine functionality needed to participate in the ligation reaction, however the presence of the secondary alcohol may hinder the reaction making it a less effective substrate than serine in this ligation method.

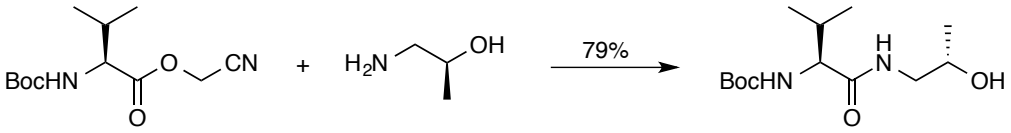

Figure 4.1: Ligation of 1-amino-2-propanol and Boc-valine CM ester.[48]

Threonine peptide assembly was examined by reactions with threonine methyl ester and the corresponding HIP, TFE, and CM activated esters of a variety of acetylated amino acids, including: alanine, valine, phenylalanine, leucine, isoleucine and proline. *N*-Acetyl protected amino acids were utilized as models, as opposed to carbamate protected amino acids, to better represent the C-terminus of a peptide segment. The acetylated amino acid CM and TFE esters are synthesized in a racemization-free manner by S_N2 reactions with the carboxylate as the nucleophile, as previously described.[137] TFE triflate

makes the TFE ester, and bromo- or chloroacetonitrile make the CM ester in fair yields for this study (Figure 4.2). The HIP esters can be synthesized in a similar manner by reaction with HIP triflate, but in poor yield. The yields of the HIP esters were much improved when prepared by coupling using the reagent *N*-(3-dimethyl aminopropyl)-*N*′-ethyl carbodiimide (EDCI) (Figure 4.2). However, coupling reactions can result in amino acid racemization due to oxazolone formation. Therefore, the reaction with EDCI was performed with the addition of the racemization suppressant hydroxybenxotriazole (HOBt) and a large excess of HIP alcohol to promote the intermolecular coupling and diminish the possibility of racemization. The peptide assembly with HIP esters result in a single diastereomer of product indicating that the conditions to synthesize the HIP esters, although not as green as alkylation, do not cause racemization. The acetyl amino acid CM, TFE, and HIP esters were used to study the structure-reactivity relationship of threonine peptide assembly (Figure 4.2).

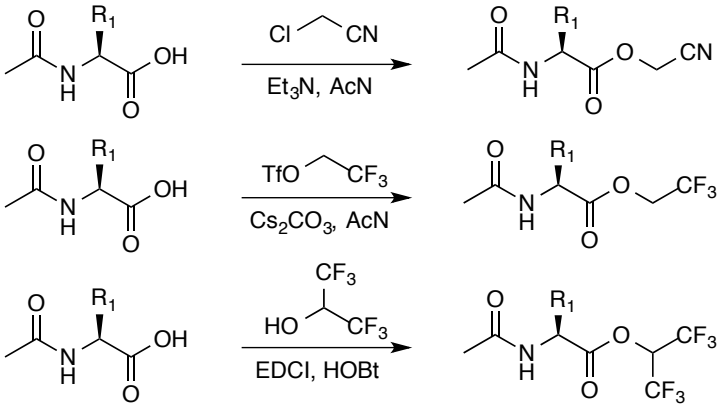

Compound #	Ac-AA	Ester	Yield (%)
4.1	Ala	HIP	92
4.2	Ala	TFE	83
4.3	Ala	CM	94
4.4	Ala	PFP	88
4.5	Val	HIP	93
4.6	Val	CM	90
4.7	Phe	HIP	96
4.8	Phe	CM	93
4.9	Leu	HIP	98
4.10	Leu	CM	96
4.11	Ile	HIP	90
4.12	Ile	CM	98
4.13	Pro	HIP	77
4.14	Pro	CM	94

Figure 4.2: Synthetic route and yield of the Ac-amino acid activated esters.

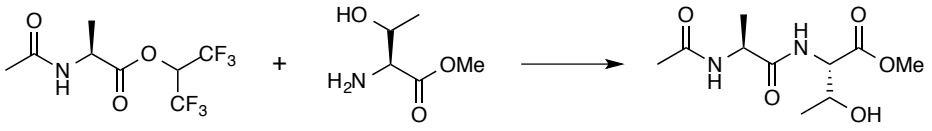

4.1 **4.0** **4.15**

Entry	Solvent[a]	Additive[b]	Time (h)	Yield (%)
a	THF	-	48	93
b	THF	TBD	19	49
c	THF	HIP-OH	60	80
d	THF	AcOH	16	94
e	Hexane	AcOH	10	85
f	Cyclohexane	AcOH	10	79
g	EtAc	AcOH	16	96
h	AcN	AcOH	38	95
i	DMF	AcOH	38	89
j	Toluene	AcOH	40	94
k	DCM	AcOH	72	90

[a] 1 M concentration; [b] Catalytic, 0.2 equiv.

Table 4.1: Threonine ligation reaction optimization at ambient temperature.

Threonine methyl ester **4.0** and acetyl (Ac) alanine HIP ester **4.1** were initially used as model substrates for ligation reaction optimization by examining the reaction parameters- solvent, time, temperature, and catalyst. Table 4.1 summarizes the results. The peptide assembly reactions were conducted at 1 M concentrations with a 50% excess of activated ester. Unreacted ester could be isolated and reused upon purification of the ligation reaction. Initially, **4.0** and **4.1** were ligated utilizing tetrahydrofuran (THF) as the solvent, and after 48 hours the corresponding dipeptide **4.15** was formed in 93% yield (Table 4.1, entry a). To try to increase the rate of reaction, a variety of transesterification catalysts were investigated (Table 4.1, entry b, c, d), with acetic acid (AcOH) proving most effective, reducing the reaction time to 16 hours while maintaining a high product

yield. Triazabicyclodecene (TBD) also drastically increased the reaction rate, however with a lower product yield of 49% (Table 4.1, entry b). The main side product of the reaction was the result of the reaction of threonine with two molecules of the alanine HIP ester, as revealed by NMR and MS, and was obtained in 39% yield (Figure 4.3). In previous work with serine peptide assembly, the use of HIP alcohol was used to catalyze the ligation. However in threonine peptide assembly, the use of HIP alcohol as an additive resulted in a slower rate of reaction. Additionally, other additives including phenol, pyridine and *N,N*-diisopropylethylamine (DIPEA) were ineffective catalysts for the ligation.

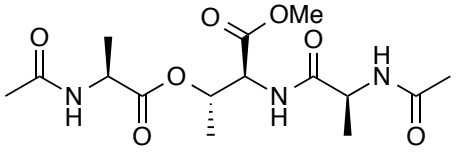

Figure 4.3: The side product in the TBD catalyzed ligation with **4.0** and **4.1**.

The effect of solvent was then investigated, maintaining the use of AcOH as the catalyst (Table 4.1, entries d-k). It was observed that the ligation rate was increased when non-polar solvents like hexane and cyclohexane were used, which is consistent with the results from the previous work with β-hydroxylamine ligations (Table 4.1, entries e and f).[48] Nonpolar solvents do not interfere with the internal hydrogen bonding between the amine and hydroxyl group of the hydroxyl amino acid, which is hypothesized to enhance the reactivity of the hydroxylamine toward transesterification.[48] Unfortunately, the poor solubility of the ligation product **4.15** resulted in incomplete reaction and diminished

yields due to the solidification of the reaction mixture prior to reaction completion (Table 4.1, entries e and f). The use of ethyl acetate as the solvent gave similar results to THF, while the other solvents investigated (Table 4.1, entries h-k) demonstrated a drastic decrease in reaction rate. THF and ethyl acetate proved to be the most suitable solvents for these ligations, providing fast reaction times with the capability to dissolve the ligation reactants, while maintaining a relatively non-polar nature. Of the two options, THF was used in further threonine ligation studies.

Next, the relative reactivity of the different ester activators was investigated (Table 4.2). The reactivity of the HIP, CM, TFE, as well as the 2,2,3,3,3-pentafluoropropyl (PFP) ester of Ac-alanine were examined by ligation with **4.0**. The reactions were conducted at 1 M concentration with 50% excess of Ac-alanine ester. Each reaction provided similar yield of the ligated product but varied in the rate of reaction. As expected, the HIP ester was the most reactive, the CM ester was the second most reactive, followed by TFE and PFP ester. This trend in ester reactivity deviated from the previous results of the ligation of *N*-Boc valine esters and the serine surrogate L-alaninol,[137] with the ester reactivity trend being HIP > PFP > TFE > CM. The difference in ester reactivity of the two ligation systems can be explained by the varying reactivity of the ligating components. Alkyl hydroxylamines can have different reactivity than hydroxyl amino acids resulting from the electron withdrawing nature of the carboxylic acid in hydroxyl amino acids, and/or the activator reactivity may be dependent on the ligation junction. Therefore, the trend in activator reactivity may not be consistent between the ligation of the various amino acids with each of the hydroxyl amino acids

(AA-Ser/Thr/Hse). This hypothesis could be examined in the future by comparing the ligation of serine, threonine and homoserine with all the different amino acid ester combinations.

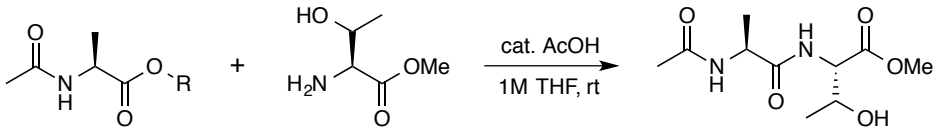

4.0 **4.15**

Entry	Ester	R	Time (h)	Yield (%)
a	HIP	$-CH(CF_3)_2$	16	94
b	CM	$-CH_2CN$	18	98
c	TFE	$-CH_2CF_3$	84	94
d	PFP	$-CH_2CF_2CF_3$	84	93

Table 4.2: Acetyl alanine ester reactivity under optimized ambient conditions.

Previous work with serine peptide assembly showed that microwave heating increases the rate of ligation without compromising reaction yield.[137] Therefore, the model reaction of threonine methyl ester **4.0** and Ac-alanine HIP ester **4.1** were examined with microwave heating under the optimized conditions of THF as solvent and AcOH as catalyst (Table 4.3, entry a and b). After two hours at 70° C, the dipeptide product **4.15** was obtained in 92% yield. Increasing the reaction time to four hours provided the product in a slightly higher yield of 96%. The ligations of **4.0** with other C-terminal amino acids were investigated utilizing microwave irradiation (Table 4.3, entries c-g). The results in Table 4.3 demonstrate that the variation in the C-terminal amino acid is

well tolerated and the successful ligation of proline, isoleucine, and valine is notable, as these amino acids are very poor substrates in NCL.[77]

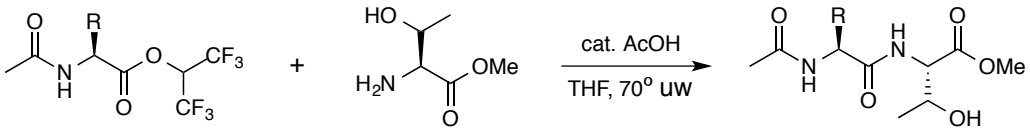

4.0 **4.15-4.20**

Entry	Ac-AA	Time (h)	Yield (%)
a	Ala	2	92
b	Ala	4	96
c	Phe	5	90
d	Pro	5	83
e	Leu	5	70
f	Ile	5	67
g	Val	5	63

Table 4.3: Threonine ligation with *N*-acetyl amino HIP esters with microwave heating.

In summary, peptide assembly by ligation of mildly activated esters has been extended to threonine. The optimized ligation conditions include the use of a relatively non-polar reaction solvent, THF, and the addition of AcOH as a transesterification catalyst. Threonine ligation can tolerate a range of C-terminal amino acids, including residues that are not compatible with NCL. The application of peptide assembly utilizing threonine ligation with mildly activated esters was demonstrated by the synthesis of a target peptide of unique therapeutic value, as described in the next section.

4.3 Application of Peptide Assembly-Synthesis of LTNF-10

Antivenoms are currently the only treatment available for the envenomation by poisonous animals including snakes, scorpions, spiders, ticks, and jellyfish.[138] Generally, antivenoms consist of antibodies that have been collected from animals that were injected with immunogens of a specific venom to induce the production of the neutralizing venom antibodies.[139] The main limitations to the use of antivenoms are that many people are allergic to the animal proteins in which the treatment is made and that the source of the toxin must be identified to administer the proper antidote. Lethal toxin neutralizing factor (LTNF) is a protein isolated from opossum (*Didelphis virginiana*) serum that was discovered to neutralize venoms and toxins from a broad range of poisonous animals, plants, and bacteria.[140] Lipps demonstrated that LTNF is effective in neutralizing venoms of a wide range of snakes, scorpions, bees, as well as neutralizing toxins including plant derived ricin and bacterial toxins botulinum and holothurin.[138] Lipps later identified a peptide fragment of LTNF, LTNF-10 of the sequence Leu-Lys-Ala-Met-Asp-Pro-Thr-Pro-Pro-Leu, to exhibit similar activity to the parent protein against venoms and toxins (Figure 4.4).[141] Due to the neutralization of a diverse range of toxins and venoms, LTNF, and more specifically, LTNF-10, has the potential to be used as a universal treatment for envenomation without the limitations that are posed by traditional antivenoms. LTNF-10 offers a synthetically accessible target with demonstrated potential for the use as an antivenom therapeutic. Komives and coworkers have recently accomplished the synthesis of a LTNF peptide fragment, by applying recombinant DNA technologies with

expression in *E. coli* to produce the LTNF peptide fragment LTNF-11 consisting of the sequence Leu-Lys-Ala-Met-Asp-Pro-Thr-Pro-Pro-Leu-Trp.[139]

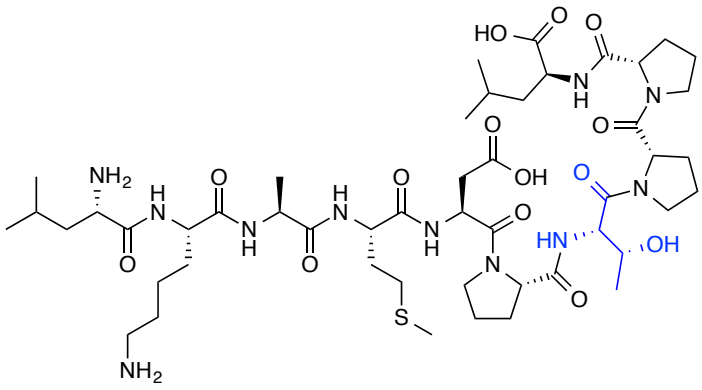

LTNF-10: Leu-Lys-Ala-Met-Asp-Pro-Thr-Pro-Pro-Leu

Figure 4.4: Structure of LTNF-10.

With our development of peptide assembly using activated esters, we decided to apply the technique toward the chemical synthesis of LTNF-10. LTNF-10 is chosen as a model target to demonstrate the utility of our method, due to its amino acid composition and its therapeutic value. The target contains a suitable ligation junction with a threonine residue in the middle of the sequence, which will provide two similarly sized peptide fragments that can be assembled by a convergent synthesis utilizing our method of threonine peptide assembly. LTNF-10 was synthesized by way of a convergent synthesis utilizing SPPS and threonine peptide assembly by the general route outlined in Figure 4.5. The two peptide fragments LTNF-10 (1-6) and LTNF-10 (7-10) were synthesized by a standard Fmoc-SPPS protocol, followed by appropriate functionalization of the fragments: assembly of the LTNF-10 (1-6) activated ester, and formation of the LTNF-

10 (7-10) benzyl ester and subsequent removal of the *N*-Fmoc protecting group to free the terminal threonine hydroxylamine moiety. The two fragments will be ligated by the previously developed threonine peptide assembly method, followed by global deprotection to afford the target peptide. This work will demonstrate the total synthesis of LTNF-10 by peptide chemical synthesis utilizing threonine peptide assembly.

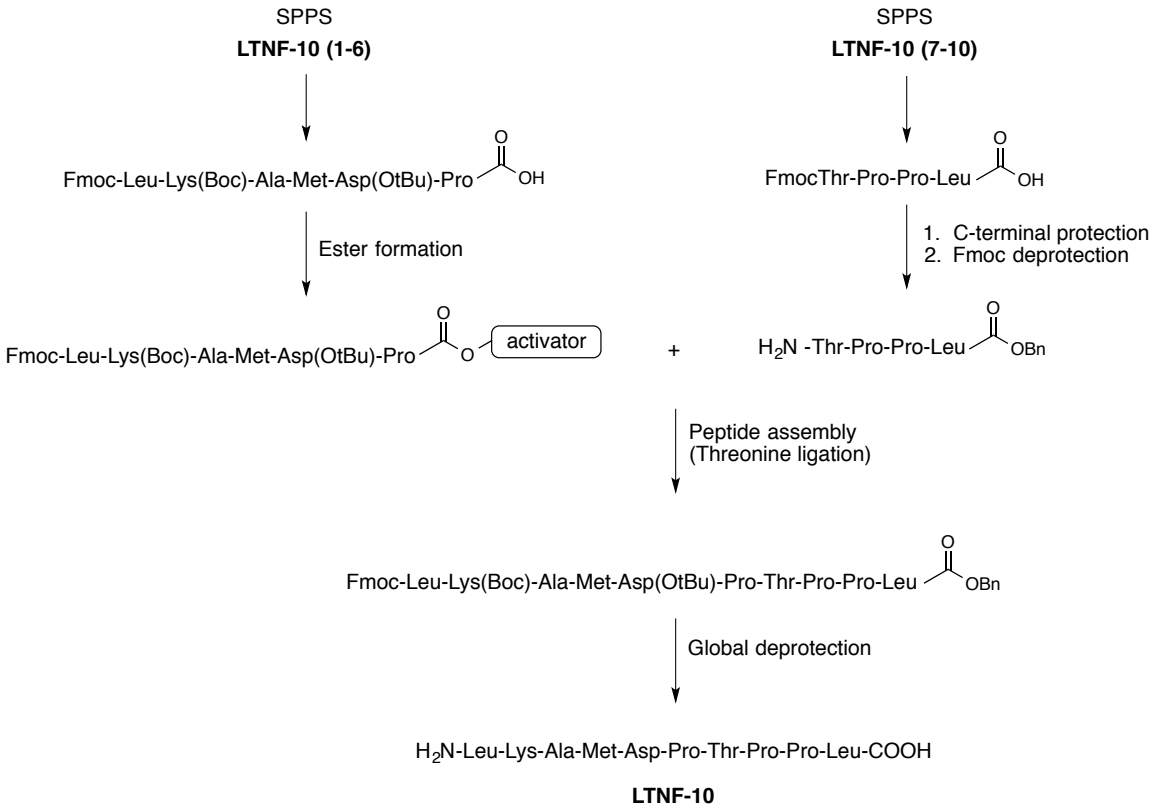

Figure 4.5: Generalized synthetic scheme for the synthesis of LTNF-10.

The LTNF-10 peptide was synthesized from the ligation of the two peptide fragments LTNF-10 (1-6) and LTNF-10 (7-10), containing six and four amino acid

residues respectively (Figure 4.5). First, the two fragments were assembled by Fmoc-SPPS utilizing 2-chlorotrityl chloride resin, HATU and DIPEA for coupling, and 4-methylpiperidine for Fmoc deprotection. The peptides were released from the resin with the side chain protecting groups intact using AcOH/TFE/DCM (1:2:7) to obtain the corresponding peptides, verified by mass spectrometry (MS), in high yield and purity (Scheme 4.1). LTNF-10 (1-6) **4.21** was obtained in 75% yield and LTNF-10 (7-10) **4.22** in 87% yield after precipitation with ether. The HIP activated ester was utilized for the ligation due to superior reactivity compared to the other tested activators, and the encouraging ligation results of the model threonine ligation (Table 4.3, entry 3). The HIP ester of LTNF-10 (1-6) **4.21** was synthesized by coupling using EDCI and racemization suppressant HOBt with an excess of HIP alcohol to obtain the LTNF-10 (1-6) HIP ester **4.23** in 81% yield. The threonine peptide fragment was prepared for ligation by treatment of LTNF-10 (7-10) **4.22** with benzyl bromide and cesium carbonate to afford the corresponding benzyl ester **4.24** in 84% yield, followed by Fmoc deprotection with 1,8-diazabicyclo[5.4.0]undec-7-ene (DBU) and 1-octanethiol to afford the LTNF-10 (7-10) benzyl ester fragment **4.25** with the unprotected N-terminus ready for ligation.

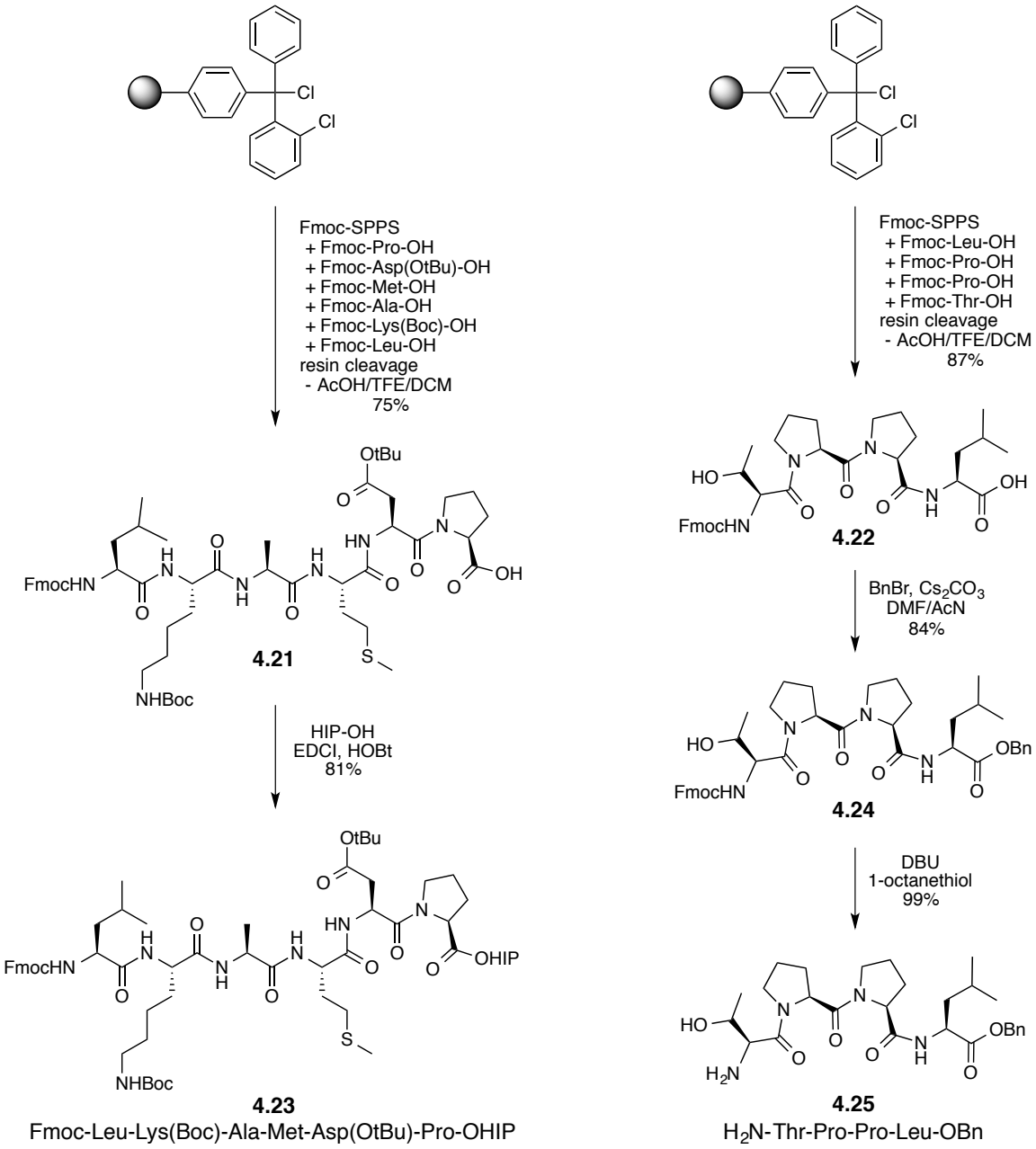

Scheme 4.1: Synthetic strategy of the two peptide fragments **4.23** and **4.25** of LTNF-10.

With the purified peptide fragments in hand, the peptide assembly was attempted. The ligation of the two peptide fragments **4.23** and **4.25** was examined at various conditions shown in Table 4.2. Originally the threonine ligation was performed with the optimized solvent THF. The typical protocol for peptide assembly is to perform reactions at 1 M concentration with 50% excess of activated ester and the addition of catalytic AcOH. However, these ligations had to be conducted at much lower concentrations due to the lack of solubility of the reactants. Initially, the ligation was performed at 0.10 M in THF at room temperature. After five days, the ligation mixture was concentrated and purified by column chromatography, although the reaction was incomplete as revealed by TLC. The product of the ligation **4.26**, verified by MS, was obtained in 17% yield (Table 4.2, entry a). The ligation was repeated in THF at a higher concentration of 0.25 M and the yield of the protected LTNF-10 **4.26** was increased to 25% (Table 4.2, entry b). Additionally, when the ligation was performed in a more polar solvent DMF, at a concentration of 0.33 M for five days, the yield was further increased to 30% (Table 4.2 entry c). In the ligation of **4.23** and **4.25**, an increase in the reaction concentration resulted in an increase in product yield. Results from previous work on peptide assembly,[48, 137] demonstrated that ligation rate is directly related to reaction concentration. Although an increase in product yield is not indicative of an increase in reaction rate, it could be a contributing factor for the observed increase in the product yield in the ligation of **4.23** and **4.25**. When the ligation was conducted with microwave heating for five hours, the yield decreased dramatically, even though the reaction had proceeded to completion, as indicated by TLC (Table 4.2, entry d).

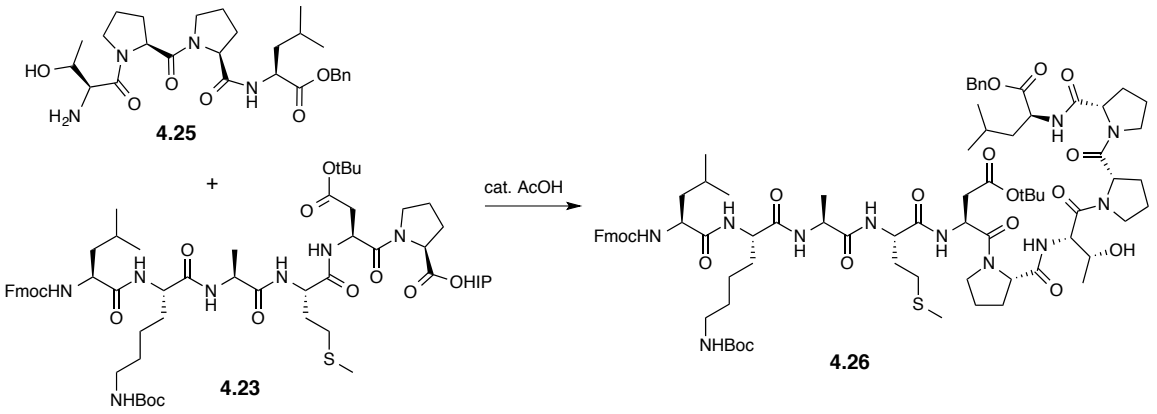

Entry	Conditions	Solvent	Concentration (M)	Yield (%)
a	5 d, rt	THF	0.10	17
b	5 d, rt	THF	0.25	25
c	5 d, rt	DMF	0.33	30
d	5 h, 70° μw	THF	0.25	10

Table 4.4: Ligation between the peptide fragments LTNF-10 (1-6) **4.23** and LTNF-10 (7-10) **4.25**.

Although the reaction rate was sluggish, the ligation of the two LTNF-10 fragments with threonine peptide assembly was successful, providing **4.26** in 30% yield. Optimization of the reaction conditions can be further investigated to improve the rate of ligation and overall yield, including utilizing a larger excess of activated ester or determining optimal microwave heating conditions that can increase the reaction rate without compromising product yield.

Global protecting group deprotection of the ligation product **4.26** was conducted to afford the desired target LTNF-10 (Scheme 4.2). Deprotection was performed in three steps. First, the C-terminal benzyl ester was cleaved by hydrogenation catalyzed by 10% palladium on activated carbon in AcOH/MeOH (1:9). Next, the amine *N*-Fmoc protecting

group was removed by treatment with 4-methylpiperidine (20% volume in DCM). Finally, the side chain protecting groups were removed by treatment with a mixture of TFA, water, and triethylsilane (95/2.5/2.5). The crude peptide was purified by ether precipitation and verified by mass spectrometry. LTNF-10 was obtained as the TFA salt in 54% yield over the three steps.

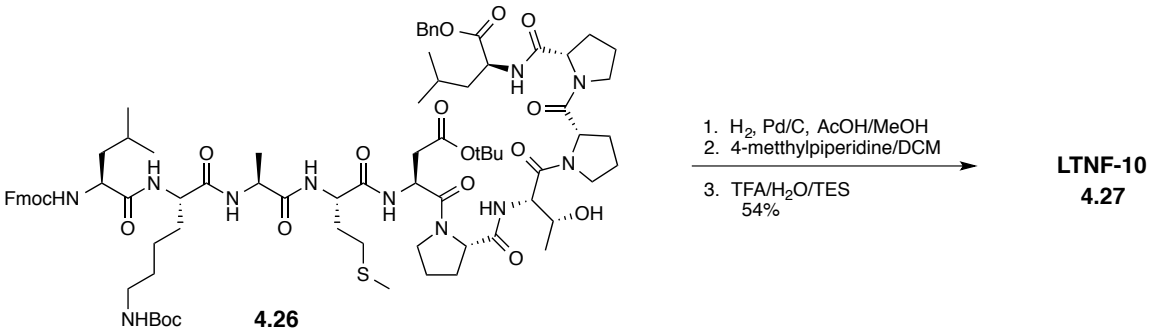

Scheme 4.2: Global deprotection of ligated product to produce LTNF-10.

The utility of peptide assembly was demonstrated by the successful synthesis of the target peptide LTNF-10 by threonine ligation. The ligation at a challenging junction between proline and threonine was achieved. Additionally, this work provides the chemical synthesis of antivenom peptide LTNF-10.

4.4 Homoserine Ligation

With the success of extending and applying the method of peptide assembly by ligation with activated esters to threonine, the ligation of homoserine was then investigated. The idea of homoserine peptide assembly was inspired by the method of methionine ligation with the use of homocysteine in NCL, followed by post-ligation modification to transform homocysteine to a methionine residue by selective methylation.[79] Selective oxidation of homoserine post peptide assembly will generate an aspartic acid residue at the ligation site (Figure 4.6). Ligation with homoserine can further broaden the scope of peptide assembly by extending to ligation to aspartic acid residue junctions.

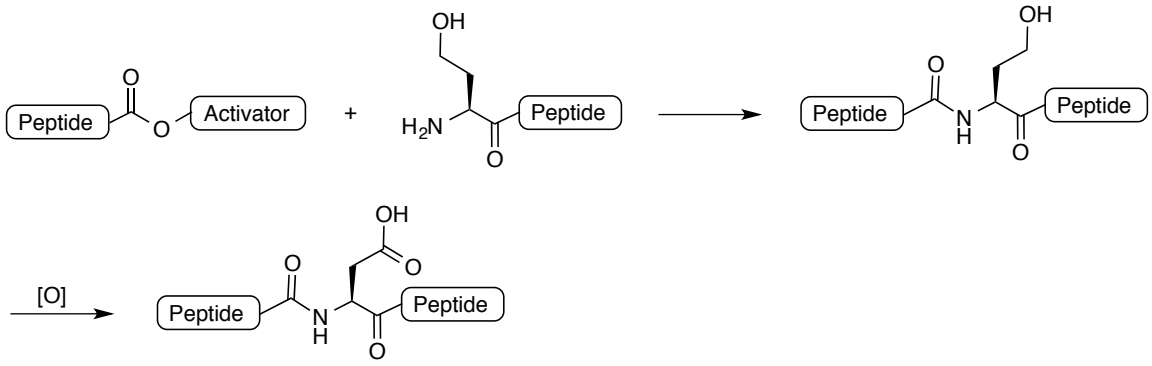

Figure 4.6: General overview of homoserine peptide assembly and subsequent oxidation to afford aspartic acid residue at the ligation site.

The trial reaction of the ligation with 3-amino-1-propanol **4.28** and Ac-valine HIP ester **4.5** demonstrated that peptide assembly is not limited to 1,2-hydroxylamine functionalities, as supported by previous studies with 3-amino-1-propanol ligations by the

Pirrung laboratory (Figure 4.7).[48] Nonetheless, ligation with homoserine will proceed through a 1,5 O→N acyl transfer pathway resulting in a six-membered ring transition state, which is less favorable and may form slower than the five membered ring transition state resulting from the 1,4 O→N acyl transfer in serine and threonine peptide assemblies. Thus, homoserine peptide assembly will be less efficient than serine peptide assembly. The structure-activity relationship of homoserine peptide assembly was investigated in a similar manner as was accomplished with threonine. The acetylated amino acids alanine, valine, phenylalanine, leucine, isoleucine, and proline were converted to the selected activated esters (CM, TFE, and HIP) and utilized in the study of homoserine peptide assembly (Figure 4.1). For the direct comparison of the reactivity of homoserine and serine in peptide assembly with the mildly activated esters, the dipeptide homoserine phenylalanine methyl ester **4.31** was proposed as a model substrate to mimic previous work on serine peptide assembly.[137] The peptide assembly with homoserine will be conducted utilizing the optimized reaction parameters: 1 M concentration in THF with a 50% excess of activated ester and the addition of catalytic AcOH.

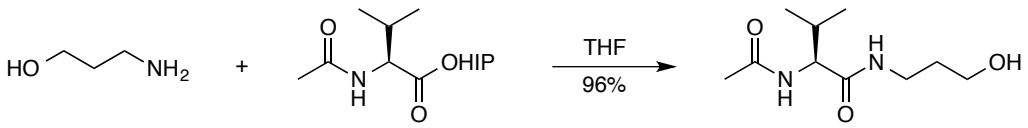

4.28 **4.5** **4.29**

Figure 4.7: Ligation of 3-amino-1-propanol and Ac-valine HIP ester.

Initially, the synthesis of the model dipeptide **4.31** was attempted by traditional peptide coupling between *N*-Boc protected homoserine **4.30** and phenylalanine methyl

ester with EDCI and HOBt (Scheme 4.3). However, it was observed that upon carboxylate activation, the formation of the corresponding lactone **4.32** was highly favored and was the dominant product of the reaction. The homoserine lactone formation proved to be a recurring issue in the development of homoserine peptide assembly.

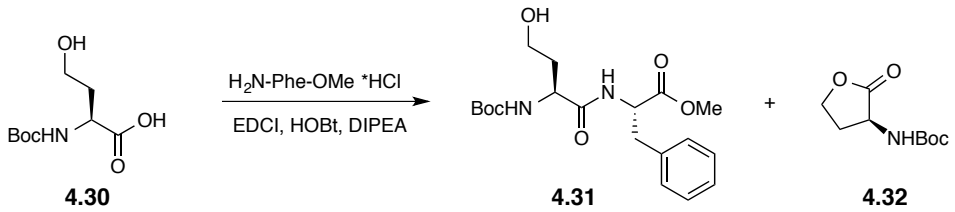

4.30 **4.31** **4.32**

Scheme 4.3: Proposed synthesis of model homoserine dipeptide.

In order to obtain the desired dipeptide, *N*-Boc homoserine with a benzyl protected alcohol **4.33** was used to afford the protected dipeptide **4.34** in 91% yield (Scheme 4.4). To afford the free hydroxylamine for ligation, first the benzyl ether was removed by hydrogenation followed by treatment with HCl to remove the *N*-Boc group and subsequent neutralization with MP-carbonate resin to afford the free amine **4.36**. The TLC analysis of **4.36** revealed that the desired amine was impure and contained a variety of side products. It was discovered that the acidic conditions of the *N*-Boc removal promoted acid catalyzed formation of the lactone, resulting in the formation of byproducts **4.37** and **4.38**. Therefore, it was necessary to avoid the use of strongly acidic reaction conditions that could promote lactone formation.

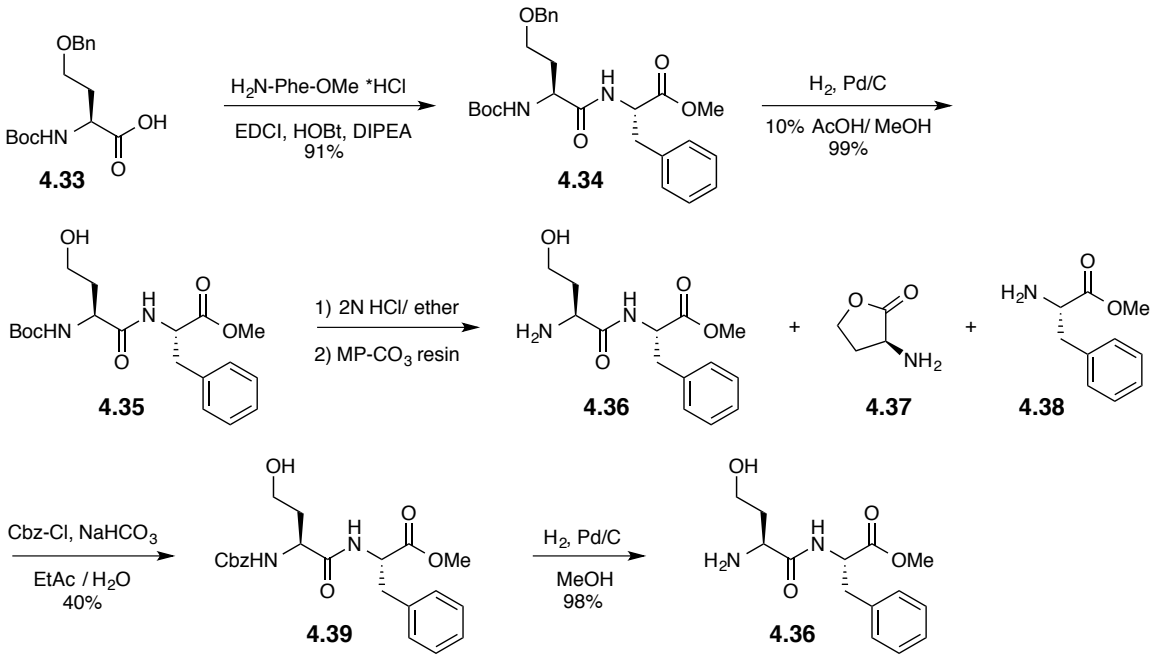

Scheme 4.4: Attempted synthesis of the model homoserine dipeptide **4.36**.

The carbobenzyloxy (Cbz) *N*-terminal protecting group was implemented to prevent further issues resulting from lactone formation. The *N*-Cbz group can be readily cleaved by hydrogenation to provide the pure amine product with minimal purification. Accordingly, the resulting reaction mixture containing **4.36** was subjected to Cbz amine protection and purified to obtain dipeptide **4.39** in 40% yield (Scheme 4.4). The *N*-Cbz dipeptide **4.39** was subjected to hydrogenation to afford the pure free hydroxylamine **4.36** for ligation, in 98% yield. Unfortunately, it was discovered in the attempt to ligate **4.36**, the main product of the ligation was the corresponding diketopiperizine (DKP) **4.40** (Scheme 4.5). Therefore, a different C-terminal protecting group on the homoserine dipeptide was required to suppress DKP formation.

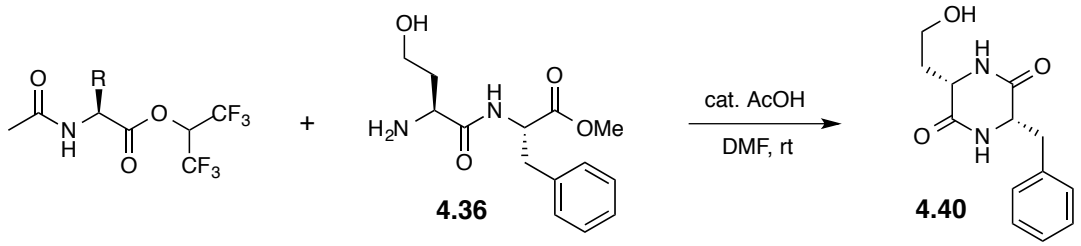

Scheme 4.5: Attempted homoserine ligation resulting in diketopiperizine formation.

At this point, the model peptide to demonstrate the ligation of homoserine in the peptide assembly needed to be redesigned. Conditions that promote the formation of homoserine lactone needed to be avoided, and a larger and less reactive C-terminal protecting group was needed to suppress DKP formation. The optimal homoserine amino acid starting material would be *N*-Cbz *O*-benzyl homoserine, so that global deprotection of the assembled dipeptide could be achieved in one step to afford pure peptide with minimal work-up. Unfortunately, the only commercially available homoserine derivatives have orthogonal amine and side chain protecting groups and are relatively expensive. A work around procedure had to be devised to synthesize pure hydroxylamine dipeptide for ligation.

Next, we decided to introduce a triphenylmethyl (trityl) amide at the C-terminus of the model dipeptide to eliminate the ligation side reaction of DKP formation. Trityl amides are particularly difficult to synthesize on bulky amino acid residues, so phenylalanine was replaced with the less sterically hindered amino acid glycine. The new ligation model of interest was the dipeptide homoserine glycine trityl amide **4.44** (Scheme 4.6). *N*-Boc-glycine **4.41** was coupled with tritylamine to generate the corresponding dipeptide **4.43** in 66% yield. HATU was the optimal coupling reagent for

this transformation. After Boc removal, the glycine trityl amide was coupled to Boc-Hse(Bn) **4.33** to obtain **4.44** in 95% yield. However, the palladium-catalyzed hydrogenation to remove the benzyl ether did not proceed as intended. In addition to removal of the benzyl ether, the trityl was also cleaved from the amide, resulting in a mixture of products.

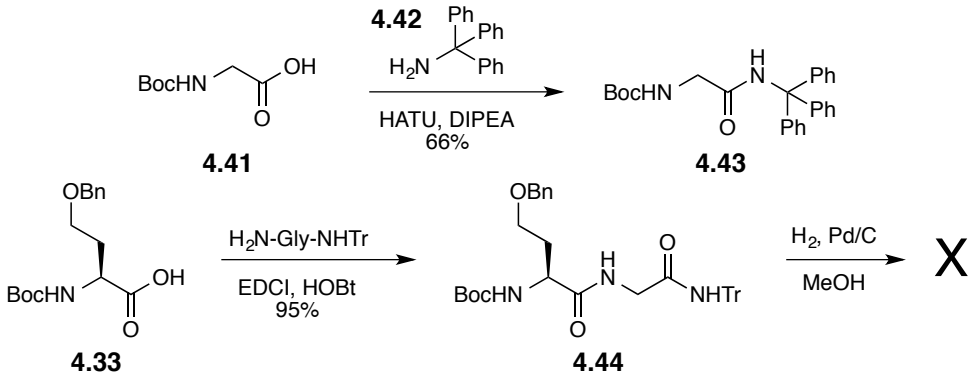

Scheme 4.6: Attempted synthesis of the model homoserine dipeptide.

Due to the incompatibility of trityl and benzyl protecting groups, a different C-terminal protection was needed. The incorporation of a *tert*-butyl amide as the C-terminus of a model homoserine dipeptide was devised and implemented. The use of *tert*-butyl amide would inhibit DKP formation, it is easily accessible by the coupling of *tert*-butyl amine, and it is stable to both hydrogenation and mild acidic conditions utilized for Boc removal. The *tert*-butyl protecting group can be removed from amides by treatment with either triflic acid[142-143] or copper (II) triflate[144]. The desired model dipeptide consisting of homoserine and phenylalanine can be generated with the *tert*-butyl amide at the C-terminus (Scheme 4.7). First, *N*-Boc-phenylalanine and *tert*-butyl amine were

coupled with HATU to provide **4.46** in 98% yield. After subsequent Boc-removal, the phenylalanine *tert*-butyl amide was coupled to **4.33** with EDCI and HOBt to obtain **4.47** in 98%. The benzyl ether was then cleaved by hydrogenation to provide **4.28** in 95% yield. Due to the formation of homoserine lactone under acidic conditions, the *N*-Boc protecting group of dipeptide of **4.48** was converted to Cbz over two steps in 58% yield. *N*-Boc removal was carefully conducted at low temperatures with minimal reaction time in attempt to optimize the product yield by suppressing lactonization. Finally, the *N*-Cbz group was removed by hydrogenation to afford pure hydroxylamine **4.49** in 97%.

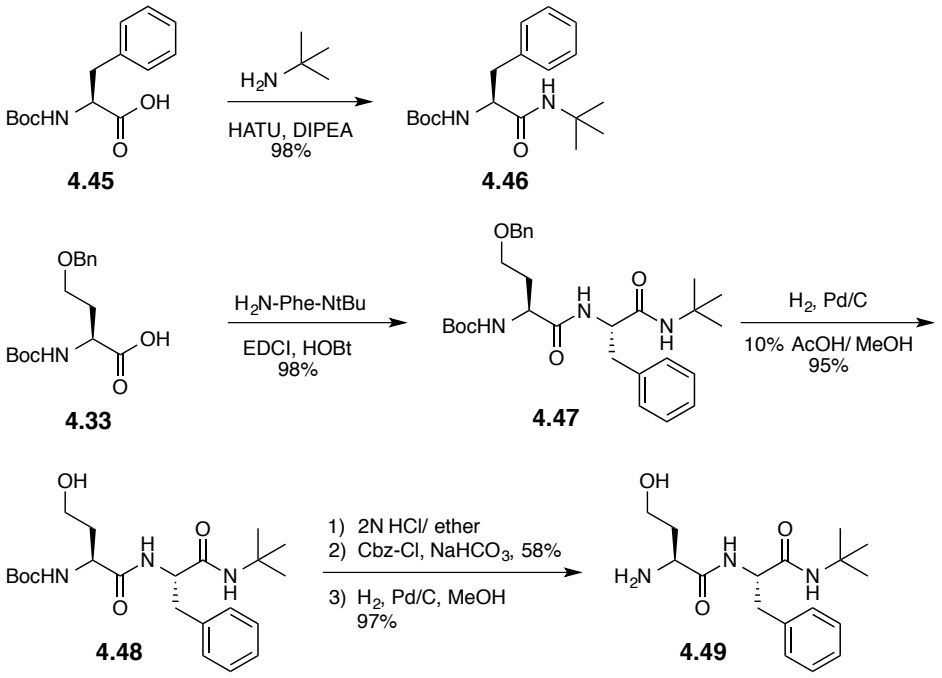

Scheme 4.7: Synthesis of model homoserine dipeptide **4.49**.

An attempt to optimize the synthesis of the target peptide by avoiding pathways that result in homoserine lactonization was investigated (Scheme 4.8). The *N*-Cbz amine protection was preformed prior to the removal of the benzyl ether to afford **4.50** in 81% yield. The generated intermediate **4.50** could then be globally deprotected in one step by palladium-catalyzed hydrogenation to obtain **4.49** to use for ligation. In theory, this synthetic route would shorten the synthesis and increase the overall yield by eliminating the least efficient step that resulted in the formation of the homoserine lactone. When deprotecting dipeptide **4.50** to afford the unprotected homoserine dipeptide **4.49**, the hydrogenation reaction was very sluggish and did not proceed to completion. After extended reaction time, decomposition of the free dipeptide was observed. This route was not successful in providing the pure hydroxylamine **4.49** for peptide assembly.

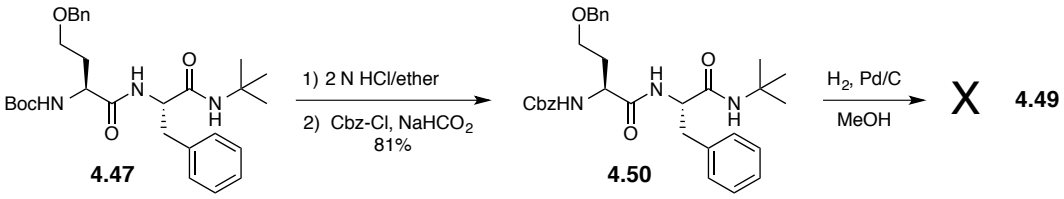

Scheme 4.8: Alternative synthetic route to the homoserine dipeptide **4.49**.

The structure-reactivity relationship of the homoserine peptide assembly was studied by ligation using the homoserine dipeptide **4.49** with various acetylated amino acid HIP, TFE, and CM activated esters. The peptide assemblies were conducted utilizing the optimized reaction parameters: reactions were preformed at 1 M concentration with a 50% excess of ester and the addition of catalytic AcOH. Due to the limited solubility

observed in previously attempted homoserine ligations, DMF was used as the reaction solvent in place of THF. The homoserine peptide assembly was first examined at ambient temperatures with a variety of acetyl amino acid esters (Table 4.5). Initially, ligation with alanine HIP ester **4.1** and **4.49** was performed and the reaction was complete within ten hours (Table 4.5, entry a). However, the compound resulting from homoserine reacting with two molecules of the alanine HIP ester was the main side product of the reaction (Figure 4.8), as indicated by NMR and MS, similar to the compound observed in the TBD catalyzed ligation between threonine and alanine. Thus, the ligation between homoserine and alanine were then examined with the other ester activators TFE and CM to compare the reactivity (Table 4.5, entries b and c). Switching away from the HIP ester resulted in an increase in product yield, although accompanied by a drastic decrease in reaction rate. Minimal amounts of the overreacted ligation product were also observed in these reactions. The poor results of the ligation between the model homoserine dipeptide and Ac-alanine HIP ester in comparison to TFE and CM can be explained by the following hypothesis. The HIP ester is the best activator to induce the ligation transesterification step and alanine has minimal steric hindrance compared to other acetylated amino acids used in this study. The combination of limited steric hindrance due to the lack of a large β-branched alkyl group and a more reactive ester allows transesterification reaction to happen more readily a second time after the ligation has occurred. This is observed more readily with HIP than with the other activators.

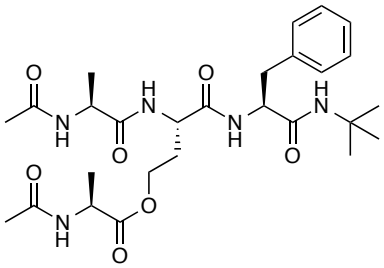

Figure 4.8: Main side product of the homoserine ligation with **4.1** and **4.49**.

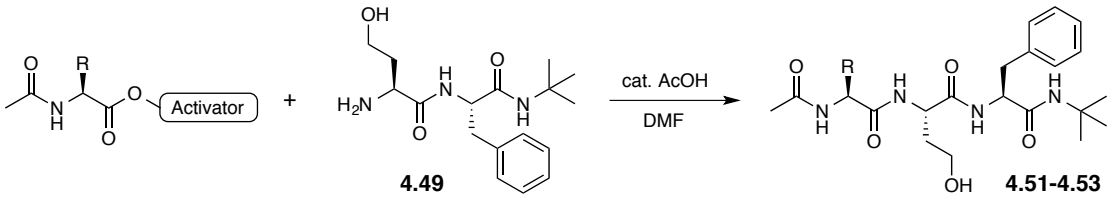

Entry	Ac-AA-OR	Time (h)	Yield (%)
a	Ala-OHIP	10	40
b	Ala-OTFE	50	84
c	Ala-OCM	30	89
d	Phe-OHIP	12	53
e	Val-OHIP	84	46

Table 4.5: Results of homoserine ligation with N-acetyl amino esters at ambient conditions.

The ligations of homoserine with phenylalanine and valine HIP esters were also examined at ambient conditions (Table 4.5, entries d and e). The ligation with phenylalanine was complete after 12 hours to obtain the corresponding tripeptide in 53% yield. When valine was employed in the homoserine ligation, the reaction was much slower and was complete after 84 hours with a yield of 46%. Additionally, the formation of various unidentified side products during the homoserine peptide assemblies resulted in diminished ligation product yields. The side products are likely due to the instability of

the homoserine peptides resulting in decomposition by lactone formation. Previous work on serine peptide assembly demonstrated the successful ligation of serine phenylalanine methyl ester with Ac-valine TFE ester, in 36 hours with 76% yield (Figure 4.9).[137] Although the serine ligation example with valine could not be reproduced identically with homoserine, indirect comparisons can be made to explain the decreased reactivity of homoserine ligations. The reaction rate of homoserine peptide assembly is notably much slower compared to serine peptide assembly. As mentioned, homoserine ligation proceeds through a 1,5 O→N acyl transfer pathway resulting in a less favorable six-membered ring transition state, which could result in the observed slower rate of reaction. Additionally, it could be possible that the initial transesterification step is not as favorable, which could be the result of weaker internal hydrogen bonding of the hydroxylamine moiety causing the hydroxyl group to be less nucleophilic and thus homoserine to be intrinsically less reactive.

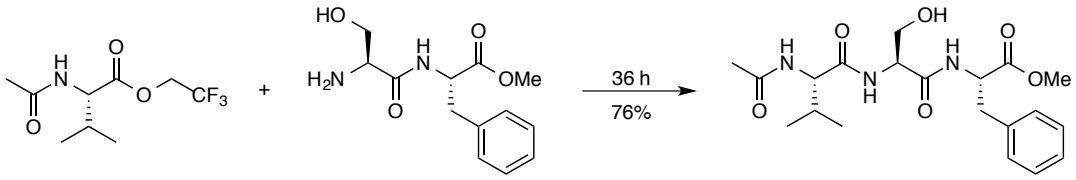

Figure 4.9: Previous work on serine peptide assembly.

Microwave heating was employed to enhance the rate of the homoserine peptide assembly reactions (Table. 4.6). As demonstrated by the results obtained from the homoserine ligation with phenylalanine and valine HIP esters (Table 4.6, entries b and d),

the rate of the reactions was increased without an increase in byproduct formation that would reduce the product yield. In two hours, phenylalanine and valine ligated tripeptides were obtained in 52% and 46% yield respectively. The ligations of **4.49** with other C-terminal amino acids were all investigated utilizing microwave heating. Results summarized in Table 4.6 demonstrate that variation in the C-terminal amino acid is well tolerated and products are obtained in fair yields. Additionally, the reactivity of HIP and CM esters were compared by homoserine ligation with microwave heating (Table 4.6). Peptide assembly with CM esters required double the reaction time to HIP esters for the ligation to proceed to completion. In most cases homoserine ligation with CM esters resulted in similar but slightly poorer product yield when compared to the HIP esters.

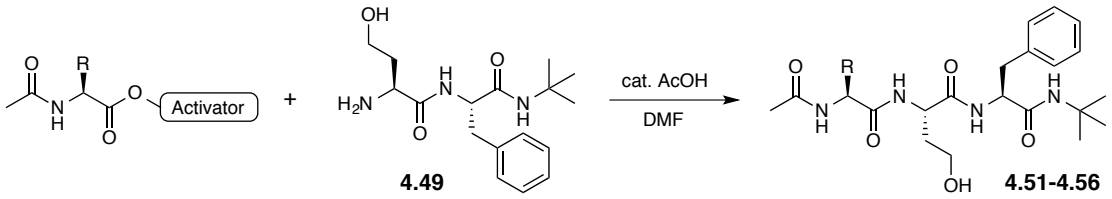

Entry	Ac-AA-OR	Time (h)	Yield (%)
a	Ala-OCM	2	62
b	Phe-OHIP	2	52
c	Phe-OCM	2	38
d	Val-OHIP	2	46
e	Val-OCM	4	41
f	Pro-OHIP	2	76
g	Pro-OCM	4	52
h	Leu-OHIP	2	34
i	Leu-OCM	4	37
j	Ile-OHIP	2	56
k	Ile-OCM	4	34

Table 4.6: Results of homoserine ligation with *N*-acetyl amino esters with microwave heating at 70 °C.

Bode and coworkers have successfully replaced the residues methionine, isoleucine, asparagine, aspartic acid, and glutamic acid with homoserine using the KAHA ligation to synthesize bioactive peptides without observing a negative impact on their bioactivity.[124] However, simple amino acid substitutions are not always tolerated and can alter the peptide structure resulting in a negative impact on the peptide activity. Therefore, we examined post-ligation oxidation to convert homoserine to an aspartic acid residue at the ligation site. A mild oxidation protocol using trichloroisocyanuric acid (TCICA) and 2,2,6,6-tetramethyl-1-piperidinyloxy (TEMPO) was explored. This method provides a mild and chemoselective oxidation of alcohols to the corresponding carboxylic acid in an efficient one–pot reaction.[145] In the application of homoserine peptide assembly, precautions need to be taken to insure the selective oxidation of homoserine at the ligation site without the oxidation of susceptible side chains of other amino acid residues. Other possible oxidation sensitive functional groups of peptides synthesized by peptide assembly have protecting groups, allowing selective oxidation of the unprotected homoserine alcohol at the ligation site. The utility of this oxidation was demonstrated with two model homoserine tripeptides **4.52** and **4.53** synthesized by homoserine peptide assembly (Table 4.7). Treatment of the homoserine tripeptides with TCICA and catalytic TEMPO and sodium bromide in basic aqueous/organic media resulted in the desired oxidized tripeptides **4.57** and **4.58** after one hour in moderate yields. These results demonstrate the utility of applying the method of homoserine peptide assembly to an aspartic acid ligation, providing additional ligation junctions that can be accessed to ligate peptide fragments by hydroxylamine peptide assembly.

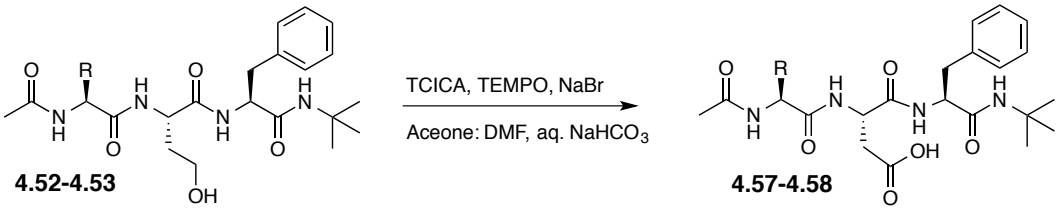

Entry	Ac-AA	Yield (%)
a	Val	75
b	Phe	62

Table 4.7: Oxidation of homoserine to aspartic acid in ligated peptides.

In summary, peptide assembly by ligation of mildly activated esters has been extended to homoserine. It has been demonstrated that homoserine peptide assembly can tolerate a variety of C-terminal amino acids, including residues that are not compatible with NCL. Post-ligation oxidation of homoserine using a mild and green method utilizing TCICA and TEMPO can be used to transform homoserine into an aspartic acid residue at the ligation site, broadening the scope of this method. Additional work is needed to further optimize the reaction conditions of homoserine peptide assembly in attempt to limit the formation of side products that diminish the ligated product yield, before applying homoserine peptide assembly to target peptides.

4.5 Conclusion

In the present work, the method of peptide assembly by ligation of hydroxyl amino acids with mildly activated esters has been applied to threonine and homoserine, broadening the scope of our peptide assembly technique. Mild oxidation of homoserine

post-ligation was achieved to transform homoserine into an aspartic acid residue at the ligation site. The structure-reactivity relationship of the peptide assemblies of threonine and homoserine with the mildly activated HIP, TFE and CM esters has been studied, demonstrating that the HIP ester was the optimal activator for these peptide assemblies. These results are consistent with the previous work on serine peptide assembly.[137] It is worth noting that ligation between alanine and homoserine benefit from a less activated ester group to limit the side product resulting from a second transesterification reaction. A variety of C-terminal amino acids were successfully ligated with the peptide assembly method, surpassing the capabilities of NCL. Extension of the hydroxylamine peptide assembly from serine to threonine and homoserine demonstrates greater utility of this method over NCL. NCL relies on ligation based on cysteine, which is one of the least prevalent amino acid residues (19th abundant) in natural peptides with an abundance of 1.7%, and it is not compatible with the ligation of C-terminal residues including valine, isoleucine and proline.[77-78] In comparison, the relative abundance in natural peptides of serine (4th abundant) is 6.9%, threonine (8th abundant) is 5.8%, and aspartic acid (10th abundant) is 5.3%, allowing for a greater access to ligation junctions that can be used to ligate peptide fragments with this method, for the use of preparative peptide synthesis.[78] In addition to the versatility of this method, ligations are racemization free and are conducted in concentrated organic media, which can be applicable for scale up and preparative peptide synthesis. The utility of this method was demonstrated by the successful synthesis of the antivenom lethal toxin neutralizing factor-10 (LTNF-10).

Part 3: Experimental Details

Chapter 5: Experimental

5.1 General Information

All reagents were purchased from commercial sources and were used without further purification, unless otherwise stated. All reactions were performed with oven-dried glassware under a nitrogen atmosphere using standard syringe and septum techniques unless otherwise stated. Microwave reactions were performed with oven-dried microwave vessels sealed under air, in a CEM Discover microwave reactor with IR temperature monitoring. Volatiles were removed under reduced pressure using a Büchi rotary evaporator. Solid phase peptide synthesis (SPPS) was performed with a Vortex-Genie 2T shaker using polypropylene syringes (10 mL) equipped with polyethylene frits as reactors. 2-Chlorotrityl chloride (2-CTC) resin was used as the solid support for SPPS. Thin layer chromatography (TLC) was performed on silica gel 60 F_{254} aluminum-backed plates. TLC analysis was performed by visualization using UV light and straining with phosphomolybdic acid (PMA) or ninhydrin solutions. Chromatographic purification of products was accomplished using flash column chromatography with silica gel 60.

All melting point data were measured on a Büchi Melting Point B-545 instrument and are uncorrected. IR spectra were obtained on a Perkin Elmer Spectrum One FT-IR spectrometer or a Bruker Alpha FT-IR spectrometer using the ATR accessory and are reported in absorption frequency (cm^{-1}). The specific rotation data were measured on a Rudolph Research Analytical AutoPol IV polarimeter. Proton (^{1}H) and carbon (^{13}C)

NMR spectra were obtained on Varian Inova 300 (300 MHz and 75 MHz, respectively), Varian Inova 400 (400 MHz and 101 MHz, respectively), Bruker Avance Neo 400 (400 MHz and 101 MHz, respectively), Varian Inova 500 (500 MHz and 126 MHz, respectively) or Bruker Avance 700 (700 MHz) spectrometers, and were internally referenced to residual deuterated solvent signals. Fluorine (^{19}F) NMR spectra were obtained on Bruker Avance Neo 400 (376 MHz) and were referenced using hexafluorobenzene as an internal standard. The data for ^{1}H NMR are reported in terms of chemical shift (δ ppm), multiplicity, coupling constant (Hz) and proton integration. The data for ^{13}C NMR are reported in terms of chemical shift (δ ppm). Mass spectra were obtained on an Agilent G3250AA LCMS instrument.

5.2 Syrbactin Experimental

***tert*-Butyl ((S)-3-((2-(2-(diethoxyphosphoryl)acetamido)ethyl)thio)-1-(((S)-1-hydroxpropan-2-yl)amino)-1-oxopropan-2-yl)carbamate (2.4).**

L-4-Thialysine hydrochloride salt (**2.1**) (0.2965 g, 1.48 mmol) was dissolved in dioxane/water (1:1, 4 mL) and cooled to 0 °C. Sodium carbonate (0.3149 g, 2.97 mmol) was added to the mixture at 0 °C. After 30 min, phosphonoacetic acid *N*-hydroxysuccinimide ester (**2.2)** (0.4352 g, 1.48 mmol) was added and the mixture was stirred for 1 h at 0 °C and for 5 days at room temperature. Boc anhydride (0.6058 g, 2.78 mmol) dissolved in a minimum amount of dioxane was added drop-wise to the reaction mixture, which was stirred for 20 h at room temperature. The reaction mixture was washed with ethyl acetate (10 mL) to remove organic impurities. The aqueous phase was acidified to pH 2 using 1N hydrochloric acid, and extracted with ethyl acetate (4 × 15 mL). The combined organic extract was dried over anhydrous magnesium sulfate and concentrated to afford **2.3** as a colorless oil. This compound was used in the subsequent step without further purification.

The crude material **2.3** (0.5112 g, 1.16 mmol) was dissolved in 11 mL dry dichloromethane and set to stir at 0 °C. *N,N*'-Dicyclohexylcarbodiimide (0.2904 g, 1.41 mmol) and *N*-hydroxysuccinimide (0.1347 g, 1.17 mmol) were added at 0 °C, followed by L-alaninol (0.18 mL, 2.31 mmol). The mixture was stirred at 0 °C for 30 min, then for 20 h at room temperature and the *N,N*'-dicyclohexylurea was filtered off. The filtrate was concentrated to afford a yellow oil that was purified by column chromatography (SiO_2,

acetone/dichloromethane gradient, 1:4 to 4:1) to afford the title compound **2.4** as a colorless oil (0.3987 g, 54%). $[\alpha]^{D}_{25}$ -14.99 (*c* 1.0, MeOH). IR (neat): 3289, 3282, 2978, 2931, 2875, 1711, 1651, 1531, 1454, 1411, 1392, 1365, 1239, 1164, 1097, 1048, 1020, 968, 865, 839, 781 cm^{-1}. ^{1}H NMR (300 MHz, $CDCl_3$): δ 7.81 (s, 1H), 7.57 (d, *J* = 5.7 Hz, 1H), 5.59 (d, *J* = 8.4 Hz, 1H), 4.37 – 4.24 (m, 1H), 4.20 – 4.07 (m, 4H), 4.05 – 3.96 (m, 1H), 3.66 (dd, *J* = 11.4, 3.4 Hz, 2H), 3.48 (dd, *J* = 11.1, 5.8 Hz, 1H), 3.27 (br s, 1H), 2.90 – 2.78 (m, 4H), 2.67 – 2.54 (m, 1H), 1.42 (s, 9H), 1.32 (q, J = 7.0 Hz, 6H), 1.16 (d, J = 6.8 Hz, 3H). ^{13}C NMR (75 MHz, $CDCl_3$): δ 170.7, 164.6, 155.9, 80.1, 66.1, 63.1, 62.9, 54.6, 47.9, 39.7, 36.7, 36.0, 34.3, 33.7, 28.4, 16.8, 16.4. HRMS calcd. for $C_{19}H_{39}N_3O_8PS$ $[M+H]^+$ 500.2195, found 500.2208.

***tert*-Butyl ((8S,11R,E)-8-methyl-5,10-dioxo-1-thia-4,9-diazacyclododec-6-en-11-yl) carbamate (2.10)**.

Dess-Martin periodinane (0.4123 g, 0.972 mmol) was added to a stirring solution of phosphono-alcohol **2.4** (0.4051 g, 0.811 mmol) in 8 mL of dry dichloromethane at room temperature and stirred for 45 min. The reaction mixture was diluted with 12 mL dichloromethane and 24 mL of a 1:1 mixture of sat $NaHCO_3$ and 2% sodium thiosulfate was added. The mixture was stirred vigorously until the organic phase became clear, then the phases were separated. The organic phase was dried over sodium sulfate, filtered, and concentrated in vacuo without warming to obtain an aldehyde that was used without purification in the subsequent step.

Tetramethylethylenediamine (0.15 mL, 1.00 mmol) and triethylamine (0.46 mL, 3.30 mmol) were added to a stirring suspension of zinc triflate (0.6566 g, 1.81 mmol) in 120 mL dry tetrahydrofuran at room temperature, and stirred for 45 minutes under an inert atmosphere. The crude phosphono-aldehyde was dissolved in 70 mL dry tetrahydrofuran and added drop-wise to the suspension over 2.5 h. The reaction mixture was stirred at room temperature for 21 h and concentrated in vacuo to ca. 10 mL. The residue was diluted with 100 mL ethyl acetate and washed with 50 mL each of brine and 1% hydrochloric acid. The organic phase was dried over magnesium sulfate and concentrated to afford a yellow oil that was purified by chromatography (SiO_2, acetone/dichloromethane gradient, 1:4 to 4:1) to afford the title compound as a white solid film (0.1624 g, 58%). Mp: 176-179 °C. $[\alpha]^{D}_{25}$ -55.38 (*c* 0.30, MeOH). IR (neat): 3308, 2978, 2933, 1706, 1663, 1635, 1494, 1455, 1393, 1367, 1247, 1225, 1159, 1095, 1057, 1030, 974, 913, 885, 848, 759, 737 cm^{-1}. ^{1}H NMR (700 MHz, CD_3OD): δ 6.72 (dd, *J* = 15.6, 4.9 Hz, 1H), 6.45 (d, *J* = 15.7 Hz, 1H), 4.54 – 4.48 (m, 1H), 4.43 (m, 1H), 3.54 – 3.46 (m, 1H), 3.26 – 3.18 (m, 2H), 3.00 (dd, *J* = 14.4, 6.1 Hz, 1H), 2.70 (ddd, *J* = 14.0, 8.6, 5.1 Hz, 1H), 2.51 – 2.43 (m, 1H), 1.45 (s, 9H), 1.33 (d, *J* = 7.1 Hz, 3H). ^{13}C NMR (126 MHz, CD_3OD): δ 172.7, 170.8, 157.2, 146.0, 121.3, 81.1, 53.8, 48.0, 42.0, 34.1, 32.4, 28.8, 18.8. HRMS calcd. for $C_{15}H_{26}N_3O_4S$ $[M+H]^+$ 344.1644, found 344.1650.

(9H-Fluoren-9-yl)methyl ((S)-3-methyl-1-(((8S,11R,E)-8-methyl-5,10-dioxo-1-thia-4,9-diaza cyclododec-6-en-11-yl)amino)-1-oxobutan-2-yl)carbamate (2.11).

The macrolactam **2.10** (0.1231 g, 0.358 mmol) was treated with hydrochloric acid in ethyl acetate (3N, 3.0 mL) and stirred for 30 min at room temperature, then concentrated in vacuo. The resulting white solid hydrochloride salt was dissolved in 4 mL dry dimethylformamide and set to stir at 0 °C. MP-Carbonate resin (2.94 mmol/g, 0.3663 g, 1.08 mmol) was added, followed by *N*-Fmoc-L-valine *N*-hydroxysuccinimide ester (0.1952 g, 0.447 mmol). The reaction mixture was stirred for 30 min at 0 °C, then 24 h at room temperature. The reaction mixture was concentrated in vacuo to obtain a white solid that was purified by column chromatography (SiO_2, methanol/dichloromethane gradient, 0:10 to 1:9) to afford a white solid (0.1217 g, 60%). Mp: 207-209 °C. $[\alpha]^{D}_{25}$ -55.43 (*c* 0.05, MeOH). IR (neat): 3282, 3063, 2959, 2925, 2872, 2854, 2463, 2409, 2375, 2353, 2338, 1692, 1635, 1538, 1450, 1390, 1342, 1290, 1249, 1237, 1219, 1163, 1135, 1101, 1084, 1033, 992, 960, 852, 795, 758, 739, 730, 668 cm^{-1}. ^{1}H NMR (400 MHz, CD_3OD): δ 7.80 (d, J = 7.5 Hz, 2H), 7.71 – 7.64 (m, 2H), 7.39 (t, J = 7.4 Hz, 2H), 7.31 (t, J = 7.3 Hz, 2H), 6.72 (dd, J = 15.6, 4.9 Hz, 1H), 6.47 (d, J = 15.8 Hz, 1H), 4.71 (d, J = 5.1 Hz, 1H), 4.54 – 4.47 (m, 1H), 4.37 (t, J = 7.1 Hz, 1H), 4.25 (t, J = 6.8 Hz, 1H), 3.99 (d, J = 6.7 Hz, 1H), 3.55 – 3.46 (m, 1H), 3.20 (d, J = 14.9 Hz, 1H), 3.07 (dd, J = 14.3, 6.1 Hz, 1H), 2.73 – 2.62 (m, 1H), 2.52 – 2.42 (m, 1H), 2.19 – 2.06 (m, 1H), 1.32 (d, J = 7.0 Hz, 3H), 0.97 – 0.93 (m, 6H). ^{13}C NMR (126 MHz, CD_3OD): δ 146.0, 128.9, 128.4, 126.4, 121.1, 68.2, 62.0, 53.0, 48.0, 41.8, 33.8, 32.7, 31.8, 30.9, 19.9, 18.8. (Partial ^{13}C NMR data due to

lack of compound solubility.) HRMS calcd. for $C_{30}H_{37}N_4O_5S$ $[M+H]^+$ 565.2485, found 565.2497.

(S)-2-(3-Dodecylureido)-3-methyl-N-((8S,11R,E)-8-methyl-5,10-dioxo-1-thia-4,9-diazacyclo dodec-6-en-11-yl)butanamide (2.12).

Compound **2.11** (19 mg, 33.6 μmol) was dissolved in 1 mL dry dimethylformamide and treated with piperidine (6 μL). The solution was stirred for 40 min and the volatiles were removed in vacuo. The reaction mixture was diluted with 1 mL dry dimethylformamide and dodecylisocyanate (16 μL, 66.4 μmol) was added. The resulting mixture was stirred at room temperature for 22 h and concentrated in vacuo to obtain a solid that was purified by column chromatography (SiO_2, methanol/dichloromethane gradient, 0:10 to 1:9) to afford a white solid (0.0140 g, 75%). Mp: 231-233 °C. $[\alpha]^D_{25}$ -28.4 (*c* 0.02, MeOH). IR (neat): 3311, 3270, 3064, 2958, 2923, 2853, 1626, 1544, 1466, 1386, 1283, 1239, 1219, 1168, 1095, 1017, 961, 915, 848, 721, 643 cm^{-1}. ^1H NMR (400 MHz, CD_3OD): δ 6.74 (dd, J = 15.6, 4.8 Hz, 1H), 6.49 (d, J = 15.6 Hz, 1H), 4.72 – 4.66 (m, 1H), 4.57 – 4.47 (m, 1H), 4.10 (d, J = 5.3 Hz, 1H), 3.59 – 3.45 (m, 1H), 3.16 – 3.06 (m, 3H), 2.77 – 2.61 (m, 1H), 2.55 – 2.41 (m, 1H), 2.23 – 2.10 (m, 1H), 1.52 – 1.41 (m, 2H), 1.36 – 1.22 (m, 20H), 1.05 – 0.72 (m, 12H). ^{13}C NMR (126 MHz, CD_3OD): δ 145.9, 121.5, 78.4, 71.5, 60.7, 56.4, 53.0, 48.0, 41.8, 41.1, 33.9, 33.2, 32.7, 32.0, 31.4, 30.9, 30.6, 28.1, 23.9, 20.1, 18.8, 18.0, 14.6. HRMS calcd. for $C_{28}H_{52}N_5O_4S$ $[M+H]^+$ 554.3740, found 554.3746.

(2S)-2-(3-Dodecylureido)-3-methyl-N-((8S,11R,E)-8-methyl-1-oxido-5,10-dioxo-1-thia-4,9-diazacyclododec-6-en-11-yl)butanamide (2.13).

Compound **2.12** (12.7 mg, 22.9 μmol) was dissolved in 1.5 mL of methanol and set to stir at 0 °C. Sodium periodate (5.7 mg, 26.6 μmol) was dissolved in 0.2 mL of water and added dropwise; the reaction mixture was stirred for 24 h and concentrated in vacuo. The crude solid was purified by column chromatography (SiO_2, methanol/dichloromethane gradient, 0:10 to 1:9) to give a white solid (7.8 mg, 60%). Mp: 204-206 °C. $[\alpha]^{D}_{25}$ -36.3 (*c* 0.024, MeOH). IR (neat): 3316, 2956, 2921, 2852, 1708, 1657, 1622, 1553, 1522, 1457, 1377, 1340, 1293, 1238, 1205, 1166, 1091, 1042, 1013, 914, 853, 815, 766, 721, 648, 580, 541, 474, 456 cm^{-1}. ^{1}H NMR (400 MHz, CD_3OD): δ 6.87 (dd, *J* = 15.5, 5.0 Hz, 1H), 6.16 (d, *J* = 15.5 Hz, 1H), 4.97 (t, *J* = 4.2 Hz, 1H), 4.57 – 4.33 (m, 1H), 4.08 (d, *J* = 5.4 Hz, 1H), 3.76 (dd, *J* = 14.6, 3.2 Hz, 1H), 3.71 – 3.64 (m, 1H), 3.49 – 3.42 (m, 1H), 3.17 (dd, *J* = 14.4, 4.4 Hz, 1H), 3.09 (t, *J* = 6.5 Hz, 1H), 2.97 – 2.88 (m, 1H), 2.19 – 2.12 (m, 1H), 1.47 – 1.42 (m, 2H), 1.39 – 1.12 (m, 20H), 1.06 – 0.73 (m, 12H). ^{13}C NMR (126 MHz, CD_3OD): δ 149.0, 120.2, 78.4, 60.6, 54.3, 54.1, 51.5, 47.9, 41.1, 37.2, 33.2, 32.0, 31.4, 30.9, 30.6, 28.1, 23.9, 20.1, 18.7, 18.0, 14.6. HRMS calcd. for $C_{28}H_{52}N_5O_5S$ $[M+H]^+$ 570.3689, found 570.3703.

General procedure for synthesizing NHS esters.

The *N*-hydroxysuccinimide esters of pyrazinecarboxylic acid and (*S*)-(+)-ibuprofen were prepared by dissolving the starting acid (0.200 g, 1.0 equiv) in dry tetrahydrofuran and setting to stir at 0 °C. *N*-Hydroxysuccinimide (1.0 equiv) was added followed by *N*,*N*'-dicyclohexylcarbodiimide (1.0 equiv). The mixture was warmed to room temperature and stirred for 24 h. The *N*,*N*'-dicyclohexylurea was removed by filtration and the filtrate was concentrated to afford a solid that was purified by column chromatography.

2,5-Dioxopyrrolidin-1-yl pyrazine-2-carboxylate (2.15).

The general procedure for the synthesis of NHS esters was followed, using pyrazine carboxylic acid. The crude product was purified by column chromatography (SiO_2, 1:4 acetone/dicloromethane) to give a white solid (0.2757 g, 77%). Mp: 161 – 164 °C. ^{1}H NMR (300 MHz, $CDCl_3$): δ 9.40 (d, *J* = 1.4 Hz, 1H), 8.90 (d, *J* = 2.3 Hz, 1H), 8.83 (dd, *J* = 2.4, 1.5 Hz, 1H), 2.95 (s, 4H). ^{13}C NMR (101 MHz, $CDCl_3$): δ 168.9, 159.6, 149.3, 147.1, 145.1, 140.1, 25.8. IR (neat): 3501, 3324, 3276, 3078, 2929, 2851, 1875, 1806, 1785, 1703, 1653, 1626, 1571, 1533, 1468, 1449, 1420, 1399, 1360, 1306, 1260, 1243, 1203, 1183, 1153, 1075, 1060, 1048, 1025, 1011, 995, 951, 892, 876, 853, 811, 782, 764, 713 cm^{-1}. HRMS calcd. for $C_9H_8N_3O_4$ $[M+H]^+$ 222.0509, found 222.0502.

2,5-Dioxopyrrolidin-1-yl (S)-2-(4-isobutylphenyl)propanoate (2.17).

The general procedure for the synthesis of NHS esters was followed, using (S)-(+)-ibuprofen. The crude product was purified by column chromatography (SiO_2, ethyl acetate/hexane gradient, 1:4 to 2:3) to give a white solid (0.2742 g, 93%). Mp: 74-76 °C. $[\alpha]^D_{25}$ 60.2 (*c* 1.0, MeOH). ^{1}H NMR (500 MHz, $CDCl_3$): δ 7.27 (d, *J* = 8.0 Hz, 2H), 7.15 (d, *J* = 7.9 Hz, 2H), 4.04 (q, *J* = 7.2 Hz, 1H), 2.79 (s, 4H), 2.47 (d, *J* = 7.2 Hz, 2H), 1.87 (dp, *J* = 13.4, 6.7 Hz, 1H), 1.64 (d, *J* = 7.2 Hz, 3H), 0.91 (d, *J* = 6.6 Hz, 6H). ^{13}C NMR (126 MHz, $CDCl_3$) δ 170.2, 169.2, 141.4, 135.6, 129.9, 129.7, 127.5, 127.4, 45.2, 42.7, 30.3, 25.8, 22.6, 19.1. IR (neat): 3054, 2959, 2904, 2851, 1862, 1839, 1800, 1765, 1741, 1631, 1513, 1446, 1432, 1380, 1363, 1342, 1313, 1261, 1238, 1207, 1182, 1144, 1088, 1047, 991, 962, 924, 871, 850, 814, 769, 728, 688, 669, 641, 560, 507, 464 cm^{-1}. HRMS calcd. for $C_{17}H_{21}NO_4Na$ $[M+Na]^+$ 326.1368, found 326.1368.

N-((S)-3-Methyl-1-(((8S,11R,E)-8-methyl-5,10-dioxo-1-thia-4,9-diazacyclododec-6-en-11-yl) amino)-1-oxobutan-2-yl)pyrazine-2-carboxamide (2.18).

Compound **2.11** (59.7 mg, 0.106 mmol) was dissolved in 2 mL dry dimethylformamide and treated with piperidine (20 μL). The solution was stirred for 30 min and the volatiles were removed in vacuo. The residue was dissolved in 2 mL dimethylformamide and pyrazine carboxylic acid *N*-hydroxysuccinimide ester (**2.15**) (48.0 mg, 0.217 mmol) was added. The resulting mixture was stirred for 20 h at room temperature and concentrated in vacuo to obtain a solid that was purified by column chromatography (SiO_2, methanol/dichloromethane gradient, 0:10 to 1:9) to give a white solid (19.8 mg, 42%).

Mp: 241-243 °C. $[\alpha]^{D}_{25}$ -35.2 (*c* 0.05, MeOH). IR (neat): 3289, 3273, 3058, 2962, 2929, 2874, 1634, 1513, 1450, 1389, 1336, 1291, 1218, 1164, 1095, 1047, 1019, 961, 889, 859, 847, 775, 731, 645, 577, 439 cm^{-1}. ^{1}H NMR (400 MHz, CD_3OD): δ 9.24 (d, J = 1.1 Hz, 1H), 8.81 (d, J = 2.4 Hz, 1H), 8.71 (dd, J = 2.3, 1.5 Hz, 1H), 6.72 (dd, J = 15.6, 4.8 Hz, 1H), 6.49 (d, J = 15.6 Hz, 1H), 4.71 (dd, J = 19.0, 4.1 Hz, 1H), 4.59 – 4.55 (m, 1H), 4.51 (dd, J = 13.9, 7.5 Hz, 1H), 3.55 – 3.46 (m, 1H), 3.27 – 3.16 (m, 2H), 3.05 (dd, J = 14.3, 6.4 Hz, 1H), 2.73 – 2.65 (m, 1H), 2.54 – 2.45 (m, 1H), 2.30 – 2.18 (m, 1H), 1.33 (d, J = 7.1 Hz, 3H), 1.05 – 0.99 (m, 6H). ^{13}C NMR (101 MHz, CD_3OD): δ 173.7, 172.7, 171.7, 170.9, 165.1, 149.0, 145.9, 145.0, 121.5, 60.5, 59.9, 53.3, 48.0, 41.9, 33.9, 32.8, 31.8, 29.7, 19.9, 18.8. HRMS calcd. for $C_{20}H_{28}N_6O_4SNa$ $[M+Na]^+$ 471.1790, found 471.1796.

(S)-2-((S)-2-(4-Isobutylphenyl)propanamido)-3-methyl-N-((8S,11R,E)-8-methyl-5,10-dioxo-1-thia-4,9-diazacyclododec-6-en-11-yl)butanamide (2.19).

Compound **2.11** (22.2 mg, 39.3 μmol) was dissolved in 1 mL dry dimethylformamide and treated with piperidine (10 μL) and the solution was stirred for 30 min and volatiles were removed in vacuo. The residue was dissolved in 1 mL dimethylformamide and (*S*)-(+)-ibuprofen *N*-hydroxysuccinimide ester (**2.17**) (27.8 mg, 91.6 μmol) was added. The resulting mixture was stirred at 0 °C for 30 min and 24 h at room temperature and concentrated in vacuo to obtain a white solid that was purified by column chromatography (SiO_2, methanol/dichloromethane gradient, 0:10 to 1:9) to give a white solid (15.2 mg, 73%). Mp: 189-191 °C. $[\alpha]^{D}_{25}$ -37.1 (*c* 0.07, MeOH). IR (neat): 3274, 3055, 2957, 2925, 2870, 1706, 1630, 1535, 1459, 1382, 1282, 1220, 1166, 1088, 1030,

908, 848, 815, 777, 718, 659, 639, 577, 459 cm^{-1}. ^{1}H NMR (300 MHz, CD_3OD): δ 7.25 (d, J = 8.1 Hz, 2H), 7.08 (d, J = 8.0 Hz, 2H), 6.72 (dd, J = 15.7, 4.9 Hz, 1H), 6.46 (d, J = 15.4 Hz, 1H), 4.60 (dd, J = 6.1, 1.9 Hz, 1H), 4.54 – 4.45 (m, 1H), 4.21 (d, J = 7.4 Hz, 1H), 4.19 – 4.11 (m, 1H), 3.75 (dd, *J* = 14.4, 7.2 Hz, 1H), 3.55 – 3.42 (m, 1H), 3.26 – 3.16 (m, 1H), 3.12 (dd, *J* = 14.5, 2.2 Hz, 1H), 2.95 (dd, J = 14.2, 6.2 Hz, 1H), 2.44 (d, J = 7.1 Hz, 2H), 2.41 – 2.33 (m, 1H), 2.12 – 2.03 (m, 1H), 1.88 – 1.78 (m, 1H), 1.46 (d, J = 7.1 Hz, 3H), 1.37 – 1.27 (m, 6H), 0.95 – 0.87 (m, 9H). ^{13}C NMR (126 MHz, CD_3OD): δ 177.7, 176.0, 173.1, 171.6, 170.9, 145.9, 141.6, 139.9, 130.5, 128.5, 121.5, 60.4, 53.1, 48.0, 47.0, 46.2, 42.0, 33.7, 32.7, 31.8, 31.6, 30.8, 30.1, 28.6, 26.4, 22.9, 19.9, 19.0, 18.8. HRMS calcd. for $C_{28}H_{42}N_4O_4SNa$ $[M+Na]^+$ 553.2825, found 553.2802.

N-((8S,11R,E)-8-Methyl-5,10-dioxo-1-thia-4,9-diazacyclododec-6-en-11-yl)pyrazine-2-carboxamide (2.20).

The macrolactam **2.10** (60.1 mg, 0.175 mmol) was treated with a solution of hydrochloric acid in ethyl acetate (3 N, 2.0 mL) and stirred for 30 min at room temperature, then concentrated in vacuo. The resulting white solid hydrochloride salt was dissolved in 2 mL dimethylformamide and MP-carbonate resin (2.94 mmol/g, 0.1801 g, 0.529 mmol) was added at 0 °C, followed by pyrazine carboxylic acid *N*-hydroxysuccinimide ester (**2.15**) (49.0 mg, 0.222 mmol). The resulting mixture was stirred at 0 °C for 15 min and 14 h at room temperature and concentrated in vacuo to obtain a solid that was purified by column chromatography (SiO_2, methanol/dichloromethane gradient, 0:10 to 1:9) to give a white solid (0.0293 g, 48%). Mp: 256-258 °C. $[\alpha]^{D}_{25}$ - 13.9 (*c* 0.13, MeOH). IR (neat): 3450,

3387, 3374, 3265, 3044, 2986, 2932, 2918, 1721, 1684, 1666, 1651, 1628, 1582, 1543, 1514, 1464, 1454, 1404, 1364, 1350, 1335, 1308, 1293, 1268, 1241, 1218, 1167, 1156, 1094, 1047, 1021, 964, 947, 907, 893, 875, 852, 843, 795, 778, 734, 716, 688, 669 cm^{-1}. ^{1}H NMR (300 MHz, CD_3OD): δ 9.25 (d, *J* = 1.4 Hz, 1H), 8.82 (d, *J* = 2.5 Hz, 1H), 8.71 (dd, *J* = 2.4, 1.5 Hz, 1H), 6.77 (dd, *J* = 15.6, 4.9 Hz, 1H), 6.49 (d, *J* = 15.7 Hz, 1H), 4.95 (dd, *J* = 5.8, 1.9 Hz, 1H), 4.61 – 4.49 (m, 1H), 3.58 (ddd, *J* = 14.7, 8.8, 4.1 Hz, 1H), 3.35 (d, *J* = 2.8 Hz, 1H), 3.28 – 3.17 (m, 2H), 2.77 (ddd, *J* = 14.4, 9.0, 5.1 Hz, 1H), 2.48 (ddd, *J* = 14.9, 9.1, 6.0 Hz, 1H), 1.37 (d, *J* = 7.1 Hz, 3H). ^{13}C NMR (126 MHz, CD_3OD): δ 171.7, 170.7, 164.3, 149.2, 146.0, 145.7, 145.1, 144.8, 121.2, 52.5, 48.1, 42.0, 33.7, 32.0, 18.8. HRMS calcd. for $C_{15}H_{20}N_5O_3S$ $[M+H]^+$ 350.1287, found 350.1298.

N-((8S,11R,E)-8-Methyl-1-oxido-5,10-dioxo-1-thia-4,9-diazacyclododec-6-en-11-yl)pyrazine-2-carboxamide (2.21).

Compound **2.20** (6.2 mg, 17.7 μmol) was dissolved in 1 mL of methanol and set to stir at 0 °C. Sodium periodate (4.3 mg, 20.1 μmol) was dissolved in 0.1 mL of water and added drop-wise, and the reaction mixture was stirred for 24 hours and concentrated in vacuo. The white crude solid was purified by column chromatography (SiO_2, methanol/dichloromethane gradient, 0:10 to 1:9) to give a white solid (6.4 mg, 98%). Mp: 250-252 °C. $[\alpha]^{D}_{25}$ -32.0 (*c* 0.05, MeOH). IR (neat): 3370, 3332, 3267, 3067, 2956, 2922, 2852, 1674, 1661, 1646, 1629, 1583, 1529, 1472, 1454, 1407, 1366, 1354, 1282, 1267, 1238, 1213, 1169, 1155, 1091, 1050, 1021, 1006, 971, 945, 908, 883, 852, 775, 734, 717, 677, 631, 582, 553, 463, 432 cm^{-1}. ^{1}H NMR (400 MHz, d_6-DMSO): δ 9.21 (s, 1H), 8.91

(d, *J* = 2.1 Hz, 1H), 8.75 (d, *J* = 7.5 Hz, 1H), 6.83 (dd, *J* = 15.3, 4.6 Hz, 1H), 6.06 (d, *J* = 15.0 Hz, 1H), 5.16 (dd, *J* = 7.5, 3.6 Hz, 1H), 4.51 (dd, *J* = 12.6, 7.3 Hz, 1H), 4.04 – 3.95 (m, 1H), 3.55 – 3.45 (m, 1H), 3.25 – 3.14 (m, 3H), 2.75 – 2.65 (m, 1H), 1.24 (d, *J* = 6.4 Hz, 3H). ^{13}C NMR (126 MHz, d_6-DMSO): δ 168.0, 165.5, 162.0, 148.2, 147.5, 143.7, 143.5, 143.3, 118.5, 55.3, 52.9, 50.5, 45.8, 36.5, 18.5. HRMS calcd. for $C_{15}H_{19}N_5O_4SNa$ $[M+Na]^+$ 388.1055, found 388.1040.

***tert*-Butyl ((8*S*,11*R*,*E*)-8-methyl-1-oxido-5,10-dioxo-1-thia-4,9-diazacyclododec-6-en-11-yl)carbamate (2.22).**

The macrolactam **2.10** (10.5 mg, 30.6 μmol) was dissolved in 1 mL of methanol and set to stir at 0 °C. Sodium periodate (8.2 mg, 38.3 μmol) was dissolved in 0.1 mL of water and added drop-wise, and the reaction mixture was stirred for 24 hours and concentrated in vacuo. The white crude solid was purified by column chromatography (SiO_2, 1:9 methanol/dichloromethane) to give a white solid (9.8 mg, 89%). Mp: 210 °C (dec.). $[\alpha]^D_{25}$ -108.76 (*c* 0.3, MeOH). IR (neat): 3417, 3295, 3218, 3094, 2975, 2927, 2467, 2387, 2263, 2204, 1710, 1671, 1632, 1535, 1469, 1366, 1249, 1162, 1018, 986, 852, 789, 668, 637, 569, 514, 432 cm^{-1}. ^{1}H NMR (700 MHz, CD_3OD): δ 6.92 (dd, J = 15.4, 4.8 Hz, 1H), 6.15 (d, J = 15.4 Hz, 1H), 4.77 (t, J = 3.5 Hz, 1H), 4.59 – 4.55 (m, 1H), 3.77 (dd, J = 14.4, 3.2 Hz, 1H), 3.73 – 3.67 (m, 1H), 3.48 (ddd, J = 16.1, 6.9, 4.5 Hz, 1H), 3.30 – 3.27 (m, 1H), 3.14 (dd, J = 14.4, 3.8 Hz, 1H), 2.96 (ddd, J = 13.9, 8.9, 7.2 Hz, 1H), 1.45 (s, 9H), 1.33 (d, J = 7.1 Hz, 3H). ^{13}C NMR (126 MHz, CD_3OD): δ 171.0, 169.7, 157.1, 149.5,

120.0, 81.4, 54.5, 54.4, 52.9, 47.9, 37.4, 28.8, 18.7. HRMS calcd. for $C_{15}H_{26}N_3O_5S$ $[M+H]^+$ 360.1588, found 360.1596.

***tert*-Butyl ((*S*)-5-(2-(diethoxyphosphoryl)acetamido)-1-(((*S*)-1-hydroxypropan-2-yl) amino)-1-oxopentan-2-yl)carbamate (2.26).**

N-Boc-L-Ornithine (**2.24**) (0.5894 g, 2.54 mmol) was dissolved in dioxane/water (1:1, 3 mL) and cooled to 0 °C. Sodium carbonate (0.3149 g, 2.97 mmol) was added to the mixture at 0 °C. After 30 min, phosphonoacetic acid *N*-hydroxysuccinimide ester (**2.2)** (0.9135 g, 3.12 mmol) was added and the mixture was stirred for 1 h at 0 °C and for 24 h at room temperature. The reaction mixture was washed with ethyl acetate (10 mL) to remove organic impurities. The aqueous phase was acidified to pH 2 using 1N hydrochloric acid, and extracted with ethyl acetate (4 × 10 mL). The combined organic extract was dried over anhydrous magnesium sulfate and concentrated to afford **2.25** as a colorless oil. This compound was used in the subsequent step without further purification.

The crude material **2.25** (1.0217 g, 2.49 mmol) was dissolved in 25 mL dry dichloromethane and set to stir at 0 °C. *N,N*'-Dicyclohexylcarbodiimide (0.6176 g, 2.99 mmol) and *N*-hydroxysuccinimide (0.2874 g, 2.50 mmol) were added at 0 °C, followed by L-alaninol (0.40 mL, 5.14 mmol). The mixture was stirred at 0 °C for 30 min, then for 20 h at room temperature and the *N,N*'-dicyclohexylurea was filtered off. The filtrate was concentrated to afford a yellow oil that was purified by column chromatography (SiO_2, acetone/dichloromethane gradient, 1:4 to 4:1) to afford the title compound **2.26** as a colorless oil (0.9960 g, 86%). IR (neat): 3287, 3087, 2978, 2933, 2873, 1711, 1649, 1539,

1453, 1392, 1366, 1295, 1240, 1163, 1097, 1048, 1021, 968, 864, 825, 783, 703 cm^{-1}. ^{1}H NMR (300 MHz, $CDCl_3$) δ 4.25 – 4.12 (m, 1H), 4.12 – 3.98 (m, 4H), 3.99 – 3.85 (m, 1H), 3.60 – 3.47 (m, 1H), 3.45 – 3.33 (m, 1H), 3.33 – 3.21 (m, 1H), 3.21 – 3.08 (m, 1H), 2.85 (d, *J* = 3.1 Hz, 1H), 2.78 (d, *J* = 3.2 Hz, 1H), 1.80 – 1.64 (m, 1H), 1.64 – 1.43 (m, 2H), 1.33 (s, 9H), 1.24 (t, *J* = 7.1 Hz, 6H), 1.05 (d, *J* = 6.6 Hz, 3H). ^{13}C NMR (75 MHz, $CDCl_3$) δ 172.4, 164.7, 156.0, 79.7, 65.7, 62.9, 53.6, 47.9, 47.5, 39.0, 36.2, 34.4, 30.6, 28.3, 24.7, 16.7, 16.3. HRMS calcd. for $C_{19}H_{39}N_3O_8P$ $[M+H]^+$ 468.2469, found 468.2458.

***tert*-Butyl ((8S,11R,E)-8-methyl-1,1-dioxido-5,10-dioxo-1-thia-4,9-diazacyclododec-6-en-11-yl)carbamate (2.29).**

Compound **2.10** (50.1 mg, 0.146 mmol) was dissolved in 2 mL MeOH/THF (1:1) and set to stir at room temperature. Oxone (0.1350 g, 0.439 mmol) was dissolved in 1 mL of water and added drop-wise, and the reaction mixture was stirred for 20 h and concentrated in vacuo. The residue was dissolved in 5 mL water and extracted with ethyl acetate (4 x 10 mL). The combined organic extract was dried over anhydrous sodium sulfate and concentrated to afford the title compound **2.29** as a white solid (54.2 mg, 99%). ^{1}H NMR (500 MHz, CD_3OD) δ 6.76 (dd, *J* = 15.8, 5.4 Hz, 1H), 6.40 (d, *J* = 15.8 Hz, 1H), 4.67 – 4.61 (m, 1H), 4.45 – 4.39 (m, 1H), 3.84 – 3.73 (m, 1H), 3.73 – 3.56 (m, 2H), 3.44 – 3.34 (m, 2H), 1.45 (s, 9H), 1.35 (d, *J* = 6.9 Hz, 3H). ^{13}C NMR (126 MHz, CD_3OD) δ 170.9, 170.9, 157.0, 147.2, 121.2, 81.5, 55.8, 54.2, 52.2, 48.4, 36.5, 28.8, 18.5. HRMS calcd. for $C_{15}H_{24}N_3O_6S$ $[M-H]^-$ 374.1391, found 374.1394.

***tert*-butyl ((3E,5S,8S,9E)-5-methyl-2,7-dioxo-1,6-diazacycloundeca-3,9-dien-8-yl) carbamate (2.30).**

Compound **2.29** (54.2 mg, 0.144 mmol) was dissolved in 1 mL carbon tetrachloride/*tert*-butanol (5:3) and set to stir at room temperature. Potassium hydroxide (14.2 mg, 0.253 mmol) was added and the reaction mixture was stirred for 4 h and concentrated in vacuo. The mixture was dissolved in sat. NH_4Cl (3 mL) and was extracted with ethyl acetate (4 x 10 mL). The combined organic extract was dried over anhydrous sodium sulfate and concentrated to afford the title compound **2.30** as a white solid (13.9 mg, 31%). HRMS calcd. for $C_{16}H_{24}N_3O_6$ $[M+HCOO]^-$ 354.1671, found 354.1701.

5.3 Peptide Assembly Experimental

General procedures for synthesizing the activated esters.

Protocol A: The acetyl AA (1 equiv) was dissolved in dichloromethane (0.1 M) and set to stir at 0 °C. EDCI (1.2 equiv), HOBt (1.2 equiv) and 1,1,1,3,3,3-hexafluoroisopropanol (10 equiv) were added to the reaction mixture. The mixture was stirred at 0 °C for 30 min, then for 4 h at room temperature. The solvent was removed in vacuo, and the residue was dissolved in ethyl acetate and washed with 1 N HCl and sat. $NaHCO_3$. The organic phase was dried over sodium sulfate, filtered, and concentrated in vacuo to afford a crude product that was purified by column chromatography.

Protocol B: The acetyl AA (1 equiv) was dissolved in acetonitrile (0.1 M) and set to stir at 0 °C. Triethylamine (2.0 equiv) was added followed by chloroacetonitrile (1.5 equiv). The mixture was stirred at 0 °C for 30 min, then for 4 h at room temperature. The solvent was removed in vacuo to afford a crude product that was purified by column chromatography.

Protocol C: The acetyl AA (1 equiv) was dissolved in acetonitrile (0.1 M) and set to stir at 0 °C. Cesium carbonate (2.0 equiv) was added followed by a triflate (TFE/PFP/HIP, 1.5 equiv). The mixture was stirred at 0 °C for 30 min, then for 16 h at room temperature. The solvent was removed in vacuo, and the residue was dissolved in ethyl acetate and washed with 1 N HCl and sat. aqueous $NaHCO_3$. The organic phase was dried over sodium sulfate, filtered, and concentrated in vacuo to afford a crude product that was purified by column chromatography.

Acetyl alanine HIP ester (4.1).

The general procedure for the synthesis of activated esters protocol A was followed, using acetyl alanine. The crude product was purified by column chromatography (SiO_2, acetone/dichloromethane gradient, 1:9 to 2:3) to give a white solid (1.9862 g, 92%). Mp: 69-71 °C. $[\alpha]^{D}_{25}$ –46.8 (*c* 1.01, MeOH). IR (neat): 3252, 3073, 2996, 2973, 1798, 1788, 1641, 1545, 1460, 1383, 1362, 1312, 1284, 1260, 1248, 1232, 1194, 1174, 1122, 1106, 1077, 1052, 1013, 961, 930, 900, 732, 688, 646, 594, 552, 536, 514, 451 cm^{-1}. ^{1}H NMR (500 MHz, $CDCl_3$) δ 6.64 (br s, NH), 5.88 – 5.61 (m, 1H), 4.82 – 4.57 (m, 1H), 2.01 (s, 3H), 1.45 (d, J = 7.3 Hz, 3H). ^{13}C NMR (101 MHz, $CDCl_3$) δ 171.0, 170.4, 120.2 (q, J = 282.4 Hz), 67.2 (p, J = 34.9 Hz), 48.2, 22.4, 17.1. ^{19}F NMR (376 MHz, $CDCl_3$) δ -76.2 (p, J = 8.3 Hz), -76.4 (p, J = 8.3 Hz). HRMS calcd. for $C_8H_9F_6NO_3Na$ $[M+Na]^+$ 304.0379, found 304.0431.

Acetyl alanine TFE ester (4.2).

The general procedure for the synthesis of activated esters protocol C was followed, using acetyl alanine and TFE triflate. The crude product was purified by column chromatography (SiO_2, acetone/dichloromethane gradient, 1:9 to 2:3) to give a white solid (0.8109 g, 83%). Mp: 60-63 °C. $[\alpha]^{D}_{25}$ –33.2 (*c* 1.01, MeOH). IR (neat): 3298, 3077, 2981, 2962, 1751, 1644, 1546, 1454, 1422, 1374, 1345, 1284, 1268, 1201, 1156, 1075, 1036, 959, 925, 893, 837, 752, 694, 642, 612, 598, 515, 436, 408 cm^{-1}. ^{1}H NMR (400 MHz, $CDCl_3$) δ 6.34 (br s, NH), 4.71 – 4.53 (m, 2H), 4.49 – 4.34 (m, 1H), 2.01 (s, 3H), 1.43 (d, J = 7.3 Hz, 3H). ^{13}C NMR (101 MHz, $CDCl_3$) δ 171.9, 170.2, 122.9 (q, J =

277.3 Hz), 60.9 (q, J = 36.9 Hz), 48.1, 23.0, 17.9. ^{19}F NMR (376 MHz, $CDCl_3$) δ -77.0 (t, J = 8.6 Hz). HRMS calcd. for $C_7H_{10}F_3NO_3Na$ $[M+Na]^+$ 236.0505, found 236.0466.

Acetyl alanine CM ester (4.3).

The general procedure for the synthesis of activated esters protocol B was followed, using acetyl alanine. The crude product was purified by column chromatography (SiO_2, acetone/dichloromethane gradient, 1:9 to 2:3) to give a white solid (0.7455 g, 94%). Mp: 62-64 °C. $[\alpha]^D_{25}$ –84.1 (*c* 1.00, MeOH). IR (neat): 3254, 3061, 2994, 2942, 1771, 1758, 1639, 1542, 1455, 1420, 1375, 1351, 1304, 1277, 1262, 1193, 1143, 1058, 1015, 996, 954, 927, 917, 861, 838, 685, 596, 554, 497, 488 cm^{-1}. ^{1}H NMR (500 MHz, $CDCl_3$) δ 6.81 (d, J = 7.0 Hz, NH), 4.76 (d, J = 15.8 Hz, 1H), 4.70 (d, J = 15.8 Hz, 1H), 4.51 (p, J = 7.1 Hz, 1H), 1.95 (s, 3H), 1.37 (d, J = 7.3 Hz, 3H). ^{13}C NMR (126 MHz, $CDCl_3$) δ 171.7, 170.4, 114.3, 49.0, 47.8, 22.6, 17.3. HRMS calcd. for $C_7H_{11}N_2O_3$ $[M+H]^+$ 171.0764, found 171.0778. ^{1}H NMR and ^{13}C NMR data are consistent with previously reported literature values.[146]

Acetyl alanine PFP ester (4.4).

The general procedure for the synthesis of activated esters protocol C was followed, using acetyl alanine and PFP triflate. The crude product was purified by column chromatography (SiO_2, acetone/dichloromethane gradient, 1:9 to 2:3) to give a clear oil (1.0636 g, 88%). $[\alpha]^D_{25}$ –38.9 (*c* 1.00, MeOH). IR (neat): 3310, 3066, 3007, 2944, 1760, 1654, 1538, 1456, 1376, 1353, 1335, 1308, 1280, 1196, 1144, 1107, 1058, 997, 976, 967,

949, 939, 899, 879, 797, 780, 752, 718, 655, 619, 588, 522, 463, 428 cm^{-1}. ^{1}H NMR (400 MHz, $CDCl_3$) δ 6.43 (d, *J* = 41.9 Hz, NH), 4.79 – 4.55 (m, 2H), 4.46 (q, *J* = 12.8 Hz, 1H), 1.99 (s, 3H), 1.40 (d, *J* = 7.3 Hz, 3H). ^{13}C NMR (101 MHz, $CDCl_3$) δ 171.8, 170.3, 120.0 (t, *J* = 34.8 Hz), 117.1 (t, *J* = 34.8 Hz), 114.6 (d, *J* = 38.3 Hz), 112.0 (d, *J* = 38.3 Hz), 109.5 (d, *J* = 38.3 Hz), 59.7 (t, *J* = 28.1 Hz), 48.1, 22.8, 17.7. ^{19}F NMR (376 MHz, $CDCl_3$) δ -86.9 (t, *J* = 11.8 Hz), -126.6 (p, *J* = 13.2 Hz). HRMS calcd. for $C_8H_{11}F_5NO_3$ $[M+H]^+$ 264.0654, found 264.0640.

Acetyl valine HIP ester (4.5).

The general procedure for the synthesis of activated esters protocol A was followed, using acetyl valine. The crude product was purified by column chromatography (SiO_2, acetone/dichloromethane gradient, 1:9 to 2:3) to give a white solid (2.1678 g, 93%). Mp: 54-58 °C. $[\alpha]^{D}_{25}$ –24.7 (*c* 1.01, MeOH). IR (neat): 3354, 3327, 3298, 2976, 2941, 2882, 1774, 1680, 1652, 1530, 1471, 1447, 1372, 1357, 1294, 1268, 1254, 1215, 1195, 1158, 1105, 1076, 1045, 1017 998, 947, 926, 906, 884, 873, 837, 811, 793, 779, 766, 713, 691, 637, 609, 598, 575, 529, 521, 478, 431 cm^{-1}. ^{1}H NMR (400 MHz, $CDCl_3$) δ 6.57 (br s, NH), 5.75 (hept, *J* = 5.9 Hz, 1H), 4.74 – 4.61 (m, 1H), 2.28 – 2.13 (m, 1H), 2.03 (s, 3H), 0.97 (d, *J* = 6.9 Hz, 3H), 0.92 (d, *J* = 6.9 Hz, 3H). ^{13}C NMR (101 MHz, $CDCl_3$) δ 170.9, 169.4, 120.4 (q, *J* = 282.2), 67.0 (p, *J* = 34.9 Hz), 57.3, 30.8, 22.7, 18.8, 17.5. ^{19}F NMR (376 MHz, $CDCl_3$) δ -76.1 (d, *J* = 4.7 Hz), -76.2 (d, *J* = 4.7 Hz). HRMS calcd. for $C_{10}H_{14}F_6NO_3$ $[M+H]^+$ 310.0872, found 310.0850.

Acetyl valine CM ester (4.6).

The general procedure for the synthesis of activated esters protocol B was followed, using acetyl valine. The crude product was purified by column chromatography (SiO_2, acetone/dichloromethane gradient, 1:9 to 2:3) to give a white solid (0.1517 g, 90%). Mp: 80-82 °C. $[\alpha]^{D}_{25}$ –58.0 (*c* 0.506, MeOH). IR (neat): 3306, 3068, 3018, 2972, 2937, 2915, 2878, 1754, 1650, 1538, 1471, 1427, 1376, 1346, 1334, 1306, 1293, 1273, 1249, 1183, 1147, 1115, 1102, 1058, 1034, 1013, 979, 942, 915, 887, 836, 754, 719, 636, 600, 567, 516, 464, 414 cm^{-1}. ^{1}H NMR (500 MHz, $CDCl_3$) δ 6.20 (d, *J* = 7.4 Hz, NH), 4.83 (d, *J* = 15.7 Hz, 1H), 4.70 (d, *J* = 15.7 Hz, 1H), 4.64 – 4.46 (m, 1H), 2.31 – 2.10 (m, 1H), 2.03 (s, 3H), 0.97 (d, *J* = 6.8 Hz, 3H), 0.94 (d, *J* = 6.8 Hz, 3H). ^{13}C NMR (126 MHz, $CDCl_3$) δ 171.0, 170.5, 114.2, 57.1, 48.9, 31.1, 23.1, 19.1, 18.0. HRMS calcd. for $C_9H_{14}N_2O_3Na$ $[M+Na]^+$ 221.0897, found 221.0889.

Acetyl phenylalanine HIP ester (4.7).

The general procedure for the synthesis of activated esters protocol A was followed, using acetyl phenylalanine. The crude product was purified by column chromatography (SiO_2, acetone/dichloromethane gradient, 1:9 to 2:3) to give a white solid (0.5776 g, 96%). Mp: 96-98 °C. $[\alpha]^{D}_{25}$ –11.2 (*c* 1.01, MeOH). IR (neat): 3339, 3066, 3034, 2976, 2943, 1777, 1647, 1534, 1497, 1456, 1443, 1384, 1357, 1272, 1240, 1191, 1158, 1141, 1108, 1092, 1031, 1014, 963, 919, 895, 855, 777, 749, 734, 697, 677, 612, 589, 555, 535, 524, 479, 462, 434 cm^{-1}. ^{1}H NMR (400 MHz, $CDCl_3$) δ 7.32 – 7.14 (m, 3H), 7.06 (d, *J* = 6.7 Hz, 2H), 5.88 (br s, NH), 5.68 (hept, *J* = 6.0 Hz, 1H), 4.93 (dd, *J* = 13.5, 7.1 Hz, 1H),

3.15 (dd, J = 14.2, 5.9 Hz, 1H), 3.00 (dd, J = 14.2, 7.0 Hz, 1H), 1.89 (s, 3H). ^{13}C NMR (101 MHz, $CDCl_3$) δ 170.2, 169.2, 134.8, 129.3, 129.1, 127.8, 121.9, 119.1, 67.4 (p, J = 34.9 Hz), 53.1, 37.3, 22.9. ^{19}F NMR (376 MHz, $CDCl_3$) δ -76.0 (p, J = 7.3 Hz), -76.2 (p, J = 7.3 Hz). HRMS calcd. for $C_{14}H_{13}F_6NO_3Na$ $[M+Na]^+$ 380.0692, found 380.0690.

Acetyl phenylalanine CM ester (4.8).

The general procedure for the synthesis of activated esters protocol B was followed, using acetyl phenylalanine. The crude product was purified by column chromatography (SiO_2, acetone/dichloromethane gradient, 1:9 to 2:3) to give a white solid (0.2335 g, 93%). Mp: 100-103 °C. $[\alpha]^D_{25}$ –4.1 (*c* 1.03, MeOH). IR (neat): 3308, 3087, 3067, 3035, 3002, 2975, 2954, 1759, 1650, 1605, 1543, 1531, 1496, 1438, 1375, 1345, 1316, 1300, 1269, 1202, 1189, 1170, 1126, 1076, 1032, 1002, 964, 934, 763, 746, 699, 664, 631, 597, 557, 492, 484, 441, 410 cm^{-1}. ^{1}H NMR (500 MHz, $CDCl_3$) δ 7.31 (dt, J = 13.6, 6.5 Hz, 3H), 7.14 (d, J = 7.2 Hz, 2H), 6.05 (d, J = 5.8 Hz, NH), 4.91 (dd, J = 12.8, 6.3 Hz, 1H), 4.77 (d, J = 15.6 Hz, 1H), 4.68 (d, J = 15.6 Hz, 1H), 3.24 – 3.04 (m, 2H), 1.98 (s, 3H). ^{13}C NMR (126 MHz, $CDCl_3$) δ 170.6, 170.1, 135.2, 129.3, 129.1, 127.7, 114.0, 53.2, 49.0, 37.7, 23.1. HRMS calcd. for $C_{13}H_{14}N_2O_3Na$ $[M+Na]^+$ 269.0897, found 269.0891. ^{1}H NMR and ^{13}C NMR data are consistent with previously reported literature values.[147]

Acetyl leucine HIP ester (4.9).

The general procedure for the synthesis of activated esters protocol A was followed, using acetyl leucine. The crude product was purified by column chromatography (SiO_2,

acetone/dichloromethane gradient, 1:9 to 2:3) to give a clear oil (0.9398 g, 98%). $[\alpha]^{D}_{25}$ – 29.6 (*c* 0.996, MeOH). IR (neat): 3271, 3076, 2965, 2877, 1786, 1656, 1546, 1472, 1441, 1384, 1358, 1288, 1269, 1228, 1199, 1109, 1033, 981, 923, 906, 880, 843, 761, 717, 687, 600, 538, 519, 451 cm^{-1}. ^{1}H NMR (400 MHz, $CDCl_3$) δ 6.37 (d, *J* = 7.3 Hz, NH), 5.73 (hept, *J* = 6.0 Hz, 1H), 4.77 – 4.63 (m, 1H), 2.02 (s, 3H), 1.79 – 1.50 (m, 3H), 1.00 – 0.90 (m, 6H). ^{13}C NMR (101 MHz, $CDCl_3$) δ 170.8, 170.3, 120.4 (q, *J* = 282.5 Hz), 67.13 (p, *J* = 34.9 Hz), 51.0, 40.6, 25.0, 22.7, 21.7. ^{19}F NMR (376 MHz, $CDCl_3$) δ -76.2 (p, *J* = 8.1 Hz), -76.3 (p, *J* = 8.1 Hz). HRMS calcd. for $C_{11}H_{16}F_6NO_3$ $[M+H]^+$ 324.1029, found 324.1046.

Acetyl leucine CM ester (4.10).

The general procedure for the synthesis of activated esters protocol B was followed, using acetyl leucine. The crude product was purified by column chromatography (SiO_2, acetone/dichloromethane gradient, 1:4 to 2:3) to give a clear oil (0.4745 g, 96%). $[\alpha]^{D}_{25}$ – 56.7 (*c* 0.988, MeOH). IR (neat): 3385, 3286, 3064, 2960, 2873, 1758, 1654, 1536, 1470, 1431, 1371, 1274, 1226, 1144, 1039, 1012, 919, 821, 693, 595, 506, 466 cm^{-1}. ^{1}H NMR (500 MHz, $CDCl_3$) δ 6.42 (br s, NH), 4.79 (d, *J* = 15.8 Hz, 1H), 4.69 (d, *J* = 15.8 Hz, 1H), 4.57 (dd, *J* = 13.2, 8.2 Hz, 1H), 1.99 (s, 3H), 1.74 – 1.47 (m, 3H), 0.92 (t, *J* = 6.8 Hz, 6H). ^{13}C NMR (126 MHz, $CDCl_3$) δ 171.9, 170.6, 114.3, 50.7, 49.0, 40.7, 24.9, 22.9, 22.8, 21.8. HRMS calcd. for $C_{10}H_{16}N_2O_3Na$ $[M+Na]^+$ 235.1053, found 235.1029.

Acetyl isoleucine HIP ester (4.11).

The general procedure for the synthesis of activated esters protocol A was followed, using acetyl isoleucine. The crude product was purified by column chromatography (SiO_2, acetone/dichloromethane gradient, 1:9 to 2:3) to give a clear oil (0.8547 g, 90%). $[\alpha]^D_{25}$ –11.0 (*c* 1.00, MeOH). IR (neat): 3292, 3058, 2974, 2942, 2884, 1785, 1651, 1539, 1463, 1386, 1361, 1285, 1270, 1226, 1191, 1127, 1109, 1075, 970, 941, 904, 869, 772, 724, 692, 671, 595, 524, 502, 467, 454, 432, 417 cm^{-1}. ^1H NMR (400 MHz, $CDCl_3$) δ 5.76 (hept, *J* = 6.0 Hz, 1H), 4.76 (dd, *J* = 8.4, 5.0 Hz, 1H), 2.05 (s, 3H), 2.03 – 1.90 (m, 1H), 1.49 – 1.36 (m, 1H), 1.30 – 1.14 (m, 1H), 0.99 – 0.93 (m, 6H). ^{13}C NMR (101 MHz, $CDCl_3$) δ 170.5, 169.4, 120.5 (q, *J* = 283.3 Hz), 67.1 (p, *J* = 35.0 Hz), 56.7, 37.7, 25.2, 23.1, 15.5, 11.6. ^{19}F NMR (376 MHz, $CDCl_3$) δ -76.1 (p, *J* = 8.2 Hz), -76.2 (p, *J* = 8.2 Hz). HRMS calcd. for $C_{11}H_{16}F_6NO_3$ $[M+H]^+$ 324.1029, found 324.1036.

Acetyl isoleucine CM ester (4.12).

The general procedure for the synthesis of activated esters protocol B was followed, using acetyl isoleucine. The crude product was purified by column chromatography (SiO_2, acetone/dichloromethane gradient, 1:9 to 2:3) to give a white solid (0.4869 g, 98%). Mp: 78-81 °C. $[\alpha]^D_{25}$ –36.2 (*c* 1.01, MeOH). IR (neat): 3294, 3057, 3012, 2969, 2937, 2882, 1752, 1651, 1536, 1457, 1432, 1371, 1345, 1293, 1273, 1231, 1177, 1142, 1106, 1032, 1002, 932, 910, 883, 781, 746, 724, 639, 602, 523, 473, 424 cm^{-1}. ^1H NMR (400 MHz, $CDCl_3$) δ 6.11 (d, *J* = 7.9 Hz, NH), 4.84 (d, *J* = 15.6 Hz, 1H), 4.70 (d, *J* = 15.6 Hz, 1H), 4.62 (dd, *J* = 8.4, 5.4 Hz, 1H), 2.03 (s, 3H), 1.97 – 1.85 (m, 1H), 1.52 –

1.38 (m, 1H), 1.29 – 1.14 (m, 1H), 0.96 – 0.91 (m, 6H). ^{13}C NMR (101 MHz, $CDCl_3$) δ 171.0, 170.4, 114.1, 56.4, 48.8, 37.8, 25.4, 23.2, 15.6, 11.6. HRMS calcd. for $C_{10}H_{16}N_2O_3Na$ $[M+Na]^+$ 235.1053, found 235.1036.

Acetyl proline HIP ester (4.13).

The general procedure for the synthesis of activated esters protocol A was followed, using acetyl proline. The crude product was purified by column chromatography (SiO_2, acetone/dichloromethane gradient, 1:9 to 2:3) to give a clear oil (0.7619 g, 77%). $[\alpha]^D_{25}$ – 63.0 (*c* 0.994, MeOH). IR (neat): 2969, 2884, 1789, 1649, 1633, 1419, 1384, 1285, 1264, 1226, 1198, 1182, 1132, 1102, 1021, 999, 960, 935, 905, 893, 841, 751, 736, 686, 616, 580, 539, 523, 479, 462, 407 cm^{-1}. ^{1}H NMR (400 MHz, $CDCl_3$) δ 5.74 (hept, *J* = 6.1 Hz, 1H), 4.60 (dd, *J* = 8.8, 4.1 Hz, 1H), 3.71 – 3.62 (m, 1H), 3.61 – 3.51 (m, 1H), 2.37 – 2.23 (m, 1H), 2.09 (s, 3H), 2.09 – 1.96 (m, 4H). ^{13}C NMR (101 MHz, $CDCl_3$) δ 170.0, 169.5, 120.5 (q, *J* = 284.0 Hz), 67.0 (p, *J* = 34.9 Hz), 58.3, 47.8, 29.4, 25.1, 22.0. ^{19}F NMR (376 MHz, $CDCl_3$) δ -76.2 (p, *J* = 7.2 Hz), -76.4 (p, *J* = 7.2 Hz). HRMS calcd. for $C_{10}H_{11}F_6NO_3Na$ $[M+Na]^+$ 330.0535, found 330.0567.

Acetyl proline CM ester (4.14).

The general procedure for the synthesis of activated esters protocol B was followed, using acetyl proline. The crude product was purified by column chromatography (SiO_2, acetone/dichloromethane gradient, 1:9 to 2:3) to give a clear oil (0.4698 g, 94%). $[\alpha]^D_{25}$ – 105.1 (*c* 0.995, MeOH). IR (neat): 3474, 2960, 2883, 1757, 1630, 1417, 1380, 1357,

1273, 1239, 1152, 1099, 1072, 1035, 1010, 953, 916, 874, 819, 693, 619, 605 cm^{-1}. ^{1}H NMR (500 MHz, $CDCl_3$) δ 4.80 (d, *J* = 15.7 Hz, 1H), 4.68 (d, *J* = 15.7 Hz, 1H), 4.45 (dd, *J* = 8.6, 3.6 Hz, 1H), 3.62 (dd, *J* = 13.6, 8.4 Hz, 1H), 3.50 (dd, *J* = 16.2, 7.0 Hz, 1H), 2.29 – 2.16 (m, 1H), 2.14 – 1.90 (m, 6H). ^{13}C NMR (126 MHz, $CDCl_3$) δ 171.0, 169.7, 114.4, 58.2, 48.9, 47.8, 29.31, 25.0, 22.2. HRMS calcd. for $C_9H_{12}N_2O_3Na$ $[M+Na]^+$ 219.0740, found 219.0713.

General procedures for peptide assembly.

Ligation protocol A: The hydroxyl amino acid or peptide (1 equiv) was dissolved in organic solvent (1 M) and set to stir at room temperature. The activated amino acid or peptide ester (HIP/TFE/CN, 1.5 equiv) was added, followed by AcOH (0.2 equiv). The reaction was monitored by TLC. After reaction completion, the mixture was concentrated in vacuo to afford a crude product that was purified by column chromatography.

Ligation protocol B: The hydroxyl amino acid or peptide (1 equiv) was added to a microwave reaction vessel and dissolved in organic solvent (1 M). The activated amino acid or peptide ester (HIP/TFE/CN, 1.5 equiv) was added, followed by AcOH (0.2 equiv) and sealed under air. The reaction was irradiated at 70 °C (300W, 5 min ramp time, 250 psi max, with stirring on). The reaction mixture was concentrated in vacuo to afford a crude product that was purified by column chromatography.

Threonine peptide assembly.

The ligations with threonine methyl ester **4.0** and the acetyl amino acid esters were performed with varying activators, solvents and utilizing both ligation protocols A and B. The results are documented in Tables 4.1, 4.2 and 4.3. The crude products were purified by column chromatography (SiO_2, acetone/dichloromethane gradient, 1:4 to 4:1) to give the title compounds. The experimental procedures reported are for the optimized reaction conditions utilizing the HIP activator and THF.

Ac-Ala-Thr-OMe (4.15).

The general procedure for threonine peptide assembly was followed, to get a white solid product. Ligation protocol A: 16 h room temperature (0.1508 g, 96%). Ligation protocol B: 4 h at 70 °C (0.1606 g, 96%). Mp: 146-149 °C. $[\alpha]^{D}_{25}$ –56.0 (*c* 0.519, MeOH). IR (neat): 3302, 3158, 3086, 2996, 2950, 2916, 2868, 2758, 1753, 1641, 1556, 1528, 1440, 1379, 1338, 1313, 1267, 1209, 1177, 1151, 1121, 1082, 1065, 1040, 1007, 992, 953, 937, 917, 896, 844, 778, 750, 699, 649, 602, 529, 460, 449 cm^{-1}. ^{1}H NMR (400 MHz, $CDCl_3$) δ 6.62 (d, *J* = 7.3 Hz, NH), 4.68 – 4.52 (m, 2H), 4.41 – 4.31 (m, 1H), 3.78 (s, 3H), 2.01 (s, 3H), 1.92 (br s, OH), 1.45 (d, *J* = 7.0 Hz, 3H), 1.22 (d, *J* = 6.5 Hz, 3H). ^{13}C NMR (101 MHz, $CDCl_3$) δ 173.0, 171.4, 170.8, 68.3, 58.0, 52.8, 49.3, 23.3, 20.2, 19.0. HRMS calcd. for $C_{10}H_{19}N_2O_5$ $[M+H]^+$ 247.1288, found 247.1286.

Ac-Phe-Thr-OMe (4.16).

The general procedure for threonine peptide assembly was followed, to get a white solid product. Ligation protocol B: 5 h at 70 °C (0.1953 g, 90%). Mp: 147-150 °C. $[\alpha]^{D}_{25}$ 1.7 (*c* 0.507, MeOH). IR (neat): 3266, 3064, 3032, 2953, 2929, 2859, 1753, 1638, 1545, 1498, 1454, 1437, 1380, 1341, 1304, 1284, 1262, 1209, 1193, 1155, 1131, 1080, 1024, 996, 957, 903, 871, 833, 763, 743, 719, 698, 633, 599, 499, 464, 419 cm^{-1}. ^{1}H NMR (400 MHz, CD_3OD) δ 7.30 – 7.25 (m, 4H), 7.24 – 7.18 (m, 1H), 4.72 (dd, *J* = 9.4, 5.4 Hz, 1H), 4.45 (d, *J* = 3.1 Hz, 1H), 4.32 – 4.24 (m, 1H), 3.71 (s, 3H), 3.18 (dd, *J* = 14.0, 5.4 Hz, 1H), 2.89 (dd, *J* = 14.0, 9.4 Hz, 1H), 1.89 (s, 3H), 1.17 (d, *J* = 6.5 Hz, 3H). ^{13}C NMR (101 MHz, CD_3OD) δ 174.4, 173.4, 172.4, 138.6, 130.4, 129.6, 127.9, 68.6, 59.4, 56.2, 53.0, 38.8, 22.5, 20.3. HRMS calcd. for $C_{16}H_{23}N_2O_5$ $[M+H]^+$ 323.1601, found 323.1604.

Ac-Pro-Thr-OMe (4.17).

The general procedure for threonine peptide assembly was followed, to get a clear oil product. Ligation protocol B: 5 h at 70 °C (0.1537 g, 83%). $[\alpha]^{D}_{25}$ –72.0 (*c* 0.518, MeOH). IR (neat): 3311, 3272, 3069, 2976, 2951, 2887, 1747, 1651, 1623, 1543, 1438, 1339, 1304, 1205, 1142, 1119, 1081, 1036, 998, 920, 897, 886, 866, 778, 692, 651, 627, 605, 534, 494, 453, 416 cm^{-1}. ^{1}H NMR (400 MHz, $CDCl_3$) δ 4.46 (dd, *J* = 9.0, 2.8 Hz, 1H), 4.28 – 4.20 (m, 1H), 3.69 (s, 3H), 3.64 – 3.54 (m, 1H), 3.48 – 3.39 (m, 1H), 2.30 – 2.09 (m, 2H), 2.04 (s, 3H), 2.02 – 1.82 (m, 3H), 1.14 (d, *J* = 6.5 Hz, 3H). ^{13}C NMR (101 MHz, CD_3OD) δ 175.2, 172.5, 172.4, 68.6, 61.2, 59.4, 52.9, 48.2, 31.0, 25.8, 22.3, 20.4. HRMS calcd. for $C_{12}H_{21}N_2O_5$ $[M+H]^+$ 273.1445, found 273.1443.

Ac-Leu-Thr-OMe (4.18).

The general procedure for threonine peptide assembly was followed, to get **4.18** as a clear oil product. Ligation protocol B: 5 h at 70 °C (0.1256 g, 70%). $[\alpha]^{D}_{25}$ –32.7 (*c* 0.513, MeOH). IR (neat): 3280, 3071, 2956, 2935, 2872, 1742, 1639, 1536, 1436, 1373, 1341, 1281, 1207, 1160, 1125, 1108, 1083, 1020, 995, 943, 898, 868, 830, 696, 597, 461, 417 cm^{-1}. ^{1}H NMR (400 MHz, CD_3OD) δ 4.53 – 4.44 (m, 2H), 4.35 – 4.26 (m, 1H), 3.74 (s, 3H), 1.99 (s, 3H), 1.79 – 1.65 (m, 1H), 1.65 – 1.53 (m, 2H), 1.17 (d, *J* = 6.5 Hz, 3H), 0.98 (d, *J* = 6.5 Hz, 3H), 0.94 (d, *J* = 6.5 Hz, 3H). ^{13}C NMR (101 MHz, CD_3OD) δ 175.4, 173.4, 172.4, 68.5, 59.2, 53.4, 52.9, 41.9, 26.0, 23.5, 22.5, 22.2, 20.4. HRMS calcd. for $C_{13}H_{24}N_2O_5Na$ $[M+Na]^+$ 311.1577, found 311.1568.

Ac-Ile-Thr-OMe (4.19).

The general procedure for threonine peptide assembly was followed, to get **4.19** as a white solid product. Ligation protocol B: 5 h at 70 °C (0.1319 g, 67%). Mp: 172-176 °C. $[\alpha]^{D}_{25}$ –28.0 (*c* 0.306, MeOH). IR (neat): 3276, 3072, 2970, 2958, 2932, 2875, 1723, 1633, 1543, 1455, 1437, 1376, 1286, 1251, 1214, 1156, 1128, 1082, 1015, 995, 961, 942, 917, 885, 865, 784, 747, 710, 669, 627, 605, 556, 501, 478 cm^{-1}. ^{1}H NMR (400 MHz, CD_3OD) δ 4.46 (d, *J* = 3.1 Hz, 1H), 4.31 – 4.27 (m, 2H), 3.73 (s, 3H), 1.99 (s, 3H), 1.91 – 1.81 (m, 1H), 1.62 – 1.52 (m, 1H), 1.26 – 1.20 (m, 1H), 1.18 (d, *J* = 6.5 Hz, 3H), 0.98 (d, *J* = 6.8 Hz, 3H), 0.93 (t, *J* = 7.5 Hz, 3H). ^{13}C NMR (101 MHz, CD_3OD) δ 174.6, 173.5, 172.4, 68.5, 59.6, 59.4, 52.8, 38.0, 26.1, 22.5, 20.4, 16.0, 11.5. HRMS calcd. for $C_{13}H_{24}N_2O_5Na$ $[M+Na]^+$ 311.1577, found 311.1553.

Ac-Val-Thr-OMe (4.20).

The general procedure for threonine peptide assembly was followed, to get a white solid product. Ligation protocol B: 5 h at 70 °C (0.1162 g, 62%). Mp: 160-164 °C. $[\alpha]^{D}_{25}$ –27.5 (*c* 0.361, MeOH). IR (neat): 3285, 3078, 2960, 2935, 2873, 1721, 1635, 1545, 1435, 1380, 1346, 1288, 1269, 1224, 1156, 1125, 1083, 1020, 964, 943, 923, 883, 855, 786, 716, 668, 629, 603, 543, 497, 456, 422 cm^{-1}. ^{1}H NMR (400 MHz, CD_3OD) δ 4.46 (d, *J* = 3.1 Hz, 1H), 4.34 – 4.26 (m, 1H), 4.25 (d, *J* = 7.5 Hz, 1H), 3.73 (s, 3H), 2.14 – 2.05 (m, 1H), 2.00 (s, 3H), 1.18 (d, *J* = 6.4 Hz, 3H), 0.99 (t, *J* = 7.0 Hz, 6H). ^{13}C NMR (101 MHz, CD_3OD) δ 174.5, 173.5, 172.5, 68.5, 60.6, 59.4, 52.8, 31.8, 22.5, 20.4, 19.8, 18.9. HRMS calcd. for $C_{12}H_{22}N_2O_5Na$ $[M+Na]^+$ 297.1421, found 297.1415.

General procedure for solid phase peptide synthesis:

a) Swelling: The 2-CTC resin was transferred to a reactor and suspended in a solution of NMP (1 mL per 150 μmol of resin) and 8 mL DCM, and was left to shake for 30 minutes. The swollen resin was washed 3 times with DCM and filtered under vacuum.

b) Coupling of the first amino acid to the resin: The initial Fmoc-AA (1 equiv) was dissolved in 2:1 DCM/NMP (1 mL per 150 μmol), treated with DIPEA (2 equiv), and added to the resin. The reactor was shaken for 1 hour, after which 0.5 mL of MeOH was added to cap the excess resin, and continued shaking for an additional 30 minutes. The resin was then filtered and washed 6 times with DMF.

c) Fmoc cleavage: The resin was treated with a solution of 20% piperidine or 4-methylpiperidine in DMF (1 mL per 150 μmol) and shaken for 10 minutes and filtered. The procedure was repeated and allowed to shake for 20 minutes. The resin was then filtered and washed 6 times with DMF.

d) Amino acid coupling: The Fmoc-AA (3 equiv) was dissolved in a solution of HATU in DMF (450 μM, 3 equiv), treated with DIPEA (3 equiv), and added to the resin. The reactor was shaken for 1 hour, filtered, and washed 6 times with DMF. Completion of the coupling was evaluated using the Kaiser test (step f). To complete the sequence, additional amino acids were added by repeating steps **c** and **d** until the last AA residue was added to the resin. The resin was then filtered, washed 4 times with DCM, then dried thoroughly under vacuum before cleavage of the peptide from the resin.

e) Peptide cleavage: The peptide was cleaved from the 2-CTC resin without side chain deprotection. The resin was suspended in the cleavage cocktail of AcOH/TFE/DCM (1:2:7, 10 mL) for 2 hours. The solvent was then collected by filtration and concentrated. The residue was suspended in diethylether and titrated for 30 minutes. The crude peptide was collected by filtration and used crude in subsequent reactions.

f) Kaiser test: The two Kaiser test reagents A and B were prepared as follows: A) dissolve 0.5 g of ninhydrin in 10 mL EtOH, and B) add 0.4 mL of a 0.1mM aq. sodium cyanide solution to 20 mL of pyridine. The Kaiser test was performed by adding 0.1 mL of reagent A and 0.1 mL of reagent B to a small amount of resin in an eppendorf tube. The suspension was then placed at 110 °C for 5 minutes. The development of a blue color

of the resin beads and/or solvent indicates the presence of unreacted primary amine. The lack of color change indicates the completion of the coupling reaction.

Fmoc-Leu-Lys(Boc)-Ala-Met-Asp(OtBu)-Pro-OH (4.21).

The general procedure for solid phase peptide synthesis was followed on a 600 μmol scale, to get **4.21** as a white solid (0.4746 g, 75%). ^{13}C NMR (126 MHz, $CDCl_3$) δ 172.5, 172.3, 171.8, 171.4, 171.1, 170.5, 168.7, 168.5, 135.9, 135.5, 128.5, 128.3, 128.2, 128.1, 127.9, 95.2, 77.8, 77.7, 66.9, 66.7, 65.3, 65.3, 61.1, 59.6, 59.4, 59.3, 58.1, 52.2, 51.9, 51.1, 47.6, 47.4, 47.3, 46.8, 41.1, 38.8, 31.6, 31.5, 29.3, 28.5, 28.1, 27.7, 27.1, 25.2, 25.0, 24.8, 24.7, 23.2, 22.9, 22.7, 22.3, 21.9, 21.1, 19.4, 19.3, 18.4, 14.2. HRMS calcd. for $C_{53}H_{78}N_7O_{13}S$ $[M+H]^+$ 1052.5373, found 1052.5402.

Fmoc-Thr-Pro-Pro-Leu-OH (4.22).

The general procedure for solid phase peptide synthesis was followed on a 150 μmol scale, to get **4.22** as a white solid (0.0846 g, 87%). ^{13}C NMR (101 MHz, CD_3OD) δ 176.1, 174.4, 172.6, 171.6, 158.7, 145.3, 142.7, 128.9, 128.3, 126.3, 121.1, 68.5, 68.2, 61.4, 60.0, 59.7, 52.3, 41.8, 30.4, 29.5, 26.0, 23.5, 22.1, 20.0. HRMS calcd. for $C_{35}H_{45}N_4O_8$ $[M+H]^+$ 649.3232, found 649.3219.

Fmoc-Leu-Lys(Boc)-Ala-Met-Asp(OtBu)-Pro-OHIP (4.23).

Peptide **4.21** (0.4355 g, 0.414 mmol) was dissolved in dichloromethane (4 mL) and set to stir at 0 °C. EDCI (95.9 mg, 0.500 mmol), HOBt (68.3 mg, 0.505 mmol) and 1,1,1,3,3,3-hexafluoroisopropanol (0.44 mL, 4.18 mmol) were added to the reaction mixture. The mixture was stirred at 0 °C for 30 min, then for 6 h at room temperature. The solvent was removed in vacuo, and the residue was dissolved in ethyl acetate and washed with 1 N HCl and sat. $NaHCO_3$. The organic phase was dried over sodium sulfate, filtered, and concentrated in vacuo to afford a crude product that was purified by column chromatography (SiO_2, acetone/dichloromethane gradient, 1:9 to 2:3) to give **4.23** as a white solid (0.4033 g, 81%). ^{13}C NMR (101 MHz, $CDCl_3$) δ 173.8, 172.8, 172.1, 171.4, 169.9, 169.0, 168.9, 156.8, 156.1, 144.5, 144.1, 141.4, 127.8, 127.2, 125.6, 125.4, 124.7, 121.9, 120.0, 119.1, 116.3, 81.1, 78.8, 67.2, 66.8, 66.5, 58.6, 56.1, 53.8, 52.1, 47.2, 42.3, 40.4, 38.6, 34.6, 30.0, 29.0, 28.5, 28.0, 25.2, 24.9, 23.0, 21.2, 15.3. ^{19}F NMR (376 MHz, $CDCl_3$) δ -76.2 (d, J = 52.7 Hz). HRMS calcd. for $C_{56}H_{77}F_6N_7O_{13}SNa$ $[M+Na]^+$ 1224.5096, found 1224.5036.

Fmoc-Thr-Pro-Pro-Leu-OBn (4.24).

Peptide **4.22** (0.2172 g, 0.335 mmol) was dissolved in acetonitrile (5 mL) and set to stir at room temperature. Cesium carbonate (0.1322 g, 0.406 mmol) and benzyl bromide (0.10 mL, 0.836 mmol) were added to the reaction mixture and stirred for 4 h. The solvent was removed in vacuo to afford a crude product that was purified by column chromatography (SiO_2, acetone/dichloromethane gradient, 1:4 to 2:3) to give **4.24** as a white solid (0.2071

g, 84%). ^{13}C NMR (101 MHz, CD_3OD) δ 174.5, 174.0, 172.9, 172.6, 171.6, 158.7, 145.3, 142.7, 137.3, 129.7, 129.5, 128.9, 128.3, 126.3, 121.1, 68.5, 68.2, 68.0, 61.2, 60.0, 59.7, 52.6, 41.4, 30.4, 29.5, 26.1, 25.9, 23.4, 22.1, 20.0. HRMS calcd. for $C_{42}H_{50}N_4O_8Na$ $[M+Na]^+$ 761.3521, found 761.3452.

H_2N-Thr-Pro-Pro-Leu-OBn (4.25).

Peptide **4.24** (0.4779 g, 0.647 mmol) was dissolved in THF (7 mL) and set to stir at room temperature. 1-Octanethiol (1.2 mL, 6.92 mmol) was added to the reaction mixture, followed by DBU (10 μL, 66.9 μmol). The reaction mixture was stirred for 1 h at room temperature and concentrated in vacuo to afford a crude product that was purified by column chromatography (SiO_2, acetone/dichloromethane gradient, 1:9 to 9:1) to give **4.25** as a white solid (0.3322 g, 99%). ^{13}C NMR (126 MHz, $CDCl_3$) δ 172.5, 172.3, 171.7, 171.4, 171.1, 170.5, 168.7, 168.5, 135.9, 135.5, 128.5, 128.3, 128.2, 128.1, 127.9, 95.3, 95.2, 77.8, 77.7, 67.0, 66.7, 65.32, 65.26, 61.1, 59.6, 59.3, 58.1, 52.2, 51.1, 47.6, 47.4, 47.3, 46.8, 41.1, 38.8, 31.6, 31.5, 29.3, 28.5, 28.1, 27.7, 27.1, 25.2, 25.0, 24.8, 24.7, 23.2, 22.9, 22.3, 21.9, 21.1, 19.4, 19.3. HRMS calcd. for $C_{27}H_{41}N_4O_6$ $[M+H]^+$ 517.3021, found 517.3033.

LTNF-10 threonine peptide assembly.

The ligations of **4.24** and **4.25** were performed with varying solvents and concentrations utilizing both ligation protocols A and B. All the results are documented in Table 4.4. The crude products were purified by column chromatography (SiO_2, acetone/dichloromethane gradient, 2:3 to 9:1) to give the title compound. The experimental procedures reported below are for the optimized reaction conditions for both ligation protocols A and B.

Fmoc-Leu-Lys(Boc)-Ala-Met-Asp(OtBu)-Pro-Thr-Pro-Pro-Leu-OBn (4.26).

The general procedure for LTNF-10 threonine peptide assembly was followed, to get a white solid product. Ligation protocol A: 5 days room temperature in 0.33 M DMF (72.9 mg, 30%). Ligation protocol B: 5 h at 70 °C in 0.25 M THF (18.9 mg, 10%). ^{13}C NMR (126 MHz, $CDCl_3$) δ 172.7, 171.9, 171.7, 170.0, 157.2, 156.7, 143.8, 141.5, 135.7, 128.7, 128.5, 128.4, 128.0, 127.4, 125.3, 120.2, 67.4, 67.1, 65.9, 61.3, 60.6, 59.9, 59.5, 59.2, 54.8, 51.2, 47.7, 47.3, 45.5, 41.2, 38.6, 38.1, 29.9, 29.7, 28.7, 28.2, 25.4, 25.0, 23.2, 23.1, 22.9, 22.4, 22.0, 21.4, 19.3. HRMS calcd. for $C_{80}H_{115}N_{11}O_{18}SNa$ $[M+Na]^+$ 1572.8034, found 1572.8057.

LTNF-10: Leu-Lys-Ala-Met-Asp-Pro-Thr-Pro-Pro-Leu (4.27).

A suspension of peptide **4.26** (72.3 mg, 46.6 μmol) and 10% palladium on activated carbon (25.9 mg) in MeOH/AcOH (5 mL, 9:1) was hydrogenated, stirring the reaction mixture at room temperature under H_2 (1 atm) for 24 h. The reaction mixture was filtered through celite and concentrated in vacuo. The crude mixture was precipitated in ether and filtered to obtain the crude peptide as a white solid used in the subsequent deprotection reaction. HRMS calcd. for $C_{73}H_{109}N_{11}O_{18}SNa$ $[M+Na]^+$ 1482.7565, found 1482.7693.

The crude peptide was treated with 20% 4-methylpiperidine in dichloromethane (2 mL) and stirred for 1 h at room temperature. The reaction mixture was concentrated in vacuo and the crude mixture was precipitated in ether and filtered to obtain the crude peptide as a white solid used in the subsequent deprotection reaction. HRMS calcd. for $C_{58}H_{100}N_{11}O_{16}S$ $[M+H]^+$ 1238.7065, found 1238.7015.

The crude peptide was treated with the deprotection cocktail of TFA/water/triethylsilane (5 mL, 95/2.5/2.5) and stirred at room temperature for 2 h. The reaction mixture was concentrated in vacuo and the crude peptide was precipitated in ether and filtered to obtain **4.27** TFA salt as a white solid (33.1 mg, 54% over three steps). ^{13}C NMR (101 MHz, CD_3OD) δ 176.1, 175.1, 174.5, 174.3, 174.2, 173.4, 172.7, 171.9, 170.9, 170.8, 68.6, 62.0, 61.4, 60.1, 57.9, 54.6, 53.8, 53.0, 52.3, 50.8, 41.8, 40.6, 36.9, 32.8, 32.6, 31.1, 30.7, 30.4, 29.6, 28.2, 26.0, 25.8, 25.5, 23.5, 23.3, 22.2, 22.0, 19.9, 17.9, 15.4. HRMS calcd. for $C_{49}H_{84}N_{11}O_{14}S$ $[M+H]^+$ 1082.5914, found 1082.5881.

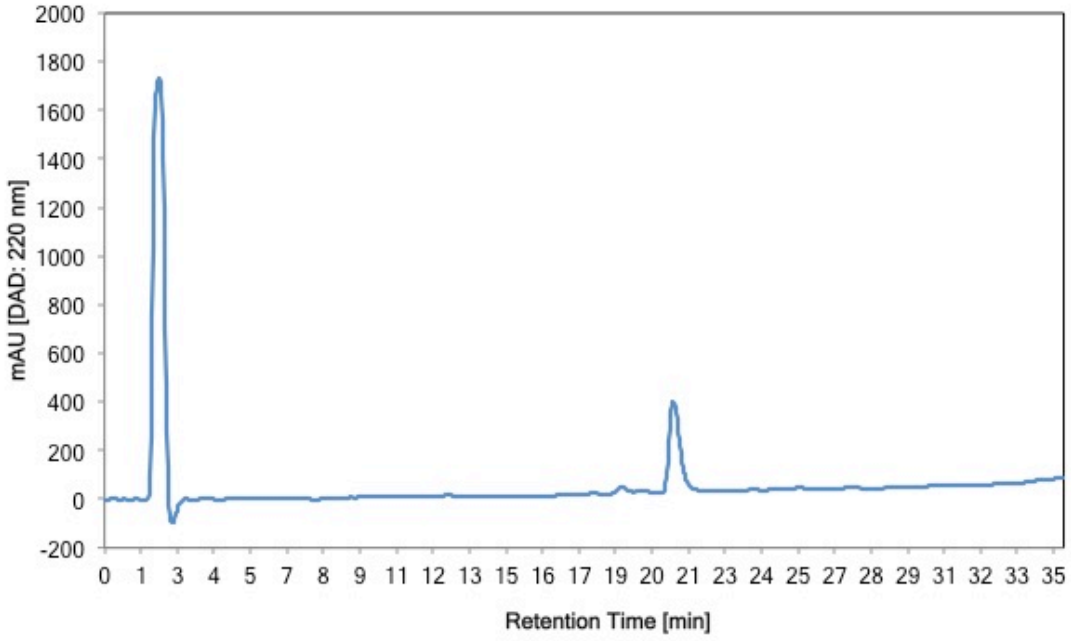

Figure 5.1: Reverse-Phase HPLC analysis of synthesized LTNF-10. A solution of LTNF-10 was manually injected onto an Agilent Eclipse Plus C_{18} RP-HPLC column, and eluted with 5% acetonitrile/ 95% water (solutions containing 0.1% TFA) isocratic for five minutes, followed by a gradient elution to 50% acetonitrile/ 50% water (solutions contain 0.1% TFA) over 30 minutes, with a flow rate of 1 mL/ min. The peak around 2 minutes corresponds to solvent and the peak around 21 minutes corresponds to LTNF-10. The chromatogram was taken at DAD 220 nm to analyze the purity of LTNF-10.

Boc-phenylalanine *tert*-butyl amide (4.46).

N-Boc phenylalanine (3.077 g, 11.6 mmol) was dissolved in dichloromethane (100 mL) and set to stir at 0 °C. HATU (5.2934 g, 13.9 mmol) was added to the reaction mixture, followed by DIPEA (2.4 mL, 14.0 mmol) and *tert*-butylamine (1.8 mL, 17.4 mmol). The mixture was stirred at 0 °C for 30 min, then for 4 h at room temperature. The solvent was removed in vacuo, and the residue was dissolved in ethyl acetate (50 mL) and washed with 1 N HCl (20 mL) and sat. $NaHCO_3$ (20 mL). The organic phase was dried over sodium sulfate, filtered, and concentrated in vacuo to afford a crude product that was

purified by column chromatography (SiO_2, acetone/dichloromethane gradient, 1:9 to 1:4) to give **4.46** as a white solid (3.6301 g, 98%). Mp: 133-135 °C (Lit. Mp: 133 °C)[148]. $[\alpha]^{D}_{25}$ 9.5 (*c* 1.01, MeOH). IR (neat): 3303, 3064, 3038, 2972, 2930, 2868, 1685, 1654, 1537, 1498, 1453, 1391, 1363, 1300, 1273, 1250, 1223, 1171, 1083, 1048, 1021, 963, 932, 915, 884, 860, 791, 733, 696, 621, 570, 553, 509, 470, 439, 411 cm^{-1}. ^{1}H NMR (400 MHz, $CDCl_3$) δ 7.34 – 7.26 (m, 2H), 7.24 (t, *J* = 7.8 Hz, 3H), 4.20 – 4.10 (m, 1H), 3.11 (dd, *J* = 13.5, 5.7 Hz, 1H), 2.91 (dd, *J* = 13.1, 8.7 Hz, 1H), 1.43 (s, 9H), 1.20 (s, 9H). ^{13}C NMR (101 MHz, $CDCl_3$) δ 170.1, 155.4, 137.3, 129.7, 128.8, 127.1, 80.1, 56.7, 51.4, 39.4, 28.7, 28.5. HRMS calcd. for $C_{18}H_{29}N_2O_3$ $[M+H]^+$ 321.2173, found 321.2201. ^{1}H NMR and ^{13}C NMR data are consistent with previously reported literature values.[148]

Phenylalanine *tert*-butyl amide.

Boc-phenylalanine *tert*-butyl amide **4.46** (2.2458 g, 7.01 mmol) was dissolved in dichloromethane (8 mL) and set to stir at room temperature. Trifluoroacetic acid (2.8 mL, 36.6 mmol) was added dropwise to the reaction mixture, stirred for 1 h, and concentrated in vacuo to afford the crude TFA salt as a white solid (2.2965 g) in 98% yield. NMR data is consistent with previously reported literature values.[149]

The crude phenylalanine *tert*-butyl amide TFA salt was dissolved in water (4 mL) and set to stir at 0 C. The pH was adjusted to 12 with sat. aq. sodium bicarbonate and stirred for 30 min at room temperature. The solution was then extracted with ethyl acetate (4 x 10 mL). The combined organic extract was dried over anhydrous sodium sulfate,

filtered, and concentrated to afford the crude product as a colorless sticky solid. The crude amino acid was used in subsequent reactions without further purification.

Boc-Hse(OBn)-Phe *tert*-butyl amide (4.47).

N-Boc-Hse(OBn)-OH (1.1796 g, 3.81 mmol) was dissolved in dichloromethane (40 mL) and set to stir at 0 °C. HOBt (0.7592 g, 4.96 mmol) was added to the reaction mixture, followed by EDCI (0.9510 g, 4.96 mmol) and phenylalanine *tert*-butyl amide (1.2678 g, 5.75 mmol). The mixture was stirred at 0 °C for 30 min, then for 6 h at room temperature. The solvent was removed in vacuo, and the residue was dissolved in ethyl acetate (25 mL) and washed with 1 N HCl (10 mL) and sat. $NaHCO_3$ (10 mL). The organic phase was dried over sodium sulfate, filtered, and concentrated in vacuo to afford a crude product that was purified by column chromatography (SiO_2, acetone/dichloromethane gradient, 1:9 to 2:3) to give **4.47** as a white solid (1.9274 g, 98%). Mp: 48-51 °C. $[\alpha]^{D}_{25}$ -24.6 (*c* 1.02, MeOH). IR (neat): 3305, 3064, 3030, 2973, 2930, 2867, 1762, 1644, 1496, 1454, 1391, 1364, 1247, 1225, 1162, 1100, 1029, 912, 863, 738, 697, 607, 519, 494 cm^{-1}. ^{1}H NMR (500 MHz, $CDCl_3$) δ 7.40 – 7.29 (m, 5H), 7.29 – 7.14 (m, 5H), 6.82 (d, *J* = 7.0 Hz, NH), 5.96 (br s, NH), 5.83 (br s, NH), 4.55 (dd, *J* = 13.0, 6.4 Hz, 1H), 4.46 (s, 2H), 4.16 (dd, *J* = 11.5, 5.6 Hz, 1H), 3.56 (d, *J* = 4.1 Hz, 2H), 3.19 (dd, *J* = 13.3, 4.5 Hz, 1H), 2.88 (dd, *J* = 13.7, 7.3 Hz, 1H), 2.11 – 1.96 (m, 2H), 1.38 (s, 9H), 1.23 (s, 9H). ^{13}C NMR (126 MHz, $CDCl_3$) δ 171.4, 169.4, 156.0, 137.8, 136.8, 129.5, 128.8, 128.6, 128.0, 127.8, 127.1, 80.2, 73.5, 68.3, 55.0, 54.4, 51.5, 38.1, 31.5, 28.6, 28.4. HRMS calcd. for $C_{29}H_{42}N_3O_5$ $[M+H]^+$ 512.3119, found 512.3078.

Boc-Hse-Phe *tert*-butyl amide (4.48).

A suspension of peptide **4.27** (3.2500 g, 6.35 mmol) and 10% palladium on activated carbon (0.1385 g) in MeOH/AcOH (50 mL, 9:1) was hydrogenated, stirring the reaction mixture at room temperature under H_2 (1 atm) for 20 h. The reaction mixture was filtered through celite and concentrated in vacuo. The crude product was dissolved in ethyl acetate (50 mL) and washed with 1 N HCl (20 mL) and sat. $NaHCO_3$ (20 mL). The organic phase was dried over sodium sulfate, filtered, and concentrated in vacuo to afford **4.48** as a white solid (2.5536, 95%). Mp: 62-66 °C. $[\alpha]^{D}_{25}$ –33.0 (*c* 1.02, MeOH). IR (neat): 3299, 3088, 3064, 3030, 2971, 2930, 1644, 1497, 1454, 1391, 1365, 1247, 1225, 1164, 1052, 1031, 904, 865, 742, 699, 647, 598, 521, 494, 426 cm^{-1}. ^1H NMR (400 MHz, $CDCl_3$) δ 7.37 – 7.29 (m, 2H), 7.29 – 7.22 (m, 3H), 7.05 (br s, NH), 5.63 (br s, NH), 5.57 (br s, NH), 4.52 (dd, *J* = 14.4, 7.9 Hz, 1H), 4.31 (d, *J* = 5.3 Hz, 1H), 3.77 – 3.58 (m, 2H), 3.16 (dd, *J* = 13.4, 5.6 Hz, 1H), 2.97 (dd, *J* = 13.6, 8.2 Hz, 1H), 2.05 – 1.91 (m, 2H), 1.82 (br s, OH), 1.44 (s, 9H), 1.22 (s, 9H). ^{13}C NMR (101 MHz, $CDCl_3$) δ 172.0, 169. 6, 156.4, 137.0, 129.7, 128.9, 127.3, 80.6, 59.3, 55.2, 52.9, 51.7, 38.7, 35.5, 28.6, 28.5. HRMS calcd. for $C_{22}H_{35}N_3O_5Na$ $[M+Na]^+$ 444.2469, found 444.2428.

H_2N-Hse-Phe *tert*-butyl amide (4.49).

Dipeptide **4.48** (2.5536 g, 6.06 mmol) was dissolved in a minimum amount of MeOH (1 mL) and set to stir at 0 °C. A solution of hydrochloric acid in ether (2 N, 15 mL) was added slowly, and the stirring was continued for 1 h. The reaction mixture was concentrated in vacuo without heat and used crude in the next step. The reaction mixture

was dissolved in water and ethyl acetate (1:1, 12 mL) and set to stir at 0 °C. Sodium bicarbonate (3.0587 g, 36.4 mL) was added slowly to the reaction mixture, followed by addition of benzyl chloroformate (1.28 mL, 9.09 mmol). The reaction was stirred at 0 °C for 15 min, then for 14 h at room temperature. The organic phase was separated, and the aqueous phase was extracted with ethyl acetate (4 x 10 mL). The organic portions were combined, dried over sodium sulfate, filtered, and concentrated in vacuo to afford a crude product that was purified by column chromatography (SiO_2, acetone/dichloromethane gradient, 1:9 to 2:3) to give the *N*-Cbz protected dipeptide as a white solid (1.6069 g, 58%). Mp: 157-159 °C. $[\alpha]^{D}_{25}$ –38.7 (*c* 0.506, MeOH). IR (neat): 3371, 3343, 3226, 3063, 3028, 3006, 2976, 2961, 2934, 2885, 2868, 1711, 1663, 1643, 1585, 1538, 1499, 1447, 1415, 1392, 1364, 1330, 1317, 1286, 1259, 1232, 1187, 1167, 1154, 1115, 1095, 1080, 1046, 1030, 994, 944, 902, 890, 845, 789, 754, 743, 716, 699, 625, 586, 575, 512, 502, 466, 450, 412 cm^{-1}. ^{1}H NMR (500 MHz, $CDCl_3$) δ 7.39 – 7.31 (m, 5H), 7.31 – 7.26 (m, 2H), 7.25 – 7.18 (m, 3H), 5.09 (q, *J* = 12.2 Hz, 2H), 4.53 (dd, *J* = 14.9, 7.6 Hz, 1H), 4.44 (dd, *J* = 12.4, 6.6 Hz, 1H), 3.72 – 3.63 (m, 1H), 3.63 – 3.55 (m, 1H), 3.07 (dd, *J* = 13.5, 6.3 Hz, 1H), 2.99 (dd, *J* = 13.2, 8.4 Hz, 1H), 2.81 (br s, OH), 2.06 – 1.89 (m, 1H), 1.88 – 1.77 (m, 1H), 1.20 (s, 9H). ^{13}C NMR (126 MHz, $CDCl_3$) δ 171.7, 169.7, 156.8, 137.1, 136.3, 129.6, 128.8, 128.8, 128.4, 128.3, 127.2, 67.4, 59.1, 55.3, 53.2, 51.6, 38.8, 35.5, 28.6. HRMS calcd. for $C_{25}H_{33}N_3O_5Na$ $[M+Na]^+$ 478.2312, found 478.2288.

A suspension of Cbz-Hse-Phe *tert*-butyl amide (1.0047 g, 2.21 mmol) and 10% palladium on activated carbon (51.0 mg) in MeOH (5 mL) was hydrogenated, stirring the reaction mixture at room temperature under H_2 (1 atm) for 1 h. The reaction mixture was

filtered through celite and concentrated in vacuo to give **4.49** as a white solid (0.6905 g, 97%) Mp: 104-107 °C. $[\alpha]^{D}_{25}$ 7.4 (*c* 0.497, MeOH). IR (neat): 3286, 3084, 3031, 2969, 2925, 2871, 1638, 1549, 1497, 1454, 1392, 1363, 1299, 1250, 1222, 1157, 1117, 1055, 1032, 962, 913, 876, 846, 732, 696, 667, 574, 494, 436 cm^{-1}. ^{1}H NMR (400 MHz, CD_3OD) δ 7.34 – 7.14 (m, 5H), 4.53 (t, *J* = 7.5 Hz, 1H), 3.68 – 3.55 (m, 2H), 3.43 (dd, *J* = 7.8, 5.5 Hz, 1H), 3.02 (dd, *J* = 13.5, 7.3 Hz, 1H), 2.91 (dd, *J* = 13.5, 7.8 Hz, 1H), 1.92 – 1.76 (m, 1H), 1.71 – 1.56 (m, 1H), 1.23 (s, 9H). ^{13}C NMR (101 MHz, CD_3OD) δ 177.2, 172.5, 138.4, 130.7, 129.6, 127.9, 60.2, 56.3, 54.1, 52.3, 39.8, 38.6, 28.9. HRMS calcd. for $C_{17}H_{28}N_3O_3$ [M+H]+ 322.2125, found 322.2102.

Homoserine peptide assembly

The ligation with homoserine dipeptide **4.49** and the acetyl amino acid esters were performed with varying activators and utilizing both ligation protocols A and B. All the results are documented in Tables 4.5 and 4.6. The crude products were purified by column chromatography (SiO_2, acetone/dichloromethane gradient, 2:3 to 4:1) to give the title compounds. The experimental procedures reported below are for the optimized reaction conditions utilizing the HIP activator and DMF.

Ac-Ala-Hse-Phe *tert*-butyl amide (4.51).

The general procedure for homoserine peptide assembly was followed, with the use of Ac-alanine CM ester in place of the HIP ester to get a white solid product. Ligation protocol A: 30 h room temperature (91.2 mg, 89%). Ligation protocol B: 2 h at 70 °C (76.8 mg, 62%). Mp: 233 °C (dec.). $[\alpha]^{D}_{25}$ –63.2 (*c* 0.519, MeOH). IR (neat): 3284, 3089, 3030, 2970, 2930, 2873, 1686, 1621, 1531, 1435, 1393, 1363, 1276, 1224, 1159, 1050, 977, 930, 882, 847, 741, 696, 602, 569, 520, 496, 451, 438, 427, 411 cm^{-1}. ^{1}H NMR (400 MHz, CD_3OD) δ 7.33 – 7.17 (m, 5H), 4.51 (dd, *J* = 9.1, 5.9 Hz, 1H), 4.32 (dd, *J* = 7.2, 5.3 Hz, 1H), 4.20 (q, *J* = 7.2 Hz, 1H), 3.56 – 3.44 (m, 1H), 3.35 – 3.26 (m, 1H), 3.15 (dd, *J* = 13.8, 5.8 Hz, 1H), 2.94 (dd, *J* = 13.7, 9.2 Hz, 1H), 2.03 (s, 3H), 1.94 – 1.82 (m, 1H), 1.79 – 1.67 (m, 1H), 1.34 (d, *J* = 7.2 Hz, 3H), 1.29 (s, 9H). ^{13}C NMR (101 MHz, CD_3OD) δ 175.7, 174.1, 173.8, 172.6, 138.9, 130.5, 129.6, 127.9, 59.7, 56.8, 53.9, 52.6, 51.7, 39.0, 34.6, 29.0, 22.7, 17.5. HRMS calcd. for $C_{22}H_{35}N_4O_5$ $[M+H]^+$ 435.2602, found 435.2627.

Ac-Phe-Hse-Phe *tert*-butyl amide (4.52).

The general procedure for homoserine peptide assembly was followed, to get a white solid product. Ligation protocol A: 12 h at room temperature (76.0 mg, 53%). Ligation protocol B: 2 h at 70 °C (66.8 mg, 52%). Mp: 245 °C (dec.). $[\alpha]^{D}_{25}$ –28.5 (*c* 0.50, MeOH). IR (neat): 3285, 3088, 3063, 3029, 2967, 2927, 1681, 1622, 1549, 1496, 1453, 1393, 1363, 1264, 1224, 1128, 1051, 1031, 956, 913, 885, 843, 823, 741, 697, 598, 578, 520, 499, 427, 411 cm^{-1}. ^{1}H NMR (500 MHz, CD_3OD) δ 7.29 – 7.16 (m, 10H), 4.54 (dd,

J = 9.6, 4.9 Hz, 1H), 4.50 (dd, *J* = 8.2, 6.7 Hz, 1H), 4.37 (dd, *J* = 7.8, 5.3 Hz, 1H), 3.52 (dt, *J* = 10.9, 5.4 Hz, 1H), 3.44 – 3.35 (m, 1H), 3.16 – 3.04 (m, 2H), 2.97 – 2.82 (m, 2H), 1.92 (s, 3H), 1.91 – 1.85 (m, 1H), 1.80 – 1.71 (m, 1H), 1.27 (s, 9H). ^{13}C NMR (126 MHz, CD_3OD) δ 174.1, 173.8, 173.6, 172.4, 138.6, 130.6, 130.3, 129.6, 129.6, 127.9, 127.9, 59.6, 56.8, 56.7, 53.4, 52.4, 39.2, 38.5, 35.1, 28.9, 22.6. HRMS calcd. for $C_{28}H_{39}N_4O_5$ $[M+H]^+$ 511.2915, found 511.2909.

Ac-Val-Hse-Phe *tert*-butyl amide (4.53).

The general procedure for homoserine peptide assembly was followed, to get a white solid product. Ligation protocol A: 84 h at room temperature (59.2 mg, 46%). Ligation protocol B: 2 h at 70 °C (59.4 mg, 46%). Mp: 254 °C (dec.). $[\alpha]^D_{25}$ –55.5 (*c* 0.418, MeOH). IR (neat): 3281, 3088, 3031, 2965, 2932, 2874, 1686, 1623, 1531, 1454, 1392, 1363, 1264, 1225, 1120, 1054, 952, 912, 887, 741, 694, 600, 528, 499, 427, 412 cm^{-1}. ^{1}H NMR (500 MHz, CD_3OD) δ 7.35 – 7.13 (m, 5H), 4.50 (dd, *J* = 8.5, 6.4 Hz, 1H), 4.40 (dd, *J* = 7.7, 5.4 Hz, 1H), 4.07 (d, *J* = 6.6 Hz, 1H), 3.58 – 3.49 (m, 2H), 3.42 – 3.34 (m, 1H), 3.09 (dd, *J* = 13.7, 6.4 Hz, 1H), 2.98 – 2.90 (m, 1H), 2.04 (s, 3H), 1.95 – 1.86 (m, 1H), 1.81 – 1.71 (m, 1H), 1.26 (s, 9H), 0.95 (t, *J* = 7.3 Hz, 6H). ^{13}C NMR (126 MHz, CD_3OD) δ 174.2, 174.1, 173.6, 172.3, 138.7, 130.6, 129.5, 127.8, 61.3, 59.6, 56.8, 53.3, 52.4, 39.2, 35.1, 31.5, 28.9, 22.6, 19.9, 18.9. HRMS calcd. for $C_{24}H_{39}N_4O_5$ $[M+H]^+$ 463.2915, found 463.2912.

Ac-Pro-Hse-Phe *tert*-butyl amide (4.54).

The general procedure for homoserine peptide assembly was followed, to get a clear oil film. Ligation protocol B: 2 h at 70 °C (83.5 mg, 76%). $[\alpha]^{D}_{25}$ –68.8 (*c* 0.50, MeOH). IR (neat): 3291, 3087, 3063, 3030, 2964, 2929, 2875, 1624, 1526, 1450, 1420, 1393, 1362, 1300, 1224, 1119, 1058, 1033, 997, 917, 876, 847, 743, 699, 661, 620, 597, 543, 498, 451, 423, 411 cm^{-1}. ^{1}H NMR (400 MHz, CD_3OD) δ 7.32 – 7.16 (m, 5H), 4.57 – 4.48 (m, 1H), 4.36 – 4.29 (m, 2H), 3.72 – 3.56 (m, 2H), 3.56 – 3.47 (m, 1H), 3.17 (dd, *J* = 13.8, 5.5 Hz, 1H), 2.94 (dd, *J* = 13.2, 10.1 Hz, 1H), 2.29 – 2.18 (m, 1H), 2.15 (s, 3H), 2.05 – 1.92 (m, 4H), 1.87 (dd, *J* = 8.7, 5.1 Hz, 1H), 1.77 – 1.65 (m, 1H), 1.30 (s, 9H). ^{13}C NMR (101 MHz, CD_3OD) δ 175.0, 173.8, 173.1, 172.6, 138.9, 130.5, 129.5, 127.8, 62.2, 59.7, 56.8, 56.7, 53.9, 52.5, 39.0, 34.4, 31.0, 29.0, 26.0, 22.7. HRMS calcd. for $C_{24}H_{37}N_4O_5$ $[M+H]^+$ 462.2789, found 462.2816.

Ac-Leu-Hse-Phe *tert*-butyl amide (4.55).

The general procedure for homoserine peptide assembly was followed, to get a white solid product. Ligation protocol B: 2 h at 70 °C (39.2 mg, 34%). Mp: 271 °C (dec.). $[\alpha]^{D}_{25}$ –58.2 (*c* 0.253, MeOH). IR (neat): 3273, 3088, 2959, 2928, 2869, 1687, 1622, 1537, 1455, 1393, 1364, 1289, 1268, 1226, 1147, 1116, 1055, 958, 935, 886, 825, 780, 743, 696, 623, 600, 525, 499, 482, 412 cm^{-1}. ^{1}H NMR (400 MHz, CD_3OD) δ 7.31 – 7.14 (m, 5H), 4.50 (t, *J* = 7.4 Hz, 1H), 4.32 (t, *J* = 6.2 Hz, 1H), 4.26 (t, *J* = 7.5 Hz, 1H), 3.56 – 3.46 (m, 1H), 3.13 (dd, *J* = 13.7, 6.0 Hz, 1H), 2.93 (dd, *J* = 13.6, 9.2 Hz, 1H), 2.03 (s, 3H), 1.94 – 1.83 (m, 1H), 1.80 – 1.65 (m, 2H), 1.56 (t, *J* = 7.3 Hz, 2H), 1.28 (s, 9H), 0.97

(d, J = 6.5 Hz, 3H), 0.93 (d, J = 6.4 Hz, 3H). ^{13}C NMR (101 MHz, CD_3OD) δ 175.4, 174.3, 173.8, 172.5, 138.8, 130.6, 129.6, 127.9, 59.7, 56.8, 54.3, 53.8, 52.6, 41.5, 39.1, 34.7, 29.0, 26.1, 23.5, 22.6, 22.0. HRMS calcd. for $C_{25}H_{41}N_4O_5$ $[M+H]^+$ 477.3071, found 477.3097.

Ac-Ile-Hse-Phe *tert*-butyl amide (4.56).

The general procedure for homoserine peptide assembly was followed, to get a white solid product. Ligation protocol B: 2 h at 70 °C (75.1 mg, 56%). Mp: 243 °C (dec.). $[\alpha]^D_{25}$ –45.9 (*c* 0.30, MeOH). IR (neat): 3273, 3087, 2965, 2931, 2876, 1686, 1622, 1536, 1455, 1393, 1364, 1286, 1265, 1225, 1154, 1054, 949, 912, 888, 741, 696, 600, 498, 427 cm^{-1}. ^{1}H NMR (400 MHz, CD_3OD) δ 7.29 – 7.17 (m, 5H), 4.49 (dd, J = 8.5, 6.3 Hz, 1H), 4.43 – 4.34 (m, 1H), 4.16 – 4.09 (m, 1H), 3.59 – 3.45 (m, 1H), 3.39 – 3.33 (m, 1H), 3.20 – 3.06 (m, 1H), 3.02 – 2.89 (m, 1H), 2.04 (s, 3H), 1.94 – 1.78 (m, 2H), 1.78 – 1.69 (m, 1H), 1.27 (s, 9H), 1.26 (d, J = 20.4 Hz, 2H), 0.98 – 0.88 (m, 6H). ^{13}C NMR (101 MHz, CD_3OD) δ 174.3, 174.1, 173.7, 172.4, 138.8, 130.6, 129.6, 127.9, 60.3, 59.6, 56.9, 53.4, 52.4, 39.1, 37.8, 34.9, 28.9, 26.4, 22.6, 16.2, 11.8. HRMS calcd. for $C_{25}H_{40}N_4O_5Na$ $[M+Na]^+$ 499.2891, found 499.2907.

General procedure for homoserine peptide oxidation.

The homoserine peptide (1 equiv) was dissolved in 3 mL acetone/DMF (2:1) and set to stir at 0 °C. An aqueous 15% solution of $NaHCO_3$ (0.5 mL) was added, followed by NaBr (0.05 equiv) and TEMPO (0.01 equiv). TCICA (2 equiv) was added over 20 min (0.5 equiv portions every 5 min). After the addition of TCICA, the reaction mixture was stirred for 2 h and 2-propanol (2 mL) was added and stirring was continued for 15 min. The reaction mixture was concentrated in vacuo. The mixture was dissolved with sat. aqueous $NaHCO_3$ (5 mL) and was washed with ethyl acetate (15 mL). The aqueous phase was acidified to pH 2 using 1N hydrochloric acid, and extracted with ethyl acetate (4 × 15 mL). The combined organic extract was dried over anhydrous sodium sulfate and concentrated to afford the oxidized peptide.

Ac-Val-Asp-Phe *tert*-butyl amide (4.57).

The general procedure for homoserine peptide oxidation was followed, to get a white solid (59.4 mg, 75%). Mp: 250 °C (dec.). $[\alpha]^{D}_{25}$ –27.2 (*c* 0.20, MeOH). IR (neat): 3205, 3059, 2972, 2916, 2884, 2831, 2779, 1778, 1754, 1693, 1535, 1454, 1416, 1397, 1220, 1061, 1050, 914, 843, 780, 759, 740, 691, 530, 446 cm^{-1}. ^{1}H NMR (400 MHz, CD_3OD) δ 7.32 – 7.15 (m, 5H), 4.50 (t, *J* = 6.2 Hz, 1H), 4.42 (t, *J* = 7.1 Hz, 1H), 4.11 (d, *J* = 5.9 Hz, 1H), 3.09 (dd, *J* = 13.8, 6.3 Hz, 1H), 2.97 (dd, *J* = 13.5, 8.2 Hz, 1H), 2.50 (dd, *J* = 18.6, 6.3 Hz, 1H), 2.18 – 2.08 (m, 1H), 2.06 (s, 3H), 1.26 (s, 9H), 0.94 (d, *J* = 6.5 Hz, 6H). ^{13}C NMR (101 MHz, CD_3OD) δ 178.0, 174.4, 173.9, 173.8, 172.5, 138.8, 130.6, 129.6,

127.8, 61.3, 57.0, 53.1, 52.4, 40.0, 39.1, 31.5, 29.0, 22.7, 19.9, 18.6. HRMS calcd. for $C_{24}H_{40}N_5O_6$ $[M+NH_4]^+$ 494.2973, found 494.3007.

Ac-Phe-Asp-Phe *tert*-butyl amide (4.58).

The general procedure for homoserine peptide oxidation was followed, to get a white solid product (43.7 mg, 62%). Mp: 253 °C (dec.). $[\alpha]^D_{25}$ –8.1 (*c* 0.40, MeOH). IR (neat): 3272, 3206, 3078, 3061, 3037, 2974, 2923, 2826, 2779, 1692, 1632, 1538, 1495, 1454, 1416, 1396, 1365, 1293, 1221, 1050, 952, 913, 844, 782, 741, 698, 608, 581, 529, 445 cm^{-1}. ^1H NMR (400 MHz, CD_3OD) δ 7.31 – 7.11 (m, 10H), 4.63 (t, *J* = 6.6 Hz, 1H), 4.58 – 4.51 (m, 1H), 4.49 – 4.42 (m, 1H), 3.11 – 2.98 (m, 2H), 2.92 (dd, *J* = 13.7, 8.0 Hz, 1H), 2.86 – 2.76 (m, 1H), 1.89 (s, 3H), 1.26 (s, 9H). ^{13}C NMR (101 MHz, CD_3OD) δ 174.0, 173.9, 173.6, 172.5, 172.2, 138.6, 138.0, 130.7, 130.6, 130.4, 129.6, 128.0, 127.9, 56.8, 56.4, 52.4, 51.5, 49.2, 39.6, 39.1, 38.7, 36.3, 28.9, 22.5 HRMS calcd. for $C_{28}H_{37}N_4O_6$ $[M+H]^+$ 525.2708, found 525.2758.

References

1. Groll, M.; Schellenberg, B.; Bachmann, A. S.; Archer, C. R.; Huber, R.; Powell, T. K.; Lindow, S.; Kaiser, M.; Dudler, R. A plant pathogen virulence factor inhibits the eukaryotic proteasome by a novel mechanism. *Nature,* **2008,** *452*, 755-8.

2. Oka, M.; Nishiyama, Y.; Ohta, S.; Kamei, H.; Konishi, M.; Miyaki, T.; Oki, T.; Kawaguchi, H. Glidobactins A, B and C, new antitumor antibiotics. I. Production, isolation, chemical properties and biological activity. *J. Antibiot. (Tokyo),* **1988,** *41*, 1331-1337.

3. Oka, M.; Ohkuma, H.; Kamei, H.; Konishi, M.; Oki, T.; Kawaguchi, H. Glidobactins D, E, F, G and H; minor components of the antitumor antibiotic glidobactin. *J. Antibiot. (Tokyo),* **1988,** *41*, 1906-9.

4. Konishi, M.; Tomita, K.; Oka, M.; Numata, K. Peptide Antibiotics. *US 4692510,* September 8, 1987.

5. Schellenberg, B.; Bigler, L.; Dudler, R. Identification of genes involved in the biosynthesis of the cytotoxic compound glidobactin from a soil bacterium. *Environ. Microbiol.* **2007,** *9*, 1640-50.

6. Oka, M.; Nishiyama, Y.; Ohta, S.; Kamei, H.; Konishi, M.; Miyaki, T.; Oki, T.; Kawaguchi, H. Glidobactins A, B and C, new antitumor antibiotics II. Structure elucidation. *J. Antibiot. (Tokyo),* **1988,** *41*, 1338-1350.

7. Shoji, J.; Hinoo, H.; Kato, T.; Hattori, T.; Hirooka, K.; Tawara, K.; Shiratori, O.; Terui, Y. Isolation of cepafungins I, II, and III from *Pseudomonas* species. *J. Antibiot. (Tokyo),* **1990,** *43*, 783-787.

8. Terui, Y.; Nishikawa, J.; Hinoo, H.; Kato, T.; Shoji, J. Structures of cepafungins I, II and III. *J. Antibiot. (Tokyo),* **1990,** *43*, 788-795.

9. Waspi, U.; Blanc, D.; Winkler, T.; Ruedi, P.; Dudler, R. Syringolin, a novel peptide elicitor from *Pseudomonas syringae* pv. *syringae* that induces resistance to pyricularia oryzae in rice. *Mol. Plant-Microbe. Interact.* **1998,** *11*, 727-733.

10. Waspi, U.; Hassa, P.; Staempfli, A. A.; Molleyres, L. P.; Winkler, T.; Dudler, R. Identification and structure of a family of syringolin variants - Unusual cyclic peptides from *Pseudomonas syringae* pv. *syringae* that elicit defense responses in rice. *Microbiol. Res.* **1999,** *154*, 89-93.

11. Bian, X.; Huang, F.; Stewart, F. A.; Xia, L.; Zhang, Y.; Muller, R. Direct cloning, genetic engineering, and heterologous expression of the syringolin biosynthetic gene cluster in E. coli through Red/ET recombineering. *Chembiochem,* **2012,** *13*, 1946-1952.

12. Bian, X.; Plaza, A.; Zhang, Y.; Muller, R. Luminmycins A-C, cryptic natural products from Photorhabdus luminescens identified by heterologous expression in Escherichia coli. *J. Nat. Prod.* **2012,** *75*, 1652-5.

13. Coleman, C. S.; Rocetes, J. P.; Park, D. J.; Wallick, C. J.; Warn-Cramer, B. J.; Michel, K.; Dudler, R.; Bachmann, A. S. Syringolin A, a new plant elicitor from the phytopathogenic bacterium *Pseudomonas syringae* pv. *syringae*, inhibits the proliferation of neuroblastoma and ovarian cancer cells and induces apoptosis. *Cell Prolif.* **2006,** *39*, 599-609.

14. Clerc, J.; Li, N.; Krahn, D.; Groll, M.; Bachmann, A. S.; Florea, B. I.; Overkleeft, H. S.; Kaiser, M. The natural product hybrid of syringolin A and glidobactin A synergizes proteasome inhibition potency with subsite selectivity. *Chem. Commun.* **2011,** *47*, 385-7.

15. Murata, S.; Yashiroda, H.; Tanaka, K. Molecular mechanisms of proteasome assembly. *Nat. Rev. Mol. Cell Biol.* **2009,** *10*, 104-15.

16. Ben-Nissan, G.; Sharon, M. Regulating the 20S proteasome ubiquitin-independent degradation pathway. *Biomolecules,* **2014,** *4*, 862-84.

17. Krahn, D.; Ottmann, C.; Kaiser, M. The chemistry and biology of syringolins, glidobactins and cepafungins (syrbactins). *Nat. Prod. Rep.* **2011,** *28*, 1854-67.

18. Angeles, A. Fung, G; Luo, H. Immune and non-immune functions of the immunoproteasome. *Front. Biosci.* **2012,** *17*, 1904-1916.

19. Huber, E. M.; Basler, M.; Schwab, R.; Heinemeyer, W.; Kirk, C. J.; Groettrup, M.; Groll, M. Immuno- and constitutive proteasome crystal structures reveal differences in substrate and inhibitor specificity. *Cell,* **2012,** *148*, 727-38.

20. Kisselev, A. F.; Callard, A.; Goldberg, A. L. Importance of the different proteolytic sites of the proteasome and the efficacy of inhibitors varies with the protein substrate. *J. Biol. Chem.* **2006,** *281*, 8582-90.

21. Borissenko, L.; Groll, M. 20S proteasome and its inhibitors: crystallographic knowledge for drug development. *Chem. Rev.* **2007,** *107*, 687-717.

22. Bachmann, A. S.; Opoku-Ansah, J.; Ibarra-Rivera, T. R.; Yco, L. P.; Ambadi, S.; Roberts, C. C.; Chang, C. E.; Pirrung, M. C. Syrbactin structural analog TIR-199 blocks proteasome activity and induces tumor cell death. *J. Biol. Chem.* **2016,** *291*, 8350-62.

23. Clerc, J.; Groll, M.; Illich, D. J.; Bachmann, A. S.; Huber, R.; Schellenberg, B.; Dudler, R.; Kaiser, M. Synthetic and structural studies on syringolin A and B reveal critical determinants of selectivity and potency of proteasome inhibition. *Proc. Natl. Acad. Sci. U.S.A.* **2009,** *106*, 6507-12.

24. Archer, C. R.; Groll, M.; Stein, M. L.; Schellenberg, B.; Clerc, J.; Kaiser, M.; Kondratyuk, T. P.; Pezzuto, J. M.; Dudler, R.; Bachmann, A. S. Activity enhancement of the synthetic syrbactin proteasome inhibitor hybrid and biological evaluation in tumor cells. *Biochemistry,* **2012,** *51*, 6880-8.

25. Laubach, J. P.; Mitsiades, C. S.; Roccaro, A. M.; Ghobrial, I. M.; Anderson, K. C.; Richardson, P. G. Clinical challenges associated with bortezomib therapy in multiple myeloma and Waldenstroms Macroglobulinemia. *Leuk. Lymphoma,* **2009,** *50*, 694-702.

26. Curran, M. P.; McKeage, K. Bortezomib: a review of its use in patients with multiple myeloma. *Drugs,* **2009,** *69*, 859-88.

27. Lawasut, P.; Chauhan, D.; Laubach, J.; Hayes, C.; Fabre, C.; Maglio, M.; Mitsiades, C.; Hideshima, T.; Anderson, K. C.; Richardson, P. G. New proteasome inhibitors in myeloma. *Curr. Hematol. Malig. Rep.* **2012,** *7*, 258-66.

28. Mullard, A. Next-generation proteasome blockers promise safer cancer therapy. *Nat. Med.* **2012,** *18*, 7.

29. Miller, Z.; Ao, L.; Kim, K. B.; Lee, W. Inhibitors of the immunoproteasome: current status and future directions. *Curr. Pharm. Des.* **2013,** *19*, 4140-51.

30. Meng, Q.; Hesse, M. Synthetic approaches toward glidobamine, the core structure of the glidobactin antibiotics. *Tetrahedron,* **1991,** *47*, 6251-6264.

31. Schmidt, U.; Kleefeldt, A.; Mangold, R. The synthesis of glidobactin A. *J. Chem. Soc. Chem. Commun.* **1992,** 1687-1689.

32. Clerc, J.; Schellenberg, B.; Groll, M.; Bachmann, A. S.; Huber, R.; Dudler, R.; Kaiser, M. Convergent synthesis and biological evaluation of syringolin A and derivatives as eukaryotic 20S proteasome inhibitors. *Eur. J. Org. Chem.* **2010,** 3991-4003.

33. Dai, C.; Stephenson, C. R. Total synthesis of syringolin A. *Org. Lett.* **2010,** *12*, 3453-5.

34. Chiba, T.; Hosono, H.; Nakagawa, K.; Asaka, M.; Takeda, H.; Matsuda, A.; Ichikawa, S. Total synthesis of syringolin A and improvement of its biological activity. *Angew. Chem. Int. Ed.* **2014,** *126*, 4936-4939.

35. Pirrung, M. C.; Biswas, G.; Ibarra-Rivera, T. R. Total synthesis of syringolin A and B. *Org. Lett.* **2010,** *12*, 2402-2405.

36. Ibarra-Rivera, T. R.; Opoku-Ansah, J.; Ambadi, S.; Bachmann, A. S.; Pirrung, M. C. Syntheses and cytotoxicity of syringolin B-based proteasome inhibitors. *Tetrahedron,* **2011,** *67*, 9950-9956.

37. Helquist, P.; Schauer, D. Mild zinc-promoted Horner-Wadsworth-Emmons reactions of diprotic phosphonate reagents. *Synthesis,* **2006,** *21*, 3654-3660.

38. Archer, C. R.; Koomoa, D. L.; Mitsunaga, E. M.; Clerc, J.; Shimizu, M.; Kaiser, M.; Schellenberg, B.; Dudler, R.; Bachmann, A. S. Syrbactin class proteasome inhibitor-induced apoptosis and autophagy occurs in association with p53 accumulation and Akt/PKB activation in neuroblastoma. *Biochem. Pharmacol.* **2010,** *80*, 170-178.

39. Chiba, T.; Matsuda, A.; Ichikawa, S. Structure-activity relationship study of syringolin A as a potential anticancer agent. *Bioorg. Med. Chem. Lett.* **2015,** *25*, 4872-7.

40. Kitahata, S.; Chiba, T.; Yoshida, T.; Ri, M.; Iida, S.; Matsuda, A.; Ichikawa, S. Design, synthesis, and biological activity of isosyringolin A. *Org. Lett.* **2016,** *18*, 2312-5.

41. Anshu, A.; Thomas, S.; Agarwal, P.; Ibarra-Rivera, T. R.; Pirrung, M. C.; Schonthal, A. H. Novel proteasome-inhibitory syrbactin analogs inducing endoplasmic reticulum stress and apoptosis in hematological tumor cell lines. *Biochem. Pharmacol.* **2011,** *82*, 600-9.

42. Opoku-Ansah, J.; Ibarra-Rivera, T. R.; Pirrung, M. C.; Bachmann, A. S. Syringolin B-inspired proteasome inhibitor analogue TIR-203 exhibits enhanced biological activity in multiple myeloma and neuroblastoma. *Pharm. Biol.* **2012,** *50*, 25-9.

43. Curatolo, W. Physical chemical properties of oral drug candidates in the discovery and exploratory development settings. *Pharm. Sci. Technol. To.* **1998,** *1*, 387-393.

44. Ishikawa, M.; Hashimoto, Y. Improvement in aqueous solubility in small molecule drug discovery programs by disruption of molecular planarity and symmetry. *J. Med. Chem.* **2011,** *54*, 1539-54.

45. Lovering, F. Escape from flatland 2: complexity and promiscuity. *Med. Chem. Commun.* **2013,** *4*, 515-519.

46. Gowardhane, A. P.; Kadam, N. V.; Dutta, S. Review on enhancement of solubilization process. *Am. J. Drug Discov. Dev.* **2014,** *4*, 134-152.

47. Vazquez, A.; Sánchez, A.; Calderón, E. Using the 9-BBN group as a transient protective group for the functionalization of reactive chains of α-amino acids. *Synthesis,* **2013,** *45*, 1364-1372.

48. Pirrung, M. C.; Zhang, F.; Ambadi, S.; Ibarra-Rivera, T. R. Reactive esters in amide ligation with β-hydroxyamines. *Eur. J. Org. Chem.* **2012,** 4283-4286.

49. Naredla, R. R.; Dash, B. P.; Klumpp, D. A. Preparation of pyrazine carboxamides: a reaction involving N-heterocyclic carbene (NHC) intermediates. *Org. Lett.* **2013,** *15*, 4806-9.

50. Fraser, R. R.; Schuber, F. J.; Wigfield, Y. Y. Conformational preference of an alpha-sulfinyl carbanion. *J. Am. Chem. Soc.* **1972,** *94*, 8795-8799.

51. Chavan, S. P.; Chavan, P. N.; Gonnade, R. G. Stereospecific synthetic approach towards Tamiflu using the Ramberg–Backlund reaction from cysteine hydrochloride. *RSC Adv.* **2014,** *4*, 62281-62284.

52. Mercer, J. A.; Cohen, C. M.; Shuken, S. R.; Wagner, A. M.; Smith, M. W.; Moss, F. R., 3rd; Smith, M. D.; Vahala, R.; Gonzalez-Martinez, A.; Boxer, S. G.; Burns, N. Z. Chemical synthesis and self-assembly of a ladderane phospholipid. *J. Am. Chem. Soc.* **2016,** *138*, 15845-15848.

53. Lusci, A.; Pollastri, G.; Baldi, P. Deep architectures and deep learning in chemoinformatics: the prediction of aqueous solubility for drug-like molecules. *J Chem. Inf. Model.* **2013,** *53*, 1563-75.

54. Lagorce, D.; Sperandio, O.; Baell, J. B.; Miteva, M. A.; Villoutreix, B. O. FAF-Drugs3: a web server for compound property calculation and chemical library design. *Nucleic Acids Res.* **2015,** *43*, W200-7.

55. Kuhn, D. J.; Hunsucker, S. A.; Chen, Q.; Voorhees, P. M.; Orlowski, M.; Orlowski, R. Z. Targeted inhibition of the immunoproteasome is a potent strategy against models of multiple myeloma that overcomes resistance to conventional drugs and nonspecific proteasome inhibitors. *Blood,* **2009,** *113*, 4667-76.

56. Kraus, J.; Kraus, M.; Liu, N.; Besse, L.; Bader, J.; Geurink, P. P.; de Bruin, G.; Kisselev, A. F.; Overkleeft, H.; Driessen, C. The novel beta2-selective proteasome inhibitor LU-102 decreases phosphorylation of I kappa B and induces highly synergistic cytotoxicity in combination with ibrutinib in multiple myeloma cells. *Cancer Chemother. Pharmacol.* **2015,** *76*, 383-96.

57. Kraus, M.; Bader, J.; Geurink, P. P.; Weyburne, E. S.; Mirabella, A. C.; Silzle, T.; Shabaneh, T. B.; van der Linden, W. A.; de Bruin, G.; Haile, S. R.; van Rooden, E.; Appenzeller, C.; Li, N.; Kisselev, A. F.; Overkleeft, H.; Driessen, C. The novel beta2-selective proteasome inhibitor LU-102 synergizes with bortezomib and carfilzomib to overcome proteasome inhibitor resistance of myeloma cells. *Haematologica.* **2015,** *100*, 1350-60.

58. Koroleva, O. N.; Pham, T. H.; Bouvier, D.; Dufau, L.; Qin, L.; Reboud-Ravaux, M.; Ivanov, A. A.; Zhuze, A. L.; Gromova, E. S.; Bouvier-Durand, M. Bisbenzimidazole derivatives as potent inhibitors of the trypsin-like sites of the immunoproteasome core particle. *Biochimie.* **2015,** *108*, 94-100.

59. Kuhn, D. J.; Orlowski, R. Z. The immunoproteasome as a target in hematologic malignancies. *Semin. Hematol.* **2012,** *49*, 258-62.

60. Nilsson, B. L.; Soellner, M. B.; Raines, R. T. Chemical synthesis of proteins. *Annu. Rev. Biophys. Biomol. Struct.* **2005,** *34*, 91-118.

61. Kent, S. B. Chemical synthesis of peptides and proteins. *Annu. Rev. Biochem.* **1988,** *57*, 957-89.

62. Bondalapati, S.; Jbara, M.; Brik, A. Expanding the chemical toolbox for the synthesis of large and uniquely modified proteins. *Nat. Chem.* **2016,** *8*, 407-18.

63. Raibaut, L.; Ollivier, N.; Melnyk, O. Sequential native peptide ligation strategies for total chemical protein synthesis. *Chem. Soc. Rev.* **2012,** *41*, 7001-15.

64. Muralidharan, V.; Muir, T. W. Protein ligation: an enabling technology for the biophysical analysis of proteins. *Nat. Methods,* **2006,** *3*, 429-38.

65. Kimmerlin, T.; Seebach, D. '100 years of peptide synthesis': ligation methods for peptide and protein synthesis with applications to beta-peptide assemblies. *J. Pept. Res.* **2005,** *65*, 229-60.

66. Chandrudu, S.; Simerska, P.; Toth, I. Chemical methods for peptide and protein production. *Molecules,* **2013,** *18*, 4373-88.

67. Fischer, E.; Fourneau, E. Ueber einige Derivate des Glykocolls. *Ber. Dtsch. Chem. Ges.* **1901,** *34*, 2868-2877.

68. Merrifield, R. B. Solid phase peptide synthesis. I. The synthesis of a tetrapeptide. *J. Am. Chem. Soc.* **1963,** *85*, 2149-2154.

69. Dawson, P. E.; Muir, T. W.; Clark-Lewis, I.; Kent, S. B. Synthesis of proteins by native chemical ligation. *Science,* **1994,** *266*, 776-9.

70. Fosgerau, K.; Hoffmann, T. Peptide therapeutics: current status and future directions. *Drug Discov. Today,* **2015,** *20*, 122-8.

71. Pedersen, S. L.; Tofteng, A. P.; Malik, L.; Jensen, K. J. Microwave heating in solid-phase peptide synthesis. *Chem. Soc. Rev.* **2012,** *41*, 1826-44.

72. Schnolzer, M.; Alewood, P.; Jones, A.; Alewood, D.; Kent, S. B. In situ neutralization in Boc-chemistry solid phase peptide synthesis. Rapid, high yield assembly of difficult sequences. *Int. J. Pept. Protein Res.* **1992,** *40*, 180-93.

73. Rohde, H.; Seitz, O. Ligation-desulfurization: a powerful combination in the synthesis of peptides and glycopeptides. *Biopolymers,* **2010,** *94*, 551-9.

74. Fotouhi, N.; Galakatos, N. G.; Kemp, D. S. Peptide synthesis by prior thiol capture. 6. Rates of the disulfide bond forming capture reaction and demonstration of the overall strategy by synthesis of the C-terminal 29-peptide sequence of BPTI. *J. Org. Chem.* **1989,** *54*, 2803-2817.

75. Dawson, P. E.; Churchill, M. J.; Ghadiri, M. R.; Kent, S. B. H. Modulation of reactivity in native chemical ligation through the use of thiol additives. *J. Am. Chem. Soc.* **1997,** *119*, 4325-4329.

76. Johnson, E. C.; Kent, S. B. Insights into the mechanism and catalysis of the native chemical ligation reaction. *J. Am. Chem. Soc.* **2006,** *128*, 6640-6.

77. Hackeng, T. M.; Griffin, J. H.; Dawson, P. E. Protein synthesis by native chemical ligation: expanded scope by using straightforward methodology. *Proc. Natl. Acad. Sci. U.S.A.* **1999,** *96*, 10068-73.

78. McCaldon, P.; Argos, P. Oligopeptide biases in protein sequences and their use in predicting protein coding regions in nucleotide sequences. *Proteins,* **1988,** *4*, 99-122.

79. Tam, J. P.; Yu, Q. Methionine ligation strategy in the biomimetic synthesis of parathyroid hormones. *Biopolymers,* **1998,** *46*, 319-27.

80. Wong, C. T.; Tung, C. L.; Li, X. Synthetic cysteine surrogates used in native chemical ligation. *Mol. Biosyst.* **2013,** *9*, 826-33.

81. Yan, L. Z.; Dawson, P. E. Synthesis of peptides and proteins without cysteine residues by native chemical ligation combined with desulfurization. *J. Am. Chem. Soc.* **2001,** *123*, 526-33.

82. Canne, L. E.; Bark, S. J.; Kent, S. B. H. Extending the applicability of native chemical ligation. *J. Am. Chem. Soc.* **1996,** *118*, 5891-5896.

83. Malins, L. R.; Payne, R. J. Recent extensions to native chemical ligation for the chemical synthesis of peptides and proteins. *Curr. Opin. Chem. Biol.* **2014,** *22*, 70-78.

84. Offer, J.; Dawson, P. E. Nα-2-mercaptobenzylamine-assisted chemical ligation. *Org. Lett.* **2000,** *2*, 23-6.

85. Low, D. W.; Hill, M. G.; Carrasco, M. R.; Kent, S. B.; Botti, P. Total synthesis of cytochrome b562 by native chemical ligation using a removable auxiliary. *Proc. Natl. Acad. Sci. U.S.A.* **2001,** *98*, 6554-9.

86. Offer, J.; Boddy, C. N.; Dawson, P. E. Extending synthetic access to proteins with a removable acyl transfer auxiliary. *J. Am. Chem. Soc.* **2002,** *124*, 4642-6.

87. Kawakami, T.; Aimoto, S. A photoremovable ligation auxiliary for use in polypeptide synthesis. *Tetrahedron Lett.* **2003,** *44*, 6059-6061.

88. Marinzi, C.; Offer, J.; Longhi, R.; Dawson, P. E. An o-nitrobenzyl scaffold for peptide ligation: synthesis and applications. *Bioorg. Med. Chem.* **2004,** *12*, 2749-2757.

89. Wan, Q.; Danishefsky, S. J. Free-radical-based, specific desulfurization of cysteine: a powerful advance in the synthesis of polypeptides and glycopolypeptides. *Angew. Chem. Int. Ed.* **2007,** *46*, 9248-52.

90. Gao, X. F.; Du, J. J.; Liu, Z.; Guo, J. Visible-light-induced specific desulfurization of cysteinyl peptide and glycopeptide in aqueous solution. *Org. Lett.* **2016,** *18*, 1166-9.

91. Haase, C.; Rohde, H.; Seitz, O. Native chemical ligation at valine. *Angew. Chem. Int. Ed.* **2008,** *47*, 6807-10.

92. Chen, J.; Wan, Q.; Yuan, Y.; Zhu, J.; Danishefsky, S. J. Native chemical ligation at valine: a contribution to peptide and glycopeptide synthesis. *Angew. Chem. Int. Ed.* **2008,** *47*, 8521-4.

93. Crich, D.; Banerjee, A. Native chemical ligation at phenylalanine. *J. Am. Chem. Soc.* **2007,** *129*, 10064-5.

94. Malins, L. R.; Payne, R. J. Synthesis and utility of beta-selenol-phenylalanine for native chemical ligation-deselenization chemistry. *Org. Lett.* **2012,** *14*, 3142-5.

95. Tan, Z.; Shang, S.; Danishefsky, S. J. Insights into the finer issues of native chemical ligation: an approach to cascade ligations. *Angew. Chem. Int. Ed.* **2010,** *49*, 9500-3.

96. Harpaz, Z.; Siman, P.; Kumar, K. S.; Brik, A. Protein synthesis assisted by native chemical ligation at leucine. *Chembiochem.* **2010,** *11*, 1232-5.

97. Ajish Kumar, K. S.; Haj-Yahya, M.; Olschewski, D.; Lashuel, H. A.; Brik, A. Highly efficient and chemoselective peptide ubiquitylation. *Angew. Chem. Int. Ed.* **2009,** *48*, 8090-4.

98. Yang, R.; Pasunooti, K. K.; Li, F.; Liu, X. W.; Liu, C. F. Dual native chemical ligation at lysine. *J. Am. Chem. Soc.* **2009,** *131*, 13592-3.

99. El Oualid, F.; Merkx, R.; Ekkebus, R.; Hameed, D. S.; Smit, J. J.; de Jong, A.; Hilkmann, H.; Sixma, T. K.; Ovaa, H. Chemical synthesis of ubiquitin, ubiquitin-based probes, and diubiquitin. *Angew. Chem. Int. Ed.* **2010,** *49*, 10149-53.

100. Shang, S.; Tan, Z.; Dong, S.; Danishefsky, S. J. An advance in proline ligation. *J. Am. Chem. Soc.* **2011,** *133*, 10784-6.

101. Townsend, S. D.; Tan, Z.; Dong, S.; Shang, S.; Brailsford, J. A.; Danishefsky, S. J. Advances in proline ligation. *J. Am. Chem. Soc.* **2012,** *134*, 3912-6.

102. Chen, J.; Wang, P.; Zhu, J.; Wan, Q.; Danishefsky, S. J. A program for ligation at threonine sites: application to the controlled total synthesis of glycopeptides. *Tetrahedron.* **2010,** *66*, 2277-2283.

103. Siman, P.; Karthikeyan, S. V.; Brik, A. Native chemical ligation at glutamine. *Org. Lett.* **2012,** *14*, 1520-3.

104. Malins, L. R.; Cergol, K. M.; Payne, R. J. Chemoselective sulfenylation and peptide ligation at tryptophan. *Chem. Sci.* **2014,** *5*, 260-266.

105. Malins, L. R.; Cergol, K. M.; Payne, R. J. Peptide ligation-desulfurization chemistry at arginine. *Chembiochem.* **2013,** *14*, 559-63.

106. Thompson, R. E.; Chan, B.; Radom, L.; Jolliffe, K. A.; Payne, R. J. Chemoselective peptide ligation-desulfurization at aspartate. *Angew. Chem. Int. Ed.* **2013,** *52*, 9723-7.

107. Shang, S.; Tan, Z.; Danishefsky, S. J. Application of the logic of cysteine-free native chemical ligation to the synthesis of Human Parathyroid Hormone (hPTH). *Proc. Natl. Acad. Sci. U.S.A.* **2011,** *108*, 5986-9.

108. Dawson, P. E. Native chemical ligation combined with desulfurization and deselenization: A general strategy for chemical protein synthesis. *Isr. J. Chem.* **2011,** *51*, 862-867.

109. Saxon, E.; Armstrong, J. I.; Bertozzi, C. R. A "traceless" Staudinger ligation for the chemoselective synthesis of amide bonds. *Org. Lett.* **2000,** *2*, 2141-3.

110. Nilsson, B. L.; Kiessling, L. L.; Raines, R. T. Staudinger ligation: a peptide from a thioester and azide. *Org. Lett.* **2000,** *2*, 1939-41.

111. Saxon, E.; Bertozzi, C. R. Cell surface engineering by a modified Staudinger reaction. *Science,* **2000,** *287*, 2007-10.

112. Soellner, M. B.; Dickson, K. A.; Nilsson, B. L.; Raines, R. T. Site-specific protein immobilization by Staudinger ligation. *J. Am. Chem. Soc.* **2003,** *125*, 11790-11791.

113. Kalia, J.; Abbott, N. L.; Raines, R. T. General method for site-specific protein immobilization by Staudinger ligation. *Bioconjug. Chem.* **2007,** *18*, 1064-1069.

114. Bode, J. W.; Fox, R. M.; Baucom, K. D. Chemoselective amide ligations by decarboxylative condensations of N-alkylhydroxylamines and alpha-ketoacids. *Angew. Chem. Int. Ed.* **2006,** *45*, 1248-1252.

115. Ju, L.; Lippert, A. R.; Bode, J. W. Stereoretentive synthesis and chemoselective amide-forming ligations of C-terminal peptide alpha-ketoacids. *J. Am. Chem. Soc.* **2008,** *130*, 4253-4255.

116. Ju, L.; Bode, J. W. A general strategy for the preparation of C-terminal peptide alpha-ketoacids by solid phase peptide synthesis. *Org. Biomol. Chem.* **2009,** *7*, 2259-2264.

117. Medina, S. I.; Wu, J.; Bode, J. W. Nitrone protecting groups for enantiopure N-hydroxyamino acids: synthesis of N-terminal peptide hydroxylamines for chemoselective ligations. *Org. Biomol. Chem.* **2010,** *8*, 3405-3417.

118. Pattabiraman, V. R.; Ogunkoya, A. O.; Bode, J. W. Chemical protein synthesis by chemoselective alpha-ketoacid-hydroxylamine (KAHA) ligations with 5-oxaproline. *Angew. Chem. Int. Ed.* **2012,** *51*, 5114-5118.

119. Wucherpfennig, T. G.; Rohrbacher, F.; Pattabiraman, V. R.; Bode, J. W. Formation and rearrangement of homoserine depsipeptides and depsiproteins in the alpha-ketoacid-hydroxylamine ligation with 5-oxaproline. *Angew. Chem. Int. Ed.* **2014,** *53*, 12244-12247.

120. Pusterla, I.; Bode, J. W. An oxazetidine amino acid for chemical protein synthesis by rapid, serine-forming ligations. *Nat. Chem.* **2015,** *7*, 668-672.

121. Wu, J.; Ruiz-Rodríguez, J.; Comstock, J. M.; Dong, J. Z.; Bode, J. W. Synthesis of human GLP-1 (7–36) by chemoselective α-ketoacid–hydroxylamine peptide ligation of unprotected fragments. *Chem. Sci.* **2011,** *2*, 1976-1979.

122. Fukuzumi, T.; Ju, L.; Bode, J. W. Chemoselective cyclization of unprotected linear peptides by alpha-ketoacid-hydroxylamine amide-ligation. *Org. Biomol. Chem.* **2012,** *10*, 5837-44.

123. Ogunkoya, A. O.; Pattabiraman, V. R.; Bode, J. W. Sequential alpha-ketoacid-hydroxylamine (KAHA) ligations: synthesis of C-terminal variants of the modifier protein UFM1. *Angew. Chem. Int. Ed.* **2012,** *51*, 9693-9697.

124. Harmand, T. J.; Murar, C. E.; Bode, J. W. Protein chemical synthesis by alpha-ketoacid-hydroxylamine ligation. *Nat. Protoc.* **2016,** *11*, 1130-47.

125. Kemp, D. S. The amine capture strategy for peptide bond formation-an outline of progress. *Biopolymers,* **1981,** *20*, 1793-1804.

126. Liu, C. F.; Tam, J. P. Chemical ligation approach to form a peptide bond between unprotected peptide segments. Concept and model study. *J. Am. Chem. Soc.* **1994,** *116*, 4149-4153.

127. Shao, J.; Tam, J. P. Unprotected peptides as building blocks for the synthesis of peptide dendrimers with oxime, hydrazone, and thiazolidine linkages. *J. Am. Chem. Soc.* **1995,** *117*, 3893-3899.

128. Liu, C. F.; Tam, J. P. Peptide segment ligation strategy without use of protecting groups. *Proc. Natl. Acad. Sci. U.S.A.* **1994,** *91*, 6584-6588.

129. Tam, J. P.; Miao, Z. Stereospecific pseudoproline ligation of N-terminal serine, threonine, or cysteine-containing unprotected peptides. *J. Am. Chem. Soc.* **1999,** *121*, 9013-9022.

130. Li, X.; Lam, H. Y.; Zhang, Y.; Chan, C. K. Salicylaldehyde ester-induced chemoselective peptide ligations: enabling generation of natural peptidic linkages at the serine/threonine sites. *Org. Lett.* **2010,** *12*, 1724-1727.

131. Wong, C. T.; Li, T.; Lam, H. Y.; Zhang, Y.; Li, X. Realizing serine/threonine ligation: scope and limitations and mechanistic implication thereof. *Front. Chem.* **2014,** *2*, 1-7.

132. Zhang, Y.; Xu, C.; Lam, H. Y.; Lee, C. L.; Li, X. Protein chemical synthesis by serine and threonine ligation. *Proc. Natl. Acad. Sci. U.S.A.* **2013,** *110*, 6657-62.

133. Lee, C. L.; Li, X. Serine/threonine ligation for the chemical synthesis of proteins. *Curr. Opin. Chem. Biol.* **2014,** *22*, 108-14.

134. Jin, K.; Sam, I. H.; Po, K. H.; Lin, D.; Ghazvini Zadeh, E. H.; Chen, S.; Yuan, Y.; Li, X. Total synthesis of teixobactin. *Nat. Commun.* **2016,** *7*, 12394.

135. Liu, H.; Li, X. Development and application of serine/threonine ligation for synthetic protein chemistry. *Org. Biomol. Chem.* **2014,** *12*, 3768-3773.

136. Zhang, Y.; Li, T.; Li, X. Synthesis of human growth hormone-releasing hormone via three-fragment serine/threonine ligation (STL). *Org. Biomol. Chem.* **2013,** *11*, 5584-5587.

137. Pirrung, M. C.; Schreihans, R. S. Native serine peptide assembly - Scope and utility. *Eur. J. Org. Chem.* **2016**, 5633-5636.

138. Lipps, B. V. Anti-lethal factor from opossum serum is a potent antidote for animal, plant and bacterial toxins. *J. Venom. Anim. Toxins,* **1999,** *5*, 56-66.

139. Komives, C. F.; Sanchez, E. E.; Rathore, A. S.; White, B.; Balderrama, M.; Suntravat, M.; Cifelli, A.; Joshi, V. Opossum peptide that can neutralize rattlesnake venom is expressed in *Escherichia coli*. *Biotechnol. Prog.* **2017,** *33*, 81-86.

140. Lipps, B. V. Part 1: Lethal toxin neutralizing factor from opossum serum. *Toxin Reviews,* **2008,** *27*, 81-92.

141. Lipps, B. V. Part 2: Conversion of the active domain of natural opossum lethal toxin neutralizing factor to a synthetic peptide, LT-10. *Toxin Reviews,* **2008,** *27*, 93-107.

142. Earle, M. J.; Fairhurst, R. A.; Heaney, H.; Papageorgiou, G. A new synthesis of primary amines using *tert*-butylamine as an ammonia equivalent: The triflic aAcid catalysed removal of N-*tert*-butyl groups from carbamates. *Synlett,* **1990**, 621-623.

143. Zhao, B.; Yuan, W.; Du, H.; Shi, Y. Cu(I)-catalyzed intermolecular diamination of activated terminal olefins. *Org. Lett.* **2007,** *9*, 4943-4945.

144. Evans, V.; Mahon, M. F.; Webster, R. L. A mild, copper-catalysed amide deprotection strategy: use of tert-butyl as a protecting group. *Tetrahedron,* **2014,** *70*, 7593-7597.

145. De Luca, L.; Giacomelli, G.; Masala, S.; Porcheddu, A. Trichloroisocyanuric:TEMPO oxidation of alcohols under mild conditions- A close investigation. *J. Org. Chem.* **2003,** *68*, 4999-5001.

146. Duca, M.; Chen, S.; Hecht, S. M. Modeling the reactive properties of tandemly activated tRNAs. *Org. Biomol. Chem.* **2008,** *6*, 3292-9.

147. Schmid, W.; Nagl, M.; Panuschka, C.; Barta, A. The BF3*OEt2-assisted conversion of nitriles into thioamides with Lawesson's reagent. *Synthesis,* **2008,** *24*, 4012-4018.

148. Martinez, L.; Martorell, G.; Sampedro, A.; Ballester, P.; Costa, A.; Rotger, C. Hydrogen bonded squaramide-based foldable module induces both beta- and alpha-turns in hairpin structures of alpha-peptides in water. *Org. Lett.* **2015,** *17*, 2980-2983.

149. Pelagatti, P.; Carcelli, M.; Calbiani, F.; Cassi, C.; Elviri, L.; Pelizzi, C.; Rizzotti, U.; Rogolino, D. Transfer hydrogenation of acetophenone catalyzed by half-sandwich Ruthenium(II) complexes containing amino amide ligands. Detection of the catalytic intermediates by electrospray ionization mass spectrometry. *Organometallics,* **2005,** *24*, 5836-5844.